ISSN 0021-9673

VOL. 664 NO. 1 MARCH 25, 1994

JOURNAL OF CHROMATOGRAPHY A

INCLUDING ELECTROPHORESIS AND OTHER SEPARATION METHODS

ELSEVIER

JOURNAL OF CHROMATOGRAPHY A

INCLUDING ELECTROPHORESIS AND OTHER SEPARATION METHODS

Scope. The *Journal of Chromatography A* publishes papers on all aspects of **chromatography, electrophoresis** and related methods. Contributions consist mainly of research papers dealing with chromatographic theory, instrumental developments and their applications. In the *Symposium volumes*, which are under separate editorship, proceedings of symposia on chromatography, electrophoresis and related methods are published. *Journal of Chromatography B: Biomedical Applications* —This journal, which is under separate editorship, deals with the following aspects: developments in and applications of chromatographic and electrophoretic techniques related to clinical diagnosis or alterations during medical treatment; screening and profiling of body fluids or tissues related to the analysis of active substances and to metabolic disorders; drug level monitoring and pharmacokinetic studies; clinical toxicology; forensic medicine; veterinary medicine; occupational medicine; results from basic medical research with direct consequences in clinical practice.

Submission of Papers. The preferred medium of submission is on disk with accompanying manuscript (see *Electronic manuscripts* in the Instructions to Authors, which can be obtained from the publisher, Elsevier Science B.V., P.O. Box 330, 1000 AH Amsterdam, Netherlands). Manuscripts (in English; *four* copies are required) should be submitted to: Editorial Office of *Journal of Chromatography A*, P.O. Box 681, 1000 AR Amsterdam, Netherlands, Telefax (+31-20) 5862 304, or to: The Editor of *Journal of Chromatography B: Biomedical Applications*, P.O. Box 681, 1000 AR Amsterdam, Netherlands. Review articles are invited or proposed in writing to the Editors who welcome suggestions for subjects. An outline of the proposed review should first be forwarded to the Editors for preliminary discussion prior to preparation. Submission of an article is understood to imply that the article is original and unpublished and is not being considered for publication elsewhere. For copyright regulations, see below.

Publication information. *Journal of Chromatography A* (ISSN 0021-9673): for 1994 Vols. 652–682 are scheduled for publication. *Journal of Chromatography B: Biomedical Applications* (ISSN 0378-4347): for 1994 Vols. 652–662 are scheduled for publication. Subscription prices for *Journal of Chromatography A*, *Journal of Chromatography B: Biomedical Applications* or a combined subscription are available upon request from the publisher. Subscriptions are accepted on a prepaid basis only and are entered on a calendar year basis. Issues are sent by surface mail except to the following countries where air delivery via SAL is ensured: Argentina, Australia, Brazil, Canada, China, Hong Kong, India, Israel, Japan, Malaysia, Mexico, New Zealand, Pakistan, Singapore, South Africa, South Korea, Taiwan, Thailand, USA. For all other countries airmail rates are available upon request. Claims for missing issues must be made within six months of our publication (mailing) date. Please address all your requests regarding orders and subscription queries to: Elsevier Science B.V., Journal Department, P.O. Box 211, 1000 AE Amsterdam, Netherlands. Tel.: (+31-20) 5803 642; Fax: (+31-20) 5803 598. Customers in the USA and Canada wishing information on this and other Elsevier journals, please contact Journal Information Center, Elsevier Science Inc., 655 Avenue of the Americas, New York, NY 10010, USA, Tel. (+1-212) 633 3750, Telefax (+1-212) 633 3764.

Abstracts/Contents Lists published in Analytical Abstracts, Biochemical Abstracts, Biological Abstracts, Chemical Abstracts, Chemical Titles, Chromatography Abstracts, Current Awareness in Biological Sciences (CABS), Current Contents/Life Sciences, Current Contents/Physical, Chemical & Earth Sciences, Deep-Sea Research/Part B: Oceanographic Literature Review, Excerpta Medica, Index Medicus, Mass Spectrometry Bulletin, PASCAL-CNRS, Referativnyi Zhurnal, Research Alert and Science Citation Index.

US Mailing Notice. *Journal of Chromatography A* (ISSN 0021-9673) is published weekly (total 52 issues) by Elsevier Science B.V., (Sara Burgerhartstraat 25, P.O. Box 211, 1000 AE Amsterdam, Netherlands). Annual subscription price in the USA US$ 4994.00 (US$ price valid in North, Central and South America only) including air speed delivery. Second class postage paid at Jamaica, NY 11431. **USA POSTMASTERS**: Send address changes to *Journal of Chromatography A*, Publications Expediting, Inc., 200 Meacham Avenue, Elmont, NY 11003. Airfreight and mailing in the USA by Publications Expediting.

See inside back cover for Publication Schedule, Information for Authors and information on Advertisements.

0021-9673/94/$07.00

Printed in the Netherlands

CONTENTS

(Abstracts/Contents Lists published in Analytical Abstracts, Biochemical Abstracts, Biological Abstracts, Chemical Abstracts, Chemical Titles, Chromatography Abstracts, Current Awareness in Biological Sciences (CABS), Current Contents/Life Sciences, Current Contents/Physical, Chemical & Earth Sciences, Deep-Sea Research/Part B: Oceanographic Literature Review, Excerpta Medica, Index Medicus, Mass Spectrometry Bulletin, PASCAL-CNRS, Referativnyi Zhurnal, Research Alert and Science Citation Index)

REGULAR PAPERS

Column Liquid Chromatography

Gas Chromatography

Electrophoresis

SHORT COMMUNICATIONS

Column Liquid Chromatography

(Continued overleaf)

Contents (continued)

JOURNAL OF CHROMATOGRAPHY A

VOL. 664 (1994)

JOURNAL OF CHROMATOGRAPHY A

INCLUDING ELECTROPHORESIS AND OTHER SEPARATION METHODS

ELSEVIER

AMSTERDAM — LONDON — NEW YORK — TOKYO

0021-9673/94/$07.00

This issue is printed on acid-free paper.

Printed in the Netherlands

ELSEVIER

Journal of Chromatography A, 664 (1994) 1–11

JOURNAL OF CHROMATOGRAPHY A

Fluorinated bonded stationary phases in micellar liquid chromatography

Shenyuan Yang, Lisa F. Resotko Kruk, Morteza G. Khaledi*

Department of Chemistry, P.O. Box 8204, North Carolina State University, Raleigh, NC 27695, USA

(First received July 28th, 1993; revised manuscript received November 12th, 1993)

Abstract

The usefulness of fluorinated bonded stationary phases in micellar liquid chromatography (MLC) is examined. Different selectivities and higher efficiencies were observed using a flurooctyl (FO) column as compared to that of a C_{18} column for both non-ionic and ionic compounds in MLC. Shortened analysis times for amino acids and small peptides and increased retention for the early eluting sulfonamides were observed on the FO column. The unique phenomenon of the simultaneous enhancement of solvent strength and selectivity that often occurs in the MLC systems with the alkyl-bonded stationary phases was also observed for the FO column. This is due to the existence of the competing partitioning equilibria in MLC and because of the interactive nature of the two eluent parameters, micelle concentration and the volume fraction of organic modifiers, both of which influence solvent strength and selectivity. Consequently, simultaneous optimization of these two parameters is the most effective strategy for the MLC systems with the fluorinated bonded stationary phases. Subsequently, the iterative regression strategy was utilized to optimize these two mobile phase parameters for a group of amino acids and small peptides. Excellent agreement was obtained between the observed optimum chromatogram and the one predicted by the iterative regression strategy using only five initial experiments. The successful application of the iterative regression optimization procedure indicates that the retention pattern in MLC with fluorinated bonded stationary phases is easily predictable. This is a similar behavior to that using hydrocarbonaceous phases and can be attributed to the linear variations in retention with the two mobile phase parameters and to the highly reproducible retention behavior in MLC.

1. Introduction

Micellar liquid chromatography (MLC) is a powerful alternative to ion-pair chromatography (IPC) for the separation of charged compounds [1–3]. This is because MLC offers a combination of several capabilities such as capability of simultaneous separation of ionic and non-ionic compounds, reproducible and predictable retention behavior, simultaneous enhancement of solvent strength and separation selectivity, and rapid gradient capability. Other unique advantages like possibility of on-column injection of physiological fluids, enhanced luminescence detection, applications in quantitative structure–biological activity relationships, low cost and low toxicity have also been reported [4–10].

The most serious drawback of MLC is the additional band broadening as compared to that in conventional reversed-phase LC with hydro-organic eluents. However, the typical MLC column efficiency is about the same as that in

* Corresponding author.

0021-9673/94/$07.00
SSDI 0021-9673(93)E1230-W

IPC at similar elution strengths [3]. Several workers have concluded that adsorption of monomer surfactants on the alkyl-bonded stationary phases in MLC contributes significantly to the band-broadening process. In general, slow kinetics of mass transfer in stationary phase and in mobile phase have been identified as the reasons behind the poor chromatographic efficiency [11–14]. In general, incorporation of additional chemical equilibria in an LC system (such as ion pairing or micelle partitioning) provides enhanced selectivity at the expense of additional band broadening.

Alkyl-bonded stationary phases have been used in nearly all of the MLC separations that have so far been reported. Fluorinated bonded stationary phases in MLC may offer several advantages over hydrocarbonaceous bonded stationary phases. First, due to the reduced interaction between hydrocarbon and fluorocarbon functional groups (as compared to the hydrocarbon–hydrocarbon interactions), it is expected that the extent of adsorption of hydrocarbon surfactants on the fluorinated bonded stationary phases be less than that on the alkyl-bonded stationary phases. Reduction in surfactant adsorption may lead to an improvement in the kinetics of mass transfer across the stationary phase in MLC and subsequently to higher column efficiencies. Second, hydrocarbon compounds are generally less retentive on fluorinated bonded stationary phases than on alkyl-bonded stationary phases. Therefore, for the separation of hydrophobic hydrocarbon compounds either lower micelle concentration is required which leads to better efficiency in MLC [13], or faster separations are achieved at a given solvent strength. Third, different chromatographic selectivity can be observed on a fluorinated bonded stationary phase especially for compounds with polar functional groups. In addition, the differences in polarities and types of interactions that exist in MLC systems with hydrocarbon ionic micelles in the mobile phase and fluorinated bonded stationary phases are larger than those in traditional MLC systems with hydrocarbon micelles and alkyl-bonded stationary phases. This might lead to a better control on retention and higher degree of selectivities. Generally, larger differences between the mobile phase and stationary phase polarities provide better selectivities [15,16].

The usefulness of fluorinated bonded stationary phases in RPLC system was first reported by Berendsen *et al.* [17]. As compared to the hydrocarbonaceous bonded stationary phases (such as C_{18}) in RPLC, fluorocarbon columns have different chemistry and offer less retention for hydrocarbon compounds and specific interactions between fluorine and some polar functional groups (such as–CHO,–$COCH_3$,–OH,–NO_2, –CN,–OCH_3,–F and–COOH) [15,18–20]. They are potentially useful for the separation of very hydrophobic hydrocarbon compounds [21], proteins [22], and some polar compounds [20].

In this paper, the usefulness of a flurooctyl (FO)-bonded stationary phase in MLC is examined with the emphasis on retention and selectivity behaviors. Retention behavior of ionic and non-ionic compounds were investigated in MLC with the FO column and sodium dodecyl sulfate (SDS) micellar eluents. The influence of the stationary phase on retention and selectivity for alkylphenone homologous series, amino acids, small peptides and sulfonamides is discussed. As expected, higher efficiencies were observed on the FO column than those on a C_{18} column for different test solutes. It was found that the simultaneous enhancement of solvent strength and selectivity, which was previously observed for the C_{18}-based MLC system [1–3], may also occur in the FO-based MLC system. The iterative regression optimization strategy [23,24] was successfully used for optimizing the separation of ten amino acids and small peptides. The effects of stationary phase on retention and selectivity for amino acids, small peptides and sulfonamides is also discussed.

2. Experimental

2.1. Chromatographic system

The chromatographic apparatus consisted of an HPLC pump (Model 400; Applied Biosys-

tems, Foster City, CA, USA) and a variable-wavelength absorbance detector (Model 783A, Applied Biosystems) set at 210 nm for amino acids and small peptides and at 254 nm for other test solutes. The HPLC system was controlled by the Chemresearch chromatographic data management system controller software (ISCO, Lincoln, NE, USA) running on a PC-88 Turbo personal computer (IDS, Paramount, CA, USA). A 5-μm particle size FO column (E.S. Industries, Berlin, NJ, USA), 150 × 4.6 mm, and a 5-μm particle size C_{18} column (Rainin Instruments, Woburn, MA, USA), 150 × 4.6 mm, were used. The columns were thermostated at 40°C by a water circulator bath (Lauda Model MT-6; Brinkmann Instruments, Westbury, NY, USA). A silica precolumn was used to saturate the mobile phase with silicates and protect the analytical column. Two 1.5-μm precolumn filters (Rainin Instruments) were placed between the silica precolumn and a VIGI injector (Valco, Houston, TX, USA) and between the injector and the analytical column. The column dead times were measured from the injection point of water samples and the first deviation of the baseline. The iterative regression program [23,24] was used to optimize and reconstruct the experimental chromatograms. The simulated chromatograms in this paper are based on a Gaussian peak shape, using the theoretical plates and the dead times experimentally observed.

2.2. Reagents

The stock solution of SDS (Sigma), was prepared by dissolving the required amount of surfactant in doubly distilled, deionized water and was filtered through a 0.45-μm nylon-66 membrane filter (Rainin Instruments). All the test solutes were obtained from Sigma. The sample solutions were prepared by diluting the stock solutions (5 mg/ml in methanol) with the mobile phase. The ionic strength was adjusted by adding phosphate buffer so that the total buffer concentration of the final solution was 0.020 *M*. After adding the required amount of organic solvents (such as 1-propanol) the pH was adjusted to 3.0. All other chemicals were obtained from Sigma, Aldrich or Fisher.

3. Results and discussion

Several mobile phase parameters such as the type/concentration of surfactant and organic solvent, pH, ionic strength and temperature can influence the MLC separations. In this study, the effects of surfactant concentration, type and volume fraction of organic solvent on the chromatographic behavior of the test solutes using a FO column and a C_{18} column were examined.

3.1. Retention behavior of homologous series

Alkyl homologous series are suitable test compounds for the investigation of retention mechanisms, especially in new RPLC systems [25,26]. The linear increase of retention (*i.e.* ln k') due to the addition of a methylene group is recognized as a measure of hydrophobic interaction in a given RPLC system.

The retention and selectivity of *n*-alkylphenones on the FO column were studied in the micellar eluents comprised of SDS micelles and an organic modifier (referred to as hybrid mobile phases [27,28]). Three different organic modifiers (1-propanol, 2-propanol and tetrafluoro-1-propanol) were investigated, and the results are listed in Table 1. It is clear from Table 1 that the retention factor (k'), instead of the logarithm of k', is linearly dependent on the carbon number (n_C) for all three hybrid eluents. For these systems, the plot of ln k' *vs.* n_C has a clear curvature and a quadratic equation provides a better correlation than the linear regression. However, a quadratic fit of k' *vs.* n_C plot does not improve the correlation. These results are consistent with those previously observed in the C_{18}-based MLC systems [27]. It has been concluded that the curvature in ln k' *vs.* n_C plots, which reflects the variation of methylene selectivity with n_C, is due to the fact that different compounds of a homologous series occupy various locations (with different microenvironment polarities) in micelles [27].

Table 1
Retention and selectivity of alkylphenones in hybrid SDS System (FO column)

Compounds	0.10 *M* SDS, 15% 2-PrOH		0.10 *M* SDS, 15% 1-PrOH		0.20 *M* SDS, 3% tetrafluoro-1-PrOH	
	k'	α	k'	α	k'	α
Octanophenone	[a]		11.25	1.18	[a]	
Heptanophenone	12.19	1.14	9.53	1.12	12.25	1.12
Hexanophenone	10.70	1.19	8.49	1.19	10.94	1.13
Valerophenone	8.96	1.27	7.16	1.26	9.69	1.15
Butyrophenone	7.03	1.39	5.69	1.38	8.46	1.18
Propiophenone	5.04	1.44	4.12	1.44	7.14	1.18
Acetophenone	3.49		2.86		6.03	
Linear regression (R^2)						
k' *vs.* n_C		0.9980		0.9978		0.9996
ln k' *vs.* n_C		0.9655		0.9586		0.9923

[a] The peaks for octanophenone were not observed at these two mobile phase conditions.

The ratio of retention factors of two compounds differing only in a–CH_2 group, $\alpha(CH_2)$, is smaller on the FO column than that on the C_{18} and C_8 columns [28] at the same mobile phase conditions. This indicates that the interaction between a–CH_2 group and the fluorocarbon phase is less than that with the alkyl phases. This observation has also been reported for conventional hydro–organic mobile phases [19]. Note that $\alpha(CH_2)$ decreases as the homologues become more hydrophobic (with one exception), which was also observed with the alkyl-bonded stationary phases [28]. It has been concluded that the $\alpha(CH_2)$ differences between the compounds in a homologous series are due to the different locations (*i.e.* the different microenvironment polarities) of solubilization in/on micelles in MLC [28]. Also note that the $\alpha(CH_2)$ values for the tetrafluoro-1-propanol-containing eluent are smaller than those for the propanol-containing eluents. This may be due to smaller differences between the polarities of the mobile phase and the stationary phase in the former case despite the fact that the hybrid mobile phase with tetrafluoro-1-propanol is the weakest. Generally, $\alpha(CH_2)$ is inversely related to solvent strength in RPLC, however, this is not the case for MLC as was shown previously [1,3].

3.2. Efficiency

The typical numbers of theoretical plates for different compounds in MLC with the FO column and the C_{18} column are listed in Table 2.

The efficiencies for amino acids, small peptides and sulfonamides are higher on the FO column than those on the C_{18} column. The higher efficiencies obtained on the FO column in MLC are perhaps partly due to the smaller adsorption of surfactant (SDS) on the FO stationary phase surface than that on the C_{18} stationary phase surface. Smaller surfactant adsorption should accelerate the mass transfer and decrease the flow anisotropy [14]. However, this should be further confirmed by studying the adsorption isotherms of the surfactant on both FO column and C_{18} column. It is also clear from Table 2 that the micelle concentration has a great effect on efficiency. The efficiencies of amino acids and small peptides were reduced by about 10 000 theoretical plates per meter with an increase in the SDS concentration from 0.050 to

Table 2
Column efficiencies in MLC[a]

Compounds	Column	Mobile phase	N (plates/m, average)	h [b]	k' range
Amino acids and peptides	FO	0.10 *M* SDS, 15% 2-propanol	23 300	8.57	1.1–3.4
Amino acids and peptides	C_{18}	0.10 *M* SDS, 15% 2-propanol	16 000	12.5	3.0–9.9
Sulfonamides	FO	0.1075 *M* SDS, 8% 1-propanol	23 300	8.57	0.9–7.4
Sulfonamides	C_{18}	0.1075 *M* SDS, 8% 1-propanol	13 300	15.0	0.5–8.4
Amino acids and peptides	FO	0.05 *M* SDS, 3% 1-propanol	26 000	7.5	9.3–21.7
Amino acids andpeptides	FO	0.20 *M* SDS, 3% 1-propanol	16 000	12.0	2.8–5.4

[a] Calculated by using Foley and Dorsey's equation [29].
[b] Reduced plate height.

0.200 *M*. These results suggest that both stationary phase and mobile phase effects contribute to band broadening in MLC [11–14].

3.3. Solvent strength and selectivity

Simultaneous enhancement of solvent strength and separation selectivity was previously reported in the C_{18}-based MLC system [1–3]. A similar behavior was also observed in the FO-based MLC system for both amino acids and small peptides (ionic compounds) and sulfonamides (non-ionic compounds at pH 3.0) using the hybrid SDS micellar mobile phase conditions (pH 3.0).

In the C_{18}-based MLC system Eqs. 1 and 2 [1–3] describe the dependence of retention factor in MLC on the volume fraction of organic solvent and the micelle concentration, respectively.

$$\ln k' = -S\varphi_{org} + \ln k'_0 \quad (1)$$

$$1/k' = (K_{mw}[M] + 1)/(P_{sw}\phi) \quad (2)$$

where k' is the retention factor of a solute, φ_{org} is the volume fraction of the organic solvent, k'_0 is the retention factor in a purely aqueous micellar mobile phase, S is the solvent strength parameter, [M] is the micelle concentration, ϕ is the phase ratio, K_{mw} is the binding constant of solute to micelles, and P_{sw} is the partition coefficient of a compound from mobile phase into stationary phase [6].

According to Eqs. 1 and 2, increasing the solvent strength in MLC through an increase in the volume fraction of organic solvent or an increase in the micelle concentration leads to a decrease in retention. Fig. 1 shows that Eqs. 1

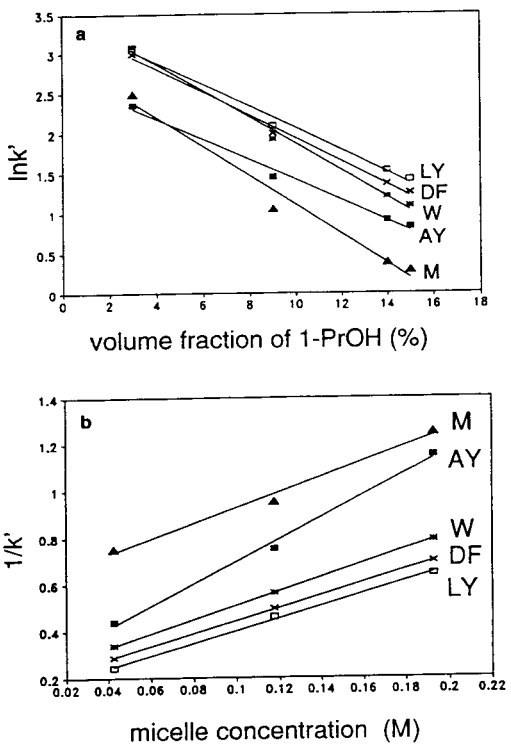

Fig. 1. The effect of (a) the volume fraction of 1-propanol (0.05 *M* SDS) and (b) the SDS concentration (15% 1-propanol) on the retention of amino acids and small peptides.

and 2 are also valid for an MLC system with fluorinated bonded stationary phase using a group of amino acids and small peptides as test compounds. Good linearity (r, the correlation coefficient, >0.99) for both ln k' *vs.* φ_{org} and $1/k'$ *vs.* [M] was obtained with the exception of Met ($r = 0.988$) in Fig. 1a, which may be due to the experimental errors. Similar results were also observed for sulfonamides.

Eqs. 3 and 4 show the dependence of selectivity in MLC systems on the volume fraction of organic solvent and micellar concentration [1].

$$\ln \alpha = -(S_2 - S_1)\varphi_{org} + (\ln k'_{0,1} - \ln k'_{0,2}) \quad (3)$$

$$\alpha = \frac{(\alpha_{sw})([M] + 1/K_{mw,1})}{(\alpha_{mw})([M] + 1/K_{mw,2})} \quad (4)$$

Eq. 3 describes the change in selectivity between compounds 1 and 2 ($\alpha = k'_2/k'_1$) when the volume fraction of organic solvent increases from φ_a to φ_b ($\varphi_b > \varphi_a$). In Eq. 4, $K_{mw,1}$ and $K_{mw,2}$ are the binding constants of solutes 1 and 2 to micelles. α_{sw} is the stationary phase partitioning selectivity ($P_{sw,2}/P_{sw,1}$) and α_{mw} is the selectivity of binding to (or partitioning into) micelles ($K_{mw,2}/K_{mw,1}$).

The experimental results for amino acids and small peptides are illustrated in Fig. 2.

Previously, it was shown that there is no direct relation between solvent strength and selectivity in MLC with alkyl-bonded stationary phases [1–3]. This is in contrast to many situations in RPLC and IPC where solvent strength and selectivity are inversely related because of the direct relationship between solvent strength parameter (S) and retention (intercept of Eq. 1, ln k'_0) [1,3,30]. In the MLC system with alkyl-bonded stationary phases, the S values for different compounds would depend on the extent of their interactions with micelles; *i.e.* S values are no longer linearly related to ln k'_0 [1–3]. This is also observed for the FO column as shown in Fig. 3. As a result, simultaneous selectivity enhancement with solvent strength can also occur in MLC systems with fluorinated bonded stationary phases.

The occurrence of simultaneous enhancement of solvent strength and separation selectivity in

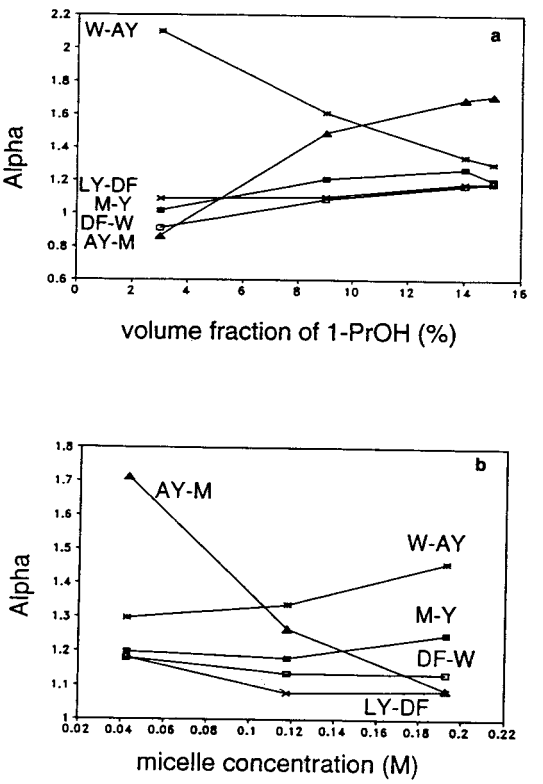

Fig. 2. The effect of (a) the volume fraction of 1-propanol (0.05 *M* SDS) and (b) the SDS concentration (15% 1-propanol) on the selectivity of amino acids and small peptides.

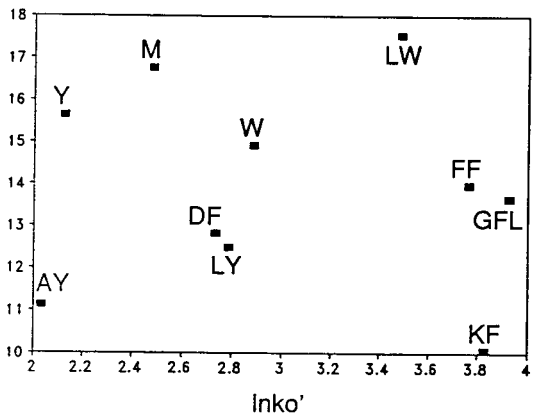

Fig. 3. The plot of solvent strength parameter (S) *vs.* ln k'_0. FO column, 0.11 *M* SDS, 1-propanol, pH 3.0.

MLC has been attributed to the existence of the competing partitioning equilibria in MLC and to the influence of micelles on the role of the organic solvents [1–3].

Selectivity in MLC is a function of the types and concentrations of micelles and organic modifiers [1,28]. Due to the different types of interactions (such as electrostatic and hydrophobic) and the competing equilibria in MLC, one can expect any forms of the selectivity behavior with the changes in the micelle concentration and the volume fraction of solvent. This is a similar behavior to that in the C_{18}-based MLC system [1–3,28]. This means that the simultaneous optimization of the volume fraction of organic solvent and the micelle concentration is necessary in the C_{18}-based MLC system [3,23,24] as well as the fluorocarbon-based MLC system.

3.4. Type of organic solvents

Snyder's selectivity triangle is a widely accepted method for the characterization of LC solvents and has been employed for solvent selection in conventional HPLC [31–35]. In this paper, the influence of various organic modifiers on retention and selectivity in the FO based MLC system was studied for sulfonamides, amino acids and small peptides.

1-Propanol (from group II), methanol (from group II), tetrahydrofuran (from group III), acetonitrile (from group VIb) and tetrafluoro-1-propanol (from group VIII) were used as organic modifiers in the FO-based MLC of sulfonamides. The effect of organic modifiers on selectivity is illustrated in Fig. 4 for two different pairs of sulfonamides (IXZ-CPD and BZD-IXZ) (see Table 3 for abbreviations). The effect of organic solvents on the separation of eight sulfonamides is illustrated in Fig. 5. The volume fractions of the organic modifiers were adjusted so that the solvent strengths (retention factors) of all five mobile phases remain approximately the same for the last eluting solute (IMD, $k' = 20$). It is clear that the organic solvents have a different influence on the selectivity for a pair of compounds (Fig. 4). However, the differences and similarities in retention pattern and selectivity

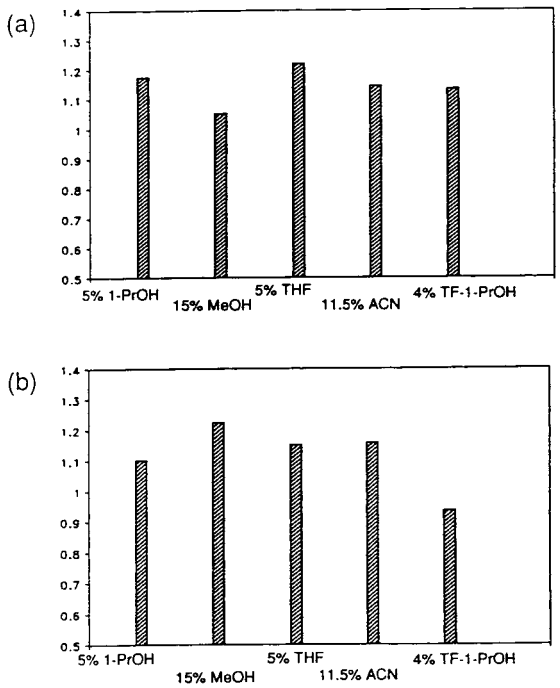

Fig. 4. The effect of organic modifiers on selectivity of sulfonamides at [SDS] = 0.02 *M*. (a) IXZ-CPD, (b) BZD-IXZ. ACN = Acetonitrile; TF = tetrafluoro.

among these five organic solvents can not be explained according to the Snyder's classification. Tetrafluoro-1-propanol has the most significant overall difference on the separation of sulfonamides, which may be due to the similarity between stationary phase and mobile phase. Similar results were also obtained for amino acids and small peptides and in the C_{18}-based MLC systems. Apparently, the existence of the competing partitioning equilibria in MLC and the influence of micelles in the mobile phase alter the effects of organic modifiers such that their role can no longer be explained according to the Snyder's classification of solvent selectivity [36].

3.5. Optimization of separation

It has been previously shown that the effects of the micelle concentration and the volume fraction of organic solvent in MLC should be

Table 3
Abbreviation of solutes

Amino acids and small peptides		Sulfonamides	
Components	Abbreviation	Components	Abbreviation
Ala–Tyr	AY	Sulfisoxazole	IXZ
Asp–Phe	DF	Sulfachloropyridazine	CPD
Leu–Tyr	LY	Sulfabenzamide	BZD
Met	M	Sulfacetamide	CTM
Trp	W	Sulfadiazine	DIA
Tyr	Y	Sulfamerazine	MRZ
Leu–Trp	LW	Sulfadimethoxine	DMX
Lys–Phe	KF	Sulfisomidine	IMD
Gly–Phe–Leu	GFL	Sulfamethazine	MTZ
Phe–Phe	FF	Sulfinpyrazone	IPZ

evaluated simultaneously. Optimization of one mobile phase variable at a time is ineffective in MLC due to the interactive nature of the variables.

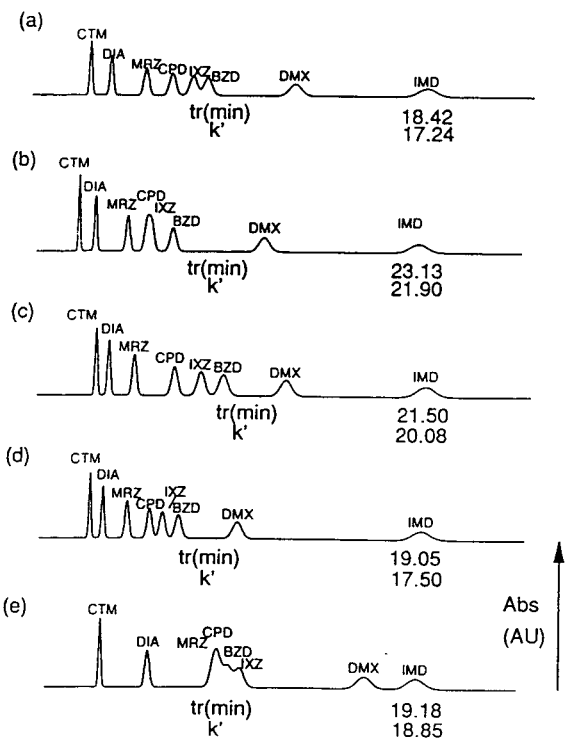

Fig. 5. The reconstructed chromatograms of a mixture of eight sulfonamides based on the experimental retention and efficiency data at 0.02 *M* SDS (a) 5% 1-propanol, (b) 15% methanol, (c) 5% tetrahydrofuran, (d) 11.5% acetonitrile, (e) 4% tetrafluoro-1-propanol.

Consequently, the iterative regression (IR) optimization design has been successfully applied for the multiparameter optimization in MLC [23,24]. This optimization strategy is based on the assumption that retention (ln k') is a linear function of the parameters within the parameter space. As shown in Eq. 1, it is certain that ln k' is linearly related to the volume fraction of organic modifier (1-propanol). According to Eq. 2, $1/k'$ is linearly proportional to the micelle concentration. However, the algorithm of the IR program that was used in this work is based on the assumption that retention (ln k') is a linear function of the two parameters (volume fraction of organic modifier and surfactant concentration) within the parameter space [23,24]. The results of the regressions between $1/k'$ *vs.* micelle concentration and ln k' *vs.* surfactant concentration are listed in Table 4 for the amino acids and small peptides. Acceptable linearity is observed for ln k' *vs.* surfactant concentration within the selected range (0.05–0.20 *M*). The experimental design for the optimization of the two important parameters, the concentration of surfactant (SDS) and the volume fraction of organic solvent (1-propanol), was based on only five initial experiments, four at the corners of a square and one at the center [23]. The corner values of the parameters are limited by the practical conditions of chromatographic systems. The lower surfactant concentration is chosen well above the critical micelle concentration of the surfactant (*ca.* 8 m*M* for SDS at ambient

Table 4
The comparison of regression

Components	$1/k'$ *vs.* [micelle]	r	$\ln k'$ *vs.* [surfactant]	r
AY	$1/k' = 4.739[M] + 0.223$	0.9977	$\ln k' = -6.423[SDS] + 1.126$	0.9976
DF	$1/k' = 2.719[M] + 0.172$	0.9999	$\ln k' = -5.902[SDS] + 1.510$	0.9909
LY	$1/k' = 2.655[M] + 0.135$	0.9988	$\ln k' = -6.474[SDS] + 1.689$	0.9843
M	$1/k' = 3.321[M] + 0.594$	0.9937	$\ln k' = -3.389[SDS] + 0.461$	0.9992
W	$1/k' = 2.997[M] + 0.210$	1.0000	$\ln k' = -5.641[SDS] + 1.339$	0.9933

Mobile phase compositions: SDS concentration range: 0.05–0.20 *M* and 15% 1-propanol. r = Correlation coefficient.

temperatures and without organic modifier) and can elute all the components. The upper surfactant concentration is controlled by a combination of some factors, such as the solubility of the surfactant in mobile phase, the viscosity of the resulting mobile phase and degradation of the efficiency at higher surfactant concentrations. The organic modifier concentration is limited to a maximum of *ca.* 15% to ensure the integrity of the micelles [23,24]. The retention of all the ten amino acids and small peptides were measured at these five mobile phase compositions. The optimum mobile phase composition of 14% 1-propanol and 0.05 *M* SDS was predicted by the IR program.

Excellent agreement exists between the predicted and the observed separation for these ten amino acids and small peptides as illustrated in Fig. 6. The plot of k' (observed) *vs.* k' (predicted) for these ten amino acids and small peptides is very good as shown in Fig. 7. Apparently, the assumed linear model of $\ln k'$ *vs.* the parameters is valid and retention behavior is reproducible. These results indicate that good separation of ionic solutes with a minimum experimental effort can be achieved in the FO-based MLC as well.

3.6. Stationary phase effect

Amino acids and small peptides (ionic compounds) and sulfonamides (non-ionic compounds at pH 3.0) were used as the test solutes to compare the stationary phase effects (FO *vs.* C_{18}) on retention, selectivity and the overall elution pattern.

The iterative regression optimization computer program [23,24] was used to optimize the separation of ten amino acids and small peptides on both the FO and C_{18} columns. The predicted optimized separations are illustrated in Fig. 8.

These ten amino acids and small peptides can be separated on a 15-cm FO column with the total analysis time of about 29 min. The same set of solutes could be separated on a 25-cm C_{18} column with the total analysis time of about 66.5

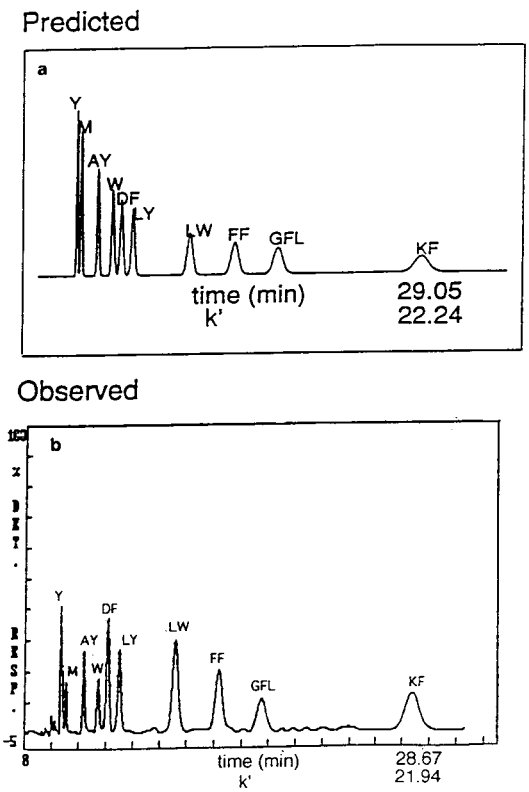

Fig. 6. The predicted (a) and observed (b) chromatograms of amino acids and peptides at the optimum mobile phase composition (0.05 *M* SDS + 14% 1-propanol) for ten amino acids and small peptides. FO column, 15 cm; pH 3.0.

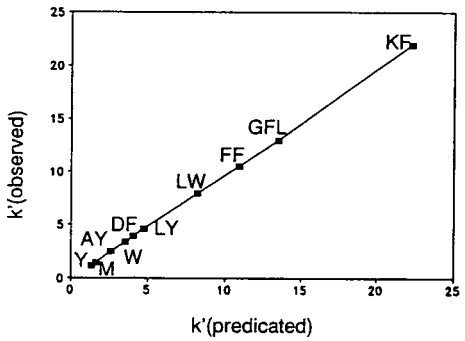

Fig. 7. The observed capacity factors *vs.* the predicted capacity factors for the ten amino acids and small peptides at the optimum mobile phase condition.

min. A shorter FO column (as compared to a C_{18} column) can be used to achieve the desired separation because of the higher efficiency gained from the faster mass transfer. Shortened analysis times are observed on the FO column due to both less interactions between fluorocarbon groups and the solutes and because of using a shorter column. Different elution orders (selectivity changes) of the solutes are observed on the FO column which indicates the different solute–stationary phase interactions. In addition, the differences in retention behavior could partly be attributed to the different mobile phase pH and organic modifiers.

To further confirm the stationary phase effect, the exact same mobile phase conditions were applied for the separation of sulfonamides on both FO and C_{18} columns. The reconstructed chromatograms of seven sulfonamides on a 15-cm FO column and a 15-cm C_{18} column are illustrated in Fig. 9 for both columns. Better separation was achieved on the FO column because of the increased retention and different selectivities for the early eluting peaks. The separations shown in Fig. 9 were obtained under non-optimized conditions using FO and C_{18} columns but were performed by using the same mobile phase composition. The same efficiency ($N = 3000$) was used to reconstruct the chromatograms for both FO and C_{18} columns; however, lower efficiency was observed on the C_{18}

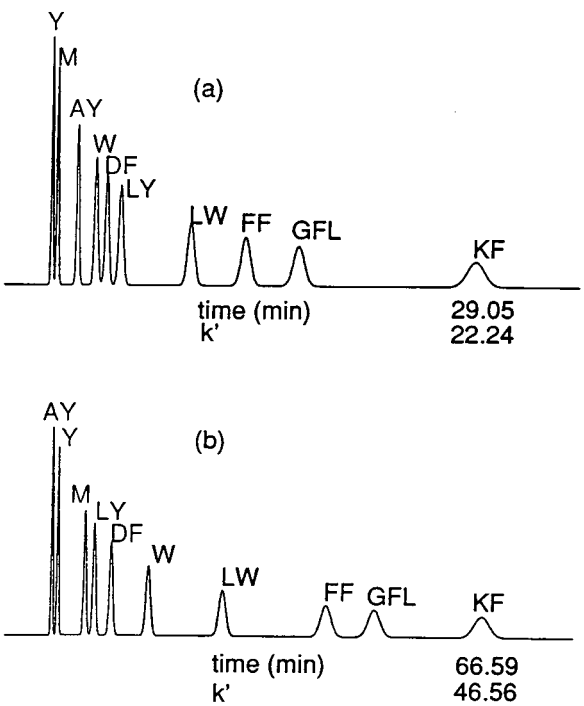

Fig. 8. The predicated optimized separation of ten amino acids and small peptides (a) 15-cm Flurooctyl column, 14% 1-propanol, 0.05 *M* SDS, pH 3.0; (b) 25-cm C_{18} column, 11% 2-propanol, 0.10 *M* SDS, pH 2.5.

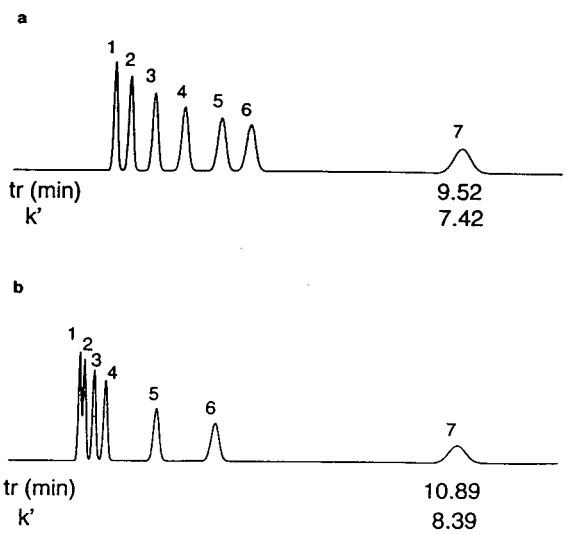

Fig. 9. The reconstructed chromatograms of seven sulfonamides based on the experimental retention data and $N = 3000$ at 0.1075 *M* SDS, 8% 1-propanol, pH 3.0 (a) 15-cm FO column, (b) 15-cm C_{18} column. Peaks: 1 = CTM; 2 = DIA; 3 = MRZ; 4 = MTZ; 5 = DMX; 6 = IMD; 7 = IPZ.

column (see Table 2). This means that a longer C_{18} column should be used to achieve the illustrated separation.

4. Conclusions

The possibility of using fluorinated bonded stationary phases in MLC was investigated. Higher efficiencies for both ionic and non-ionic compounds in MLC were obtained on the fluorinated bonded stationary phase probably because of the faster mass transfer. Shortened analysis times for hydrophobic compounds and increased retention for hydrophilic compounds were observed on a FO column. Better and faster separations can be obtained on the FO column for some compounds. In addition to the remedies that have already been suggested [11,13], the poor efficiency in MLC system might be improved by using stationary phases on which surfactant is less adsorbed. Stationary phase is a very important factor in MLC because it affects efficiency and overall separation. However, additional studies on the effect of stationary phase on efficiency and separation in MLC are needed.

5. Acknowledgement

This work was supported by a research grant from the U.S. National Institutes of Health (GM 38738).

6. References

[1] M.G. Khaledi, J.K. Strasters, A.H. Rodgers and E.D. Breyer, *Anal. Chem.*, 62 (1990) 130.
[2] A.S. Kord and M.G. Khaledi, *Anal. Chem.*, 64 (1992) 1894.
[3] A.S. Kord and M.G. Khaledi, *Anal. Chem.*, 64 (1992) 1901.
[4] D.W. Armstrong and S.J. Henry, *J. Liq. Chromatogr.*, 3 (1980) 657.
[5] L.J. Cline Love, J.G. Habarta and J.G. Dorsey, *Anal. Chem.*, 56 (1984) 1132A.
[6] D.W. Armstrong, *Sep. Purif. Methods*, 14 (1985) 213.
[7] J.G. Dorsey, *Adv. Chromatogr.*, 27 (1987) 167.
[8] W.L. Hinze, in W.L. Hinze and D.W. Armstrong (Editors), *Ordered Media in Chemical Separation (ACS Symposium Series*, No. 324), American Chemical Society, Washington, DC, 1987, Ch. 1, p. 2.
[9] M.G. Khaledi, *Trends Anal. Chem.*, 7 (1988) 293.
[10] M.G. Khaledi and E.D. Breyer, *Anal. Chem.*, 61 (1989) 1040.
[11] J.G. Dorsey, M. DeEchegaray, and J.S. Landy, *Anal. Chem.*, 55 (1983) 924.
[12] D.W. Armstrong, T, J. Ward and A, Berthod, *Anal. Chem.*, 58 (1986) 579.
[13] P. Yarmchuk, R. Weinberger, R.F. Hirsch and L.J. Cline Love, *J. Chromatogr.*, 283 (1984) 47
[14] A. Berthod, M.F. Borgerding and W.L. Hinze, *J. Chromatogr.*, 556 (1991) 263.
[15] H.A.H. Billiet, P.J. Schoenmakers and L. de Galan, *J. Chromatogr.*, 218 (1981) 443.
[16] P.J. Schoenmakers, H.A.H. Billiet and L. de Galan, *Chromatographia*, 15 (1982) 205.
[17] G.E. Berendsen, K.A. Pikaart and L. de Galan, *Anal. Chem.*, 52 (1980) 1990.
[18] P. Varughese, M.E. Gangoda and R.K. Gilpin, *J. Chromatogr. Sci.*, 26 (1988) 401.
[19] P.C. Sadek and P.W. Carr, *J. Chromatogr.*, 288 (1984) 25.
[20] N.D. Danielson, L.G. Beaver and J. Wangsa, *J. Chromatogr.*, 544 (1991) 187.
[21] G. Felix and C. Bertrand, *J. High Resolut. Chromatogr. Chromatogr. Commun.*, 8 (1985) 362.
[22] X. Geng and P.W. Carr, *J. Chromatogr.*, 269 (1983) 96.
[23] J.K. Strasters, E.M. Breyer, A.H. Rodgers and M.G. Khaledi, *J. Chromatogr.*, 511 (1990) 17.
[24] J.K. Strasters, S.-T. Kim and M.G. Khaledi, *J. Chromatogr.*, 586 (1991) 221.
[25] E. Grushka, H. Colin and G. Guiochon, *J. Chromatogr.*, 248 (1982) 325.
[26] H. Colin, G. Guiochon, Z. Yun, J.C. Diez-Masa and P. Jandera, *J. Chromatogr. Sci.*, 21 (1983) 179.
[27] M.G. Khaledi, E. Peuler and J. Ngeh-Ngwainhi, *Anal. Chem.*, 59 (1987) 2738.
[28] M.G. Khaledi, *Anal. Chem.*, 60 (1988) 876.
[29] J.P. Foley and J.G. Dorsey, *Anal. Chem.*, 55 (1983) 730.
[30] P.J. Schoenmakers, H.A.H. Billiet and L. de Galan, *J. Chromatogr.*, 185 (1979) 179.
[31] L.R. Snyder, *J. Chromatogr. Sci.*, 16 (1978) 223.
[32] L.R. Snyder and J.J. Kirkland, *Introduction to Modern Liquid Chromatography*, Wiley, New York, 2nd ed., 1979, p. 260.
[33] S.C. Rutan, P.W. Carr, W.J. Cheong, J.H. Park and L.R. Snyder, *J. Chromatogr.*, 463 (1989) 21.
[34] J.L. Glajch, J.J. Kirkland, K.M. Squire and J.M. Minor, *J. Chromatogr.*, 199 (1980) 57.
[35] R.M. Smith, *J. Chromatogr.*, 324 (1985) 243.
[36] A.S. Kord and M.G. Khaledi, *J. Chromatogr.*, 631 (1993) 125.

ELSEVIER

Journal of Chromatography A, 664 (1994) 13–25

JOURNAL OF CHROMATOGRAPHY A

Immobilized metal affinity membrane adsorbers as stationary phases for metal interaction protein separation

Oscar-Werner Reif[a], Volker Nier[a], Ute Bahr[b], Ruth Freitag*[,a]

[a]*Institut für Technische Chemie, Universität Hannover, Callinstrasse 3, 30167 Hannover, Germany*

[b]*Institut für medizinische Physik und Biophysik, Universität Münster, Robert-Koch Strasse 31, 48149 Münster, Germany*

(First received August 25th, 1993; revised manuscript received November 18th, 1993)

Abstract

Novel immobilized metal affinity membrane adsorbers (IMA-MA) were studied for potential use as stationary phases for protein separation. Protein adsorption on IMA-MA loaded with Cu(II), Ni(II), Zn(II) and Co(II) ions was compared as a function of the flow-rate and the ionic strength of the elution buffer. To exclude the possibility of mixed-mode interaction in the experiments, the binding of proteins similar in terms of hydrophobicity, isoelectric point, size and mass-to-charge ratio but differing in their number of surface histidine residues was investigated. Matrix-assisted laser desorption/ionization mass spectrometry was used to distinguish between these proteins in the eluted fractions. Salt concentration of at least 0.5 *M* NaCl and flow-rates below 2 ml min^{-1} were found suitable to ensure an adsorption mechanism based on affinity interaction between the proteins and the chelated metal ions. In an application study, the IMA-MA and conventional chelating Sepharose fast flow columns were compared for the isolation of a recombinant fusion protein (EcoR V), which carried a polyhistidine sequence (HIS_6-tag) at the N-terminus.

1. Introduction

Immobilized metal affinity chromatography (IMAC) is a sensitive method for protein separation, which allows one to distinguish between proteins differing only by a single histidine residue on their respective surfaces [1]. Starting in 1975, when Porath *et al.* [2] first extended the concept of ligand-exchange chromatography, introduced more than a decade before by Helfferich [3], to the separation of biomolecules, IMAC has been used to separate complex protein mixtures [4–7] and to investigate the surface topography of their histidine residues [8,9]. Moreover, recent advances in genetic engineering may prove to be a great incentive towards the development of efficient IMAC techniques [10–13]. It has become possible to fuse an affinity tag to either terminus of a recombinant protein, and this has been shown to facilitate protein purification considerably. While larger tags such as protein A or glutathione-S-transferase have to be cleaved off to obtain the active and stable protein, a small polyhistidine sequence at the N-terminus of a recombinant protein serves to enhance the affinity of the fusion protein to IMAC phases to a high degree without influencing the protein's integrity and activity overmuch [14,15].

IMAC is based on the interaction of a Lewis acid (electron pair donor), *i.e.*, a chelated metal ion, with an electron acceptor group on the

* Corresponding author.

0021-9673/94/$07.00
SSDI 0021-9673(93)E1261-W

surface of the protein. Save for some exceptions, such as the well documented affinity of certain phosphoproteins for Fe(III) ions [16], proteins are assumed to interact mainly through their histidine and, to a lesser extent, their tryptophan residues with the immobilized metal ions. Nitrogen as a Lewis base of intermediate hardness should interact best with Lewis acids of similar polarizability, such as Cu(II), Zn(II), Ni(II) or Co(II). Such ions can be fixed to a chromatographic support through chelating agents such as the terdentate ligand iminodiacetic acid (IDA). The nature of the chelating agent is of great importance. If a large number of the coordination sites of the metal ion are involved, the ion is stably immobilized and bleeding becomes less likely. The affinity to proteins is, however, decreased. Elution in IMAC involves most commonly the lowering of the pH of the mobile phase below 6, which causes protonation of the side-chains of most histidine residues. Competitive elution in a gradient of increasing histidine, glycine or imidazole concentration, elution in a salt or organic modifier gradient and elution of the protein–metal ion complexes with EDTA have also been described.

Compared with other chromatographic methods based on affinity interactions, IMAC is taken to be superior in terms of ligand stability, capacity, recovery of active protein and cost. Columns can be repeatedly stripped and reloaded with metal ions. Compared with other liquid chromatographic (LC) methods, however, examples of practical applications have been few in IMAC. One reason may be the limited theoretical basis currently available for the design of the chromatographic experiment, and another the paucity of available stationary phases for IMAC, compared with, *e.g.*, ion-exchange or reversed-phase chromatography. Traditionally, soft and semi-rigid polysaccharide-based stationary phases carrying IDA chelating groups are used in IMAC. In addition, a few silica- and polymer-based carriers suitable for HPLC applications are available [6,17–20]. The aim of the work described in this paper was to investigate the potential of a new type of stationary phase, namely membrane adsorbers (MA) carrying IDA groups, for protein separation.

2. Experimental

2.1. Chemicals

Proteins were of analytical-reagent grade or better and were purchased from Sigma. Bulk chemicals were obtained from Fluka. Buffer and sample solutions were prepared with deionized water and prefiltered through a 0.2-μm membrane (Sartorius, Göttingen, Germany).

2.2. Stationary phases

Immobilized metal affinity membrane adsorbers (IMA-MA) were obtained from Sartorius. The membranes themselves consisted of a hydrophilic copolymer carrying chelating IDA groups. They are between 170 and 190 μm thick, have an average pore size of 0.45 μm and are stable in the pH range 2–13. Two types of ready-to-use IMA-MA units were available. In the first option, a single membrane with a cross-sectional area of 5.4 cm^2 was encased in a suitable filter holder; in the second option, a stack of five membranes each with a cross-sectional area of 20 cm^2, *i.e.*, a total filtration area of 100 cm^2, was placed in a larger filter holder. The maximum operating pressures of the units were 400 and 700 kPa, respectively. Both filter holders were equipped with male and female Luer lock connectors for easy insertion into the chromatographic systems. New IMA-MA were stored dry at room temperature. Between use the IMA-MA were kept in the appropriate equilibration buffer with 0.001 *M* NaN_3 added as a bacteriostatic agent. For the preparation of the active IMA-MA, 20 ml of a 0.5 *M* solution of the sulphate salt of the metal ion to be immobilized were passed through the unit at a flow-rate of 1 ml min^{-1}. The respective equilibration buffers were used to prepare the loading solution. Prior to the loading step the IMA-MA were washed with pure equilibration buffer. If a decrease in capacity was observed during the experiments, the IMA-MA were stripped of all metal ions by washing with 10 ml of 0.5 *M* EDTA solution at a flow-rate of 1 ml min^{-1}. Reloading was carried out after excessive washing with equilibration buffer as described above.

Chelating Sepharose fast flow (Pharmacia, Uppsala, Sweden) was used to slurry pack IMAC columns (1 cm I.D., various lengths). Three column volumes of water were pumped through followed by 30 ml of 0.1 *M* $NiSO_4$ or $CuSO_4$ solution at a flow-rate of 1 ml min^{-1}. Subsequently the column was flushed with 120 ml of water. The column was equilibrated with three column volumes of the initial buffer before sample injection and washed with methanol–water (1:5, v/v) after use.

2.3. Instrumentation

For the experiments concerning the purification of recombinant EcoR V, the IMA-MA and the chelating Sepharose fast flow columns were integrated into a fast protein liquid chromatographic (FPLC) system (Pharmacia), which consisted of two P 500 pumps, a Model 2141 UV detector, a Superrac fraction collector and an MV7 injection valve. All components were controlled by an LCC 500 unit. Data analysis was carried out using conventional FPLC software. All other experiments were carried out using an HPLC system assembled from a Model 64 pump (Knauer, Berlin, Germany) which allowed flow-rates up to 40 ml min^{-1}, an injection valve (Valco, Houston, TX, USA) and a Model 7215 UV–Vis detector (ERMA, Tokyo, Japan). The gradient was controlled by an Autochrom System 300 and an Autochrom valve box (obtained from ERC, Regensburg, Germany). An SP 4290 integrator (Spectra-Physics, San Jose, CA, USA) and an R4 integrator (Shimadzu, Kyoto, Japan) were used for collection and analysis of the chromatographic data. Protein fractions were collected using a Retriever 500 (ISCO, Lincoln, NE, USA).

2.4. Methods

Protein concentrations were established according to Bradford [21] or Lowry *et al.* [22] using bovine serum albumin (BSA) as a standard protein. Concentrations of metal ions in solution were established by titration with 0.1 *M* EDTA against murexide as indicator [23]. Sodium dodecyl sulphate polyacrylamide gel electrophoresis (SDS-PAGE) was carried out according to Laemmli [24] using a laboratory-made apparatus. The activity of EcoR V was determined as follows. EcoR V splits λ-DNA into 22 fragments [25], which can be separated on agarose slab gels and quantified after staining with ethidium bromide [26]; 1 U of the restriction enzyme will split 1 μg of λ DNA within 1 h at 37°C.

To determine the protein-binding capacity of the IMA-MA, human serum albumin (HSA, 0.5 mg ml^{-1}) was loaded on to the metal ion-saturated IMA-MA at a flow-rate of 1 ml min^{-1} until saturation was reached, *i.e.*, until the protein concentration in the eluate was constant again. After washing, the retained protein was eluted and quantified. A 0.025 *M* phosphate buffer (pH 8.0) containing 0.5 *M* NaCl was used for loading and washing. For elution a 0.025 *M* acetate buffer (pH 3.5) containing 0.5 *M* NaCl was used. All chromatographic experiments were repeated three times. The capacity of a given stationary phase for metal ions was established by pumping 0.1 *M* $NiSO_4$ or $CuSO_4$ solution through the unit (flow-rate 1 ml min^{-1}) until saturation. By monitoring the metal ion concentration in the eluate using the methods described above, the amount of metal ions retained on the chromatographic support could be calculated. The larger IMA-MA were used in the capacity measurements. Capacities were calculated as μmol cm^{-2} and mg cm^{-2} for metal ions and proteins, respectively, by dividing the total amount retained on the IMA-MA by the cross-sectional area (20 cm^2).

For matrix-assisted laser ionization/desorption mass spectrometry (MALDI-MS) measurements, a Vision 2000 laser time-of-flight mass spectrometer (Finnigan MAT, Bremen, Germany) was used. Samples were dissolved in acetonitrile–water containing 0.1% trifluoroacetic acid (1:2 v/v) at a concentration of *ca.* 1 mg ml^{-1}. A 10 g l^{-1} solution of 2,5-dihydroxybenzoic acid in the same solvent was used as a matrix. For measurements, 1 μl of sample and 1 μl of matrix were mixed on a metal target and allowed to dry.

2.5. Bacterial culture

Escherichia coli LK 111 λ/pLBM/pUHE/His Th RV (2) was used as the expression system. The strain produces the restriction endonuclease EcoR V with the chelating peptide (CP) His_6 at the N-terminus. Expression is controlled by the lac-promotor. The strain is resistant to the antibiotics ampicillin and chloramphenicol. Strain maintenance was done on agar plates using LB medium (10 g l^{-1} casein peptone, 10 g l^{-1} NaCl, 5 g l^{-1} yeast extract) with an ampicillin concentration of 75 μg ml^{-1} and a chloramphenicol concentration of 30 μg ml^{-1}. *E. coli* cultures were performed in shaking flasks filled with 200 ml of LB medium with similar antibiotic concentrations added. After inoculation, the culture was left to grow overnight at 30°C. Production of EcoR V was induced by the addition of isopropyl β-D-thiogalactopyranoside (IPTG) at concentrations between 0.2 and 2 m*M*. After 2–3 h the bacteria were centrifuged off at 3000 *g* (4°C) and stored at −20°C. Cell lysis was achieved by sonication (5 min, 100 W, 0°C). Subsequently the cell debris was removed by centrifugation at 35 000 *g* (4°C). The supernatant was filtered through a 0.2-μm membrane (Sartorius).

3. Results and discussion

3.1. Characterization of immobilized metal affinity membrane adsorbers

For assessment of the general suitability of the IMA-MA as stationary phases for protein IMAC, the capacities of the IMA-MA for metal ions and proteins were determined. In Table 1 the capacities for Cu(II) and Ni(II) ions, *i.e.*, the two most commonly used ions in IMAC, are compiled, together with the protein capacities established for IMA-MA saturated with the respective metal ions, taking HSA as a probe. The metal ion capacity of the IMA-MA is higher for Cu(II) than for Ni(II). At the same time, more HSA is bound per μmole of immobilized Cu(II) than per μmole of immobilized Ni(II). In all instances capacities found for the 20 cm^2 IMA-MA were sufficiently high for the semi-preparative tasks required in our laboratory. When HSA was repeatedly adsorbed on the IMA-MA and eluted in a pH gradient (pH 8.0–3.5) at a flow-rate of 1 ml min^{-1}, a decrease in capacity was observed after five cycles. After 25 cycles, the capacity had decreased by *ca.* 10%. The effect was seen for both the Cu(II)–IMA-MA and the Ni(II)–IMA-MA systems. In order to prevent the capacity decrease from biasing the experiments, all metal ions were removed from the IMA-MA with an EDTA wash after five chromatographic experiments and the MA reloaded with fresh metal ions during the investigations described below. Under these circumstances, an IMA-MA could be used for several hundred experiments without a decline in performance. The protein recovery was well over 90% and no evidence of unspecific or irreversible protein binding was found.

3.2. Influence of the chelated metal on protein separation

Cu(II), Ni(II), Zn(II) and Co(II) are the most commonly used metal ions in protein IMAC. In order to investigate the influence of the metal ion species on the protein separation power of the IMA-MA, a mixture of proteins that differ in

Table 1
Capacities of the IMA-MA for Cu(II) and Ni(II) ions and capacities of the saturated supports for human serum albumin (HSA)

Species	IMA-MA	Cu(II)–IMA-MA	Ni(II)–IMA-MA
Ni(II)	59.25 μmol cm^{-2}		
Cu(II)	65.75 μmol cm^{-2}		
HSA		1.13 mg cm^{-2}	0.81 mg cm^{-2}

the number of their surface histidine residues (HIS) had to be designed. Cytochrome *c* from tuna heart (t-Cyt *c*, no HIS), cytochrome *c* from horse heart (e-Cyt *c*, 1 HIS) and dog myoglobin (d-Myo, 2 HIS) were chosen. The 20 cm^2 IMA-MA units were used for these investigations. Proteins are most commonly eluted from IMAC phases by protonation of the histidine residues, *i.e.*, by lowering the pH of the eluent to <6. As metal ions are substantially washed out from the chelating phase if the pH is lowered too much, pH gradients were only applied down to a value of 4 in our experiments. Proteins that did not elute under these conditions were eluted in an imidazole gradient, *i.e.*, through the introduction of a competing electron donor. A 5-ml volume of a sample containing a total of 3.5 mg of each cytochrome species and 1.5 mg of d-Myo was loaded on to the IMA-MA at pH 7 and eluted at a flow-rate of 0.5 ml min^{-1} in a two-step gradient of decreasing pH (first step) and increasing imidazole concentration (second step). Fractions of 1 ml were collected and the protein content was determined. On the Cu(II)–IMA-MA only t-Cyt *c*, *i.e.*, the protein without surface histidine residues, appears in the breakthrough, whereas e-Cyt *c* and d-Myo are retained and well separated (Fig. 1a). This corresponds to results published in the literature, where one HIS residue is usually reported as sufficient for the retention on a Cu(II)–IMAC column, and proteins varying by only one HIS residue can be

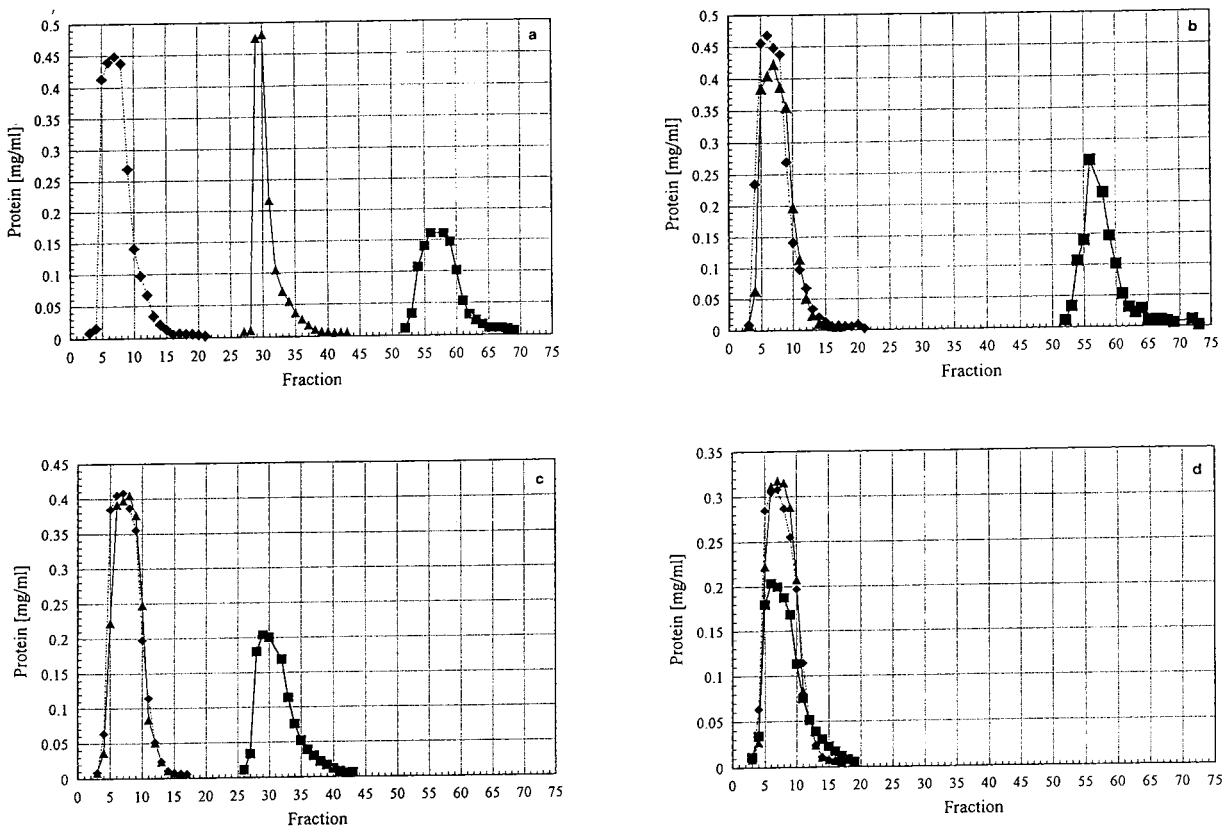

Fig. 1. Separation of proteins on IMA-MA with different chelated metal ions: (a) Cu(II); (b) Ni(II); (c) Zn(II); (d) Co(II). IMA-MA size: 20 cm^2. Buffer A = 0.02 *M* phosphate–0.75 *M* NaCl (pH 7.0); buffer B = 0.05 *M* acetate–0.75 *M* NaCl (pH 4.0); buffer C = 0.05 *M* acetate–0.75 *M* NaCl–0.1 *M* imidazole (pH 4.2). Sample: e-Cyt *c* 3.5 mg, t-Cyt *c* 3.5 mg, d-Myo 1.5 mg. Gradient: fractions 0–24 buffer A, fractions 24–49 buffer B, fractions 49–75 buffer C. Flow-rate: 0.5 ml min^{-1}. Sample volume: 5 ml. ◆ = t-Cyt *c*; ▲ = e-Cyt *c*; ■ = d-Myo.

separated [9,27,28]. Whereas e-Cyt *c* is eluted in the pH-step, d-Myo is desorbed only by introducing the competing electron donor imidazole. On the Ni(II)– (Fig. 1b) and Zn(II)–IMA-MA (Fig. 1c) the two cytochromes appear together in the breakthrough, whereas d-Myo is retained in both instances. However, whereas the elution of d-Myo from the Ni(II)–IMA-MA requires conditions similar to those for its elution from Cu(II) phases, *i.e.*, an imidazole gradient, a simple pH decrease will elute the protein from the Zn(II) phase. A higher affinity of the d-Myo to the Ni(II)– than to the Zn(II)–IMA-MA can thus be assumed. None of the test proteins were retained on the Co(II)–IMA-MA (Fig. 1d). On the whole, the retention behaviour of the test proteins on the IMA-MA mirrors that established for conventional IMAC phases, where the affinity of most proteins towards the immobilized metals follows the order Cu(II) > Ni(II) > Zn(II) > Co(II). Only the fact that not even d-Myo was retained on the Co(II)–IMA-MA is surprising, as proteins with two HIS residues are usually reported to show some affinity to Co(II)-saturated IMAC phases [8].

Some workers, *e.g.*, Sulkowski [8], recommend the addition of 1 m*M* imidazole to the equilibration buffer, especially if an imidazole gradient is to be used for elution in IMAC, as a beneficial influence on the separation efficiency is often observed. In order to establish how such an addition influences the performance of the IMA-MA, t-Cyt *c* and e-Cyt *c* were separated in a pH gradient on a Cu(II)–IMA-MA in the presence of 1 m*M* imidazole in both the equilibration and the elution buffer (Fig. 2). Under these conditions neither t-Cyt *c* nor e-Cyt *c* is retained on the IMA-MA, even though the latter protein had been retained well on the same stationary phase in the absence of imidazole. Apparently, the affinity of e-Cyt *c* for the Cu(II)–IMA-MA is reduced sufficiently to prevent retention in the presence of imidazole.

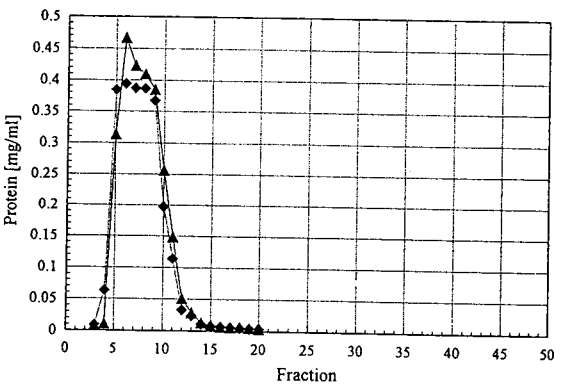

Fig. 2. Separation of proteins on Cu(II)–IMA-MA in the presence of imidazole. IMA-MA size: 20 cm^2. Buffer A = 0.02 *M* phosphate–0.75 *M* NaCl (pH 7.0)–1 m*M* imidazole; buffer B = 0.05 *M* acetate–0.75 *M* NaCl (pH 3.9)–1 m*M* imidazole. Sample: t-Cyt *c* 3.5 mg, e-Cyt *c* 3.5 mg. Gradient: fractions 0–24 buffer A, fractions 24–50 buffer B. Flow-rate: 0.5 ml min^{-1}. Sample volume: 5 ml. ◆ = t-Cyt *c*; ▲ = e-Cyt *c*.

3.3. *Influence of flow-rate of elution buffer on protein separation*

MA phases have no interparticular void volume. Concomitantly, mass transport through the pores is convective. As a consequence, adsorption equilibria are generally reached quickly and high volumetric flow-rates can be used without impairing the separation efficiency [29]. In addition, MA can be used at higher volumetric flow-rates than conventional LC and HPLC columns, owing to their negligible flow resistance. Fast separations therefore become possible, often cited as a major advantage of MA phases over conventional chromatographic supports. The effect of the volumetric flow-rate on the sample distribution over an MA has already been investigated using a strong ion exchanger MA of a geometric design similar to that of the IMA-MA used in these investigations [29]. The feasibility of using flow-rates of 60 ml min^{-1} and more has been established for protein separations on these ion exchanger MA. The general possibility of fast protein separation as a result of an interaction with immobilized metal ions, on the other hand, has already been suggested by Bonn *et al.* [30], who demonstrated the superiority of micropellicular, *i.e.*, non-porous, supports over conventional porous stationary phases in this respect. The fastest volumetric flow-rates applied in that case were 2 ml min^{-1}. El Rassi and Horvath [6] found the efficiency of chelated metal phases to be lower than expected, which

they ascribed to the slow interaction kinetics of the affinity-based adsorptive reaction. Such slow interaction kinetics, however, should limit the maximum applicable flow-rate. A study of the influence of the elution buffer flow-rate on protein separation on the IMA-MA was therefore considered necessary.

A mixture of 0.1 mg each of α-chymotrypsinogen, β-lactoglobulin and lysozyme in 0.02 *M* phosphate buffer (pH 6) was separated in a two-step NaCl gradient (0–0.5 *M* NaCl) on a Ni(II)–IMA-MA at various flow-rates; the 5.4-cm^2 units were used. Protein fractions were collected and analysed by SDS-PAGE. β-Lactoglobulin was not retained under these conditions, α-chymotrypsinogen was eluted in the first salt step (*ca.* 20% B) and lysozyme in the second step, *i.e.*, at 100% B. Fig. 3 shows that an efficient separation could be achieved even at flow-rates of 35 ml min^{-1}, thus decreasing the time required for complete separation to less than 2 min. According to these results, the flow-rate of the elution buffer does not present a limiting factor on the efficiency of protein separations on the IMA-MA. This finding was surprising and considered to require further investigation. Mixed-mode retentions, where the metal–chelate affinity interaction is, *e.g.*, overlaid with a hydrophobic or ion-exchange interaction, are possible with the supports used in protein IMAC. The low salt concentration of the loading buffer used in the experiment above may conceivably have furthered such an ion-exchange interaction. Taking the isoelectric points of the proteins into account, a chromatogram similar to that depicted in Fig. 3 would also ensue if the separation had been carried out on a cation exchanger MA. Moreover, such a separation should indeed be independent of the mobile phase flow-rate in the range examined, as we have recently been able to demonstrate [29].

To investigate this further, e-Cyt *c* and d-Myo were separated at various flow-rates in the presence of at least 0.75 *M* NaCl in the equilibration and the elution buffer, on both Cu(II)– and Ni(II)–IMA-MA. As before, a two-step pH and imidazole gradient was used for elution. At a flow-rate of 1 ml min^{-1} a chromatogram similar

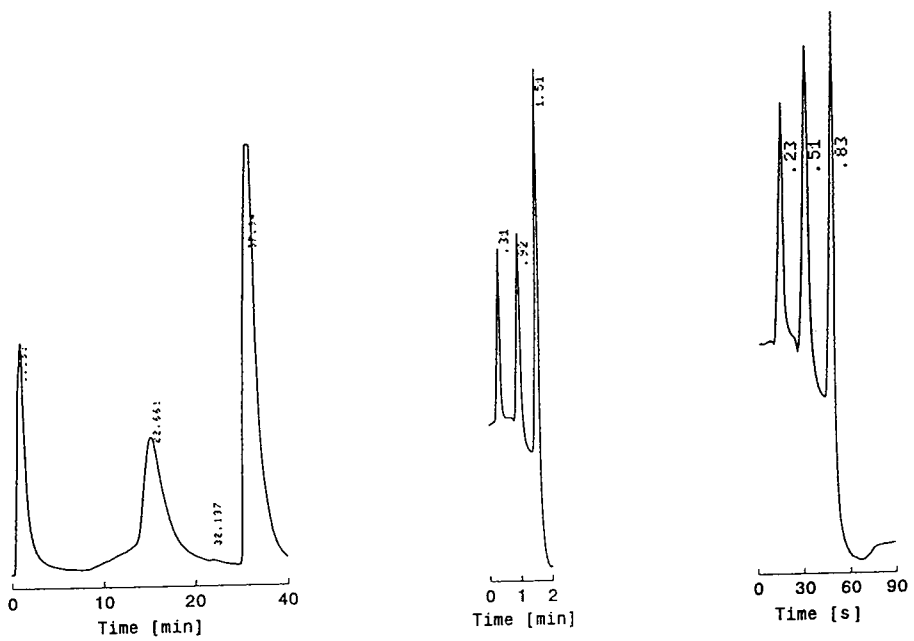

Fig. 3. Separation of β-lactoglobulin, α-chymotrypsinogen and lysozyme on a Cu(II)–IMA-MA as a function of flow-rate. Flow-rate: (a) 1, (b) 15 and (c) 35 ml min^{-1}. IMA-MA size: 5.4 cm^2. Buffer A = 0.02 *M* phosphate (pH 6.0); buffer B = 0.02 *M* phosphate–0.5 *M* NaCl (pH 6.0). Sample: 0.1 mg β-lactoglobulin, 0.1 mg α-chymotrypsinogen, 0.1 mg lysozyme; sample volume, 1 ml. Gradient: step 1, 0% B; step 2, 20% B, step 3, 100% B.

to that shown in Fig. 1a was obtained for the Cu(II)–IMA-MA (Fig. 4a). Whereas a small amount of both proteins appears in the breakthrough, the major part of the e-Cyt *c* is eluted by the pH shift and the major part of the d-Myo by the imidazole step. At 2.5 ml min^{-1} the protein concentration in the breakthrough is much higher than at 1 ml min^{-1} (Fig. 4b). Analysis of the peak fractions by SDS-PAGE revealed that fractions 25–40 contain both e-Cyt *c* and d-Myo. Apparently some d-Myo is already eluted by the pH shift under these conditions. At a flow-rate of 5 ml min^{-1} only d-Myo is retained at all on the IMA-MA (Fig. 4c). However, this protein is now split into two equally sized portions, one of which is eluted by the pH shift (fractions 25–40) and the other by the imidazole step (fractions 52–70). Similar results were obtained when e-Cyt *c* and d-Myo were separated on a Ni(II)–IMA-MA, using a step gradient from 0.02 *M* phosphate buffer (pH 7.0) containing 0.75 *M* NaCl to 0.04 *M* acetate buffer (pH 4.0) containing 0.8 *M* NaCl and 0.1 *M* imidazole. The two proteins were separated well at a flow-rate of 1 ml min^{-1}. At a flow-rate of 2.5 ml min^{-1} only a fraction of the d-Myo was retained, while most of the d-Myo broke through with the e-Cyt *c*.

From the data presented, it can be deduced that the efficiency of some protein separations on the IMA-MA decreases rapidly with increasing flow-rate of the elution buffer, whereas other protein mixtures separate almost independently of this parameter. So far the reason for this difference can only be speculated upon. The salt concentration used in the separations of e-Cyt *c* and d-Myo may have been sufficiently high to suppress an ion-exchange interaction, whereas such an effect may have been operative in the separation of β-lactoglobulin, α-chymotrypsinogen and lysozyme. A definite statement concerning the flow-rate dependence of metal–chelate affinity interaction chromatography would require the study of the separation of two proteins that vary in the number of surface histidine residues, but only insignificantly in their isoelectric point, their hydrophobicity, their ternary structure or their size, as a function of flow-rate.

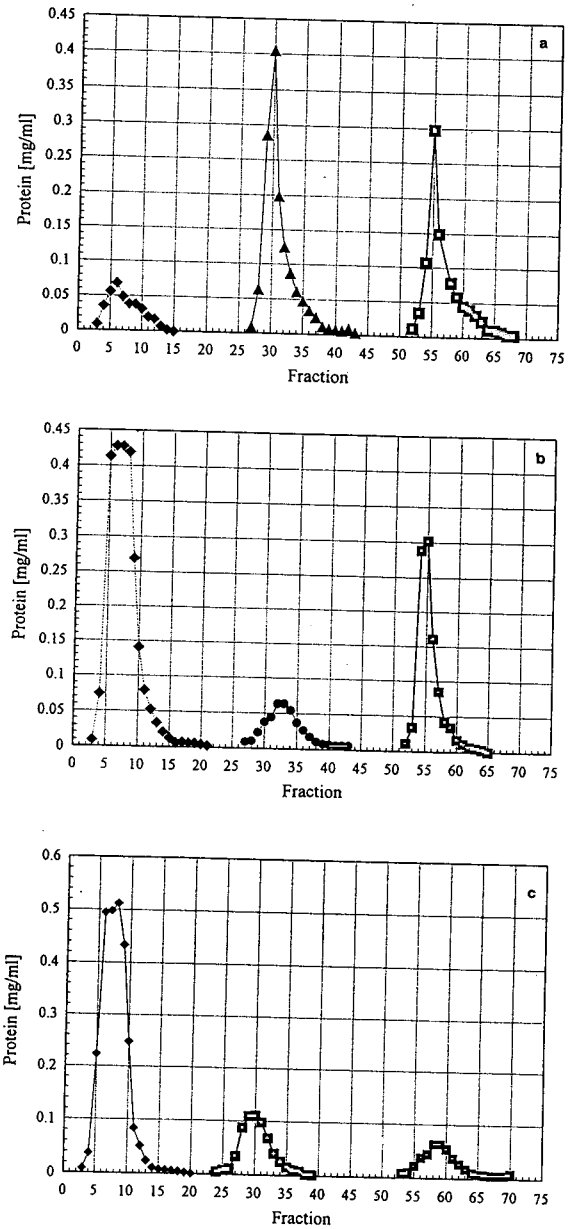

Fig. 4. Separation of e-Cyt *c* and d-Myo on a Cu(II)–IMA-MA as a function of flow-rate. Flow-rate: (a) 1, (b) 2.5 and (c) 5 ml min^{-1}. IMA-MA size: 20 cm^2. Buffer A = 0.02 *M* phosphate–0.75 *M* NaCl (pH 7.0); buffer B = 0.04 *M* acetate–0.8 *M* NaCl (pH 4.5); buffer C = 0.04 *M* acetate–0.8 *M* NaCl–0.1 *M* imidazole (pH 4.0). Gradient: fractions 0–24 buffer A, fractions 24–49 buffer B, fractions 49–75 buffer C. Sample: e-Cyt *c* 3 mg, d-Myo 2.5 mg; sample volume 5 ml. ◆ = Breakthrough; ▲ = e-Cyt *c*; □ = d-Myo; ○ = e-Cyt *c* and d-Myo.

t-Cyt *c* and e-Cyt *c* are two proteins that resemble each other strongly but differ in the number of their surface histidine residues, as pointed out before. Owing to their similarity, however, the determination of the individual concentrations of these two proteins in the collected protein fractions by conventional, *i.e.*, chromatographic or electrophoretic, methods would be difficult. Here recent progress in mass spectrometry becomes significant. New soft-ionization methods allow the ionization and measurement of sensitive proteins *in toto*. As the molecular masses of t-Cyt *c* and e-Cyt *c* differ by about 100 u, the analysis of the fraction composition by MALDI-MS is possible. Thus, the separation of t-Cyt *c* and e-Cyt *c* on a Cu(II)–IMA-MA with a pH step gradient as a function of flow-rate was investigated and MALDI-MS was used to analyse each peak composition.

At a flow-rate of 1 ml min^{-1} two protein peaks were collected, one in the breakthrough and the other during the pH gradient. According to the MALDI mass spectra, only t-Cyt *c* is found in the breakthrough fractions (Fig. 5a), e-Cyt *c* being retained on the IMA-MA (Fig. 5b). If the flow-rate is raised to 2.5 ml min^{-1}, again two protein peaks are observed in the chromatograms. However, a mixture of t-Cyt *c* and e-Cyt *c* is now found in the breakthrough, according to the MALDI mass spectrum (Fig. 5c). Still, significant amounts of e-Cyt-*c* are retained on the IMA-MA and eluted by the pH step. The trend becomes more pronounced if the flow-rate is raised to 5 ml min^{-1}. Under these circumstances, only a small portion of the e-Cyt *c* is retained on the IMA-MA at all, while most of this protein co-elutes with the t-Cyt *c* in the breakthrough. It must therefore be assumed that the flow-rate limit for protein separation on IMA-MA phases is indeed considerably lower than that determined for MA used as stationary phases in other, less specific, chromatographic techniques.

3.4. *Influence of ionic strength of elution buffer*

Ion exchange-based interactions seem to be of consequence in protein separations on IMA-MA

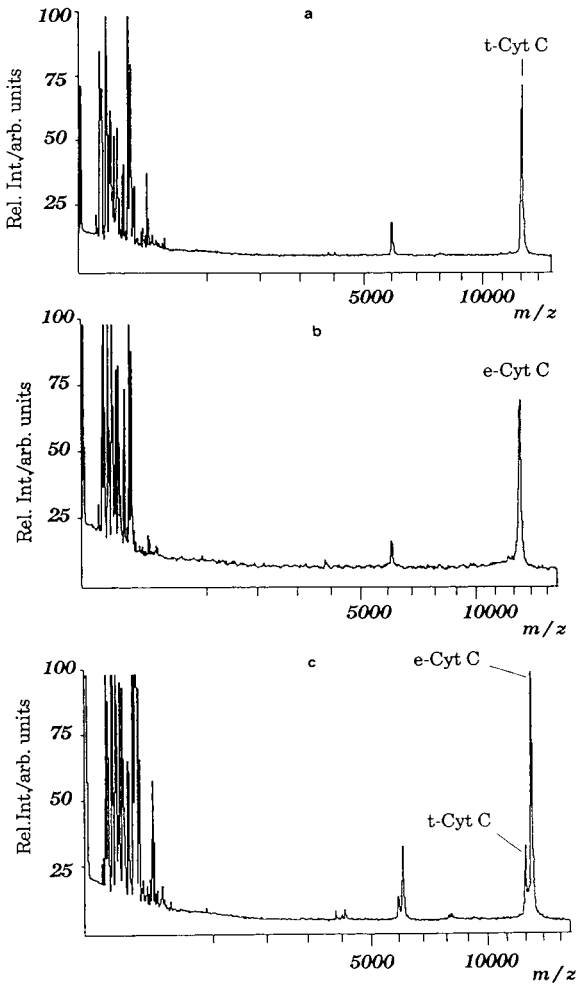

Fig. 5. (a) Mass spectrum of the protein-containing fractions of the breakthrough collected during the separation of t-Cyt *c* and e-Cyt *c* on a Cu(II)–IMA-MA at a flow rate of 1 ml min^{-1}. The singly and doubly charged molecules of t-Cyt *c* are detected. IMA-MA size: 20 cm^2. Buffer A = 0.02 *M* phosphate–0.75 *M* NaCl (pH 7.0); buffer B = 0.05 *M* acetate–0.75 *M* NaCl (pH 4.2). Gradient: fractions 0–24 buffer A, fractions 24–50 buffer B. Sample: 3-Cyt *c* 2.5 mg, t-Cyt *c* 3.5 mg; sample volume, 5 ml. (b) Mass spectrum of the protein-containing fractions eluted by the pH gradient during the separation of t-Cyt *c* and e-Cyt *c* on a Cu(II)–IMA-MA at a flow-rate of 1 ml min^{-1}. The singly, doubly and triply charged molecules of e-Cyt *c* are detected. Separation conditions as in (a). (c) Mass spectrum of the protein-containing fractions of the breakthrough collected during the separation of t-Cyt *c* and e-Cyt *c* on a Cu(II)–IMA-MA at a flow-rate of 2.5 ml min^{-1}. The singly, doubly and triply charged molecules of t-Cyt *c* and e-Cyt *c* are detected. Separation conditions as in (a).

phases. The influence of the ionic strength of the elution buffer therefore had to be investigated. A high salt concentration should suppress the ion exchange mechanism by shielding charges present on either the proteins or the support. However, at too high a salt concentration, hydrophobic interactions between the proteins and the support may occur [6,7]. For the purpose of these investigations t-Cyt *c* and e-Cyt *c* were separated on Cu(II)–IMA-MA in a pH step gradient. Various amounts of NaCl were added to the buffers. The composition of each protein peak was again analysed using MALDI-MS. If a minimum of 0.5 *M* NaCl was added, t-Cyt *c* and e-Cyt *c* were well separated (Fig. 6a). As their average hydrophobicities, isoelectric points and surface charge distributions are nearly identical, the separation can safely be attributed to differences in their affinity to the chelated Cu(II) ions. When the NaCl concentration of the buffers was lowered to 0.1 *M* the chromatogram depicted in Fig. 6b ensued. Again, two separate peaks are present. However, according to the MALDI-MS measurements, neither peak consists of a pure protein. In fact, there seems to be no difference in the retention behaviour of the two cytochrome *c* species under these conditions, which strongly argues for an ionic interaction between the proteins and the stationary phase, rather than an interaction based on the affinity for the chelated metal ions. A similar picture emerged when no NaCl was added to the buffer (Fig. 6c). The major portion of both the t-Cyt *c* and the e-Cyt *c* was retained on the stationary phase, presumably owing to an ion-exchange mechanism, and eluted in the pH gradient. According to the MALDI-MS measurements, no separation takes place between the proteins and their elution profiles are identical.

3.5. Application of IMA-MA to the purification of $(HIS)_6$-tagged EcoR V

The isolation of recombinant proteins that carry a polyhistidine tag is currently perhaps the most promising application of IMAC. Even trace amounts of tagged proteins can be removed from complex cell lysates in a single-step operation. As an example of a successful application of the

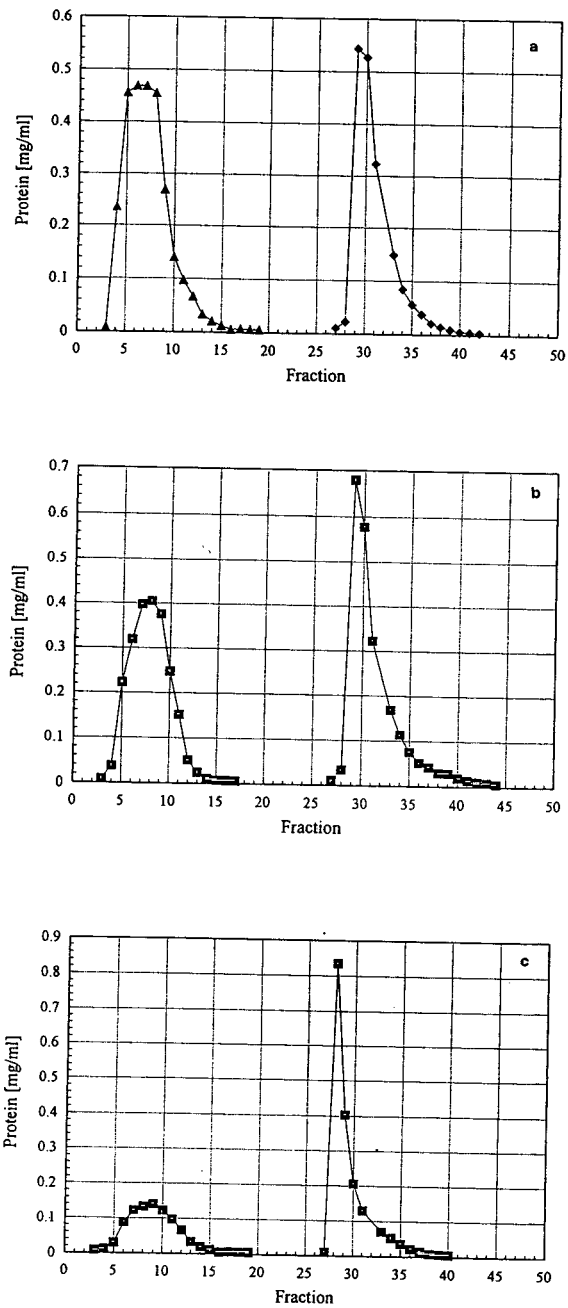

Fig. 6. Separation of e-Cyt *c* and t-Cyt *c* on a Cu(II)–IMA-MA with different NaCl concentrations in the buffer: (a) 0.5, (b) 0.1 and (c) 0 *M* NaCl in buffers A and B. IMA-MA size: 20 cm^2. Buffer A = 0.025 *M* phosphate (pH 7.0); buffer B = 0.05 *M* acetate (pH 4). Gradient: fractions 0–24 buffer A, fractions 24–50 buffer B. Sample: e-Cyt *c* 2.6 mg, t-Cyt *c* 3.2 mg; sample volume, 5 ml. Flow-rate: 1 ml min^{-1}. ▲ = t-Cyt *c*; ◆ = e-Cyt *c*; □ = t-Cyt *c* and e-Cyt *c*.

IMA-MA, the 5.4-cm^2 Ni(II)–IMA-MA units were used to isolate $(HIS)_6$-tagged EcoR V, an *E. coli* restriction endonuclease, from cell lysates of *E. coli*. The results obtained with the IMA-MA were compared with those achieved with conventional Ni(II)–IMAC columns, made by slurry packing of chelating Sepharose fast flow. The protein capacity of one 5.4-cm^2 Ni(II)–IMA-MA unit was found to be roughly the same as that of 1 ml of swollen gel. Stacks of up to ten MA could be used with a concomittant linear increase in the capacity before the pressure limit of the individual units was surpassed.

For the isolation of EcoR V the filtered cell lysate was loaded on to the stationary phase which had been equilibrated with the initial buffer. Subsequently the support was washed with this buffer until all UV-active, non-adsorbed components had been flushed out. Elution could be achieved in a pH gradient (7.0–5.8), a salt gradient (0.5–1.5 *M* NaCl) or an imidazole gradient (0–1 *M*). Fractions of 1 ml were collected and analysed using SDS-PAGE. The enzyme activity was determined as described above. Fractions collected during the pH and salt gradients contained a number of proteins. EcoR V was not isolated by these operations. This is not surprising, as both of these agents obviate the histidine–metal interaction in an all-or-nothing fashion. The number of histidine residues present is of little consequence under these circumstances. When imidazole is added to the eluting buffer, however, adsorption equilibria are readjusted instead. In this case the number of histidine residues is of great significance. Consequently, EcoR V could be separated from the other *E. coli* proteins in a gradient of increasing imidazole concentration.

When the fractions were checked for co-eluting metal ions by adding dimethylglyoxime, traces of Ni(II) ions were found. By decreasing the final imidazole concentration of the gradient to 0.25 *M*, the washing out could be prevented, while EcoR V was still isolated. Fig. 7a shows the separation on the Ni(II)-loaded Sepharose fast flow column under optimized conditions. According to the analysis by SDS-PAGE, the first peak contains a number of proteins, while the second peak contains one major protein together with one impurity. EcoR V activity is found only in the second peak. As according to the SDS-PAGE analysis the molecular mass of the main protein found in the second peak is *ca.* 30 000, we assumed this protein to be EcoR V. The impurity, which amounts to 13% of the total protein content of the second peak, has a molecular mass of *ca.* 89 000. The total protein content of the *E. coli* cell lysate after centrifugation and filtration was 10.2 mg ml^{-1} and that of the pooled EcoR V containing fractions 0.22 mg ml^{-1}. As a result of the chromatographic purification process, the specific activity was increased by a factor of 33 from $1.36 \cdot 10^4$ to $4.55 \cdot 10^5$ U mg^{-1}.

When a similar linear imidazole gradient was used to isolate EcoR V on a Ni(II)–IMA-MA, the chromatogram shown in Fig. 7b ensued. No distinct protein peaks could be collected. Analysis of the fractions by SDS-PAGE showed, however, that a certain amount of separation did take place, *i.e.*, fractions collected after *ca.* 40 min contained large amounts of EcoR V. Better results in terms of resolution were obtained when the final buffer concentration was reached in a step gradient (Fig. 7c). Whereas a linear gradient has a sharpening effect on the analyte zones in column gradient elution, in MA gradient elution a step gradient is more suitable, or else radial differences in the volumetric flow-rate across the MA will lead to zone broadening. The purities and specific activities of the EcoR V isolated on the IMA-MA were only insignificantly higher than those found for EcoR V purified on the Sepharose column. The IMA-MA were stable for at least 4 months of use. In daily laboratory routine they proved to be less labour intensive than the Sepharose columns, less time being required for washing and equilibration. The capacity of the system was easily adapted to the product concentration determined in the cell lysate by choosing the optimum number of MA units, rather than packing a new column.

4. Conclusions

IMAC is a sensitive and selective method for protein separation. Proteins similar in their

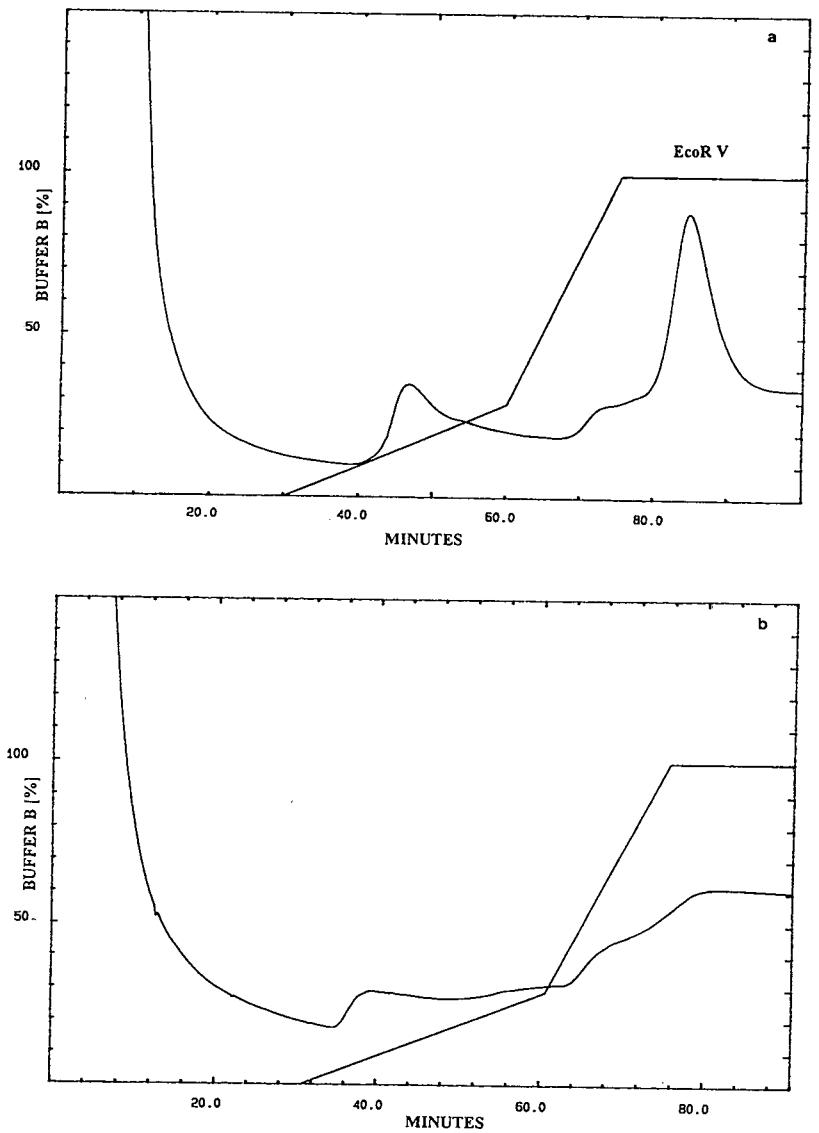

Fig. 7. Purification of $(HIS)_6$-tagged EcoR V by metal–chelate affinity chromatography. (a) Separation on a Ni(II) Sepharose fast flow column; (b) separation on a Ni(II)–IMA-MA using a linear gradient; (c) separation on a Ni(II)–IMA-MA using a step gradient. IMA-MA size: 5.4 cm^2. Buffer A = 0.3 *M* phosphate–1 m*M* dithioerythritol–0.5 *M* NaCl–10 m*M* imidazole (pH 7.0); buffer B = 0.3 *M* phosphate–1 m*M* dithioerythritol–0.5 *M* NaCl–0.25 *M* imidazole. Flow-rate: 1 ml min^{-1}.

physico-chemical parameters can be separated. However, the chromatographic conditions have to be controlled carefully, otherwise mixed-mode retention may become a problem. The membrane absorber units introduced here are interesting alternatives to conventional LC columns in protein IMAC. The IMA-MA are commercially available, comparatively inexpensive units that can be used instantaneously and are easy to handle. Scale-up is extremely simple, as up to ten units can be used in a stack, with a concomitant linear increase in the overall capacity. Conditions can be found where the IMA-MA are similar to standard IMAC columns in terms of

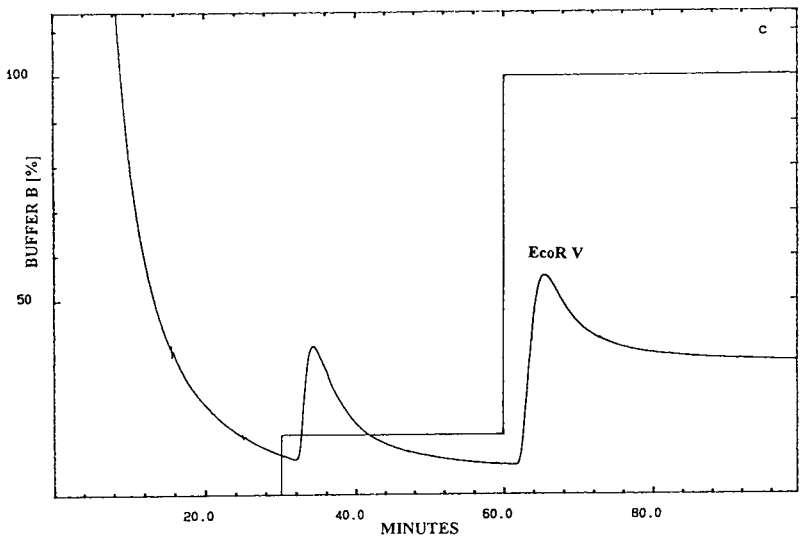

Fig. 7 *(continued).*

resolution and capacity. First attempts to use the IMA-MA for the routine isolation of a biotechnological product have yielded promising results.

5. References

[1] J.W. Wong, R.L. Albright and N.H.L. Wang, *Sep. Purif. Methods*, 20 (1991) 49.

[2] J. Porath, J. Carlsson, I. Olsson and G. Belfrage, *Nature*, 258 (1975) 598.

[3] F. Helfferich, *Nature*, 189 (1961) 1001.

[4] B. Lönnerdal and C.L. Keen, *J. Appl. Biochem.*, 4 (1982) 203.

[5] L. Fanou-Ayi and M. Vijayalakshmi, *Ann. N.Y. Acad. Sci.*, 413 (1983) 300.

[6] Z. El Rassi and Cs. Horváth, *J. Chromatogr.*, 359 (1986) 241.

[7] Z. El Rassi and Cs. Horváth, in K.M. Gooding and F.E. Regnier (Editors), *HPLC of Biological Macromolecules, Methods and Applications*, Marcel Dekker, New York, 1990, pp. 179–212.

[8] E. Sulkowski, *Trends Biotechnol.*, 3 (1985) 1.

[9] E.S. Hemdan, Y.-J. Zhao, E. Sulkowski and J. Porath, *Proc. Natl. Acad. Sci. U.S.A.*, 86 (1989) 1811.

[10] R. Gentz, C.-H. Chen and C.A. Rosen, *Proc. Natl. Acad. Sci. U.S.A.*, 86 (1989) 821.

[11] T. Moks, L. Abrahmsen, B. Oesterlöf, S. Josephson, M. Oestling, S.O. Enfors, I. Persson, B. Nilsson and M. Uhlen, *Bio/Technology*, 5 (1987) 379.

[12] J. Germio and D. Bastia, *Proc. Natl. Acad. Sci. U.S.A.*, 81 (1984) 4692.

[13] H.M. Sassenfeld and S.J. Brewer, *Bio/Technology*, 2 (1984) 76.

[14] E. Hochuli, W. Bannwarth, H. Döbeli, R. Gentz and D. Stüber, *Bio/Technology*, 6 (1988) 1321.

[15] R. Janknecht, G. de Martynoff, J. Lou, R.A. Hipskind, A. Nordheim and H.G. Stunnenberg, *Proc. Natl. Acad. Sci. U.S.A.*, 88 (1991) 8972.

[16] L. Andersson and J. Porath, *Anal. Biochem.*, 154 (1986) 250.

[17] T. Seshadi, U. Kampschulze and A. Kettrup, *Fresenius' Z. Anal. Chem.*, 300 (1980) 124.

[18] T. Seshadi and A. Kettrup, *Fresenius' Z. Anal. Chem.*, 310 (1982) 1.

[19] M. Gimpel and K. Unger, *Chromatographia*, 17 (1983) 200.

[20] H. Takayanagi, D. Hatano, K. Fujimura and T. Audo, *Anal. Chem.*, 57 (1985) 1840.

[21] M. Bradford, *Anal. Biochem.*, 72 (1976) 248.

[22] O.H. Lowry, N.J. Rosebrough, A.L. Farr and R.J. Randall, *J. Biol. Chem.*, 193 (1951) 25.

[23] G. Jander and E. Blasius, *Einführung in das Anorganisch-Chemische Praktikum*, S. Hirzel Verlag, Stuttgart, 12th ed., 1984, p. 326.

[24] U.K. Laemmli, *Nature*, 227 (1970) 680.

[25] G.V. Kholmina, B.A. Rebentish, Y.S. Skoblov, A.A. Mironov, Y. Yankovskii, Y.I. Kozlov, L.I. Glatman, A.E. Moroz and V.G. Debabov, *Dokl. Akad. Nauk SSSR*, 253 (1980) 495.

[26] K. Hebenbrock, *Ph.D. Thesis*, University of Hannover, Hannover, 1993.

[27] M. Belew, T.T. Yip, L. Andersson and R. Ehrnström, *Anal. Biochem.*, 164 (1987) 457.

[28] T.T. Yip, Y. Nakagawa and J. Porath, *Anal. Biochem.*, 183 (1989) 159.

[29] O.-W. Reif and R. Freitag, *J. Chromatogr. A*, 654 (1993) 29.

[30] G.K. Bonn, K. Kalghatgi, W.C. Horne and Cs. Horváth, *Chromatographia*, 30 (1990) 484.

ELSEVIER

Journal of Chromatography A, 664 (1994) 27–32

JOURNAL OF CHROMATOGRAPHY A

Hydrophobic interaction chromatography of proteins on an Alkyl-Superose column

Géza Rippel[a], László Szepesy*[,b]

[a]Department of Agricultural Chemical Technology, Technical University of Budapest, Budafoki u. 8, H-1521 Budapest, Hungary

[b]Department of Chemical Technology, Technical University of Budapest, Budafoki u. 8, H-1521 Budapest, Hungary

(First received February 2nd, 1993; revised manuscript received November 23rd, 1993)

Abstract

The effects of ammonium sulphate, sodium acetate and sodium citrate on the retention of proteins were investigated under gradient conditions on an Alkyl-Superose column. It was found that the salts exert different effects on the retentions of hydrophobic and hydrophilic proteins. Retention data were evaluated according to the linear solvent strength theory of gradient elution. The calculated ln k–salt molality relationships revealed specific and complex effects of the different salts on the retention behaviour of the proteins having different hydrophobicities.

1. Introduction

Two high-performance chromatographic techniques are available for separating biopolymers by virtue of their differing hydrophobicities, reversed-phase liquid chromatography (RPLC) and hydrophobic interaction chromatography (HIC). In both techniques hydrophobic functional groups are bound to the support, undergoing a London-type dispersion interaction with the hydrophobic regions or patches on the surface of the biopolymers. However, there are considerable differences between the two methods as regards the separation of biologically active substances, *e.g.*, proteins. In contrast to the strongly hydrophobic RPLC stationary phases, in HIC packings the functional groups are more sparsely distributed, producing moderately hydrophobic surfaces and resulting in a mild hydrophobic interaction.

Retention depends on the type of stationary phase (type of ligand, chain length of ligand, ligand density) [1–5] and on the characteristics of the mobile phase such as type of salt, initial salt concentration, gradient time, flow-rate, temperature, pH and addition of the organic modifiers [6–15].

In a previous study [16] we examined the effect of the stationary phase on the retention of proteins by comparing three commercially available HIC columns of different types. It was shown that the effect of the salt type used differed considerably on the various stationary phases. In this paper, further results are given on

* Corresponding author.

0021-9673/94/$07.00
SSDI 0021-9673(93)E1258-2

the effect of different salts on the separation of proteins on an Alkyl-Superose column.

2. Experimental

2.1. Instrumentation

A fast protein liquid chromatographic (FPLC) system (Pharmacia–LKB, Uppsala, Sweden) was used, consisting of an LCC-500 controller, two P-500 pumps, a UV-M monitor, an MV-7 injector with a 25-μl sample loop and a REC-482 two-channel detector. The chromatograms were acquired, evaluated and stored by a Labchrom chromatographic data station (Labinform, Budapest, Hungary), consisting of a dual-channel interface card and software running on a standard IBM PC/AT computer.

An Alkyl-Superose HR 10/10 column (Pharmacia–LKB) containing neopentyl ligands on an agarose support, with particle size 10 μm, was used.

2.2. Materials

Analytical-reagent grade ammonium sulphate, trisodium citrate, sodium acetate, phosphoric acid and sodium hydroxide were purchased from Reanal (Budapest, Hungary). Distilled water was prepared by double distillation in the laboratory.

The proteins used were the same as studied previously [16]. Cytochrome *c* (CYT), ribonuclease A (RNA), ovalbumin (OVA), lysozyme (LYS) α-chymotrypsinogen A (CHY) were obtained from Sigma (St. Louis, MO, USA). It is worth noting that this set of proteins is routinely used in studies on HIC because their surface hydrophobicities (termed here simply hydrophobicities) differ widely; they are listed above in order of increasing hydrophobicity.

2.3. Procedures

Gradient measurements were carried out with a linear inverse gradient from 2 to 0 *M* salt (0 to 100% B) in 0.05 *M* sodium phosphate buffer with pH adjusted to 7.0 with 0.1 *M* NaOH. With sodium acetate, the starting eluent contained 5 *M* salt in order to achieve retention in the same range as with the other two salts. This initial concentration was determined experimentally and was in good agreement with results in the literature [17,18]. The flow-rate was 0.3–0.5 ml/min. Samples were prepared by dissolving about 1 mg of each protein in 1 ml of doubly distilled water prior to injection. Each sample was chromatographed at four different gradient times (10, 15, 20 and 25 min). All the measurements were repeated at least twice and the average data are used throughout this paper.

3. Results and discussion

First gradient measurements were carried out on the Alkyl-Superose column with three different salts as eluent constituents using the protein samples given above. In order to compare the retention data of different runs, the apparent retention factors, k_g, were calculated for each run according to the literature [19,20]:

$$k_g = (t_g - t_m)/t_m \quad (1)$$

where t_g is the retention time under gradient conditions and t_m is the mobile phase hold-up time.

The data in Table 1 indicate that in most instances not only the absolute but also the relative retention, *i.e.*, the selectivity, is also changed by varying the type of the salt used in the eluent. For better comparison and evaluation of the effect of salt type, the apparent capacity factors, k_g, measured at the same gradient times in the three salt solutions were plotted against each other.

In Fig. 1, the k_g values measured in sodium citrate are plotted against those measured in ammonium sulphate. It can be seen that the retentions of the different proteins did not change similarly with variation in the type of eluent. CHY and LYS have higher retention in ammonium sulphate but RNA and CYT show significantly higher retention in sodium citrate.

Table 1
Apparent retention factors (k_g) of proteins obtained with different eluents

Gradient former[a]	t_G (min)	k_g				
		CHY	LYS	OVA	RNA	CYT
Ammonium sulfate (2–0 *m*)	10	0.891	0.677	0.469	0.384	0.004
	15	1.108	0.869	0.656	0.448	0.005
	20	1.305	1.110	0.768	0.532	0.007
	25	1.518	1.240	0.895	0.576	0.009
Sodium citrate (2–0 *m*)	10	0.727	0.647	0.544	0.552	0.207
	15	0.968	0.943	0.834	0.811	0.305
	20	1.270	1.233	1.083	1.068	0.389
	25	1.554	1.555	1.324	1.304	0.503
Sodium acetate (5–0 *m*)	10	1.038	0.615	0.274	0.109	0.064
	15	1.417	0.847	0.380	0.148	0.073
	20	1.699	1.069	0.463	0.195	0.092
	25	1.978	1.230	0.542	0.230	0.106

For conditions, see text.
[a] *m* = Molality.

As the former are known to have higher surface hydrophobicity and the latter have relatively hydrophilic characteristics, this means that replacing ammonium sulphate with sodium citrate, providing nearly the same average retentions for the samples, decreases the retention of the hydrophobic and increases those of the hydrophilic proteins.

In Fig. 2, the k_g values measured in sodium acetate are plotted against those measured in

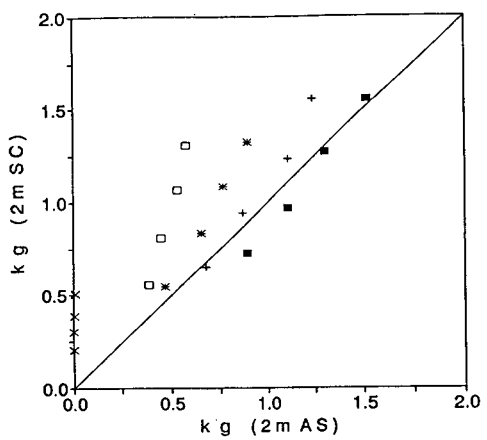

Fig. 1. Plots of apparent retention factors, k_g, of proteins determined in sodium citrate (SC) against those determined in ammonium sulphate (AS). The points represent data obtained at the same gradient time (10, 15, 20 and 25 min). ■ = CHY; + = LYS; * = OVA; □ = RNA; × = CYT.

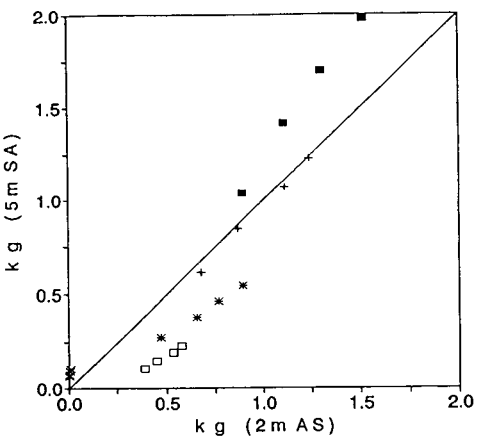

Fig. 2. Plots of apparent retention factors, k_g, of proteins determined in sodium acetate (SA) against those determined in ammonium sulphate (AS). The points represent data obtained at the same gradient time (10, 15, 20 and 25 min). Symbols as in Fig. 1.

ammonium sulphate. Although the comparison shows smaller differences between the hydrophobic and the hydrophilic proteins, the pattern of the data indicates an opposite tendency. In this instance substituting sodium acetate for ammonium sulphate increases the retention of the hydrophobic and decreases those of the hydrophilic proteins when using eluents providing nearly identical average retentions for the components.

It is well known from other studies [6–10] that changing the salt type is one of the most important parameters for modulating retention and selectivity in HIC. It has been demonstrated recently that the effect of the salt type used differs considerably on various stationary phases [16]. In order to characterize an HIC column for a given separation, the effect of salt type should be determined with different salts.

To evaluate retention and selectivity in HIC under different conditions, either isocratic or gradient measurements have been carried out and reported in the literature. As isocratic measurements are laborious and time consuming, we used the gradient data for the determination of the retention factor as a function of salt molality usually determined under isocratic conditions.

In HIC, the retention of the components can be described as

$$\ln k = \ln k_w + Sm \quad (2)$$

where m is the molality of the salt and $\ln k_w$ and S are the intercept and slope of the profile respectively, considered to be constants in a given chromatographic system. When a linear gradient is applied, the characteristic constants of Eq. 2 can be calculated from the results of two runs differing only in the duration of the gradient in accordance with the linear solvent strength (LSS) theory [19,20]. The applicability of the LSS theory under HIC conditions has been proved experimentally in some instances [21].

In addition, under LSS conditions the retention factor at the half of the column is characteristic for each component. This median value k_m determines the resolution with gradient elution just as does k in an isocratic separation. This k_m value corresponds to an average salt molality m_m in each gradient run. This pair of values furnish a good approximation for the description of the ln k–solvent strength relationship even if the retention profile is curved, *i.e.*, Eq. 2 is not valid. These median values can be calculated by using the fundamental equations of gradient elution described by Snyder and co-workers [21–23].

From the data for four different gradient runs, six independent pairs can be formed. If the retention times could be measured without error and the LSS conditions held strictly true, one S and ln k_w and four k_m and m_m values would be obtained for each protein. However, under real conditions the use of four gradient data will result in six S and ln k_w and twelve k_m and m_m values, which makes it possible to explore the error of the calculated values and the validity of the LSS model used, *i.e.*, the linearity of the profiles.

For the calculations, a program was written in C and was compiled and run on the computer used for the data acquisition. Although the applicability of the LSS model under HIC conditions has been demonstrated [21], we checked the predicted retention times in ammonium sulphate under isocratic conditions. The salt concentration of the eluent was varied in the range spanned by the m_m values calculated. As good agreements were found for all the proteins investigated, the retention profiles calculated from the data obtained with the other two salts were accepted without further examination. In Figs. 3 and 4 the results obtained for CHY and LYS are presented. It is seen that the measured value (triangles) fit the calculated profile (solid line) well and the median values (squares) do not indicate any significant curvature.

The characteristic constants of Eq. 2 for the proteins in the different eluents are presented in Table 2. These values are averages of the six values calculated from the independent pairs of retention times. The examination of the predicted profiles reveals that the effect of the salt change is more complex than for gradient measurements. Replacing ammonium sulphate with sodium citrate results in an increase in retention at identical concentration but the relative positions of the components are also altered. All the slope values are increased and the intercepts are

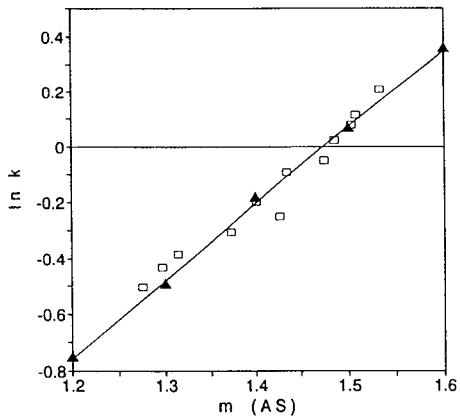

Fig. 3. Retention profile (solid line) of α-chymotrypsinogen A (CHY) calculated from the LSS model of gradient elution. AS = Ammonium sulphate. □ = Characteristic calculated median values; ▲ = retention data obtained experimentally. For details, see text.

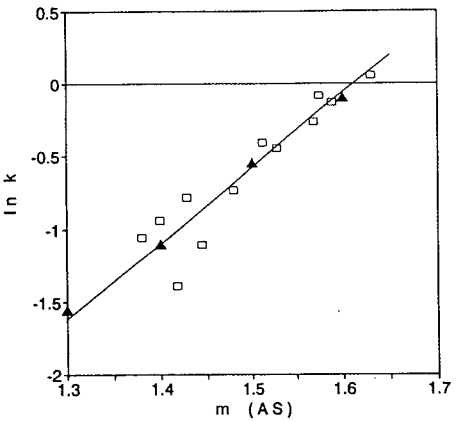

Fig. 4. Retention profile (solid line) of lysozyme (LYS) calculated from the LSS model of gradient elution. AS = Ammonium sulphate. Symbols as in Fig. 3. For details, see text.

decreased. The changes in the parameters are smaller for the hydrophobic proteins (CHY, LYS) and larger for the hydrophilic proteins.

The effect of sodium acetate is different. The retention profiles of the hydrophobic proteins are highly flattened and the intercepts are larger than with ammonium sulphate, but the effect for the hydrophilic proteins is very similar to that with sodium citrate.

4. Conclusions

The effect of the salt type on the retention of standard proteins on an Alkyl-Superose column was investigated by gradient measurements. It was found that the salts have different effects on the retention of the hydrophobic and hydrophilic proteins. At salt concentrations giving nearly the same average retentions of the components, sodium acetate in comparison with ammonium sulphate increased the retention of the hydrophobic and decreased those of the hydrophilic proteins. With sodium citrate the retention of the hydrophilic proteins increased whereas that of the hydrophobic proteins decreased. The relative retentions, *i.e.*, selectivities, were also different in the different salts.

It has been found that the ln k–salt molality relationship, usually determined under isocratic conditions, can be calculated from the data obtained with gradient elution via the linear solvent strength model. Comparison of the calculated retention profiles revealed that a change in salt modifies more specifically the behaviour of the proteins having different hydrophobicities than was shown by the gradient data. Replacing

Table 2
Slope and intercept values of the retention profiles of the proteins calculated from the LSS model

Protein	Ammonium sulphate		Sodium citrate		Sodium acetate	
	S	ln k_w	S	ln k_w	S	ln k_w
CHY	2.770	−4.083	5.980	−4.664	0.736	−0.893
LYS	5.182	−8.263	14.715	−10.171	1.344	−4.109
OVA	7.002	−12.318	33.043	−26.198	2.728	−12.181
RNA	4.391	−8.713	13.223	−12.247	16.517	−77.350
CYT	5.566	−13.481	48.633	−77.596	9.521	−48.522

ammonium sulphate with sodium citrate increased the slope and decreased the intercept of the ln k *vs.* salt molality profiles, but the effect was more pronounced for the hydrophilic proteins. Sodium acetate exerted the opposite effect on the hydrophobic proteins, *i.e.*, the slopes decreased and the intercepts increased, but the same effect on the hydrophilic proteins. This means that varying the salt in the eluent will result in significant changes not only in the overall retention of the proteins but also in the selectivity of the separations.

5. Acknowledgement

We gratefully acknowledge the support given by the Hungarian Academy of Sciences under grant OTKA 1998/91.

6. References

[1] Y. Kato, T. Kitamura and T. Hashimoto, *J. Chromatogr.*, 266 (1983) 49.
[2] N. Cooke, P. Shieh and N. Miller, *LC·GC Int.*, 3, No. 1 (1990) 9.
[3] Y. Kato, T. Kitamura and T. Hashimoto, *J. Chromatogr.*, 360 (1986) 260.
[4] J. Kleinmann, J. Plicka, P. Smidl and V. Svoboda, *J. Chromatogr.*, 479 (1989) 327.
[5] D.L. Gooding, M.N. Schmuck, M.P. Nowlan and K.M. Gooding, *J. Chromatogr.*, 359 (1986) 331.
[6] N.T. Miller and B.L. Karger, *J. Chromatogr.*, 326 (1985) 45.
[7] J.L. Fausnaugh and F.E. Regnier, *J. Chromatogr.*, 359 (1986) 131.
[8] W.R. Melander, Z.El Rassi and Cs. Horváth, *J. Chromatogr.*, 469 (1989) 3.
[9] J.A. Smith and M.O'Hare, *J. Chromatogr.*, 496 (1989) 71.
[10] Y. Kato, T. Kitamura, S. Nakatani and T. Hashimoto, *J. Chromatogr.*, 483 (1989) 401.
[11] T.S. Reid and D.J. Gisch, *LC·GC*, 5 (1987) 986.
[12] S. Hjertén, K. Yao, K.O. Erikson and B. Johansson, *J. Chromatogr.*, 359 (1986) 99.
[13] R.M. Chicz and F.E. Regnier, *J. Chromatogr.*, 500 (1990) 503.
[14] M.L. Heinitz, L.A. Kennedy, W. Kopaciewicz and F.E. Regnier, *J. Chromatogr.*, 443 (1988) 173.
[15] L. Szepesy and G. Rippel, *LC·GC Int.*, 5, No. 11 (1992) 24.
[16] L. Szepesy and G. Rippel, *Chromatographia*, 34 (1992) 391.
[17] M.L. Schmuch, M.P. Nowlan and K.M. Gooding, *J. Chromatogr.*, 371 (1986) 55.
[18] S.A. Berkowitz, *Anal. Biochem.*, 164 (1987) 254.
[19] L.R. Snyder, in Cs. Horváth (Editor), *High-Performance Liquid Chromatography —Advances and Perspectives*, Vol. 1, Academic Press, New York, 1980, p. 207.
[20] L.R. Snyder, M.A. Stadalius and M.A. Quarry, *Anal. Chem.*, 55 (1983) 1412A.
[21] L.R. Snyder and M.A. Stadalius, in Cs. Horváth (Editor), *High-Performance Liquid Chromatography —Advances and Perspectives*, Vol. 4, Academic Press, New York, 1986, p. 195.
[22] M.A. Stadalius, H.S. Gold and L.R. Snyder, *J. Chromatogr.*, 296 (1984) 31.
[23] M.A. Quarry, R.L. Grob and L.R. Snyder, *Anal. Chem.*, 58 (1986) 907.

ELSEVIER

Journal of Chromatography A, 664 (1994) 33–38

JOURNAL OF CHROMATOGRAPHY A

Separation of closely related intrinsic membrane polypeptides of the photosystem II light-harvesting complex (LHC II) by reversed-phase high-performance liquid chromatography on a poly(styrene–divinylbenzene) column

Ingo Damm[☆], Beverley R. Green*

Botany Department, University of British Columbia, Vancouver, BC V6T 1Z4, Canada

(First received July 12th, 1993; revised manuscript received December 20th, 1993)

Abstract

The three closely related intrinsic membrane polypeptides of the photosystem II light-harvesting complex (LHC II) were successfully resolved on a PRP-1 poly(styrene–divinylbenzene) column using a three-stage linear water–acetonitrile gradient containing 0.1% trifluoroacetic acid. The hydrophobic proteins of photosystem I (PS I-200) and photosystem II core particles were also separated by this method, showing that membrane proteins of different sizes and hydrophobicities can be resolved in this system.

1. Introduction

Mixtures of hydrophobic membrane proteins are usually analyzed by polyacrylamide gel electrophoresis (PAGE) in the presence of sodium dodecyl sulphate (SDS), which separates denatured, detergent-bound proteins on the basis of their molecular mass in the absence of complicating factors such asglycosylation [1]. Although this method is reasonably fast (several hours), it would be very useful to have a rapid alternative method which would separate membrane proteins on some basis other than molecular mass. Reversed-phase (RP) HPLC is extensively used for separation of soluble proteins, but has had only limited application to the separation of intrinsic membrane proteins [2–7] because of the many technical difficulties due to their highly hydrophobic nature [2–4].

The photosystem (PS) II light-harvesting complex (LHC II) is the major chlorophyll–protein complex of green plant photosynthetic membranes [8,9]. It has three hydrophobic polypeptides of M_r 25 000–28 000, all of which have three membrane-spanning helices [10] and are very similar in amino acid sequence [11,12]. Since they are intrinsic membrane polypeptides, they can only be released from the membrane with high concentrations of detergent, and are insoluble in aqueous solutions in the absence of detergent. In tomato, the type I LHC II polypeptide is four amino acids longer than the type II polypeptide, and has one less positive charge; the type III polypeptide is 11 amino acids shorter and has two fewer positive charges [12]. The

* Corresponding author.

☆ Present address: Institut für Pharmakologie und Toxikologie, Universität Rostock, D-(O)-2600 Rostock-1, Germany.

0021-9673/94/$07.00
SSDI 0021-9673(93)E0065-3

three types have 74% residue identity. Optimum separation of the denatured polypeptides on SDS-PAGE requires overnight electrophoresis in the presence of 4 *M* urea [12]. In this paper we report that a PRP-1 poly(styrene–divinylbenzene) reversed-phase column can be used to separate the three spinach LHC II polypeptides rapidly and in a different order from SDS-PAGE. To our knowledge, this is the first report of the use of this type of column for separation of intrinsic membrane proteins.

2. Methods

LHC II was isolated from washed thylakoids (photosynthetic membranes) solubilized with 1.2% Triton X-100 according to Ryrie *et al.* [13]. PS II core preparations were prepared according to ref. 14. In some cases, LHC II was prepared as a by-product of this procedure. PS I preparations with different amounts of associated antenna chlorophyll (PS I-200, PS I-100) were isolated according to Mullet *et al.* [15] and Haworth *et al.* [16].

Aliquots of LHC II corresponding to 100 μg chlorophyll (approximately 200 μg protein) were precipitated in 80% aqueous acetone at room temperature and collected by centrifugation. The pellet was dried under a stream of nitrogen, dissolved in 50–100 μl of acetonitrile–formic acid (2:1, v/v) and filtered through a 0.45-μm nylon filter (Cole-Parmer). The filtrate was injected immediately onto the HPLC column to avoid acid-induced degradation of the polypeptides. PS I and II preparations were treated the same way.

The HPLC system consisted of a Waters 600E gradient system (Waters, Milford, MA, USA) with an U6K injector and a Waters 994 photodiode array detector. The detector was routinely set to 215 nm. HPLC-grade acetonitrile and trifluoroacetic acid (TFA) were purchased from BDH (Canada). Distilled water was filtered through a 0.22-μm GSWP filter (Millipore). Reversed-phase chromatography was carried out on a 10-μm poly(styrene–divinylbenzene) PRP-1 column, (150 × 4.1 mm, 7.5 nm pore size, Hamilton, NY, USA) at a flow-rate of 0.5 ml/min and a temperature of 25°C. A guard column of the same material was used in all experiments. The three-stage linear gradient started with 90% A (0.1% TFA in water) and 10% B (0.1% TFA in acetonitrile) reaching 63% B after 52.5 min, 70% B after 80 min and 100% B after 90 min. Other columns investigated were a PRP-3 poly(styrene–divinylbenzene) column (50 × 4.1 mm; 30 nm pore size, Hamilton) and a silica-based RP-8 column (250 × 4 mm; 30 nm pore size, 10 μm particle size) from Merck (Darmstadt, Germany).

SDS-PAGE separations were according to ref. 12 on a 14% polyacrylamide gel containing 4 *M* urea, 0.8 *M* Tris, pH 8.8. HPLC fractions were dried under nitrogen before being solubilized in 2% SDS, 10 m*M* dithiothreitol, 65 m*M* Tris, pH 6.8.

3. Results

The LHC II polypeptides were completely solubilized in acetonitrile–formic acid (2:1, v/v) after removal of pigments by acetone extraction. Separation of the three polypeptides was achieved with a PRP-1 column with a pore size of about 7.5 nm, using a three-stage linear acetonitrile–water gradient in the presence of 0.1% TFA (Fig. 1). Fig. 1 shows the separation of two major peaks (1 and 2) and a shoulder (3), which is clearly visualized on an expanded scale (Fig. 1, inset).

Fig. 2a shows a similar sample of purified spinach LHC II separated by high-resolution SDS-PAGE containing 4 *M* urea. Type I, II and III polypeptides are numbered according to their relative molecular masses which are approximately 27 000, 26 000 and 25 000 in spinach [14]. Samples were collected from HPLC separations such as the one in Fig. 1, evaporated, dissolved in electrophoresis buffer and separated by urea-SDS-PAGE. Fig. 2b shows that peak 1 contains the type II polypeptide. The central fraction of peak 2 contained only the type I polypeptide (Fig. 2e), while the shoulder (peak 3) was enriched for the type III polypeptide (Fig. 2c, d). Taking into account the difficulty in collecting fractions that correspond exactly to the peaks

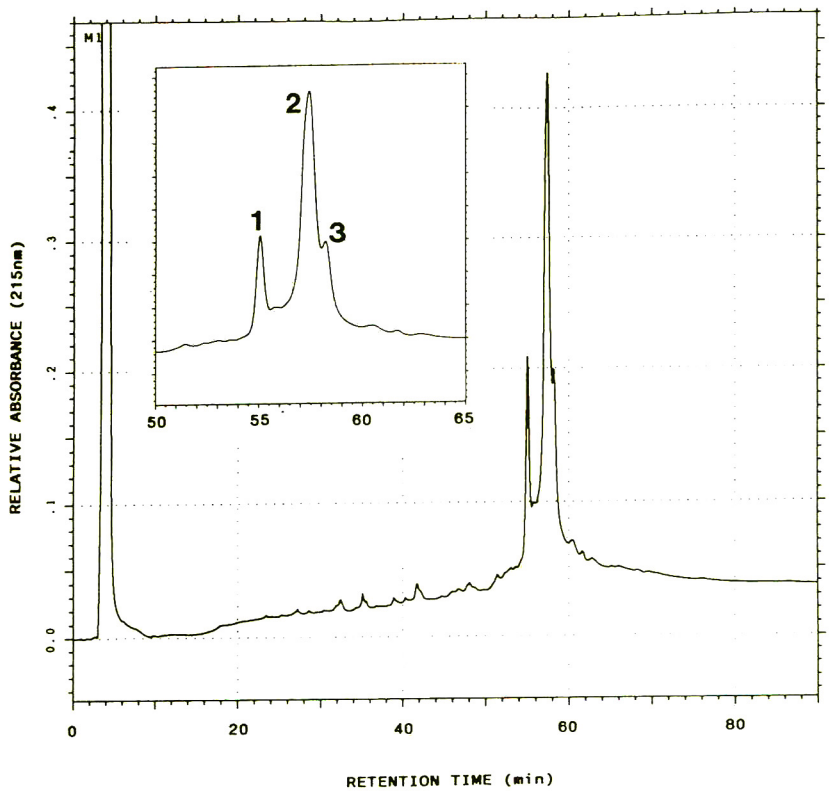

Fig. 1. Separation of the three types of spinach LHC II polypeptides on a PRP-1 column with a three-stage 10 to 90% gradient of acetonitrile in water, 0.1% TFA (see Methods). Inset: expanded scale showing relevant segment of the profile. See text.

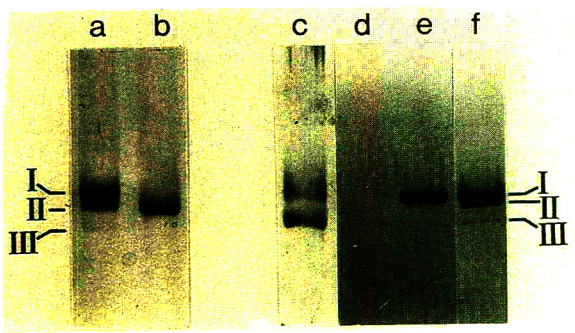

Fig. 2. SDS-PAGE separation of LHC II fractions from the PRP-1 HPLC column. (a–b) and (c–f) are from two different runs. All samples Coomassie-stained except for (c) which was silver stained. (a) Purified LHC II, (b) peak 1, (c and d) peak 3, (e) peak 2, (f) purified LHC II.

in question, we can conclude that peaks 1, 2 and 3 correspond to types II, I and III, respectively. This shows that the PRP-1 column is resolving the three polypeptide types in a different order from SDS-PAGE, and therefore is separating them on some basis other than molecular mass.

LHC II was isolated from several different plants and separated by HPLC (Fig. 3) and by SDS-PAGE (Fig. 4). Each plant has a somewhat different profile on HPLC, as would be expected from its SDS-PAGE separation. Pea has one major peak on HPLC (Fig. 3a) and apparently no type II band on SDS-PAGE (Fig. 4c). The barley type III polypeptide separates well from types I and II on SDS-PAGE (Fig. 4a), although the latter are not as well resolved from each other as they are in spinach. On HPLC (Fig. 3b), there is one major peak and a well-separated shoulder which is probably the type III poly-

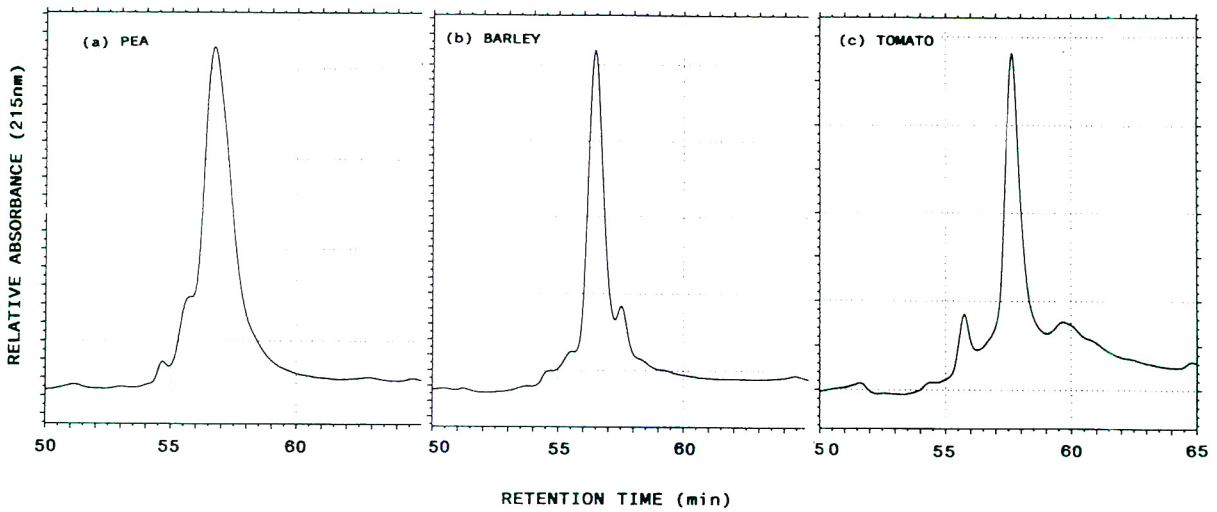

Fig. 3. HPLC separation of LHC II preparations from several plants. (a) Pea, (b) barley, (c) tomato.

peptide by analogy with spinach. The HPLC profile of tomato LHC II (Fig. 3c) is similar to that of spinach, as is its SDS-PAGE profile (Fig. 4d), although the two tomato type III bands are not resolved on HPLC the way they are on SDS-PAGE.

In order to determine if the HPLC separation method might be useful for resolving more complex mixtures of photosynthetic membrane proteins, it was challenged with a sample of a crude PS I preparation (PS I-200) (Fig. 5a) containing 17–20 polypeptides [15], and a PS II core preparation (Fig. 5b) containing 6–8 major polypeptides by SDS-PAGE [14]. There was no apparent problem with solubilization of either sample, in spite of the fact that the core proteins of both photosystems are even more hydrophobic than the LHC II proteins [8]. These results show that a large number of membrane proteins of different sizes and hydrophobicities can be separated by this method.

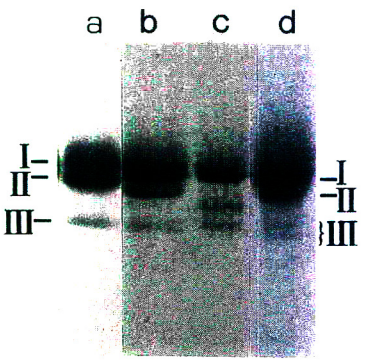

Fig. 4. SDS-PAGE separation of LHC II preparations from several plants. (a) Barley, (b) spinach, (c) pea, (d) tomato.

Over 200 injections of 50–100 μg protein on the same column over a period of months gave reproducible peak patterns. This included several large-scale preparations of LHC II, all of which gave the same retention times for the three polypeptides. There was rarely an indication of protein adsorbed to the separating column and no evidence for specific loss of any LHC II polypeptide. Occasionally some protein would be removed from the guard column after cleaning with acetonitrile or methanol. Although most trial separations involved variations of the water–acetonitrile gradient program, it was found that the addition of as little as 5% propanol to the acetonitrile caused a large shift in peak positions (data not shown). Although the presence of propanol resulted in higher back pressure in the column, it might be useful for resolving a minor protein peak migrating close to or underneath a major peak in the acetonitrile–water system.

Two other columns were tested for membrane

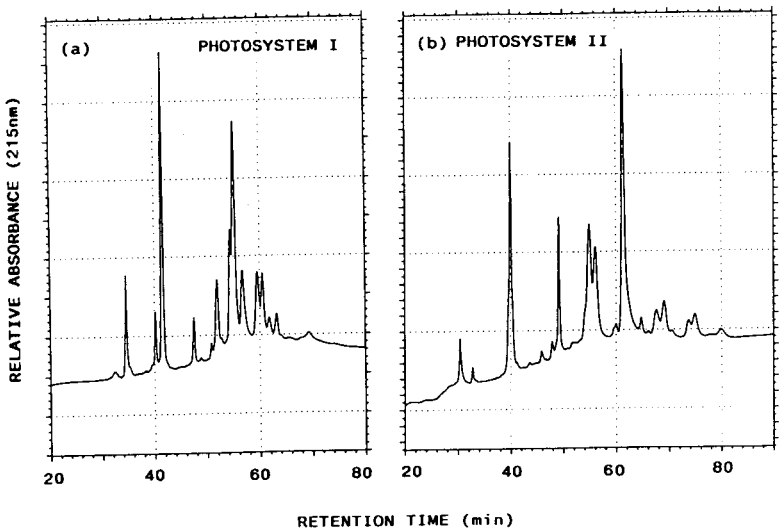

Fig. 5. HPLC separation of polypeptides from photosynthetic particles. (a) Photosystem I-200, (b) Photosystem II core particles.

protein separation. A short PRP-3 column (50 mm × 4.1 mm) with a pore size of 30 nm separated types I and II polypeptides, but no resolution of type III was obtained with any gradient conditions tried. A silica-based wide-pore RP-8 column (30 nm pore size, 10 μm particle size, 250 × 4 mm) did not give reproducible results.

4. Discussion

The HPLC separation method we report here is applicable to a wide range of photosynthetic membrane proteins. It is capable of separating LHC II proteins which have a high degree of sequence identity and differ in length by as little as four amino acids. With a preparation time of about 10 min and a running time of less than 90 min, this HPLC separation is faster than SDS-PAGE methods of comparable resolving power. The volatile buffer system means that it can be used preparatively for sequence analysis. Most importantly, however, it separates polypeptides on a different basis from SDS-PAGE. The polymeric reversed-phase column is probably more successful for separating membrane proteins because there are no silanol groups which could interact with polar groups on the protein [17,18]. Our results suggest such columns may be very useful for a wide range of membrane proteins with different molecular weights and hydrophobicities.

5. Acknowledgements

We should like to thank Dr. G.H.N. Towers for the use of the HPLC system, Mr. Filipe Balza for helpful advice, Mr. Dingren Shen for his generous and cheerful assistance, and the Natural Sciences and Engineering Research Council of Canada for financial support.

6. References

[1] U.K. Laemmli, *Nature*, 277 (1970) 680.
[2] M. Kehl and F. Lottspeich, *J. Chromatogr.*, 477 (1989) 131.
[3] G.W. Welling, R. van der Zee and S. Welling-Wester, *J. Chromatogr.*, 418 (1987) 223.
[4] F.E. Regnier, *J. Chromatogr.*, 418 (1987) 115.
[5] N.E. Tandy, R.A. Dilley and F.E. Regnier, *J. Chromatogr.*, 266 (1983) 577.
[6] S.D. Power, M.A. Locherie and R.O. Poyton, *J. Chromatogr.*, 266 (1983) 577.
[7] P.S. Parkes-Loach J.R. Sprinkle and P.A. Loach, *Biochemistry*, 27 (1988) 2718.
[8] B.R. Green, *Photosyn. Res.*, 15 (1988) 3.

[9] B.R. Green, K. Kloppstech and E. Pichersky, *Trends Biochem. Sci.*, 16 (1991) 181.
[10] W. Kuehlbrandt and D.N. Wang, *Nature*, 350 (1991) 130.
[11] P.R. Chitnis and J.P. Thornber, *Photosyn. Res.*, 16 (1988) 41.
[12] B.R. Green, D. Shen, R. Aebersold and E. Pichersky, *FEBS Lett.*, 305 (1992) 18.
[13] I.J. Ryrie, J.M. Anderson and D.J. Goodchild, *Eur. J. Biochem.*, 107 (1980) 345-354.
[14] E.L. Camm and B.R. Green, *Biochim. Biophys. Acta*, 974 (1989) 180.
[15] J.E. Mullet, J.J. Burke and C.J. Arntzen, *Plant Physiol.*, 65 (1980) 814.
[16] P. Haworth, J.L. Watson and C.J. Arntzen, *Biochim. Biophys. Acta*, 724 (1983) 151.
[17] B.S. Welinder, *J. Chromatogr.*, 542 (1991) 83.
[18] P.H. Corran, in R.W.A. Oliver (Editor), *HPLC of Macromolecules*, IRL Press, Oxford, 1989, pp. 127–156.

ELSEVIER

Journal of Chromatography A, 664 (1994) 39–43

JOURNAL OF CHROMATOGRAPHY A

Determination of patulin in apple juice by high-performance liquid chromatography with diode-array detection

B. Bartolomé*, M.L. Bengoechea, F.J. Pérez-Ilzarbe, T. Hernández, I. Estrella, C. Gómez-Cordovés

Instituto de Fermentaciones Industriales, CSIC, c/ Juan de la Cierva 3, 28006-Madrid, Spain

(First received September 7th, 1993; revised manuscript received November 8th, 1993)

Abstract

A method is described for the detection of patulin in apple juice and the simultaneous determination of the phenolic composition. Spectral data obtained with diode-array detection showed that patulin can be easily distinguished from compounds eluting under the same conditions. The detection limit for patulin was 8.96 μg/l.

1. Introduction

Patulin (Fig. 1) is a mycotoxin produced by several species of moulds (*Penicillium*, *Aspergillus* and *Bissochlamys*) [1]. It is particularly produced by the apple-rotting fungus *Penicillium expansum*, thus being of toxicological concern in apple products such as apple juice. However, patulin has also been detected in grape juice [2], barley, wheat and corn [3] and with growth of fungus in pears, bananas, pineapples, grapes, peaches and apricots [4].

There is increasing interest in developing methods for the detection and determination of patulin in foodstuffs, owing to its toxic activity and its teratogenicity, carcinogenicity and mutagenicity [5] as tested in laboratory animals. No data are available about the toxicity of patulin in humans, but some governments (Switzerland, Sweden, Belgium, Russian Federation and Norway) have established a maximum permitted concentration of 50 μg/l in apple juice [5,6].

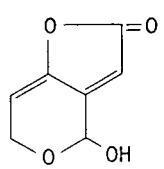

Fig. 1. Structure of patulin, 4-hydroxy-4*H*-furo[3,2-*c*]pyran-2(6*H*)one.

Although patulin is removed from juices during fermentation [2,7], its level is only decreased by about 20% during common processes in fruit-juice production [8]. Patulin is therefore a good indicator to detect the quality of the fruit used in the manufacture of juices. For these reasons, a number of methods have been developed for detecting and determining patulin in fruit juices. TLC methods have been rapidly replaced by HPLC [2,5,6,8–14].

Sample preparation involves two steps; (a) extraction with ethyl acetate and (b) a purification step, such as partitioning with aqueous sodium carbonate solution [10,13], elution through a silica gel [5,8,11,12] or Extrelut [2,9]

* Corresponding author.

0021-9673/94/$07.00
SSDI 0021-9673(93)E1257-Z

column or the use of a Sep-Pak cartridge [6]. In HPLC, reversed-phase columns are employed with different solvents, with UV detection between 272 and 280 nm.

All of the reported methods have the unique purpose of detecting patulin and none of the studies consider the compounds eluting under the same conditions. Only Leuenberger *et al.* [9] and Lehmann and Wald [11] reported that 5-hydroxymethyl-2-furaldehyde (a compound formed in thermal treatments) elutes under the same conditions as patulin.

In this paper we present a method for the detection and determination of patulin and also phenolic compounds naturally occurring in fruits. These have proved to be useful for characterizing fruit juices [14] and for detecting adulteration [15,16]. The method involves HPLC with diode-array detection (DAD). Patulin can be distinguished from phenolics in contaminated apple juice by its chromatographic and spectral features. The study of different parameters obtained from spectral data [17] permits the differentiation of patulin from over 60 low-molecular-mass phenolic compounds.

2. Experimental

2.1. Sample preparation

Different amounts of a solution of patulin [2.25 mg/l in acetonitrile–water (80:20, v/v)] were added to commercial apple juices that contained no traces of patulin. After being homogenized, the samples were extracted. Previous tests showed that the extraction of patulin with ethyl acetate is more efficient than that with diethyl ether, so the initial method for extracting non-flavonoid phenolics and 3-flavanols from fruit juices [14] was modified. The juices were not concentrated, but only ethyl acetate was used, and the number of extractions, the ratio of organic phase to the aqueous phase and the final volume of the sample were changed, in order to increase the recovery of patulin. No qualitative differences were found between the phenolic profiles of an apple juice extracted by the two methods. Therefore, samples (25 ml) were extracted six times with ethyl acetate (20 ml). The organic solutions were combined, dried for 30 min with anhydrous sodium sulphate, filtered and evaporated to dryness. The residue was dissolved in 1 ml of methanol–water (50:50, v/v) and 10 μl were injected into the HPLC apparatus. Samples were prepared and analysed in triplicate.

2.2. HPLC conditions

The equipment was obtained from Waters (Milford, MA, USA): a Model 600E pump system controller, a U6K universal injector and a Model 991 photodiode-array detector. The column was reversed-phase Nova-Pak C_{18} (300 × 3.9 mm I.D.). The gradient elution conditions are given in Table 1; solvent A was water–acetic acid (98:2, v/v) and solvent B was water–methanol–acetic acid (68:30:2, v/v/v). Detection was performed by scanning from 210 to 400 nm with an acquisition speed of 1 s. Spectra were recorded after subtracting the solvent absorption. Injections were made in duplicate.

2.3. Identification of compounds

Identification was achieved by comparing the retention times and the spectral data (obtained by DAD) with those for standards obtained from Sigma (Deisenhofen, Germany) and Aldrich (Steinheim/Albuch, Germany). *p*-Coumaric acid derivatives, for which standards were not avail-

Table 1
Mobile phase gradient composition and flow-rate (gradient curve No. 5)

Time (min)	Flow-rate (ml/min)	A (%)[a]	B (%)[a]
0	0.8	100	0
59	0.8	20	80
65	0.8	20	80

[a] A = water–acetic acid (98:2, v/v); B = water–methanol–acetic acid (68:30:2, v/v/v).

able, were previously identified by hydrolysis [18].

2.4. Statistical analysis

The data were subjected to statistical analysis utilizing the Statgraphics program (Statistical Graphics, Rockville, MD, USA).

3. Results and discussion

3.1. Identification of patulin

The chromatographic method utilized, which was initially intended for separating the highly complicated phenolic content of fruit juices, was also able to separate patulin in apple juice. It can be detected when present in concentrations below the toxic level (the limit of detection is 8.96 μg/l), even among other compounds with a higher UV response or present at higher concentrations (Fig. 2).

In other substrates, where patulin could be co-eluting with interfering compounds, the UV spectrum obtained by DAD permits the identification of the mycotoxin.

In previous work [17], we studied using the same chromatographic conditions 65 low-molecular-mass phenolic compounds that are common in vegetable substrates. The UV spectra and several spectral parameters derived from them are different from those of patulin (Table 2) as follows. The spectrum of patulin consists of a unique band (see also Fig. 3), whereas that of any of the studied low-molecular-mass phenolics presents at least two bands in the same wavelength range. The spectral band of patulin originates from overlapping of the absorption bands corresponding to two conjugated chromophoric groups, *i.e.*, the carbonyl group and the diene. The convexity interval of the band, defined as the distance (in nm) between the inflection points before and after the maximum, has a value that is near that of a carbonylic band in a phenolic compound when this band overlaps one of the bands of the aromatic ring. This confirms the overlapping of bands explained for patulin.

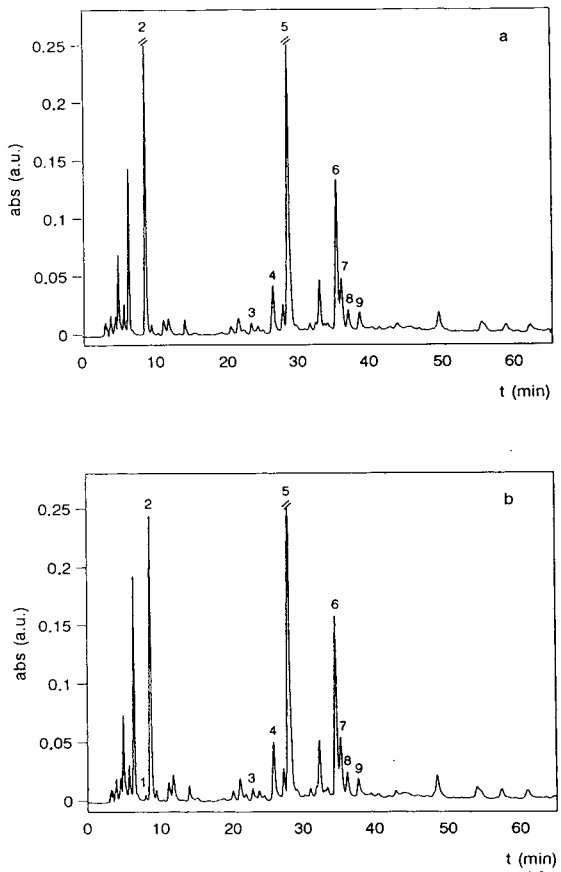

Fig. 2. Chromatograms of an apple juice (a) devoid of patulin (below the detection limit) and (b) spiked with 44.12 μg/l of patulin. Peaks: 1 = patulin; 2 = 5-hydroxymethyl-2-furaldehyde + furan-2-carboxylic acid; 3 = (+)-catechin; 4 = caffeic acid; 5 = chlorogenic acid; 6 = *p*-coumaroylquinic acid; 7 = *p*-coumaric acid; 8 = *p*-coumaroylglucose; 9 = (−)-epicatechin.

Other spectral parameters studied in the previous work [17], such as absorbance ratios at different wavelengths and the positions of the maxima in the second-order derivative spectrum, are also useful for confirmation of the identity of patulin.

3.2. Recovery of patulin

As the extraction of a compound may be affected by the other substances present in the sample, we calculated the recovery of patulin from an apple juice spiked with patulin to final concentrations of 89.46, 44.12, 17.86 and 8.96

Table 2
Values of the chromatographic parameters obtained with diode-array detection

Parameter	Patulin		5-Hydroxymethyl-2-furaldehyde		Furan-2-carboxylic acid	
Retention time (min)	8.0		8.6		8.9	
Absorbance maxima (nm)	275.4		231.5	282.2	229.8	252.3
Convexity intervals (nm)	36		–	30.6	–	26.0
260/320 nm absorbance ratio	13.6		15.7		390.6	
270/300 nm absorbance ratio	3.0		1.46		14.8	
Absorbance maxima (nm) in the second-derivative spectrum	239.3	309.5	249.7	309.5	232.8	275.7

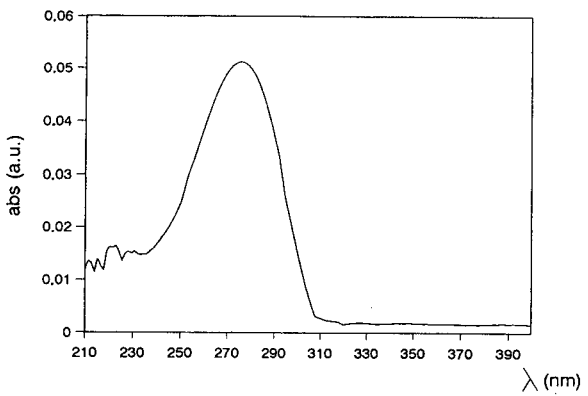

Fig. 3. UV spectrum of patulin.

μg/l. The determination of patulin was performed at 280 nm by the external standard method. A calibration graph with a higher correlation coefficient was obtained when working with peak area ($r = 0.99898$) than with peak height ($r = 0.96111$).

The recovery of patulin (Table 3) decreases with increasing concentration, ranging from 82.3% to 42.0% (because at very low concentrations the partition coefficient does not show a linear behaviour). The value of 8.96 μg/l can be considered as the detection limit of the method as lower concentrations do not allow a proper definition of the spectrum. This value is close to those reported in the literature.

Table 3
Recovery of patulin added to commercial apple juices

Concentration present (μg/l)	Concentration found (μg/l)	Recovery (%)	S.D. (%)
89.46	73.81	82.3	5.6
44.12	33.11	75.0	5.5
17.86	9.93	55.6	2.2
8.96	3.76	42.0	7.7

Results based on three replicate analyses.

3.3. Applicability

The chromatograms of a commercial apple juice without patulin and spiked with 44.12 μg/l (below the concentration considered critical by legislators) are shown in Fig. 2. Peak 1 corresponds to patulin and peaks 3–9 to phenolic compounds usually found in apples.

The nearest peak to that of patulin, peak 2, is not a phenolic compound, but appears in industrially produced fruit juices. It has been identified as a mixture of 5-hydroxymethyl-2-furaldehyde and furan-2-carboxylic acid. DAD permitted the identification of these compounds, their separate spectra to be obtained and the spectral parameters mentioned above to be acquired (Table 2). Although those compounds are related to patulin, also having a furan ring, they can be distinguished from it by the presence of two bands in their spectra and by the values of the spectral parameters.

4. Conclusions

The usefulness of DAD in the identification of a compound such as patulin in apple juice, in the

presence of other compounds occurring at very different concentrations, and having similar or dissimilar chemical attributes, has been demonstrated. These compounds can be naturally occurring in the fruits (phenolics), or can be formed during the industrial treatment applied to juices (furfurals).

The detection limit of patulin is slightly less than 8.96 μg/l, with a recovery of 42%, which increases to 75% for the legally critical concentration of 50 μg/l and above. The chromatographic system allows the determination of patulin very rapidly (less than 9 min) if it is the unique purpose of the analysis; the complete run allows the phenolic composition of the juice to be studied simultaneously, study for authentication or quality control purposes.

5. Acknowledgements

We acknowledge the assistance provided by Mr. Luis Piñal and financial support from the Comisión Interministerial de Ciencia y Tecnología (Project ALI92-0928).

6. References

[1] R. Martín, P.E. Hernández and B. Sanz, *Rev. Agroquím. Tecnol. Aliment.*, 30 (1990) 315.
[2] B. Altmayer, K.W. Eichhorn and R. Plapp, *Z. Lebensm.-Unters.-Forsch.*, 175 (1982) 172.
[3] J. Harwig, B.J. Blanchfield and G. Jarvis, *J. Food Sci.*, 42 (1977) 1225.
[4] W.G. Ikins, in D.Y.C. Fung and R.F. Matthews (Editors), *Instrumental Methods for Quality Assurance in Foods*, Marcel Dekker, New York, 1991, p. 117.
[5] R.E. Brackett and E.H. Marth, in G. Charalambous (Editor), *Liquid Chromatographic Analysis of Food and Beverages*, Academic Press, New York, 1979, p. 499.
[6] R. Rovira, F. Ribera, V. Sanchis and R. Canela, *J. Agric. Food Chem.*, 41 (1993) 214.
[7] E.E. Stinson, S.F. Osman and D.D. Bills, *J. Food Sci.*, 44 (1979) 788.
[8] H. Stray, *J. Assoc. Off. Anal. Chem.*, 61 (1978) 1359.
[9] U. Leuenberger, R. Gausch and E. Baumgartner, *J. Chromatogr.*, 161 (1978) 303.
[10] H. Tanner and C. Zanier, *Mitt. Geb. Lebensmitteluntersuch. Hyg.*, 75 (1984) 506.
[11] D. Lehmann and B. Wald, *Dtsch. Lebensm.-Rundsch.*, 86 (1990) 216.
[12] G.M. Ware, C.W. Thorpe and A.E. Pohland, *J. Assoc. Off. Anal. Chem.*, 57 (1974) 1111.
[13] T.E. Möller and E. Josefsson, *J. Assoc. Off. Anal. Chem.*, 63 (1980) 1055.
[14] B. Fernández de Simón, J. Pérez-Ilzarbe, T. Hernández, C. Gómez-Cordovés and I. Estrella, *J. Agric. Food Chem.*, 40 (1992) 1531.
[15] B. Wald and R. Galensa, *Z. Lebensm.-Unters.-Forsch.*, 188 (1989) 107.
[16] R.L. Rousseff, *J. Assoc. Off. Anal. Chem.*, 71 (1988) 798.
[17] B. Bartolomé, M.L. Bengoechea, M.C. Gálvez, F.J. Pérez-Ilzarbe, T. Hernández, I. Estrella and C. Gómez-Cordovés, *J. Chromatogr. A*, 655 (1993) 119.
[18] J. Pérez-Ilzarbe, T. Hernández and I. Estrella, *Z. Lebensm.-Unters.-Forsch.*, 192 (1991) 551.

ELSEVIER

Journal of Chromatography A, 664 (1994) 45–53

JOURNAL OF CHROMATOGRAPHY A

Preparative separation and isolation of three α bitter acids from hop, *Humulus lupulus* L., by centrifugal partition chromatography

A.C.J. Hermans-Lokkerbol *, R. Verpoorte

Leiden/Amsterdam Center for Drug Research, Division of Pharmacognosy, Center for Bio-Pharmaceutical Sciences, Leiden University, P.O. Box 9502, 2300 RA Leiden, Netherlands

(First received August 10th, 1993; revised manuscript received December 10th, 1993)

Abstract

Centrifugal partition chromatography was used for the preparative separation of bitter acids from a crude supercritical carbon dioxide extract of hop cones. The main α-acids, humulone, cohumulone and adhumulone were obtained pure in one chromatographic run with the system toluene–0.1 *M* triethanolamine · HCl pH 8.4 in water. The two-phase system was optimized for pH and the effect of ethylene glycol on the separation was investigated.

1. Introduction

The bitter taste of beer is caused by the presence of iso-α-acids, which during the brewing process are formed from the α-acids, present in the hop extracts. The extracts of hop cones, the female inflorescence of *Humulus lupulus* L., also contain the closely related β-acids. The main α-acids are humulone, cohumulone and adhumulone; the corresponding main β-acids are lupulone, colupulone and adlupulone (Fig. 1). In our studies on the biosynthesis of bitter acids in hop [1], we need relatively large amounts of the pure compounds. Also for brewery experiments on the taste of beer, the pure compounds are useful, in order to estimate the individual contribution of each bitter acid to final taste and foam formation. Despite the obvious need for these compounds they are not commercially available. This is caused on the one hand by their instability, on the other by the difficulty to separate these compounds.

For the isolation and purification of natural

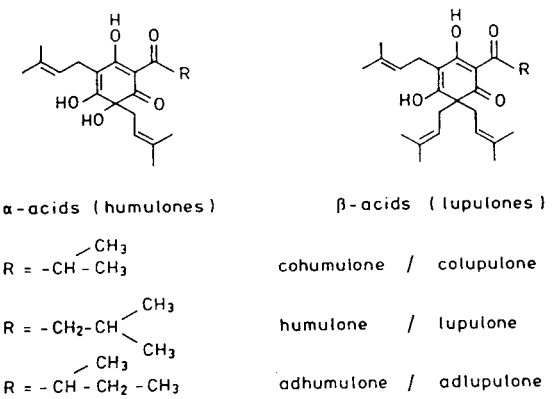

Fig. 1. Chemical structures of main hop bitter acids.

* Corresponding author.

0021-9673/94/$07.00
SSDI 0021-9673(93)E0042-S

products liquid–liquid chromatography is often the method of choice; it is a gentle method without the risk of decomposition or irreversible adsorption of the often unstable compounds by a solid stationary phase. Particularly in recent years counter-current chromatography (CCC) has been shown to be such an efficient liquid–liquid chromatographic method for the purification of natural products from complex plant extracts [2–4].

For the isolation of hop bitter acids two solvent systems for CCC have been described. Fischer *et al.* [5] used the non-aqueous system hexane–*tert.*-butyl methyl ether–acetonitrile (10:1:10) for small-scale separation (circa 24 mg) of the bitter principles from a crude carbon dioxide hop extract in an Ito multi-layer coil separator extractor. The bitter acids eluted as three peaks: the ascending side of the first peak contained cohumulone, while humulone and adhumulone eluted as the rest of the peak. The second and third peak contained the corresponding β-acids. In their experiments, replacement of the ether modifier with dichloromethane (13:3:7) increased the number of theoretical plates for four test compounds.

The second system described in literature for the separation of the three major α-acids consisted of benzene as upper phase and an aqueous buffer solution pH 8.4 (triethanolamine, hydrochloric acid and 25% ethylene glycol) as lower phase [6]. The separation was achieved by classical counter-current distribution, a tedious and time-consuming method.

In our attempts to isolate and purify the hop bitter acids we used centrifugal partition chromatography (CPC). In case of CPC the stationary phase is retained in the column by a centrifugal force, while the driving force for the movement of the mobile phase is a pump, allowing much shorter run times than in the more classic CCC methods such as the Craig type of apparatus and droplet CCC, in which the stationary phase is retained by gravity. The risk of decomposition of labile compounds is thus reduced considerably.

In this paper we report the successful purification of the main α-acids from a crude supercritical carbon dioxide hop extract. Based on the two-phase solvent systems which have been reported in literature for the counter-current separation of the hop bitter acids [5,6] systems were developed suited for a rapid separation of the bitter acids by CPC. Special attention was paid to the physical and chemical properties of the solvent systems and their influence on selectivity and efficiency of CCC.

2. Experimental

2.1. Hop extract

Crude supercritical carbon dioxide hop extract was obtained from Mr. L.C. Verhagen (Heineken Brewery, Zoeterwoude, Netherlands)

2.2. HPLC

System A

System A consisted of the following. Pump: type 2150 LKB (Bromma, Sweden); injector: Rheodyne, type 7125, equipped with a 10-μl loop; precolumn: 20 × 2 mm I.D., Uptight C-130B (Upchurch Scientific, Oak Harbor, WA, USA), packed with LiChrosorb RP-18, particle size 5 μm (Merck, Darmstadt, Germany); column: 250 × 4.6 mm I.D., LiChroma Rosil C_{18}D, particle size 5 μm (Alltech, Breda, Netherlands) (the column was always used at room temperature); detector: variable-wavelength monitor, type 2151 LKB; integrator: Shimadzu type CR-501; eluent: methanol–water–85% phosphoric acid (85:17:0.25, v/v/v), filtered over a 0.45-μm nylon membrane filter (type NL17, Schleicher & Schüll, Dassel, Germany) and degassed by means of helium.

With flow-rate 1.50 ml min^{-1} the pressure was 180 bar and the retention times were 7.6 min (cohumulone), 9.2 min (humulone and adhumulone), 12.7 min (colupulone) and 15.8 min (lupulone and adlupulone).

System B

System B is a modification of a gradient system described by David *et al.* [7] and enables separation of humulone and adhumulone. Pump:

type 2150 LKB; precolumn: 20 × 2 mm I.D., Uptight C-130B (Upchurch Scientific), packed with LiChrosorb RP-18, particle size 5 μm (Merck); column: 100 × 4.6 mm I.D., Chromsep microspher C_{18}, particle size 3 μm (Chrompack, Bergen op Zoom, Netherlands) (the column was always used at room temperature); detector and integrator: photodiode array detector, type 990 (Waters); injector: autosampler, type Wisp 710B (Waters); eluent: 5 m*M* cetyltrimethylammonium bromide (CTAB, Merck, for synthesis) in acetonitrile–water–85% phosphoric acid (6:4:0.5, v/v/v), filtered over a 0.45-μm nylon membrane filter (type NL17, Schleicher & Schüll) and degassed by vacuum.

With flow-rate 1.00 ml min^{-1} pressure was 165 bar and retention times were 7.8, 9.8 and 10.3 min for cohumulone, humulone and adhumulone, respectively.

2.3. CPC apparatus

For all experiments a modular Sanki (Kyoto, Japan) centrifugal partition chromatograph (type LLN) was used. It consists of a power supply (Model SPL), a centrifuge (Model NMF), a loop sample injector plus flow director (Model FCU-V), equipped with a 3.4-ml loop, and a triple-head constant-flow pump (Model LBP-V). To a UVIS 200 detector (Linear Instruments, Reno, NV, USA) a Panasonic Pen-recorder (Model VP-67222A) was connected. Fractions were collected by means of a LKB 17000 Minirac fraction collector. In all experiments six cartridges (total internal volume 125 ml) were used. The pressure was limited to 60 bar.

2.4. Preparation of two-phase solvent systems for CPC

The 0.1 *M* triethanolamine · HCl pH 8.4 in 25% ethylene glycol in water was prepared by dissolving 15.0 g triethanolamine (Sigma, St. Louis, MO, USA) in water. The pH was adjusted to 8.4 with hydrochloric acid and the volume was brought to 730 ml. To this solution 250 ml ethylene glycol were added and the total volume was brought to 1000 ml.

The solvents of the two-phase systems were mixed thoroughly at room temperature for 1 h; the two phases were separated in a separation funnel before use, leaving some ml of the lower layer in the upper layer and *vice versa*, thus guaranteeing saturation.

2.5. Determination of partition coefficients

The partition coefficient (k) is defined as c_{org}/c_{aq} (or $c_{non\text{-}polar}/c_{polar}$) for two-phase systems. Hop carbon dioxide extract (2–10 mg) was added to 10 ml of each of both phases of the solvent system. The mixture was shaken vigorously, kept in the dark at room temperature for 1 h, put in an ultrasonic bath for 2 min and set aside for the layers to separate. The concentration of the compounds in each of the layers was measured: part of the layer was evaporated until dryness, taken up in methanol, centrifuged 2 min at 15 500 *g* (14 000 rpm) and injected in the HPLC system. In case the layer was aqueous, the sample was not evaporated, but diluted with methanol, centrifuged and injected as such.

2.6. Determination of settling times

Volumes of 10 ml of both phases of an already saturated system were shaken by hand in a stoppered graduated cylinder during 10 s. The cylinder was put in an upright position and time was measured until complete separation of the phases. The mean of three measurements was taken. Settling times with hop extract were determined in the same manner by addition of *ca.* 10 mg of the extract. In case no separation was obtained within 3 min, the qualification "emulsion" was given.

2.7. Determination of polarity

In each of the two phases of a solvent system a small amount (*ca.* 0.02 mg ml^{-1}) of Reichardt's dye (Aldrich, Steinheim, Germany) was dissolved. The absorption maximum between 350 and 900 nm (λ_{max}) was determined. Polarity, expressed as E_tN, was calculated according to the method used by Gluck and Wingeier [8]:

$E_tN = (28\,590\lambda_{max}^{-1} - 30.7)(32.4)^{-1}$

Non-polar liquids have an E_tN close to zero and E_tN of polar liquids is close to 1.

2.8. Determination of the volume of the stationary and the mobile phase in the cartridges (V_s and V_m, respectively)

The cartridges of the CPC were filled with the stationary phase. Under experimental conditions (flow, centrifugal speed, flow direction) mobile phase was pumped through the cartridges. The effluent was led into a graduated cylinder. Pumping was continued about 30 min after the first mobile phase was eluted. The volume of the stationary phase in the cylinder was corrected for volume of inlet and outlet tubing to give V_m; the volume of the stationary phase in the cartridges, V_s, is $(125 - V_m)$ ml.

2.9. CPC sample preparation and operation

A weighed amount of the hop extract was dissolved in 3 ml stationary phase and centrifuged 2 min at 15 500 *g* (14 000 rpm) in an Eppendorf centrifuge; the supernatant was injected in the CPC system.

2.10. Extraction of the bitter acids from the aqueous phase after CPC separation

CPC fractions were combined, according to the HPLC analysis results (yielding a volume of V_{fr} ml), acidified with 2 *M* hydrochloric acid until pH 2.5–3 and extracted twice with 0.5 V_{fr} ml chloroform. The combined chloroform layers were extracted once with V_{fr} ml slightly acidified water and filtered over a paper filter, wetted with chloroform. After addition of some methanol the solvents were evaporated under vacuum; if necessary traces of toluene were removed by addition of methanol and repeated vacuum evaporation. Especially the β-, but also the α-acids are unstable compounds. Decomposition occurred, even after storage under nitrogen in the dark at −15°C. Stability was observed to be enhanced when the bitter acids were stored in methanol at −20°C. It is suspected that light has an adverse effect on the stability of the compounds. No decomposition was observed in the crude carbon dioxide extract, kept in the dark at 4°C.

3. Results and discussion

CPC was first developed by Murayama *et al.* [9] and has been studied in detail by Berthod and co-workers [10–15]. Many two-phase solvent systems for CCC have been described for all types of compounds. Reviews of solvent system applications as well as of instrumentation are published regularly [2–4]. A wide choice of two-phase systems is available; nevertheless the search for an optimal or even satisfactory solvent system for a special separation problem can be tedious and time consuming, as many factors influence the ultimate performance of the chromatography.

As each CPC run is quite time consuming, methods are needed which can be used to predict the behaviour of a particular solvent system for the desired separation. Measuring partition coefficients of the solutes and determining settling times of the two-phase systems are such methods.

By measurement of the partition coefficients of the solutes, the selectivity of a solvent system can easily be investigated. As the bitter acids are not available as pure compounds, the partitioning between the two phases has to be measured with crude extracts and the concentration of the individual compounds in the two phases has to be determined by means of HPLC analysis.

By measuring settling times [16] information is obtained about viscosity and interfacial tension which are important parameters of the solvent systems, because they affect the efficiency and separation capacity of the column. Low viscosity enables fast mass transfer of the solutes within the phases; low interfacial tension favours fast mass transfer between the phases. However, due to the formation of emulsions, it can also be the cause of flooding, which not only results in a noisy detector signal but also in a considerable loss of efficiency, capacity and reproducibility of

the chromatographic system. As already reported by Foucault and Nakanishi [17] for proteins, also hop extracts can cause quite large changes in settling time and even cause the formation of emulsions (see below). This results in temporary flooding during the elution of high concentrations of the bitter acids. The interfacial tension lowering properties of the bitter acids is well known, as they are also connected with the stability of the foam of beer.

Thus for a series of two-phase systems we determined the partition coefficients and separation factors of the bitter acids. The solvent systems tested were among others based on the systems reported by Fischer *et al.* [5], as well as some commonly applied systems. Settling times and polarities of the phases were measured. The results are presented in Table 1. Of the water-containing systems neither the highly polar butanol-containing systems 6 and 7, nor the less polar chloroform-containing 8 were promising for the separation of the bitter acids, because of small separation factors. No further attempts were made to improve selectivity by means of other modifiers.

Based on the results of the tests of the selectivity and the settling times, systems 1, 2 and 3 were selected for further studies in CPC for the separation of the bitter acids. All systems were suitable for use in CPC, no problems with flooding were encountered. The selectivity was in accordance with the data for the partition coefficients, given in Table 1. Best results were obtained with system 3, the system used by Fischer *et al.* [5]. This system was tested in both descending and ascending mode. In Fig. 2 the chromatograms of both modes are given. Analysis of fractions of the experiment in ascending mode (Fig. 2B) in HPLC system B (allowing the separation between adhumulone and humulone), showed that the first α-acid-containing fractions contained only adhumulone, which could not be detected in later fractions. From this it is concluded that there was some resolution between humulone and adhumulone. But no complete resolution of all three α-acids was achieved.

Therefore further studies were made with the solvent system as reported by Verzele and De Keukeleire [6]. In this slightly basic aqueous system (benzene–pH 8.4 aqueous buffer containing triethanolamine, hydrochloric acid and 25% ethylene glycol) the partition coefficients were reported as: 0.74 for cohumulone, 1.35 for humulone and 2.00 for adhumulone. To avoid the use of the carcinogenic benzene, we tested a system containing toluene. The triethanolamine concentration in the aqueous layer was 0.1 *M*, with a pH of 8.4, set by means of hydrochloric acid. The solvent system showed quite large differences in the partitioning coefficients for the three α-acids. The settling times were quite high and with hop extracts emulsions were formed (Table 2). Because of the high selectivity the system was tested in the CPC. In descending mode with the aqueous phase as mobile phase, nearly baseline separation was achieved between cohumulone and humulone, while adhumulone eluted in the end of the second, humulone-containing, peak. The β-acids were eluted after mode reversion with only little resolution. The pH of the aqueous phase of this system was optimized for the α-acids separation; partition at pH values between 6.5 and 9.0 is visualized in Fig. 3A. Partition coefficient values should preferably be between 0.2 and 5 to ensure a good balance between resolution and elution volume (analysis time); this corresponds with a percentage between 17 and 83% in the upper layer. For toluene as the stationary phase, best results are thus expected for pH values between 8.0 and 8.6 (Fig. 3A). Partition coefficients are strongly pH dependent, indicating that the retention mechanism mainly works by ion-pair partitioning.

Chromatographic performance of system 10 was examined at a slightly elevated temperature (30°C); V_s and pressure were the same as at room temperature, the retention volumes were *ca.* 30% lower; however, the selectivity was not changed.

In order to investigate the role of ethylene glycol in the separation of the α-acids, settling times and partition coefficients were determined for systems containing 0–25% ethylene glycol. As expected settling times increase with increasing ethylene glycol percentage (see Table 2). Partition coefficients decrease with increasing

Table 1
Some physico-chemical parameters of two-phase systems tested for the separation of α bitter acids

No.	System	Partition coefficient				Separation factor			Polarity (E_tN)		Settling times (s)	
		cohum k_1	(ad)hum k_2	colup k_3	(ad)lup k_4	k_2/k_1	k_3/k_2	k_4/k_3	Upper phase	Lower phase	Without hop extract	With hop extract
1	Hexane–dichloromethane–acetonitrile (13:3:7)	0.407	0.450	0.616	0.714	1.11	1.37	1.16	0.348	0.418	– [c]	– [c]
2	Hexane–dioxane–acetonitrile (13:3:7)	0.318	0.366	0.523	0.602	1.15	1.43	1.15	0.309	0.418	– [c]	– [c]
3	Hexane–*tert.*-butyl methyl ether–acetonitrile (10:1:10)	0.363	0.437	0.628	0.795	1.20	1.44	1.27	– [a]	0.444	– [c]	– [c]
4	Hexane–acetonitrile	0.231	0.278	0.568	0.717	1.20	2.04	1.26	– [a]	0.451	5	7
5	Hexane–methanol–water (100:99:1)	0.220	0.252	0.315	0.343	1.15	1.25	1.09	0.648	0.724	11	13
6	*n*-Butanol–water	>250	>250	>250	>250				0.657	– [a]	28	emulsion
7	*n*-Butanol–acetic acid–water (4:1:5)	>250	>250	>250	>250				– [b]	– [b]	43	47
8	Chloroform–methanol–water (5:6:4)	>250	>250	>250	>250				0.742	0.592	22	emulsion

Abbreviations: cohum = cohumulone; (ad)hum = humulone and adhumulone; colup = colupulone; (ad)lup = lupulone and adlupulone.
[a] The solubility of Reichardt's dye is too low to be able to measure the absorption maximum.
[b] The method is not applicable to acidic solutions.
[c] Not determined.

Table 2
Correlation between physico-chemical parameters and ethylene glycol concentration in the two-phase system toluene–0.1 *M* triethanolamine · HCl pH 8.4 in water

System No.	Glycol in aqueous layer (%, v/v)	Partition coefficient c_{org}/c_{aq}			Separation factor		Polarity (E_tN)		Settling times (s)	
		cohumulone k_1	humulone k_2	adhumulone k_3	k_2/k_1	k_3/k_2	Upper phase	Lower phase	Without hop extraction	With hop extraction
9	25	0.64	1.57	1.88	2.47	1.20	0.214	0.918	136 [b]	emulsion
10	20.3	0.83	1.93	2.36	2.32	1.22	– [a]	– [a]	82 [b]	emulsion
11	12.2	1.33	3.29	3.81	2.47	1.16	– [a]	– [a]	60 [b]	emulsion
12	4.1	1.77	4.47	6.40	2.52	1.43	– [a]	– [a]	35 [b]	emulsion
13	0	2.45	6.32	10.95	2.58	1.73	0.129	[c]	33 [b]	emulsion

[a] Not determined.
[b] The aqueous layer stayed turbid after separation of layers.
[c] The solubility of Reichardt's dye is too low to be able to measure the absorption maximum.

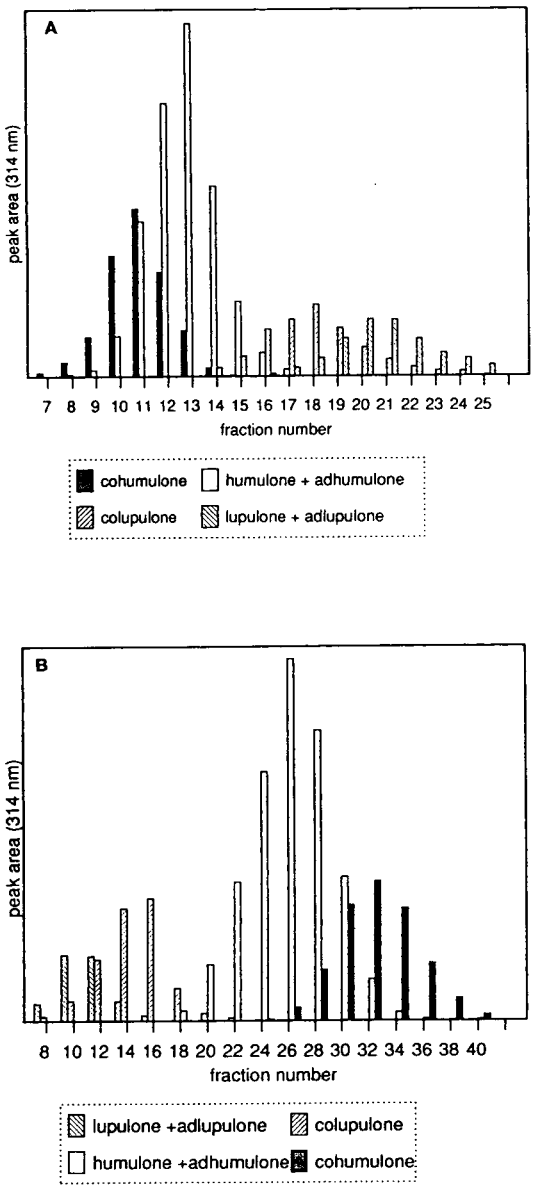

Fig. 2. Composition of fractions after CPC separation of a crude supercritical carbon dioxide hop extract as analyzed by HPLC (system A). Two-phase system: hexane–*tert.*-butyl methyl ether–acetonitrile (10:1:10, v/v/v). (A) Descending mode; rotation speed 1000 rpm; flow-rate 2.75 ml min^{-1}; pressure 29 bar; amount injected 40 mg; fraction size 3.2 ml; total elution volume after 25 fractions is 130 ml; total run time 48 min. (B) Ascending mode; rotation speed 1200 rpm; flow-rate 2.8 ml min^{-1}; V_s 80 ml; pressure 44 bar; amount injected 50 mg; fraction size 3.9 ml; total elution volume after 41 fractions is 250 ml; total run time 54 min.

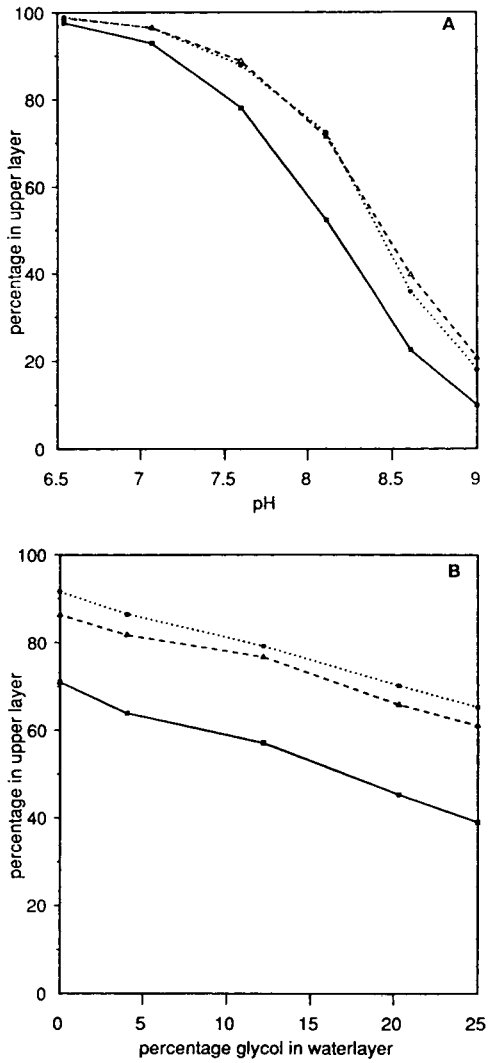

Fig. 3. Partitioning of α-acids in different two-phase systems. The percentage in the upper layer is calculated from the partition coefficients. (A) Two-phase systems: toluene–0.1 *M* triethanolamine in 25% ethylene glycol in water; the pH of the aqueous phase is set with hydrochloric acid; the pH values of the aqueous layers after addition of the hop extract are used in the graph. (B) Two-phase systems: toluene–0.1 *M* triethanolamine · HCl pH 8.4 in solutions of the indicated percentage (v/v) ethylene glycol in water. ■ = Cohumulone; △ = humulone; ○ = adhumulone.

ethylene glycol concentration, resulting in larger retention volumes and thus longer chromatographic runs (see Table 2 and Fig. 3B). On the other hand the separation factors increase, espe-

cially for adhumulone/humulone. Moreover, absence of ethylene glycol in the solvent system is also advantageous, considering isolation and further purification of the α-acids from the aqueous layer. In the ethylene glycol-free system higher pH values decreased the partition coefficients (and so diminished elution volumes), but there was also a slightly lower separation factor between adhumulone and humulone. On the other hand no improvement of the separation can be expected at pH <8.4 because of the increase of partition coefficient values of the α-acids at lower pH values. So pH 8.4 is regarded optimal for the preparative isolation of the main α-acids from hop carbon dioxide extract, both in a system with and without ethylene glycol. Results of the separation of the α-acids from hop carbon dioxide extracts by means of CPC with both systems (Nos. 9 and 13 in Table 2) are shown in Fig. 4. Using system 13 from 500 mg hop extract (total content α-acids 45.4%) 59 mg cohumulone, 82 mg humulone and 18 mg adhumulone were obtained within 5 h. Identity and purity (estimated $\geq$ 95%) were confirmed by NMR, UV spectra and HPLC (system A).

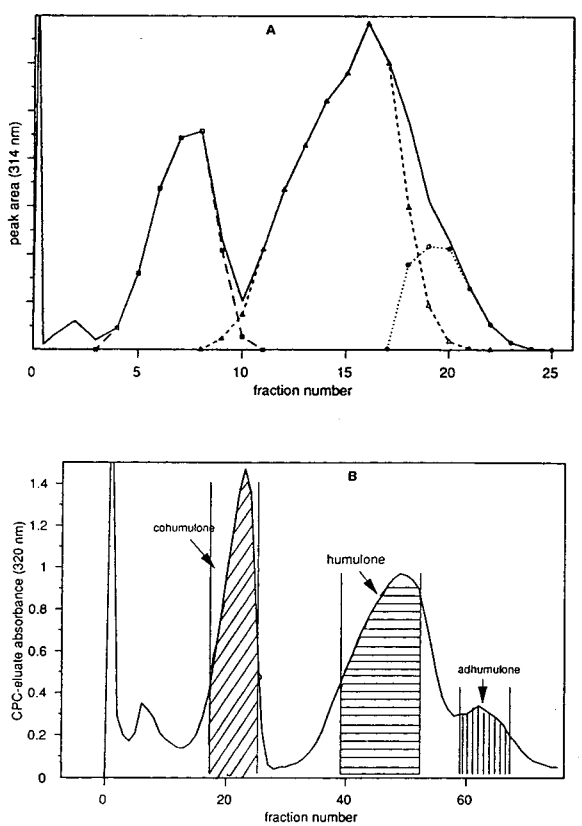

Fig. 4. CPC separations of α-acids from a crude supercritical carbon dioxide hop extract. (A) Two-phase system: toluene–0.1 *M* triethanolamine · HCl pH 8.4 in 25% ethylene glycol in water; descending mode; experimental conditions: rotation speed 800 rpm, flow-rate 2.17 ml min^{-1}, V_s 81 ml, amount injected 480 mg, fraction size 8.7 ml; total elution volume after 26 fractions is 260 ml, total run time 2 h; CPC separation was monitored by HPLC analysis (system B) of the fractions; dotted line (○) = adhumulone; broken lines: □ = cohumulone, △ = humulone; solid line = total peak area. (B) Two-phase system: toluene–0.1 *M* triethanolamine · HCl pH 8.4 in water; descending mode; experimental conditions: rotation speed 1000 rpm, flow 2.6 ml min^{-1}, V_s 81 ml, pressure 47 bar, amount injected 500 mg, fraction size 10.1 ml, total elution volume after 79 fractions is 850 ml, total run time 5 h; isolation of the bitter acids from the indicated fractions resulted in 59 mg cohumulone, 89 mg humulone and 18 mg adhumulone.

4. Conclusions

The three main α-acids, humulone, cohumulone and adhumulone, can be obtained pure from hop carbon dioxide extracts after separation by CPC, using the two-phase system toluene–0.1 *M* triethanolamine · HCl pH 8.4 in water. For analytical purposes an aqueous layer containing 0.1 *M* triethanolamine · HCl pH 8.4 in 2% (v/v) ethylene glycol in water can be used; in this system separation factors are somewhat lower but run times are shorter, retention volumes smaller and detection limits lower.

5. Acknowledgements

We wish to thank Mr. L.C. Verhagen (Heineken Brewery, Zoeterwoude, Netherlands) for the kind gift of hop extracts and Dr. J. Schripsema for running and analyzing the NMR spectra.

6. References

[1] S.-Y. Fung, J. Brussee, R.A.M. van der Hoeven, W.M.A. Niessen, J.C. Scheffer and R. Verpoorte, *J. Nat. Prod.*, in press.

[2] J.B. McAlpine and J.E. Hochlowski, in G.H. Wagman and R. Cooper (Editors), *Natural Products Isolation* (*Journal of Chromatography Library*, Vol. 43), Elsevier, Amsterdam, 1989, p. 1.
[3] A. Marston, I. Slacanin and K. Hostettmann, *Phytochem. Anal.*, 1 (1990) 3.
[4] D.E. Schaufelberger, *J. Chromatogr.*, 538 (1991) 45.
[5] N. Fischer, B. Weinreich, S. Nitz and F. Drawert, *J. Chromatogr.*, 538 (1991) 193.
[6] M. Verzele and D. De Keukeleire, *Chemistry and Analysis of Hop Bitter Acids* (*Developments in Food Science*, Vol. 27), Elsevier, Amsterdam, 1991, p. 33.
[7] F. David, P. Sandra, W.S. Pipkin and J. Smith, *Hewlett-Packard Application Note 228-115*, Hewlett-Packard, May 1990.
[8] S. Gluck and M. Wingeier, *J. Chromatogr.*, 547 (1991) 69.
[9] W. Murayama, T. Kobayashi, Y. Kosuge, H. Yano, Y. Nunogaki and K. Nunogaki, *J. Chromatogr.*, 239 (1982) 643.
[10] A. Berthod and D.W. Armstrong, *J. Liq. Chromatogr.*, 11 (1988) 547.
[11] A. Berthod and D.W. Armstrong, *J. Liq. Chromatogr.*, 11 (1988) 567.
[12] A. Berthod, J.D. Duncan and D.W. Armstrong, *J. Liq. Chromatogr.*, 11 (1988) 1171.
[13] A. Berthod and D.W. Armstrong, *J. Liq. Chromatogr.*, 11 (1988) 1187.
[14] A. Berthod, Y.I. Han and D.W. Armstrong, *J. Liq. Chromatogr.*, 11 (1988) 1441.
[15] A. Berthod and D.W. Armstrong, *J. Liq. Chromatogr.*, 11 (1988) 1457.
[16] Y. Ito, *CRC Crit. Rev. Anal. Chem.*, 17 (1986) 65.
[17] A. Foucault and K. Nakanishi, *J. Liq. Chromatogr.*, 11 (1988) 2455.

ELSEVIER

Journal of Chromatography A, 664 (1994) 55–61

JOURNAL OF CHROMATOGRAPHY A

Separation of picrocrocin, *cis-trans*-crocins and safranal of saffron using high-performance liquid chromatography with photodiode-array detection

Petros A. Tarantilis[a,b], Moschos Polissiou*[,a], Michel Manfait[b]

[a]*Laboratory of General Chemistry, Department of General Sciences, Agricultural University of Athens, 75 Iera Odos, 118 55 Athens, Greece*

[b]*Laboratoire de Spectroscopie Biomoléculaire, Faculté de Pharmacie, Université de Reims Champagne–Ardenne, 51 rue Cognacq Jay, 51096 Reims Cedex, France*

(First received October 12th, 1993; revised manuscript received November 26th, 1993)

Abstract

High-performance liquid chromatography with photodiode-array detection was used to separate picrocrocin (bitter-tasting component, glucoside of safranal), *cis/trans*-crocins (carotenoids, glucosyl esters of crocetin) and safranal (flavour, monoterpene aldeyde) of saffron. All components of pure red Greek saffron were extracted from dried stigma with 50% methanol. These compounds were detected, separated collected and identified simultaneously using a Merck LiChroCART 125-4 Superspher 100 RP-18 (4 μm) column and as mobile phase a linear gradient from 20% to 100% acetonitrile in water in 20 min with a detection wavelength at 308 nm.

1. Introduction

Saffron, in filaments, is the dried, dark-red stigmata of *Crocus sativus* L. flowers [1]. It is used both as a spice for flavouring and colouring food preparations and as a drug in medicine. It has also been used as a perfume. Foods that have been spiced with saffron include cream and cottage cheese, bouillabaisse, chicken, rice and paella [2].

Crocus sativus L. plants are now cultivated in various parts of the world such as India, Iran, China, Spain and Greece. In Greece, cultivation takes place in the region of Macedonia, Krokos Kozanis area. It seems probable that the village of Krokos derived its name from this plant. In ancient Greek "kroki" meant a string or filament (Iliad IX and XII). A definite identification of *Crocus sativus* L. dates from about 1700–1600 BC in the form of a fresco painting in the palace of Minos at Knossos in Crete. Another fresco, dated about 1500 BC, is at Akrotini on the Island of Thera (Santorini) [2].

The colouring components of saffron are crocins, which are unusual water-soluble carotenoids (glucosyl esters of crocetin). The major component is a digentiobiosyl ester of crocetin [$C_{44}H_{64}O_{24}$, 8,8′-diapo-ψ,ψ′-carotenedioic acid bis(6-O-β-D-glucopyranosyl-β-D-glucopyranosyl) ester]. Safranal ($C_{10}H_{14}O$, 2,6,6-trimethyl-1,3-cyclohexadiene-1-carboxaldehyde), one of the main components responsible for the aroma of saffron, is a monoterpene aldehyde. The principal bitter-tasting substance is picrocrocin, a

* Corresponding author.

0021-9673/94/$07.00
SSDI 0021-9673(93)E1270-A

glucoside of safranal ($C_{16}H_{26}O_7$, 4-(β-D-glucopyranosyloxy)-2,6,6-trimethyl-1-cyclohexene-1-carboxaldehyde) [3–10]. Structures of the compounds are shown in Fig. 1.

One stigma of saffron weighs about 2 mg and each flower has three stigmata; 150 000 flowers must be carefully picked one by one to obtain 1 kg of spice. At present, the price on the international market is *ca.* US$ 900–1000/kg. The small retail packets of saffron, seldom over 2 g and often only 0.25 g, cost US$ 10–15/g.

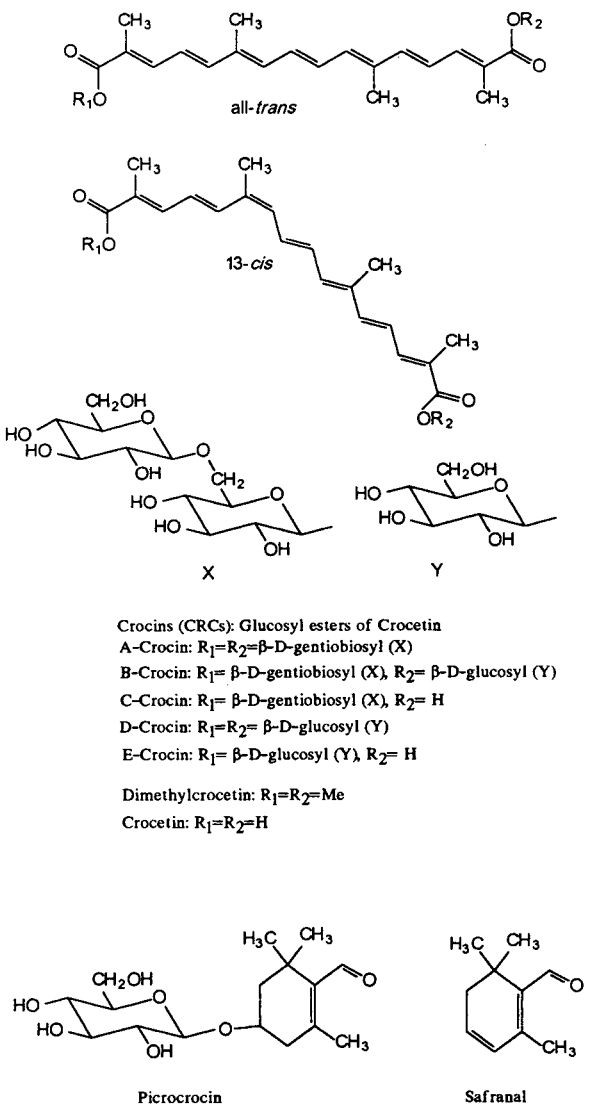

Fig. 1. Structures of saffron components.

Dietary factors play a significant role in both cancer promotion and prevention. Carotenoids are one of the most common dietary compounds that have been studied as cancer-preventive agents [11,12]. Recently, extracts from natural products and saffron have also been shown to exhibit anticancer activity [13–15].

High-performance liquid chromatography (HPLC) has been shown to be the most efficient technique for the analysis of sensitive compounds in complex extracts of natural products. Photodiode-array (PDA) detection is useful for the determination of *cis/trans* isomers. The aim of this work was to separate the components of saffron using HPLC–PDA for the determination of quality or impurities.

2. Experimental

2.1. Plant materials

Stigmata of pure red Greek saffron were kindly supplied by the Cooperative of Saffron, Krokos Kozanis. The flowers were hand picked and the stigmata were separated from the petals and the stamens and dried, in October 1992.

2.2. Sample preparation and standards

Careful attention was paid during the extraction and preparation of saffron components. All solvents were pure and specifically ethers were free from peroxide or contained the antioxidant butylated hydroxytoluene (BHT).

Extraction of the dried saffron intact stigma

For the determination of saffron components, 1 ml of methanol and 1 ml of water were added to one intact stigma saffron, followed by maceration for about 24 h in the dark at ambient temperature with occasional stirring [1,8].

Extraction of saffron in a Soxhlet extractor

Saffron (20 g) was successively and exhaustively extracted with light petroleum (b.p. 40–60°C),

diethyl ether (0.03% BHT) and methanol in a Soxhlet extractor in the dark. The light petroleum extract contained non-glucoside carotenoids and lipids. The diethyl ether extract contained lipids and picrocrocin. The methanol extract contained the glucoside carotenoids of saffron (crocins-CRCs) [3]. All solutions were evaporated to dryness in the dark at 25°C using a Rota Vapor (Buchi, Flawil, Switzerland).

Solution of saffron methanolic extracts in a Soxhlet extractor

For analytical purposes, 1.5 mg of dried methanol extract of saffron from a Soxhlet extractor were dissolved in 2 ml of methanol–water (50:50).

Compounds

Crocetin (CRT), pyridine salt, *ca.* 95%, from saffron was obtained from Sigma (St. Louis, MO, USA) and crocetin (CRT) free acid was produced from a dried methanol extract of saffron in a Soxhlet extractor, in basic (1% KOH) and acidic (1% HCl) solution. Dimethylcrocetin (DMCRT) was also produced from a methanol solution of saffron in basic (1% KOH) solution.

Picrocrocin (PCRC) was purified from the dried diethyl ether extract of saffron in a Soxhlet extractor [3]. It was then diluted with methanol and passed through a 0.45-μm filter (Millipore, Bedford, MA, USA) and purified using HPLC. Safranal (SFRN) was also extracted from saffron using three different extraction methods: (a) steam distillation (SD) under normal pressure (100 g of saffron), (b) micro-steam distillation (MSD) (10 g of saffron) and (c) vacuum headspace (VHS) (20 g of saffron) [16,17], and was purified using HPLC.

Picrocrocin and safranal are very sensitive compounds and produce oxidized and decarboxylated derivatives which may be obtained enzymatically or non-enzymatically during flower growth and the processing and storage of saffron. Further, it should be noted that the method of isolation of the fragrance is a more important step. Artifacts are produced by the SD and MSD extraction procedures. The VHS method for the isolation of safranal from stigmata is rapid and uncomplicated. The volatile components are distilled at low temperature, thus providing the fragrance concentrate form.

2.3. Equipment

UV–visible spectra were obtained using a Philips (Amsterdam, Netherlands) PU8700 UV–Vis spectrophotometer.

HPLC instrumentation

(a) A Waters (Milford, MA, USA) sample injector (20-μl loop), two Model 510 pumps, a Model 680 automated gradient controller, a Model 991 PDA detector interfaced with an NEC power mate 386/25 personal computer, Waters 991-3D chromatogram measuring software (PDA) and a Model 5200 printer–plotter were used. A Merck (Darmstadt, Germany) LiChroCART 125-4 Superspher 100 RP-18 (4 μm) column was employed. The mobile phase was a linear gradient from 20 to 100% acetonitrile in water in 20 min, with an elution profile from 0 to 30 min. The solvent flow-rate was 0.5 ml/min and the column pressure was 4.97 MPa. Detection was performed simultaneously at 220–500 nm.

(b) A Waters Model U6K universal injector (1-ml loop), two Model 510 pump, a Model 680 automated gradient controller, a μBondapak C_{18} (10 μm, 125 Å) column (300 × 7.8 mm I.D.), a UV spectrophotometric detector, and a Model 740 integrated data module system were used, together with an LKB Model 2112 fraction collector. The mobile phase was a linear gradient from 20 to 100% acetonitrile in water in 20 min, with an elution profile from 0 to 25 min. The solvent flow-rate was 5 ml/min and the column pressure 12.76 MPa. Detection was performed at 250, 308 and 328 nm. Fractions were collected automatically by the fraction collector (50 drops per tube or 1.6 ml per tube).

Two Hamilton (Reno, NV, USA) straight-edged needle syringes (25 and 250 μl) were used to inject the samples on to the column. Acetonitrile was of HPLC grade from Aldrich (St. Louis, MO, USA) and water was purified using a

Milli-Q+ system from Millipore (Bedford, MA, USA). All solvents were filtered through a 0.45-μm Millipore filter before use.

3. Results and discussion

3.1. UV–visible spectra

Picrocrocin had a UV–visible spectrum with a broad band at 250 nm and a shoulder at 350 nm. Safranal had an absorption maximum at 308 nm. It is consistent with the presence of a cyclic conjugated aldehyde.

The UV–visible spectra of aqueous saffron solutions had three absorption bands. The first at 256 nm corresponds to glycoside bonds of crocins, the second at 323 nm is attributed mainly to the presence of *cis* double bonds in the polyene conjugated system of crocins, characteristic of the absorption for all the mono-*cis*-carotenoids, and the third band between 400 and 500 nm, with λ_{max} at 440 nm, is characteristic of most all-*trans*-carotenoids [7,18,19]. However, shifts in λ_{max} and the molar absorptivity are readily induced by changing the solvent [18]; thus, in pure methanol saffron showed four peaks at 253, 319, 430 and 455 nm ($\lambda_{max} = 430$ nm), while methanol–water (50:50) resulted in three peaks at 256, 323 and 437 nm ($\lambda_{max} = 437$ nm).

3.2. High-performance liquid chromatography

Fig. 2 shows the results for (A) a methanol–water (50:50) extract of dried saffron intact stigma, (B) a methanol–water (50:50) saffron extract obtained in a Soxhlet extractor and (C) a mixture of methanol–water (50:50) extract of dried saffron intact stigma, crocetin and dimethylcrocetin detected at 440 nm. Peaks 3, 4, 5, 6 and 9 belong to the *trans*-crocins and peaks 7 and 8 to the *cis*-crocins. Peaks 11 and 12 can be identified as crocetin and dimethylcrocetin, respectively.

A comparison between profiles A and B shows that the second extract contains more *cis* isomers than the first. In addition, three minor peaks appeared, which belong to carotenoid derivatives, with retention times of 14.4, 16.8 and 26.3 min. The last peak is consistent with the presence of dimethylcrocetin (peak 12) (Fig. 2B).

The isomerization from the *trans* to the *cis* form and the production of dimethylcrocetin and the other minor unknown peaks are greatly dependent on the extraction method. In fact, the conjugated double bond systems of the saffron carotenoids are very sensitive especially to light, heat, oxygen and acids, and glycoside bonds are readily hydrolysed by alkaline and acidic reactions.

Crocins as all carotenoids are stable only in their natural plant cell environment, and are subject to considerable degradation once isolated. Common causes of pigment loss include heat-induced isomerization from the *trans* to the *cis* form, epoxidation in the presence of oxygen or peroxide, acidic degradation of naturally occurring epoxides to furanoid oxides and photosensitized degradation catalysed by metals [18–21].

Fig. 2 also showed that the retention times for *trans*/*cis*-crocins are between 8.5 and 15 min, for *trans*/*cis*-crocetin 20 and 20.5 min (broad peaks, co-eluted) and for *cis*/*trans*-dimethylcrocetin 25.8 and 26.3 min. These results contradict those of Sujata *et al.* [10]. They used similar conditions but the peaks characterized as crocetins (crocetin 1–4), in fact, correspond to *cis*,*trans*-crocins because the retention time of crocetin (pyridine salt and free acid form), used as a standard, is much longer than those of crocins (glycosyl esters of crocetin).

Fig. 3 shows the chromatographic profiles of a methanol–water (50:50) extract of the dried saffron intact stigma, which were obtained simultaneously at three different wavelengths, (A) 250, (B) 308 and (C) 440 nm. Peaks 1 and 10 with retention times of 5.5 and 18.5 min, respectively, were identified as picrocrocin and safranal from the UV–visible spectrum and confirmed by comparison with the chromatographically separated compounds. Peak 2 with a retention time of 6.5 min had a UV–visible spectrum similar to that of picrocrocin with two absorption bands,

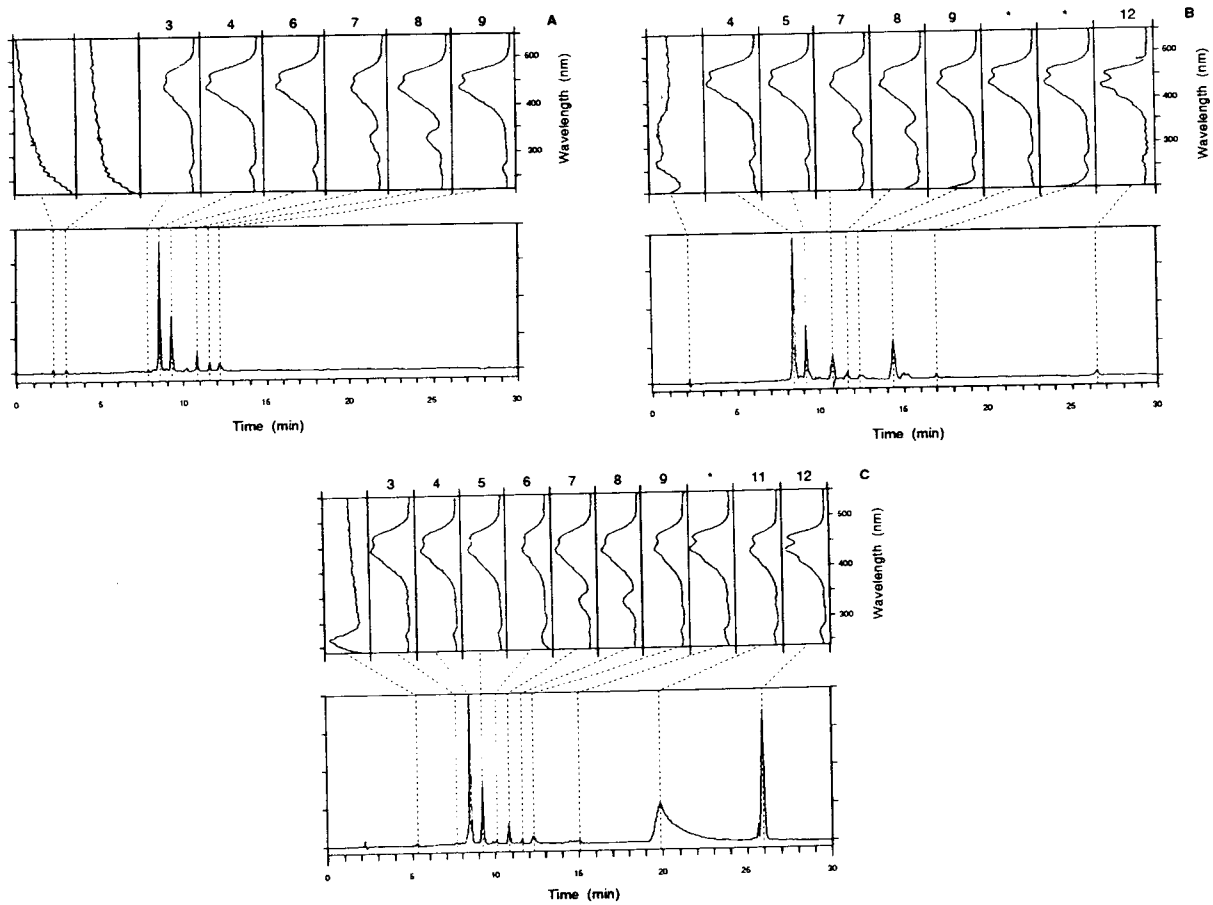

Fig. 2. Chromatograms of (A) a methanol–water (50:50) extract of dried saffron intact stigma, (B) a methanol–water (50:50) saffron extract obtained in a Soxhlet extractor and (C) a mixture of methanol–water (50:50) extracts of dried saffron intact stigma, CRT and DMCRT detected at 440 nm. Column, Merck LiChroCART 125-4 Superspher 100 RP-18 (4 μm); mobile phase, linear gradient from 20 to 100% acetonitrile in water in 20 min, with an elution profile from 0 to 30 min; solvent flow-rate, 0.5 ml/min; column pressure, 4.97 MPa. Peaks: 3–6 and 9 = *trans*-crocins; 7 and 8 = *cis*-crocins; 11 = crocetin; 12 = dimethylcrocetin.

the first at 265 nm and the second at 345 nm, but it is not picrocrocin.

From these profiles, it can be seen that detection at 308 nm is the most appropriate wavelength because all the main constituents of saffron are recorded and especially safranal, for which Sujata *et al.* [10] suggested that it was better to carry out another isocratic analysis separately.

Finally, the main factor that can limit complete resolution in the chromatographic separation of natural products on non-end-capped reversed-phase C_{18} columns is the deposition of lipid materials on the columns (Fig. 3A, retention time 22 min) [19]. In order to avoid these interferences from lipid materials, the columns were frequently washed with methanol, dichloromethane and acetone.

4. Conclusions

The HPLC profile of the methanol–water (50:50) extract of dried stigma of saffron, using a

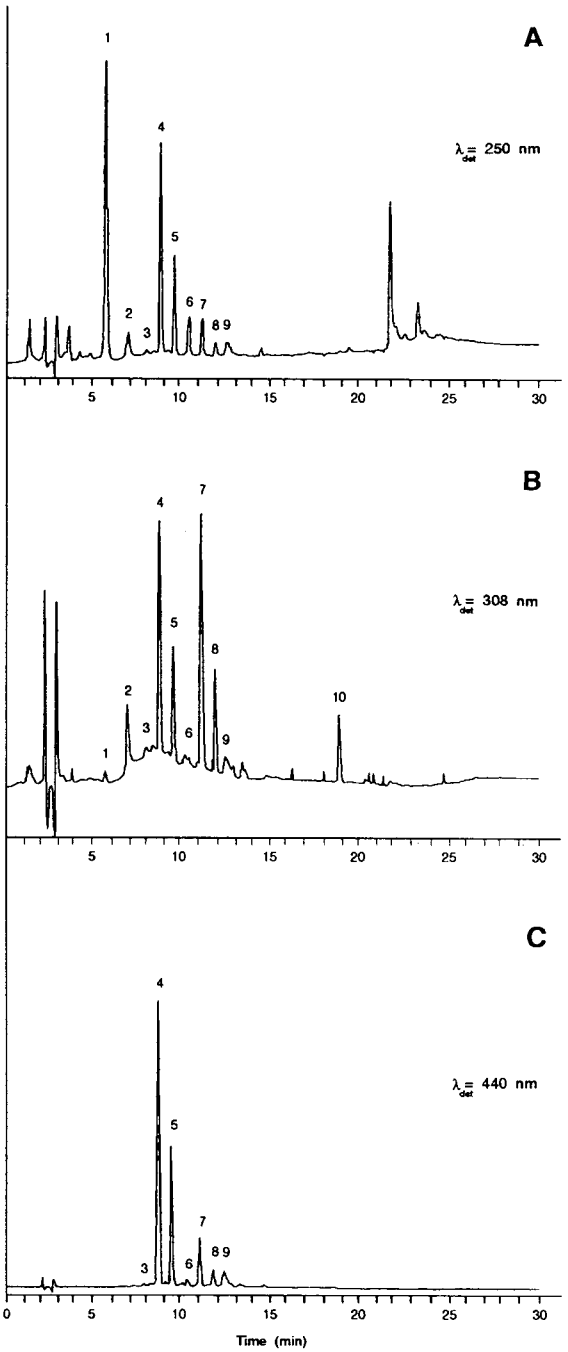

Fig. 3. Chromatograms of a methanol–water (50:50) extract of dried saffron intact stigma recorded at (A) 250, (B) 308 and (C) 440 nm. Conditions as in Fig. 2. Peaks: 1 = picrocrocin; 2 = unidentified; 3–6 and 9 = *trans*-crocins; 7 and 8 = *cis*-crocins; 10 = safranal.

Merck, LiChroCART 125-4 Superspher 100 RP-18 (4 μm) column and a linear gradient from 20 to 100% acetonitrile in water in 20 min with detection at 308 nm is useful for the determination of quality and impurities, because it gives information about all sensitive components (picrocrocin, *cis*/*trans*-crocins and safranal) of saffron.

5. Acknowledgements

We thank the Cooperative of Saffron, Krokos Kozanis, for providing the stigmata of saffron. We are also grateful to Professor B. Desoize, Director of the Laboratory of Pharmacology, Institut Jean-Godinot, Reims, France, for the generous supply of the HPLC system and Miss R. Dufour for technical assistance. This research was supported by a grant from the Ministry of Industry, Energy and Technology, General Secretariat of Research and Technology, Greece.

6. References

[1] *International Standard, Saffron —Specification, ISO 3632*, International Organization for Standardization, Geneva, 1980.
[2] D. Basker and M. Negbi, *Econ. Bot.*, 37 (1983) 228.
[3] R. Kuhn and A. Winterstein, *Ber. Dtsch. Chem. Ges.*, 67 (1934) 344.
[4] N.S. Zarghami and D.E. Heinz, *Phytochemistry*, 10 (1971) 2755.
[5] H. Pfander and F. Wittwer, *Helv. Chim. Acta*, 58, 6 (1975) 1608.
[6] H. Pfander and M. Rychener, *J. Chromatogr.*, 234 (1982) 443.
[7] G. Speranza, G. Dada, P. Manitto, D. Monti and P. Grammatica, *Gazz. Chim. Ital.*, 114 (1984) 189.
[8] D. Basker and M. Negbi, *J. Assoc. Publ. Anal.*, 3 (1985) 65.
[9] H. Himeno and K. Sano, *Agric. Biol. Chem.*, 51 (1987) 2395.
[10] V. Sujata, G.A. Ravishankar and V.L. Venkataraman, *J. Chromatogr.*, 624 (1992) 497.
[11] K.A. Steinmetz, J.D. Potter and A.R. Foloson, *Cancer Res.*, 53 (1993) 536.
[12] W. Stahl, A.S. Sundquist, M. Hanusch, W. Schwarz and H. Sies, *Clin. Chem.*, 39 (1993) 810.
[13] S.C. Nair, B. Pannikar and K.R. Panikkar, *Cancer Lett.*, 57 (1991) 109.

[14] H. Morjani, P. Tarantilis, M. Polissiou and M. Manfait, *Anticancer Res.*, 10 (1990) 1398.
[15] P. Tarantilis, M. Polissiou, H. Morjani, P. Avot, A. Bel Jebbar and M. Manfait, *Anticancer Res.*, 12 (1992) 1889.
[16] M. Frutos, J. Sanz and I. Martinez-Castro, *Chromatographia*, 25 (1988) 861.
[17] W. Rodel and M. Petrzika, *J. High Resolut. Chromatogr.*, 14 (1991) 771.
[18] A.G.H. Lea, in R. Macrae (Editor), *HPLC in Food Analysis*, Academic Press, London, 2nd ed., 1988, Ch. 8, p. 277.
[19] C.A. O'Neil and S.J. Schwartz, *J. Chromatogr.*, 624 (1992) 235.
[20] R.C. Mordi, *Chem. Ind. (London)*, (1993) 79.
[21] E. Lesellier, A. Tchapla, C. Marty and A. Lebert, *J. Chromatogr.*, 633 (1993) 9.

ELSEVIER

Journal of Chromatography A, 664 (1994) 63–70

JOURNAL OF CHROMATOGRAPHY A

HPLC purification and separation of 5,5′-substituted-2,4-imidazolidinedithiones

J.C. Hill, G.M. Flannery, B.A. Fraser*

Division of Cytokine Biology, Center for Biologics Evaluation and Research, Food and Drug Administration, 8800 Rockville Pike, Bethesda, MD 20892, USA

(First received October 18th, 1993; revised manuscript received November 30th, 1993)

Abstract

Several 5,5′-substituted-2,4-imidazolidinedithiones, synthesized from aldehydes or ketones, have been purified by HPLC using poly(styrene–divinylbenzene) packings. Purified 5,5′-substituted-2,4-imidazolidinedithiones have been identified in column effluent by UV absorbance and corroborated by mass spectrometry. Several silica-based, polymeric, and poly(styrene–divinylbenzene)-based packings were evaluated as matrices for resolution of a mixture of purified 5,5′-substituted-2,4-imidazolidinedithiones.

1. Introduction

The 5,5′ - substituted - 2,4 - imidazolidinedithiones (2,4-dithiohydantoins) have proven to be of interest in several areas. These compounds are analogues of various drugs, such as phenytoin (5,5′-diphenyl-2,4-imidazolidinedione) [1], and have been evaluated as potential therapeutics [2]. As a synthetic tool, 5,5′-substituted-2,4-imidazolidinedithiones have been used to assist the curing of halogenated polymers [3].

Synthesis of 5,5′-substituted-2,4-imidazolidinedithiones from ketones was initially reported by Carrington [4]. This synthesis was a modification of that method developed by Bucherer and Steiner [5] for synthesis of imidazolidinediones (hydantoins) from ketones, sodium cyanide, and ammonium carbonate. Carrington observed that replacement of sodium cyanide with ammonium cyanide and replacement of ammonium carbonate with carbon disulfide lead to the synthesis of 5,5′-substituted-2,4-imidazolidinedithiones. Using this synthetic approach, many 5,5′-substituted-2,4-imidazolidinedithiones have been made from ketones [4] and aldehydes [6].

While numerous papers report on the synthesis and characterization of these compounds [4,6–8], no methods have been published for their HPLC purification. Our need for reference materials necessitated the development of an HPLC method for the purification of 5,5′-substituted-2,4-imidazolidinedithiones. The reported molar absorptivity, on the order of 27 000 at 296 nm [8], made these compounds suitable candidates for UV detection after HPLC separation. This paper reports on methods for both preparative and analytical HPLC purification of 5,5′-substituted-2,4-imidazolidinedithiones. Verification of 5,5′-substituted-2,4-imidazolidinedithiones in HPLC fractions by ^{252}Cf plasma de-

* Corresponding author.

0021-9673/94/$07.00
SSDI 0021-9673(93)E1283-6

sorption time-of-flight mass spectrometry is also described. Additionally, a mixture was formulated from the purified 5,5′-substituted-2,4-imidazolidinedithiones and then used to assess the ability of several different column packings to resolve the mixture.

2. Experimental

2.1. Materials

Aldehydes (acetaldehyde, 2-methylbutyraldehyde, 2-ethylbutyraldehyde, octyl aldehyde), ketones (acetone, 2-butanone), and other chemicals were purchased from Aldrich (Milwaukee, WI, USA) in the highest purity available. All solvents were HPLC grade. Chromatography was conducted on a Hewlett-Packard (Avondale, PA, USA) 1050 HPLC system with autosampler and variable wavelength detector. Semi-preparative (30.5 × 0.7 cm) and analytical (15 × 0.41 cm) 10-μm poly(styrene–divinylbenzene) PRP-1 columns were obtained from Hamilton (Reno, NV, USA). An analytical (15 × 0.46 cm) 3-μm polymeric C_{18} column was purchased from Interaction (San Jose, CA, USA). Analytical Cyano (20 × 0.46 cm) 5-μm, Amino (22 × 0.46 cm) 5-μm, and Velosep C_{18} (10 × 0.32 cm) 3-μm silica columns were purchased from Brownlee (San Jose, CA, USA).

2.2. Synthesis of 5,5′-substituted-2,4-imidazolidinedithiones

The 5,5′ - substituted - 2,4 - imidazolidinedithiones were synthesized from their respective aldehydes or ketones following that chemistry described by Carrington [4]. The proposed reaction scheme [8] is illustrated in Fig. 1. Equimolar amounts of the selected aldehyde or ketone, sodium cyanide, ammonium sulfate, and carbon disulfide were added to a reaction vessel and covered with an excess of ethylene glycol dimethyl ether (glyme)/1,1,2-trichlorotrifluoroethane (1:2, v/v). This mixture was refluxed overnight with mixing. The solvent was removed from the reaction mixture in a rotary evaporator. Three washes with methyl formate, followed by drying, removed excess cyanide. The reaction mixture was then suspended in methanol and filtered; the 5,5′-substituted-2,4-imidazolidinedithione was precipitated upon addition of an excess of 10 *M* HCl. The 5,5′-substituted-2,4-imidazolidinedithione was then isolated by vacuum filtration and recrystallized from methanol.

2.3. Purification of 5,5′-substituted-2,4-imidazolidinedithiones

Initial purification of each 5,5′-substituted-2,4-imidazolidinedithione was achieved using a Hamilton 10 μm PRP-1 column (30.5 × 0.7 cm). Solvent A was methanol–glyme–water (3:3:44, v/v/v) and solvent B was methanol–glyme–water–acetonitrile (5:6:2:37, v/v/v/v). The elution program was: 100% A for 10 min, 0–100% B from 10 to 80 min, 100% B from 80 to 90 min, returning to 100% A from 90 to 120 min. Samples for injection were prepared by suspending recrystallized 5,5′-substituted-2,4-imidazolidinedithione in methanol such that a 1:100 dilution of the resulting solution gave an absorbance at 296 nm of 0.2 to 0.3 AU. The

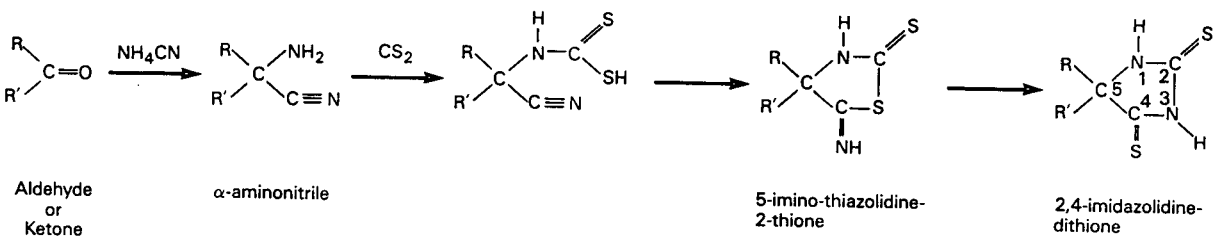

Fig. 1. Reaction scheme for synthesis of 5,5′-substituted-2,4-imidazolidinedithiones.

column was maintained at 40°C; the effluent was monitored at 296 ± 2 nm; the injection volume was 500 μl; the flow rate was 1 ml/min; and V_0 was 4 ml. Fractions were collected at 1-min intervals with a Gilson 201 fraction collector (Middleton, WI, USA). The 5,5′-substituted-2,4-imidazolidinedithione was initially identified by its absorbance at 296 nm and corroborated by mass spectrometry.

Those fractions containing the 5,5′-substituted-2,4-imidazolidinedithione were pooled, dried *in vacuo*, and further purified using a Hamilton 10-μm, PRP-1 column (15 × 0.41 cm). Solvent A was methanol–glyme–acetonitrile–water (2:3:4:41, v/v/v/v) and solvent B was methanol–glyme–acetonitrile–water (3.4:4.1:16.1:26.4, v/v/v/v). The elution program was: 100% A for 5 min, 0–100% B from 5 to 60 min, 100% B from 50 to 60 min, return to 100% A from 60 to 70 min, and equilibrate at 100% A from 70 to 80 min. Samples for injection were prepared by suspending the dried fractions in methanol such that a 1:10 dilution of the resulting solution gave an absorbance at 296 nm of 0.1 to 0.2 AU. The column was maintained at 40°C; the effluent was monitored at 296 ± 2 nm; the injection volume was 10 μl; the flow rate was 0.5 ml/min; and V_0 was 2 ml. Fractions were collected every minute; the 5,5′-substituted-2,4-imidazolidinedithione was identified by its absorbance at 296 nm and corroborated by mass spectrometry.

2.4. Mass spectrometry

Fractions collected from HPLC effluent, which potentially contained 5,5′-substituted-2,4-imidazolidinedithiones based on their absorbance at 296 nm, were pooled, dried *in vacuo*, and suspended in methanol. As noted by Edward [8], 5,5′-substituted-2,4-imidazolidinedithiones are oxidizable, high melting anions. Based on this information we chose to screen the UV absorbing fractions for the presence of 5,5′-substituted-2,4-imidazolidinedithiones using a ^{252}Cf plasma desorption time-of-flight mass spectrometer (Foster City, CA, USA) under negative ionization. A portion (1%) of each pool was applied to an aluminum–mylar foil and allowed to dry. The foils were then loaded into the mass spectrometer. Data were acquired for 1 000 000 fissions at −10 kV acceleration potential.

3. Results

3.1. Purification of 5,5′-substituted-2,4-imidazolidinedithiones

The 5,5′-substituted-2,4-imidazolidinedithiones were synthesized following that chemistry outlined in Fig. 1. For each 5,5′-substituted-2,4-imidazolidinedithione, the starting aldehyde or ketone and the substituents at the 5- and 5′-positions are listed in Table 1. The 5,5′-substituted-2,4-imidazolidinedithiones were purified initially by recrystallization from methanol. These crystals were washed with water, dried, and resuspended in methanol.

Next, each 5,5′-substituted-2,4-imidazolidinedithione was purified by semi-preparative HPLC. A representative chromatogram for this purification of a 5,5′-substituted-2,4-imidazolidinedithione after crystallization is presented in Fig. 2A. For this example the starting material was acetone, which reacted with the ammonium cyanide and carbon disulfide to produce 5,5′-dimethyl-2,4-imidazolidinedithione. The absorbance profile, monitored at 296 nm, indicates some column fall-through prior to the initiation of the gradient. Within the gradient, three peaks (identified as peak I, II, and III, respectively) eluted from the column which could correspond to the desired product. For each peak, the corresponding fractions were pooled and sampled for evaluation by mass spectrometry.

Mass spectrometric evaluation of the three peaks was conducted to corroborate the UV absorbance data and aid in selection of that fraction which would be purified further. Of the three fractions evaluated, peak III was the only one found to contain the desired analyte (Fig. 2B). Evident in the mass spectrum is an ion intensity at m/z 159, consistent with loss of a proton from the analyte, corresponding to

Table 1
5,5′-substituted-2,4-imidazolidinedithiones synthesized from aldehydes or ketones

Derivative	Starting material	R groups[a]		Molecular mass
		5	5′	
C1	Acetaldehyde	CH_3–	H–	146
C2	Acetone	CH_3–	CH_3–	160
C3	2-Butanone	CH_3–	CH_3–CH_2–	174
C4	2-Methylbutyraldehyde	CH_3–CH_2–$CH(CH_3)$–	H–	188
C5	2-Ethylbutyraldehyde	CH_3–CH_2–$CH(CH_2CH_3)$–	H–	202
C7	Octyl aldehyde	CH_3–$(CH_2)_6$–	H–	230

[a] See Fig. 1 for structure of 5,5′-substituted-2,4-imidazolidinedithione.

$(M-H)^-$ (Table 1). Also evident in the mass spectrum are several intensities which correspond to unknown products of the reaction.

The fraction containing the 5,5′-dimethyl-2,4-imidazolidinedithione was further purified by analytical HPLC chromatography, as summarized in Fig. 3A. Evident in the UV tracing, monitored at 296 nm, are peaks at the initiation of the gradient which correspond to the column fall-through. Additionally, material was observed to elute from the column at 20 min. This material was collected for evaluation by mass spectrometry. Comparison of this HPLC profile to that recorded for the separation of the crude reaction mixture (Fig. 2A) shows that there has been a reduction in the complexity of the mixture.

Mass spectrometry of this material, as shown in Fig. 3B, revealed the most intense ion in the mass spectrum to be m/z 159, consistent with $(M-H)^-$ (Table 1). Also evident in the mass spectrum was an ion intensity at m/z 143, which is consistent with $(M-H)^-$ for either a 5,5′-substituted-2-, or a 5,5′-substituted-4-imidazolidinethione. Comparison of this mass spectrum to that obtained at the previous HPLC step, Fig. 2B, indicates that there has been an overall reduction in noise with a corresponding enhancement in signal for the analyte.

For each aldehyde or ketone listed in Table 1, the synthesis, purification, and identification of the corresponding 5,5′-substituted-2,4-imidazolidinedithione were conducted in a manner similar to that described above for the acetone derivative.

3.2. Mixture analysis

A mixture was formulated which contained each of the 5,5′-substituted-2,4-imidazolidinedithiones. Separation of this mixture of 5,5′-substituted-2,4-imidazolidinedithiones on a poly(styrene–divinylbenzene)-based packing is illustrated in Fig. 4. Initiation of the gradient coincides with column fall-through. After this fall-through, the 5,5′-substituted-2,4-imidazolidinedithiones elute from the column in order of increasing aliphatic nature, reflecting the number of carbons at the 5- and 5′- positions. With the exception of a fused doublet for C1 and C2, each component is baseline resolved.

Using this mixture, a variety of column packings, under identical reversed-phase gradient and solvent conditions, were studied to identify that one best suited for the separation of 5,5′-substituted-2,4-imidazolidinedithiones. Analysis of these data, summarized in Table 2, indicates that the polymer-based packings are better at retaining the 5,5′-substituted-2,4-imidazolidinedithion-

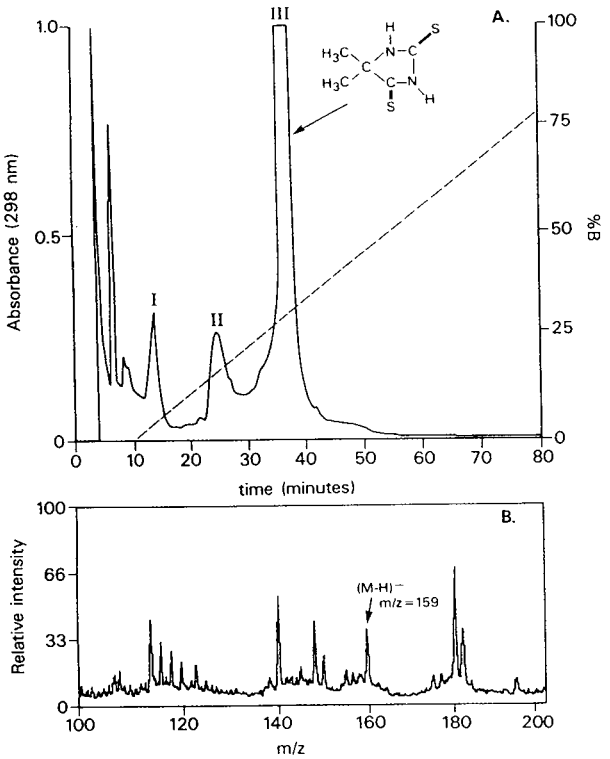

Fig. 2. Separation and characterization of recrystallized 5,5′-dimethyl-2,4-imidazolidinedithione. (A) Chromatogram from semi-preparative purification of 20 μg of 5,5′-dimethyl-2,4-imidazolidinedithione. Stationary and mobile phases, and chromatographic conditions are described in Experimental section. Indicated peaks were sampled for analysis by mass spectrometry. (B) Mass spectrum of HPLC peak III. The ion at m/z 159 is consistent with $(M-H)^-$, loss of a proton from the analyte.

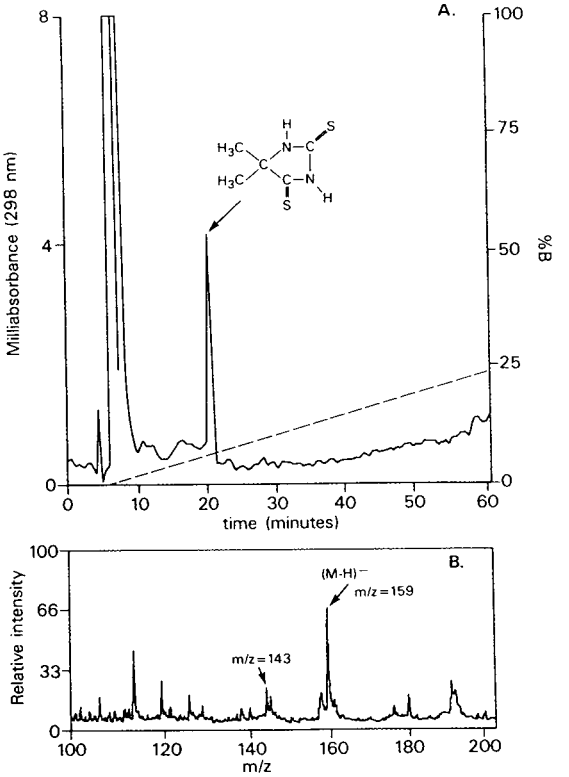

Fig. 3. Separation and characterization of purified 5,5′-dimethyl-2,4-imidazolidinedithione. (A) Chromatogram from analytical purification of 90 ng of 5,5′-dimethyl-2,4-imidazolidinedithione obtained from semi-preparative purification. Indicated peak was sampled for analysis by mass spectrometry. Stationary and mobile phases, and chromatographic conditions are described in Experimental section. (B) Mass spectrum of HPLC peak. The ion at m/z 159 is consistent with $(M-H)^-$, loss of a proton from 5,5′-dimethyl-2,4-imidazolidinedithione; the ion at m/z 143 is consistent with $(M-H)^-$ for a 5,5′-dimethyl-2- or a 5,5′-dimethyl-4-imidazolidinethione.

es than the silica-based packings. Examination of the data from the silica-based packings also indicates that, as the retentive strength of the bonded phase decreases [9], the retention of the more aliphatic 5,5′-substituted-2,4-imidazolidinedithiones also decreases. This trend is not as pronounced for the polymer-based packings. For the solvent and gradient conditions employed, the best peak shapes were obtained from the PRP-1 poly(styrene–divinylbenzene) packing; the other polymeric packing exhibited notable peak broadening and trailing. Based on analysis of these data, the PRP-1 packing appears to be best for separation of a mixture of 5,5′-substituted-2,4-imidazolidinedithiones.

4. Discussion

The available literature indicates that little has been reported about the chromatographic purification of 5,5′-substituted-2,4-imidazolidinedithiones. Carrington, in his initial studies [4], had

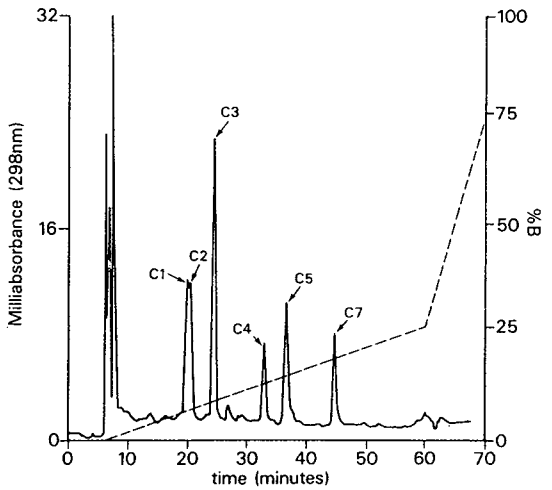

Fig. 4. Separation of a mixture of 5,5′-substituted-2,4-imidazolidinedithiones (250 ng C1, 275 ng C2, 575 ng C3, 200 ng C4, 400 ng C5, and 275 ng C7). Stationary phase: Hamilton, 10 μm, PRP-1 column (0.41 × 15 cm). Solvent A: methanol–glyme–acetonitrile–water (2:3:4:41, v/v/v/v), solvent B: methanol–glyme–acetonitrile–water (3.4:4.1:16.1:26.4, v/v/v/v).

explored the use of carbon as a means for removing contaminants from the derivatives, only to abandon this approach in later studies in favor of recrystallization from methanol [4]. Chubb and Edward [10] attempted to isolate the imine precursor of these compounds from a reaction mixture by chromatography on Florisil. This isolation attempt failed and the failure was attributed to the possibility that the precursor rearranged to form the product on the Florisil. These attempts at purifying or isolating compounds from the reaction mixture suggested that some type of phase chromatography might be useful for the purification of 5,5′-substituted-2,4-imidazolidinedithiones. Our attempts to develop normal-phase HPLC chromatographic methods for the purification of the derivatives from the reaction mixture, following the guidelines described by Snyder *et al.* [11,12], were unsuccessful at either purifying the derivatives or resolving a mixture of the derivatives (unpublished data).

Even though a practical method for the normal-phase HPLC purification and separation of 5,5′-substituted-2,4-imidazolidinedithiones was not found, some important information about the solubility of the derivatives was obtained. The derivatives were observed to be soluble primarily in alcohols, non-aqueous organic acids, organic bases, and ethers. Attempts to mix various other solvents (*i.e.*, water or non-polar compounds) with solutions of the derivatives resulted in precipitation of the derivatives. The optimum solubility of the derivatives was empiri-

Table 2
Adjusted retention volumes for 5,5′-substituted-2,4-imidazolidinedithiones separated from a mixture using different HPLC column packings

Derivative[a]	Retention volume, V'_R (ml)[b]				
	Si-C_{18} [c]	PS-C_{18} [d]	Si-CN [e]	Si-NH_2 [f]	PS [g]
C1	1.2	6.6	2.8	1.3	6.3
C2	1.2	7.8	2.8	1.4	6.9
C3	1.8	10.1	3.5	1.5	8.9
C4	5.0	12.6	5.5	1.6	13.4
C5	7.3	14.6	7.3	1.7	15.0
C7	12.6	20.8	9.8	1.9	18.7

[a] See Table 1 for definition of derivative code.
[b] Solvents and gradient, held constant for all columns, as described in Experimental.
[c] Brownlee Velosep C_{18} 3 μm, 100 × 3.2 mm.
[d] Interaction Polymeric ACT-1 3 μm, 150 × 4.6 mm.
[e] Brownlee Cyano 5 μm, 200 × 4.6 mm.
[f] Brownlee Spheri-5 amino 5 μm, 220 × 4.6 mm.
[g] Hamilton poly(styrene–divinylbenzene) PRP-1 10 μm, 150 × 4.1 mm.

cally observed to lie within a narrow range of polarity. Based on these observations, attempts were made to develop a reversed-phase HPLC method for the purification of these derivatives.

Initially, reversed-phase separations were hindered by the tendency of the derivatives to precipitate as solvent polarity increased. Using solvents with a polarity such that the derivatives remained soluble, the less aliphatic derivatives were observed to fall through silica packings but retain on polymer packings. Based on this observation, the initial solvent composition was optimized such that the C2 derivative was retained on a semi-preparative, poly(styrene–divinylbenzene)-packed HPLC column. After optimization of the initial solvent, the C7 derivative was used as a reference analyte for formulating a solvent that, under gradient conditions, eluted the more aliphatic derivatives from the poly(styrene–divinylbenzene) packing. These solvents and gradient conditions were used for the semi-preparative purification of 5,5′-substituted-2,4-imidazolidinedithiones. Slight modifications of the solvents and gradient were made to optimize the separation obtained from the analytical, poly(styrene–divinylbenzene)-packed HPLC column.

Development of an HPLC method for purification and identification of 5,5′-substituted-2,4-imidazolidinedithiones was facilitated by the use of mass spectrometry. The 5,5′-substituted-2,4-imidazolidinedithiones exhibit maximum molar absorptivities at 296 nm [8]. The 5,5′-substituted-2- or 5,5′-substituted-4-imidazolidinethiones, reaction side products, exhibit maximum molar absorptivities at 264 nm [8]. High concentrations of 5,5′-substituted-2- or 4-imidazolidinethiones in the crude reaction product can contribute measurable absorbance at 296 nm, complicating correct identification of 5,5′-substituted-2,4-imidazolidinedithiones based on UV absorption data (see Fig. 2A). Mass spectrometric evaluation of collected fractions was used to corroborate those fractions containing 5,5′-substituted-2,4-imidazolidinedithiones based on the theoretical mass of the analyte ion, $(M-H)^-$. Measurable absorbance at 296 nm coupled with a correct mass for the $(M-H)^-$ ion, served to distinguish 5,5′-substituted-2,4-imidazolidinedithiones from 5,5′-substituted-2- or 4-imidazolidinethione side products.

Mass spectrometric evaluation of collected HPLC fractions also allowed for qualitative evaluation of purity. The intent of these evaluations was not to identify reaction side products, but to identify 5,5′-substituted-2,4-imidazolidinedithiones by correlation of expected masses, calculated from the structure of the derivative, with those masses for ions observed in the mass spectra. Purity was assessed as an overall reduction of the number of peaks within the mass spectra, relative to the $(M-H)^-$ ion of interest, as a result of sequential chromatographic steps. As illustrated in Fig. 2A, several peaks eluted from the semi-preparative, poly(styrene–divinylbenzene)-packed HPLC column after the fall-through. All of these peaks exhibited absorbance at 296 nm, especially peak III. Corroboration of peak III as that containing the desired species was made based on its mass spectrum, Fig. 2B. Evident in this mass spectrum is a peak which is consistent with the $(M-H)^-$ ion of the desired compound. Also present in the mass spectrum are numerous other peaks, attributed to products from side reactions. Mass spectrometric evaluation after an additional step of purification (Fig. 3B) indicates that the greatest ion intensity is consistent with the $(M-H)^-$ ion of the desired compound; the number of additional ion intensities is notably reduced.

Development of a reversed-phase purification method using a poly(styrene–divinylbenzene)-packed HPLC column allowed for a comparison of several silica and polymer packings. The objective was to determine which packing afforded the best separation of a mixture of 5,5′-substituted-2,4-imidazolidinedithiones. As summarized in Table 2, packings were selected which covered the full range of reversed-phase interactions [9]. In all cases a mixture, composed of the indicated derivatives, and each individual derivative were analyzed. Retention times were determined from the mixture analysis for all packings except the amino-silica packing, where retention times were determined from the analysis of the individual derivatives.

In the first two columns of Table 2, silica and polymeric C_{18} (highly retentive) packings are compared. Due to the constraints on solvent polarity to maintain the derivatives in solution, the derivatives, especially the less aliphatic ones, are not retained on the silica C_{18} packing to the extent that they are retained on the polymeric C_{18} packing. For the more aliphatic derivatives an increase in retention volume follows increasing methylene substitution at C5 of the 5,5′-substituted-2,4-imidazolidinedithiones (Table 1). The third column in Table 2 lists data for a cyano-silica packing, which is somewhat less retentive than a C_{18} packing. Analysis of the data shows that overall retention of the derivatives is less, reflecting the decreasing retentive strength; however, the less aliphatic derivatives were retained to a greater extent than on the silica C_{18} packing. The fourth column in Table 2 represents a further reduction of the retentive strength of the packing material. For the amino-silica packing, the retention volumes for the derivatives are nearly similar. Finally, the fifth column in Table 2 contains data from a poly-(styrene–divinylbenzene) packing. Retention of the less aliphatic compounds is similar to that observed for the polymeric C_{18} packing, but the retention volumes are slightly less for the more aliphatic derivatives. From these data one can speculate that the 5,5′-substituted-2,4-imidazolidinedithiones perhaps interact with the poly-(styrene–divinylbenzene) packings through the 5-membered ring, elution of the less aliphatic derivatives from the packing being strongly influenced by this interaction; whereas elution of the more aliphatic derivatives is less influenced by this interaction and more influenced by their aliphatic side chain. The crossover between these two modes of interaction appears to occur between the C3 and C4 derivatives.

5. Conclusion

Using the chemistry described by Carrington [4], several 5,5′-substituted-2,4-imidazolidinedithiones have been synthesized. Following synthesis, these compounds were purified by reversed-phase HPLC using poly(styrene–divinylbenzene)-packed HPLC columns, following the methods described in this paper. The identity of each purified 5,5′-substituted-2,4-imidazolidinedithione was established by UV absorbance at 296 nm and corroborated by time-of-flight ^{252}Cf plasma desorption mass spectrometry. This is the first time that methods for HPLC purification and separation of 5,5′-substituted-2,4-imidazolidinedithiones have been reported. The chromatographic procedures described in this paper should facilitate further analysis and characterization of this class of compounds.

6. References

[1] J. Philip, I.J. Holcomb and S.A. Fusari, in K. Florey (Editor), *Analytical profiles of Drug Substances*, Academic Press, New York, 1984, pp. 417–445.
[2] H.R. Henze and P.E. Smith, *J. Amer. Chem. Soc.*, 65 (1943) 1090–1092.
[3] A. Suzui and Y. Matoba, *German Pat.*, DE 3107940 A1, January 14, 1982.
[4] H.C. Carrington, *J. Chem. Soc.*, (1947) 681–683.
[5] H.T. Bucherer and W. Steiner, *J. Prakt. Chem.*, 140 (1934) 291–316.
[6] A.H. Cook, I. Heilbron and A.L. Levy, *J. Chem. Soc.*, (1947) 1598–1609.
[7] A.H. Cook, I. Heilbron and A.L. Levy, *J. Chem. Soc.*, (1948) 201–206.
[8] J.T. Edward, in N. Kharasch and C.Y. Meyers (Editors), *The Chemistry of Organic Sulfur Compounds*, Vol. 2, Pergamon Press, New York, 1966, Ch. 11, pp. 287–309.
[9] L.R. Snyder, J.L. Glajch and J.J. Kirkland, *Practical HPLC Method Development*, John Wiley and Sons, New York, 1988, p. 67.
[10] F.L. Chubb and J.T. Edward, *Can. J. Chem.*, 59 (1981) 2724–2728.
[11] L.R. Snyder and J.J. Kirkland, in *Introduction to Modern Liquid Chromatography*, John Wiley and Sons, New York, 1979, Ch. 7.
[12] L.R. Snyder, J.L. Glajch and J.J. Kirkland, *in Practical HPLC Method Development*, John Wiley and Sons, New York, 1988, Chs. 4, 5, and 9.

Journal of Chromatography A, 664 (1994) 71–76
Elsevier Science Publishers B.V., Amsterdam

CHROM. 25 629

Gas–liquid chromatographic study of thermodynamics of solution of some alkanes on liquid crystal stationary phases

Albertine E. Habboush*, Sabri M. Farroha and Abdul-Latif Y. Kreishan

Chemistry Department, College of Science, University of Baghdad, Jadiriya, Baghdad (Iraq)

(First received March 25th, 1993; revised manuscript received October 4th, 1993)

ABSTRACT

A gas–liquid chromatographic study of the interaction and elution characteristics of C_5–C_9 normal, branched and cyclic alkanes using liquid crystalline stationary phases and at different column temperatures of 60–100°C for *p*-(*n*-hexyloxy)phenyl *p'*-methoxybenzoate and 90–150°C for *p*-pentyloxyphenyl *p'*-ethoxyazoxybenzoate as stationary phases is reported. Negligible surface effects at the liquid crystal–solid support interface were ensured using a high loading (20%, w/w) of liquid crystal stationary phase on 80–100-mesh Chromosorb W AW DMCS. The results are interpreted in terms of activity coefficients and related thermodynamic quantities.

INTRODUCTION

Gas–liquid chromatography (GLC) is an effective method for the investigation of the properties of solvents and the behaviour of solutes in liquid crystals. Martire *et al.* [1] established the feasibility of GLC for the thermodynamic investigation of liquid crystals using seven hydrocarbon solutes. Zielinski *et al.* [2] studied the GC and thermodynamics of divinylbenzene separations on 4,4'-dihexoxyazoxybenzene liquid crystal stationary phase. Chow and Martire [3] supported the concept of a two-phase (bulk gaseous phase and bulk liquid crystal phase) GLC partitioning process and hence of negligible surface effects at both the carrier gas–liquid crystal and liquid crystal–solid support interfaces, provided that a liquid crystal film thickness of greater than 1000 Å is present. Later they studied the infinite dilution thermodynamic solution properties of non-mesomorphic solutes in nematogenic liquid crystals [4].

The activity coefficients of *n*-heptane dissolved in 4,4'-dihexyloxyazobenzene obtained from chromatographic measurements showed good agreement with the results obtained by statistical methods [5]. The values of the coefficients are different in particular phases of the liquid crystal [6,7]. Seifert and Kraus [8] investigated the solution behaviour of liquid crystal phases in capillary GC and correlated the partial molar free excess enthalpy differences at the transition temperatures with the heats of transition. Soják *et al.* [9] stated that liquid crystals as stationary phases in GC possess shape-selective separation properties for structural and geometrical isomers of hydrocarbons and the selectivity increases with the high separation efficiency of capillary columns. Soják and co-workers [10,11] investigated the separation of diastereomeric C_8–C_{20} alkanes using mesogenic stationary phases in a

* Corresponding author.

0021-9673/94/$07.00
SSDI 0021-9673(93)E1068-B

capillary GC column. A comparison of the retentions of the diastereomers on mesogenic and non-mesogenic phases showed the effect of mesophase diastereoselectivity.

Coca *et al.* [12] discussed the thermodynamic properties of 22 solutes at infinite dilution in the mesophases of 4,4′-bis(heptyloxy)azobenzene in relation to solute–solvent (liquid crystal) interactions as conditioned by the degree of order in the liquid crystal. Habboush *et al.* [13] dealt with the comparative GC behaviour of liquid crystal and polyester stationary phases at different column temperatures.

The aim of this investigation was to study the thermodynamics of solution in the two liquid crystalline stationary phases using C_5–C_9 normal, branched and cyclic alkanes as model solutes and to correlate the measured thermodynamic quantities and structures of both the stationary phases and solutes.

EXPERIMENTAL

p-(*n*-Hexyloxy)phenyl *p*′-methoxybenzoate and *p*-pentyloxyphenyl *p*′-ethoxyazoxybenzene were used as the stationary phases:

$$CH_3\text{–}O\text{–}C_6H_4\text{–}COO\text{–}C_6H_4\text{–}O\text{–}C_6H_{13}$$

$$K \overset{55°C}{\rightleftharpoons} N \overset{78°C}{\rightleftharpoons} I$$

$$C_2H_5\text{–}O\text{–}C_6H_4\text{–}\overset{\overset{O}{\uparrow}}{N} = N\text{–}C_6H_4\text{–}O\text{–}C_5H_{11}$$

$$K \overset{60°C}{\rightleftharpoons} N \overset{136°C}{\rightleftharpoons} I$$

These phases were kindly prepared in Dr. G. Kraus's laboratory at Martin Luther University (Halle, Germany) for the purpose of thermodynamic studies. The transition temperatures and the purities of the two liquid crystals were determined by differential scanning calorimetry. The measurements yielded estimate purities of 99.7% for the former stationary phase and 99.8% for the latter.

All hydrocarbons and solvents were purchased from Fluka and BDH and Chromosorb from Johns-Manville.

Columns were made of stainless-steel tubing (6 ft. × 0.25 in I.D.; 1 ft. = 30.48 cm, 1 in. = 2.54 cm) and each column was packed with 20% (w/w) of stationary phase on 80–100-mesh Chromosorb W AW DMCS to ensure negligible surface effects on the liquid crystal–solid support and gas–liquid interfaces. Coating of the support was carried out as follows. An accurately known mass of the liquid crystal was dissolved in chloroform and added quantitatively to an accurately known mass of the support already wetted with chloroform in a fluted round-bottomed flask, followed by gradual solvent elimination through rotary vacuum evaporation. The dried coated stationary phase was transferred to a clean bottle and accurately weighed. The columns before packing were thoroughly washed with successive portions of acetone, methanol and diethyl ether. The mass of the loaded liquid crystal was calculated. The packing composition was checked by averaging the results for three separate Soxhlet solvent extractions carried out on a carefully weighed amount of fresh packing. The packed column was then conditioned in the gas chromatograph at a suitable temperature for 12 h with a nitrogen purge prior to use.

A Beckman GC-45 gas chromatograph equipped with a flame ionization detector was used with an optimum carrier gas (nitrogen) flow-rate of 30 ml min^{-1} at NTP. Recording was done on Beckman Model 10 1-mV recorder. Temperature dependence was studied in the crystalline–nematic–isotropic regions at a minimum of six reasonably spaced temperatures.

Normal, branched and cyclic alkanes were uses as sample components. The sample sizes ranged form 0.1 to 0.4 μl. Injections were made with a 1 μl Hamilton syringe. Each individual liquid sample and each mixture was run twice; no differences were found in the retention times when the compounds were injected individually or as a mixture, and the reproducibility was within 1%.

The solute peak retention times past the air peak were determined by taking the averages of at least four measurements obtained on two separate days. Also, early values were reproducible at the end of the experiment within the accuracy of the measurements of 1%. It was established that the solute retention times were independent of sample size, and hence that

operation was taking place in the Henry's law region (*i.e.*, infinite dilution). Further, it was found when an internal standard was used that the relative retention times were independent of the loading (15 and 20% were examined). This confirmed that solute adsorption on the solid support and the gas–liquid interface was negligible.

RESULTS AND DISCUSSION

Specific retention volumes, V_g, were calculated from the corrected peak retention times and the column operating conditions by using the well known equation derived by Littlewood *et al.* [14]. Solute vapour pressures were calculated using Antoine's equations and constants [15]. The solute activity coefficients at infinite dilution, γ^∞, were calculated for the two liquid crystal stationary phases in the temperature range 60–110°C on *p*-(*n*-hexyloxy)phenyl *p'*-methoxybenzoate and 90–150°C on *p*-pentyloxyphenyl *p'*-ethoxyazoxybenzene with 10°C increments from the following equation [16]:

$$\gamma^\infty = \frac{17.04 \cdot 10^7}{M_1 p_2^0 V_g} \quad (1)$$

where M_1 is the molecular mass of the stationary phase and p_2^0 is the vapour pressure of the pure solute vapour (mmHg; 1 mmHg = 133.322 Pa). The logarithms of the solute activity coefficients, γ^∞, obtained were plotted against the reciprocal of the absolute column temperature (Figs. 1 and 2). The partial molar excess enthalpy, ΔH_e^∞, of mixing at infinite dilution were calculated from an equation formulated by Habboush and Al-Bazi [17] for the direct calculation of ΔH_e^∞ from the specific retention volume and vapour pressure of a solute at two temperatures as follows:

$$\Delta H_e^\infty = 2.303R \cdot \frac{T_1 T_2}{T_2 - T_1} \cdot \log\left(\frac{p_2 V_g^{T_2}}{p_1 V_g^{T_1}}\right) \frac{T_1}{T_2} \quad (2)$$

The results are given in Table I. The excess partial molar free energy, ΔG_e^∞, and the partial molar excess entropy, ΔS_e^∞, of mixing at infinite dilution were calculated using the following equations:

TABLE I

EXCESS MOLAR ENTHALPY, ΔH_e^∞, (kcal/mol) AND ENTROPY, ΔS_e^∞ (cal/mol·K) OF ALKANES ON THE TWO LIQUID CRYSTAL STATIONARY PHASES

1 cal = 4.184 J.

No.	Compound	*p*-Pentyloxyphenyl *p'*-ethoxyazoxybenzene				*p*-(*n*-Hexloxy)phenyl *p'*-methoxybenzoate			
		Mesophase		Isotropic		Mesophase		Isotropic	
		ΔH_e^∞	ΔS_e^∞	ΔH_e^∞	ΔS_e^∞	ΔH_e^∞	ΔS_e^∞	ΔH_e^∞	ΔS_e^∞
1	Pentane	9.17	24.87	2.88	6.62	4.35	13.30	2.40	6.50
2	Hexane	4.34	12.44	3.91	9.63	5.97	18.43	1.92	5.95
3	Heptane	4.20	12.46	3.84	9.87	4.93	15.70	1.09	3.70
4	Octane	4.65	13.94	4.14	10.88	4.64	15.05	3.80	11.15
5	Nonane	3.68	11.51	3.96	10.65	8.00	25.21	2.47	7.92
6	2,4-Dimethylpentane	4.97	14.37	2.23	5.75	2.71	9.22	2.31	6.91
7	2,3-Dimethylpentane	4.54	13.23	3.67	9.37	4.25	13.70	2.79	8.14
8	2,2,4-Trimethylpentane	4.71	13.96	3.80	9.87	4.44	14.51	2.96	8.83
9	2,4-Dimethylhexane	4.95	14.72	3.92	10.24	4.78	15.50	3.04	9.12
10	3-Methylheptane	4.66	13.95	3.02	8.10	5.20	16.69	3.54	10.43
11	Cyclopentane	3.82	10.57	4.05	9.59	4.48	13.62	1.30	3.56
12	Cyclohexane	4.31	12.32	3.10	7.66	4.96	15.38	1.08	3.27

TABLE II

EXCESS FREE ENERGY, ΔG_0^∞ (cal/mol) OF ALKANES ON *p*-(*n*-HEXYLOXY)PHENYL *p'*-METHOXYBENZOATE AT DIFFERENT TEMPERATURES

No.	Compound	60°C	70°C	80°C	90°C	100°C	110°C
1	Pentane	268	210	133	77	22	−15
2	Hexane	428	354	279	227	182	154
3	Heptane	512	454	369	337	285	270
4	Octane	575	523	436	395	357	348
5	Nonane	649	647	556	548	486	460
6	2,4-Dimethylpentane	481	451	341	298	270	283
7	2,3-Dimethylpentane	499	449	350	295	243	207
8	2,2,4-Trimethylpentane	585	535	436	381	329	294
9	2,4-Dimethylhexane	592	538	432	392	358	322
10	3-Methylheptane	585	526	433	388	384	337
11	Cyclopentane	252	192	110	62	27	2
12	Cyclohexane	371	309	224	189	137	118

$$\Delta G_e^\infty = RT \ln \gamma^\infty \quad (3)$$

$$\Delta G_e^\infty = \Delta H_e^\infty - T\,\Delta S_e^\infty \quad (4)$$

$$\ln \gamma^\infty = \frac{\Delta H_e^\infty}{RT} - \frac{\Delta S_e^\infty}{R} \quad (5)$$

as given by Langer and Purnell [18]. The data are given in Tables II and III.

The values of the activity coefficients obtained are >1 except for pentane on *p'*-pentyloxyphenyl *p'*-ethoxyazoxybenzene in the temperature range 120–150°C, which indicates a positive deviation from ideality. Inspection of the plots of log γ^∞ *versus* $1/T$ (Figs. 1 and 2) illustrates that at the transition temperatures both a discontinuity and a change in slope occur, indicating that the solute molecules experience a marked change in environment as they enter a new phase, *i.e.*, the interaction of solutes with the solvent in the mesophase region differs from the interaction in the isotropic liquid. Further, the activity coefficients of *n*-alkanes in the two stationary phases decrease in the order nonane > octane > heptane > hexane > pentane.

Inspection of the values of the partial molar excess free energy of mixing at infinite dilution,

TABLE III

EXCESS FREE ENERGY, ΔG_e^∞ (cal/mol) OF ALKANES ON *p*-PENTYLOXYPHENYL *p'*-METHOXYAZOXYBENZENE AT DIFFERENT TEMPERATURES

No.	Compound	90°C	100°C	110°C	120°C	130°C	140°C	150°C
1	Pentane	154	105	46	−11	−68	−151	−194
2	Hexane	351	296	248	97	143	68	20
3	Heptane	494	446	402	355	297	230	186
4	Octane	608	546	512	459	418	350	307
5	Nonane	663	616	594	557	510	435	396
6	2,4-Dimethylpentane	459	392	347	292	225	146	117
7	2,3-Dimethylpentane	470	391	369	313	247	202	143
8	2,2,4-Trimethylpentane	556	497	455	400	335	274	232
9	2,4-Dimethylhexane	599	538	495	443	384	303	260
10	3-Methylheptane	602	543	506	455	400	320	288
11	Cyclopentane	168	114	68	12	−15	−93	−147
12	Cyclohexane	339	283	237	187	140	66	26

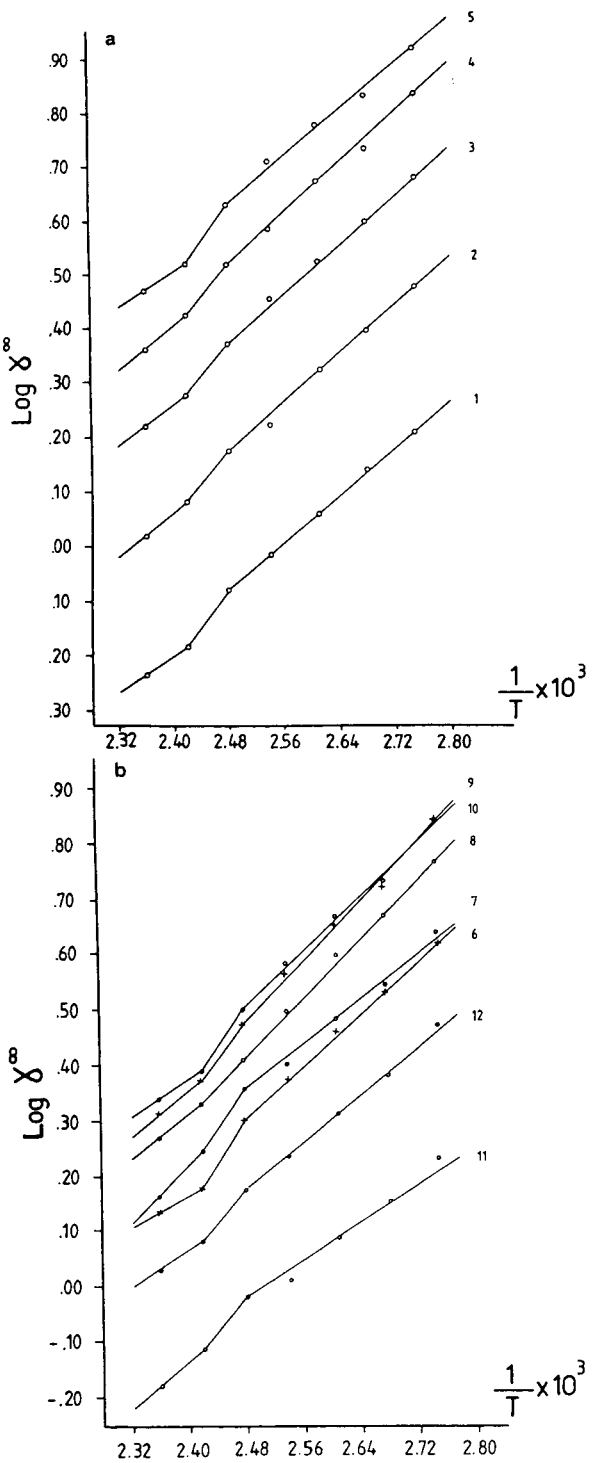

Fig. 1. (a) Plot logarithm of the activity coefficients of (a) *n*-alkanes and (b) branched and cyclic alkanes *versus* reciprocal of absolute temperature on *p*-pentyloxyphenyl *p'*-ethoxyazoxybenzene. The numbering is as in Table I.

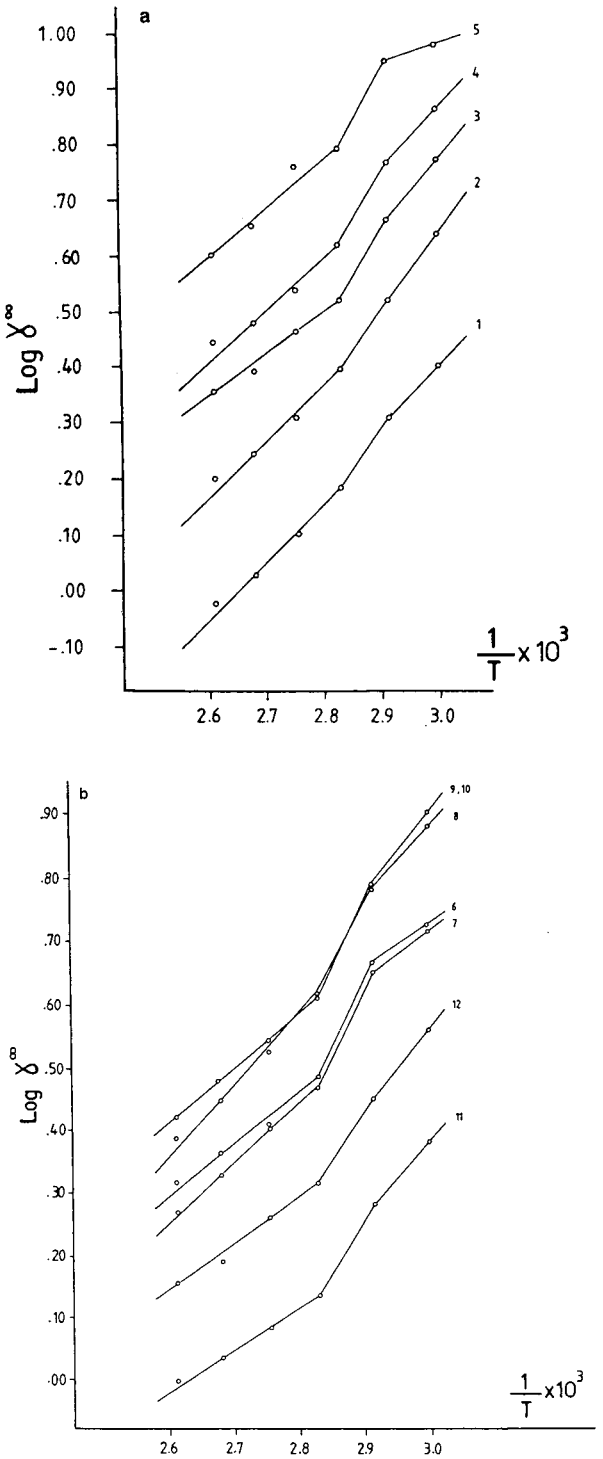

Fig. 2. (a) Plot of logarithm of the activity coefficients of (a) *n*-alkanes and (b) branched and cyclic alkanes *versus* reciprocal of absolute temperature on *p*-(*n*-hexyloxy)phenyl *p'*-methoxybenzoate. The numbering is as in Table 1.

ΔG_e^∞, of paraffins in the two liquid crystalline stationary phases in Tables II and III reveals that free energy differences exist and are appreciable. The probable reason is that alkane molecules must "straighten out" and "stiffen up" to offer the maximum interaction cross-section to the rod-like liquid crystal molecules [1,2].

The results in Table I show that the excess molar enthalpies are positive in both phases, which indicates a strong endothermic mixing effect. It is also clear from Table I that the excess molar enthalpies in the mesophase region are greater than in the isotropic melt, which means that the solution process in an anisotropic liquid needs more energy because of the difficulty of dissolving molecules in a highly ordered structure [19–21].

It is also clear from Table I that the excess molar enthalpies, ΔH_e^∞, are accompanied by high positive entropies, ΔS_e^∞.

REFERENCES

1 O.E. Martire, P.A. Blasco, P.F. Carone, L.C. Chow and H. Vicini, *J. Phys. Chem.*, 72 (1968) 3489.
2 W.L. Zielinski, D.H. Freeman, D.E. Martire and L.C. Chow, *Anal. Chem.*, 42 (1970) 176.
3 L.C. Chow and D.E. Martire, *J. Phys. Chem.*, 73 (1969) 1127.
4 L.C. Chow and D.E. Martire, *J. Phys. Chem.*, 75 (1971) 2005.
5 H.T. Peterson, D.E. Martire and W. Linder, *J. Phys. Chem.*, 76 (1972) 596.
6 A.A. Jeknavorian, P. Barrett, A.C. Watterson and E.F. Barry, *J. Chromatogr.*, 107 (1975) 317.
7 J.F. Bocquet and C. Pommier, *J. Chromatogr.*, 117 (1976) 315.
8 K. Seifert and G. Kraus, *J. Chromatogr.*, 192 (1980) 97.
9 L. Soják, G. Kraus, P. Farkaš and I. Ostrovský, *J. Chromatogr.*, 294 (1984) 155.
10 L. Soják, I. Ostrovský, P. Farkaš and J. Janák, *J. Chromatogr.*, 356 (1986) 105.
11 L. Soják, I. Ostrovský, G. Kraus and I.G. Andronikashvili, *J. Chromatogr.*, 436 (1988) 47.
12 J. Coca, I. Melina and S.H. Langer, *Chromatographia*, 25 (1988) 825.
13 A.E. Habboush, S.M. Farroha and A.Y. Kreishan, *J. High Resolut. Chromatogr.*, 14 (1991) 242.
14 A.B. Littlewood, C.G. Phillips and D.T. Price, *J. Chem. Soc.*, (1955) 1480.
15 R.R. Dreisbach, *Physical Properties of Chemical Compounds* (*Advances in Chemistry Series*, No. 15), American Chemical Society, Washington, DC, 1955.
16 D.E. Martire and L.Z. Pollara, *Adv. Chromatogr.*, 1 (1966) 335.
17 A.E. Habboush and S.J.S. Al-Bazi, *J. Chromatogr. Sci.*, 16 (1978) 296.
18 S.H. Langer and J.H. Purnell, *J. Phys. Chem.*, 67 (1963) 263.
19 H. Kellar, *Fresenius' Z. Anal. Chem.*, 198 (1963) 254.
20 H. Kelker and H. Winterscheidt, *Fresenius' Z. Anal. Chem.*, 220 (1966) 1.
21 H. Keller and A. Verhelst, *J. Chromatogr. Sci.*, 7 (1969) 79.

ELSEVIER

Journal of Chromatography A, 664 (1994) 77–87

JOURNAL OF CHROMATOGRAPHY A

Determination of selenium by gas chromatography–electron-capture detection using a rapid derivatization procedure

Abdusalam Elaseer*, Graham Nickless

Environmental and Analytical Chemistry Section, School of Chemistry, University of Bristol, Cantock's Close BS8 1TS, UK

(First received August 20th, 1993; revised manuscript received December 3rd, 1993)

Abstract

A rapid method of determination of selenium by gas chromatography with electron-capture detection using 3-bromo-5-trifluoromethyl-1,2-diaminobenzene as complexing ligand was investigated. The temperature-dependent reaction was kinetically evaluated and at 100°C the time for the quantitative formation of piazselenol can be reduced to less than 5 min without any discrepancies in the quantitative determination of selenium. The method was applied to the determination of the organoselenium compounds evolved from incubated sediments. The compounds were separated and identified as dimethylselenide and dimethyldiselenide using GC–MS.

1. Introduction

Selenium is often present in the environment in many forms as a result of microbiological transformation of the inorganic forms to organoselenium species. The concentration of the selenium is of particular concern as there is a narrow range between the essential and toxic concentrations of the element to living organisms. The transformation of inorganic selenium forms to the more volatile but less toxic organoselenium species is an important link in the global cycling of the element [1]. The toxicity of certain inorganic selenium species to some living organisms is some three orders of magnitude greater than alkyl selenides [2]. Toxic levels of selenium can be easily introduced into the food chain through green plants as a result of high plant uptake from contaminated soils, sediments and agricultural drainage water [3]. In recent years, gas chromatography (GC) has been extensively used for the detection and determination of ultra-trace amounts of selenium in such environmental samples. The method is based on the selective complexation of the selenium with the 1,2-diaminobenzene ligand in acidic media to form the piazselenol (**I**). Nakashima and Tôei [4] were the first to demonstrate the unique sensitivity of electron-capture detection (ECD) to the introduction of electron-withdrawing groups substitution into the diaminobenzene ligand (**II**). Since then, various substituted 1,2-diaminobenzenes [4–10] have been examined to increase the ECD sensitivity. Shimoishi [5] synthesized and tested the chromatographic properties of thirteen piazselenol derivatives. He reported that 4,6-dibromopiazselenol had the best sensitivity and distribution ratio. In 1988, Al-Attar and Nickless [10] prepared and demonstrated the supremacy of the 3-bromo-5-trifluoromethyl-1,2-diamino-

* Corresponding author.

0021-9673/94/$07.00
SSDI 0021-9673(93)E0015-M

benzene with respect to the sensitivity, shorter retention time and chromatographic peak shape which made GC–ECD an attractive procedure among the various methods [13–16] used to determine selenium.

Choice of the diamine reagent depends mainly upon the chromatographic properties of the formed piazselenol and the electron-withdrawing groups present. The retention time determines the resolution of the selenium peak from among other peaks of co-extracted materials. The levels of selenium present in environmental samples is likely to be very low, probably at the pg/g level. Therefore, of vital importance is a capability of detecting and determining such levels likely to be present. Any reduction in the time necessary for the quantitative formation of the piazselenol would substantially increase the advantages of the GC–ECD method.

The abbreviations CF_3/Br-PDA and Br_2-PDA refer to the 3-bromo-5-trifluoromethyl-1,2-diaminobenzene and 3,5-dibromo-1,2-diaminobenzene ligands, respectively. Similarly, CF_3/Br-PDSe and Br_2-PDSe refer to the respective piazselenols.

The quantitative formation of piazselenol at room temperature is, however, a time consuming process but the reaction rate is temperature dependent. Therefore, the concept of high-temperature derivatization is a novel and desirable trend. Thus, in 1992. Johansson and Olin [11] successfully derivatized Se(IV) using 3,5-dibromo-1,2-diaminobenzene at 100°C, the quantitative formation of piazselenol being completed in 5 min. In addition, they reported a small loss when extraction of piazselenol was made from large volumes (over 100 ml). However, a standard solution of Se(IV), treated as the sample is recommended for accurate analysis of real samples.

The objectives of the present study were (i) to investigate the possibility of using a high-temperature (≤ 100°C) derivatization step based on the reaction between the Se(IV) and CF_3/Br-PDA as a ligand for the quantitative determination of selenium and (ii) to apply the method to the determination of selenium in the volatilization products resulting from microbiological action on selenium containing sediments.

The CF_3/Br-PDA was preferred to the others ligands proposed in the literature because (a) the limit of detection is in the low pg level of concentration, (b) the piazselenol so formed is stable to an acid-washing procedure required to remove the excess ligand, (c) the reagent is commercially available in fair state of purity, (d) the retention time of the piazselenol is short at reasonable isothermal column temperatures, so minimizing column bleed and consequent contamination of the electron-capture detector and (e) the distribution ratio of the formed piazselenol is high and was verified using standard reference materials producing good results [10]. Quantitative piazselenol extraction is obtainable by a single extraction as will be proved by the present study.

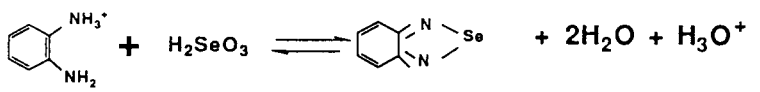

(I)

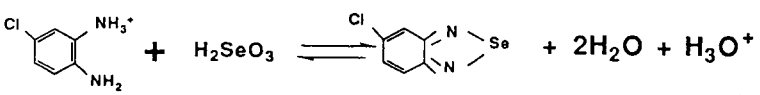

(II)

2. Experimental

2.1. Instrumentation

GC was carried out using a Carlo Erba 4160 gas chromatograph equipped with a nickel-63 electron-capture detector and Hewlett-Packard electronic integrator Model 3390 A.

The piazselenol extracts were separated on 10 m × 0.53 mm fused-silica (film thickness 2.65 μm) HP-1 cross-linked methylsilicone capillary column. Typical separation conditions were: oven temperature, 120°C; injector temperature, 260°C; injection was performed in splitless mode using 1-μl injections. The nickel-63 pulsed electron capture (Carlo Erba HF-25) was used in the constant-current pulse-modulation mode with a pulse voltage of 50 mV, 0.1-μs pulse and reference current of 10 nA. Detector temperature, 250°C; hydrogen was used as a carrier gas at a flow-rate of 10 ml/min and make-up gas was nitrogen at 50 ml/min. The kinetic studies were performed in 1-cm quartz cuvettes using a Pye-Unicam SP-1700 UV spectrophotometer equipped with a thermostatted cell holder.

2.2. Materials

All glassware was washed with detergent solution (Micro-liquid laboratory cleaner), rinsed with tap water, then distilled water and placed in 40% (v/v) nitric acid for at least 48 h. The glassware was finally rinsed with double-distilled water and oven dried at 60°C before use.

All-glass double-distilled water was used for preparing standards and dilutions. AnalaR (BDH, Poole, UK) hydrochloric, perchloric, nitric and formic acids were used without further purification. Reagent-grade elemental selenium, sodium selenite and selenium dioxide were obtained from BDH, 3-bromo-5-trifluoromethyl-1,2-diaminobenzene purchased from Maybridge (Trevillett, Tintagel, UK) was purified and converted to the chloride form by recrystallization from hydrochloric acid [10], 1,2-diamino-3,5-dibromobenzene hydrochloride was obtained from Aldrich, UK.

Solutions of 8.83 m*M* of each of the diamine reagents were prepared by dissolving 0.257 g of CF_3/Br-PDA and 0.267 g of Br_2-PDA in 100 ml of 0.25 *M* HCl and 0.5 *M* $HClO_4$, respectively. The solutions were purified by extraction with 25 ml toluene (AnalaR) and were kept in the dark at 4°C. Further working solutions of both reagents were prepared by appropriate dilution with 0.25 *M* hydrochloric acid.

Selenium(IV) stock solution of 1 mg/ml was prepared from sodium selenite (0.219 g) in 0.25 *M* hydrochloric acid.

A solution of 1 μg/ml Se(IV) was first prepared from selenium stock solution, and from this solution 0.01 μg/ml Se was prepared by serial dilution with 0.25 *M* HCl.

The standard working solutions used for the calibration were prepared as follows: in a series of 10-ml volumetric flasks containing 0.25 *M* HCl, a volume of 100, 200, 300, 400 or 500 μl of 0.01 μg/ml Se standard was added and the volumes were made up with 0.25 *M* HCl.

2.3. Internal standard: lindane

A stock solution of 0.0418 g of 99% lindane obtained from Pan Britannica (Waltham Abbey, UK), was dissolved in AnalaR toluene (100 ml). A series of working standard solutions containing 25 ng/ml of lindane was prepared by serial dilution of the stock standard solution.

2.4. Kinetic experiments

The rate of reaction was followed by adding 0.1 ml of 126.6 μ*M* Se(IV) into a quartz cuvette containing 3 ml of 0.3 m*M* CF_3/Br-PDA preheated to the desired temperature in a thermostatted cell holder. Absorbance measurements of the piazselenol was immediately started and measured every 60 s. The reaction of the selenium(IV) and the CF_3/Br-PDA was followed at the characteristic wavelength 334 nm for the CF_3/Br-PDSe maximum absorbance as indicated by Fig. 1, using temperatures of 20, 40, 60 and 80°C for the kinetic study. The data were collected and printed by automatic recording of

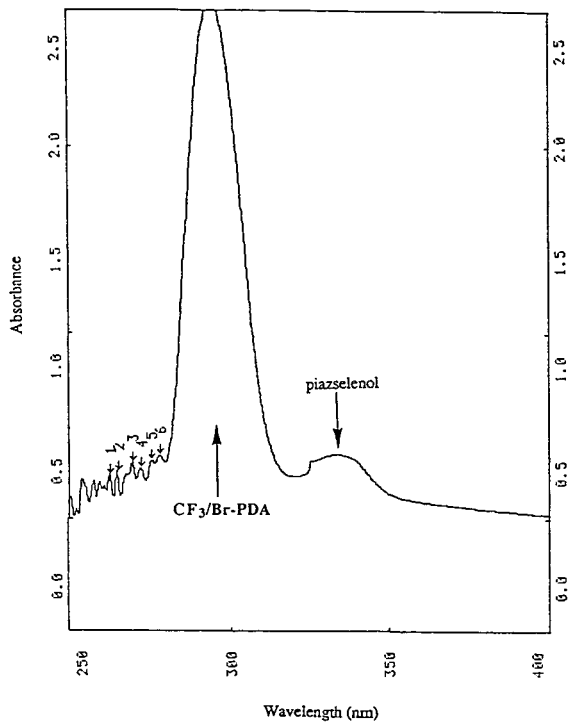

Fig. 1. UV absorption spectrum of 4-bromo-6-trifluoromethylpiazselenol. Maximum absorbance at the analytical wavelength (334 nm).

the absorbance A_{max} of the formed piazselenol using a Philips printer. A non-linear least-squares calculation was implemented. The SAS. NLIN program was used to fit the model to the experimental data [17].

2.5. Derivatization at elevated temperature

A 100 ng/l Se(IV) solution (10 ml) in 0.25 *M* HCl was heated in 20-ml screw-capped vials [18] in a thermostatted water bath at the desired temperature (20–100°C). When the required temperature had stabilized, 0.1 ml of 8.83 m*M* CF_3/Br-PDA was added and the vials were recapped and heated. After $5t_{1/2}$ (where $t_{1/2}$ is the half-life of the CF_3/Br-PDSe reaction), the vials were removed and cooled to room temperature in a cold water bath. The piazselenol formed was extracted as in the general procedure.

2.6. General procedure for extraction of piazselenol

The piazselenol was transferred quantitatively together with 5 ml double-distilled water to a 50-ml separating funnel and 5 ml of toluene (AnalaR) containing 25 ng/ml lindane as an internal standard was added. The mixture was vigorously shaken for 5 min and the aqueous phase discarded. The toluene extracts were washed twice with 3 ml of 50% (v/v) perchloric acid (sp.gr. 1.7 g/ml) and once with double-distilled water, then dried over anhydrous sodium sulphate prior to injection into the GC–ECD.

2.7. Extraction efficiency

The efficiency of a single extraction of the piazselenol was assessed. Thus, a series of piazselenol solutions of volume 20 ml containing varying concentrations of selenium were prepared at 100°C for 5 min, ranging from 0.0, 1.0, 2.0, 3.0, 4.0, to 5.0 ng of Se(IV). Each solution was extracted by the general procedure, and the aqueous solution retained. To this residual aqueous solution were added 0.2 ml of 8.83 m*M* CF_3/Br-PDA solution. The derivatization procedure was carried out at room temperature for the calculated $5t_{1/2}$ for piazselenol formation. The resultant solutions were extracted with 1 ml toluene as in the general procedure, 1 μl was injected for GC–ECD.

In order to test the extraction at successively lower concentrations of selenium, the procedure was repeated twice more. A similar concentration series based either on 100- or 250-ml sample volumes containing up to 5.0 ng of Se(IV) were treated in an exactly similar manner.

2.8. Sediments incubation experiments

The organoselenium compounds were generated from incubated (50 g dry mass) batches of three different sediments collected from River Avon. The sediments were placed in 250-ml Erlenmeyer flasks. A solution mixture of 20 ml containing 5 mg Se(IV) [19], and nutrient broth

(0.5%), D-Glucose (0.1%), yeast extract (0.05%) was added to promote microorganism growth. The flasks were connected to an air flow system at 20 ml/min. The generated organoselenium compounds were trapped in 15 ml nitric acid (AnalaR). The traps were sampled and analysed every 4 to 6 days for Se content using GC–ECD.

2.9. Determination of the evolved organoselenium compounds trapped in nitric acid

The nitric acid sample (1 ml) was mixed with 20 μl of 30% (w/v) hydrogen peroxide in a closed quartz tube and irradiated with a 700-W UV lamp for 3 h to decompose the organoselenium compounds [20]. An aliquot of between 0.25 to 0.5 ml depending on the selenium concentration of the decomposed sample solution together with 1 ml of formic acid [21] (sp.gr. 1.2 g/ml) was transferred to a 150-ml beaker and the nitrate expelled by heating on a boiling water bath until the disappearance of the nitrous fumes. The residue was transferred quantitatively with 4 ml double-distilled water into a 20-ml screw-capped vial. Hydrochloric acid (5 ml), hydrobromic acid (0.5 ml) and 3% (v/v) bromine water (0.05 ml) were added and the vial tightly screw capped. The mixture was heated for 30 min at 100°C to reduce Se(VI) and to oxidize Se(0) and Se(−II) to Se(IV). The vial was removed and hydroxyammonium chloride ($NH_2OH \cdot HCl$, 1 ml of 1 *M* aqueous solution) [22] added to reduce any excess bromine, then 0.5 ml of 8.83 m*M* CF_3/Br-PDA were added and the vial returned to the boiling water bath for a further 5 min. It was then removed, cooled to room temperature in a cold-water bath and the piazselenol was extracted as in the general procedure.

2.10. GC–mass spectrometry (MS)

GC–MS was performed on a Varian 3400 GC system interfaced with a Finnigan ITS 40 ion-trap mass spectrometer. The volatiles were separated on a capillary column, 50 m CP Sil 13, 5 μm film thickness coupled to a 50 m CP Sil 13, 2.5 μm column. Helium was used as carrier gas at 1 ml/min. Temperature programming, 50°C (1 min) increased to 100°C at 10°C/min. The sample was injected through a modified gas loop injector using a gas-tight syringe 50 ml from which only 50 μl were injected through the injector loop. Spectra were acquired in the electron impact (EI) mode, 70 eV, Auto Ion control in Finnigan MAT ion trap; with mass resolution 1 u; electron emission 11 mA; multiplier voltage 1600 V; acquire time 90 min; scanning continuously over a mass range 50–250 u at a rate of 0.599 s/scan; peak threshold 10 counts. Retention times: $(CH_3)_2Se$, 11.4 min (*m/z* 110) and $(CH3)_2Se_2$, 36.5 min (*m/z* 190).

3. Results and discussion

3.1. Rate of reaction

The abbreviations within square brackets, including Se(IV), denote concentrations. In general, diamines which are ionized to a greater extent at low pH should have a faster reaction rate [5]. In the acid concentration 0.01–6 *M* for the high-temperature derivatization the reaction rate is very dependent on (i) the form of the electronegative group attached to the benzene ring and (ii) the concentration ratio of the CF_3/Br-PDA and selenious acid in the reactant mixture.

Comparing Br_2-PDSe and CF_3/Br-PDSe, the CF_3 group is of greater electron-withdrawing ability than Br, so resulting in a more favourable electron density on the N atoms to allow ready reaction with the selenious acid.

In the following section, as will be confirmed by the kinetic results, the expected rate (*r*) equation of piazselenol (Piaz) formation was:

$$r = d[Piaz]/dt = -d[Se(IV)]/dt = K_2'[Se(IV)][CF_3/Br\text{-}PDA] \quad (1)$$

where K_2' is the rate constant.

Under the experimental conditions, and using Ostwald's isolation method, Eq. 1 was experimentally tested using excess reagent. How-

ever, in order to confirm the proposed rate equation, the experimental data were fitted to the integrated second-order rate equation:

$$\ln [\text{Se(IV)}] = \ln [\text{Se(IV)}]_0 - K_2[\text{CF}_3/\text{Br-PDA}]t \quad (2)$$

Eq. 2 is more conveniently expressed as

$$\ln [\text{Se(IV)}] = \ln [\text{Se(IV)}]_0 - kt \quad (3)$$

where $k = K_2[\text{CF}_3/\text{Br-PDA}]$ and $[\text{Se(IV)}]_0$ represents the initial selenium concentration; K_2 is the second order rate constant. In a series of experiments at 20°C, firstly the initial concentration of selenium was varied at constant ligand concentration (Fig. 2). The slopes of the resultant lines are equal. Next the reagent concentration was varied at constant selenium concentration. The k values of the three lines are different depending on the ligand concentration but the K_2 values are the same (Fig. 3). However, the proposed rate equation is confirmed. The second-order rate constants for different temperatures were determined by fitting the experimental results obtained from a series of temperature dependent piazselenol formation curves (Fig. 4) to the negative exponential equation, by non-linear least squares,

$$A_t = A_{\max} - b\, e^{-kt} \quad (4)$$

where A_t = absorbance of the piazselenol at time t and $A_{\max}$ = absorbance of the piazselenol at time infinity.

The results are presented in Table 1.

The activation energy in J mol^{-1} was calculated from the slope of the Arrhenius plot, $\ln K_2$ *vs.* $1/T$ in the temperature-dependent second-order reaction:

$$\ln K_2 = 27.75 - 57\,600/RT \quad (5)$$

Comparison of the CF_3/Br-PDA with the previously evaluated Br_2-PDA ligand [11] shows

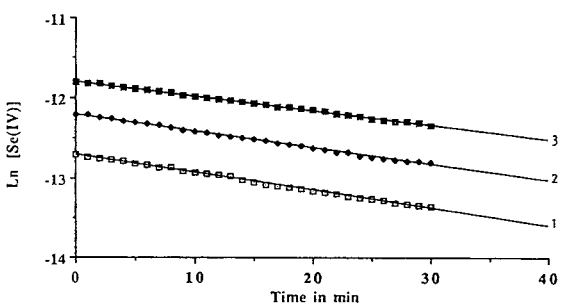

Fig. 2. Determination of the rate constant of CF_3/Br-PDSe formation. The [CF_3/Br-PDA] was kept at 0.29 mM and the [Se(IV)] was varied: 1 = 3.056 μM, 2 = 4.98 μM and 3 = 7.47 μM.

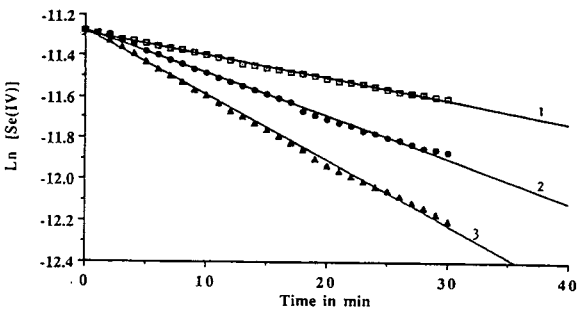

Fig. 3. Determination of the rate constant of CF_3/Br-PDSe formation. The total [Se(IV)] was kept at 12.7 μM and the [CF_3/Br-PDA] was varied: 1 = 0.206 mM, 2 = 0.309 mM and 3 = 0.463 mM.

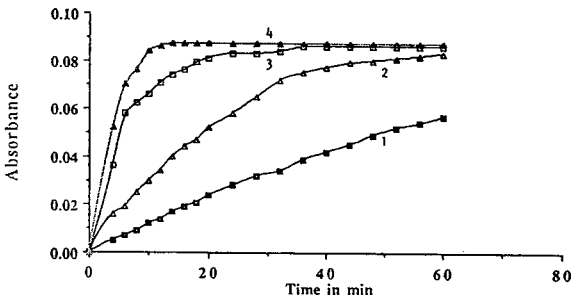

Fig. 4. Determination of the temperature dependence of piazselenol formation, The rate constant was calculated at the following temperatures: 1 = 20°C, 2 = 40°C, 3 = 60°C and 4 = 80°C.

Table 1
The second-order rate constants for varying temperatures

Temperature (°C)	Average K_2(l/mol · min)
20	61 (2)
40	277 (5)
60	1048 (11)
80	3405 (32)

Determined three times with 0.3 mM CF3/Br-PDA and 4.22 μM Se(IV) using absorbance at 334.0 nm.
Values in parentheses are the estimated standard deviations.

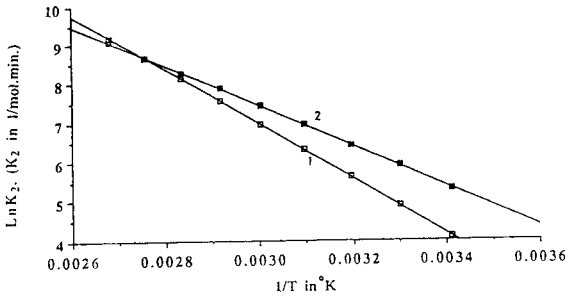

Fig. 5. Determination of Arrhenius activation energy (EA) for CF_3/Br-PDSe by plotting the ln K_2 *vs.* $1/T$. K_2 for Br_2-PDA from ref. 11 for comparison: 1 = CF_3/Br-PDA and 2 = Br_2-PDA.

that the activation energy of the CF_3/Br-PDA is greater, and hence the rate of the reaction is slower as a function of temperature until a temperature of 90°C is reached as indicated in Fig. 5. The determination of the $5t_{1/2}$ value, with 0.1 m*M* CF_3/Br-PDA at 20 to 100°C is presented in Table 2 which indicates that quantitative formation of piazselenol is completed in less than 4 min at 100°C.

3.2. The efficiency of the extraction

An investigation to provide information of the efficiency of a single extraction of the piazselenol was carried out by varying the concentrations of selenium and differing concentration-to-volume ratios. A second extraction of the residual aqueous phase (originally treated at 100°C) with excess ligand at room temperature was carried out. In all cases, no selenium was detected in the analysis of the second toluene extract, even though it was only one fifth of the original volume of toluene used in the general procedure.

So providing an adequate test for both the efficiency of extraction and the quantitative formation of the piazselenol after high-temperature derivatization. Therefore, providing clear evidence that the distribution coefficient for CF_3/Br-PDSe at least as great as that for Br_2-PDSe [11]. Moreover, the room temperature derivatization method previously described [10] provides entirely satisfactory results.

Table 2
The time required for quantitative piazselenol formation

Temperature (°C)	$5t_{1/2}$ (min)
20	564
30	260
40	125
50	63
60	33
70	18
80	10
90	6
100	3.6

Estimated times of 5 half times ($5t_{1/2}$) calculated at 0.1 m*M* CF3/Br-PDA.

3.3. Calibration

In order to evaluate the efficacy of the high temperature derivatization of the CF_3/Br-PDSe method, analyses were performed for known concentrations of Se(IV) contained in the synthesized piazselenol (CF_3/Br-PDSe). The results obtained were compared with those obtained for the identical concentrations of Se derivatized at 100°C for 5 min.

The results obtained are shown in Fig. 6, which indicate quantitative piazselenol formation.

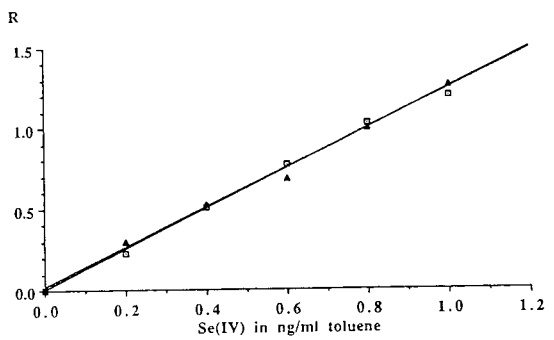

Fig. 6. Calibration plot for piazselenol. Comparison of synthesized piazselenol and 100°C for 5 min derivatized Se(IV). *R* is the area ratio between piazselenol and the internal standard: ▲ = synthesized piazselenol and □ = high-temperature derivatization. $y = 0.0183 + 0.978x$; $r^2 = 0.983$.

3.4. The evolved organoselenium compounds as total selenium

The use of CF_3/Br-PDA reagent facilitates the quantitative detection of the selenium evolved during the course of a few days of incubation. The determination was carried out in a manner in which three possible interferents were considered:

(i) The organoselenium compounds were decomposed for 3 h with UV-irradiation after addition of hydrogen peroxide. However, all the selenium was transferred into inorganic selenium form which forms the basis of the reaction of the diaminobenzene reagent with the selenium.

(ii) The nitrate was expelled to avoid interference [20] with both the reduction of Se(VI) to Se(IV) and oxidation of the diaminobenzene ligand. Any traces were eliminated by addition of hydroxyammonium hydrochloride [22], so allowing all the ligand present to provide quantitative complexation of selenium without loss of any reagent by oxidation.

(iii) The reduction, oxidation of the selenium species to Se(IV) and the high-temperature derivatization were carried out in screw-capped vials to prevent any discrepancies in quantitative selenium determination due to volatilization during the heating process [18]. The digestion method is, however, a collective demonstration of the previously established work, which provided an adequate digestion and suitable reaction media for both reactants. Fig. 7 illustrates a typical GC–ECD chromatogram obtained by the method described in the text.

Quantitation of selenium was carried out using the peak area data obtained from integration. The calibration graph was generated by plotting the peak area ratio *versus* the concentration of the standards. The area ratio of the unknown sample concentration was determined by comparison with the calibration graph using the programmed regression analysis method. The 4-bromo-6-trifluoromethylpiazselenol with capillary GC–ECD gives a linear calibration relationship. The detection limit, 0.083 ng Se/ml was calculated from the calibration graph using the method described by Liteanu and Rica [23].

The results are presented in Table 3.

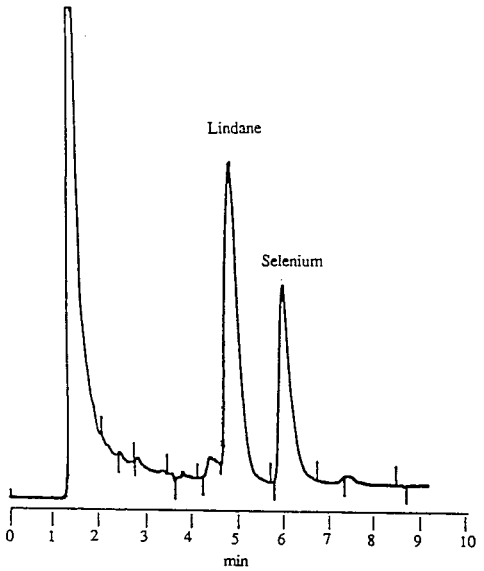

Fig. 7. Chromatogram of toluene extracts of 1 ng Se(IV)/10 ml sample solution with 0.1 m*M* CF_3/Br-PDA at 100°C for 5 min. The piazselenol was extracted with 5 ml toluene containing the internal standard, washed twice with 3 ml of 50% $HClO_4$ and once with double distilled water. The volume of 1 μl was injected in the GC–ECD system.

3.5. Separation and identification of organoselenium compounds

The volatiles above the incubated sediments were separated by withdrawing a 500-μl gas

Table 3
The evolved selenium at selected time intervals

Incubation period in days	Total evolved selenium in μg/kg sediment		
	Raybridge	Staverton	Keynsham
4	143	35	5
6	436	40	7
10	564	56	15
14	572	71	20
20	647	119	23
24	905	ND[a]	ND[a]
28	1125	187	32

Replicate determinations were carried out.
[a] Not determined.

sample with a gas-tight Hamilton 1750 pressure-lock gas syringe and injecting it directly into the GC–flame ionization detection system. The result obtained (Fig. 8) indicates the prominent two peaks at retention times 4 and 9 min. The peaks were identified later as dimethyl selenide and dimethyl diselenide, respectively, using GC–MS. The selenium-containing fragments are often easily recognized in mass spectra from the very characteristic groups of peaks resulting from the typical distribution of the six natural selenium isotopes. However, the peak arising from the most abundant ^{80}Se isotope is in general chosen to represent the selenium-containing fragments. Low-molecular-mass organoselenium compounds are labile towards heat and initial vaporization of the sample gives rise to decomposition before ionization, resulting in separation of the elemental selenium. In such cases the resultant mass spectra shows either no molecular ion or one with very low abundance [24], so explaining the relatively low parent peak of the dimethyl selenide $(CH_3)_2Se$ (reaction 6) obtained from the GC–MS analyses of the volatiles Fig. 9A.

The mass spectra for the dimethyl diselenide $(CH_3)_2Se_2$ shows three fragmentation patterns presented in Fig. 9B, which gives a clear picture of the prominent ^{80}Se isotope indicated by the presence of the appropriate metastable peaks as a result of elimination of a methyl radical from the molecular ion as a dominant process (reaction 7a), forming the fragments at m/z 175 and at m/z 160.

The more complex spectra observed are consequences of the alternative losses of other

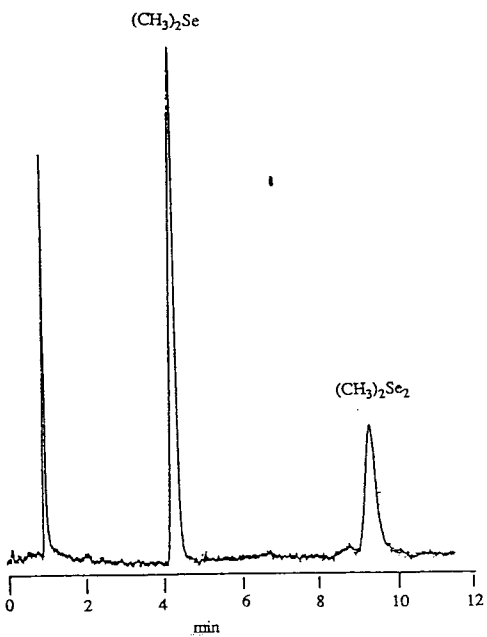

Fig. 8. Chromatogram of the separated organoselenium compounds volatilized from selenium amended sediment. Headspace 500 ml was injected into 20% SE-30 column. Temperature programmed 50°C (2 min) increased by 30°C/min to 120°C, nitrogen flow-rate 30 ml/min using flame ionization detection.

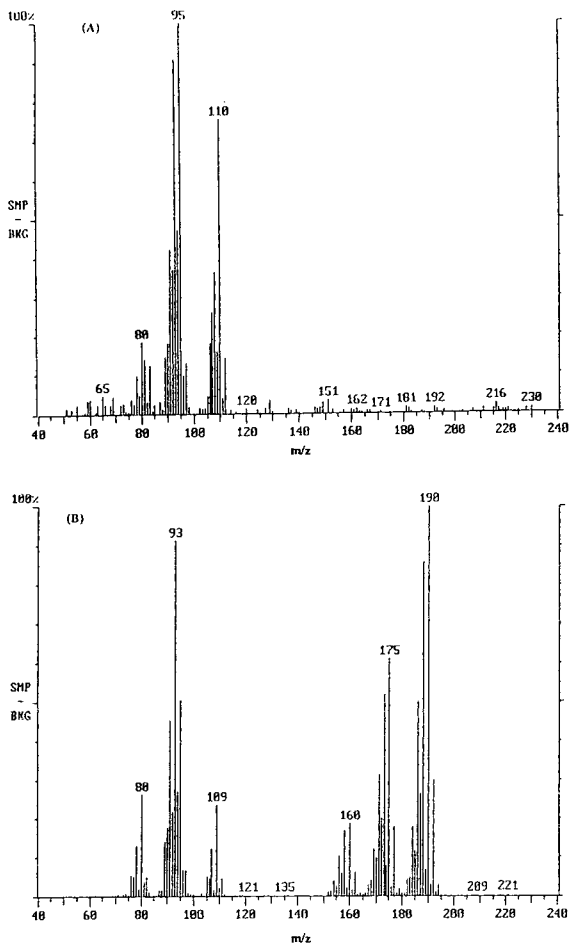

Fig. 9. GC–MS of (A) dimethylselenide and (B) dimethyldiselenide. Y-axis represent relative abundance.

$$[CH_3\text{–}Se\text{–}CH_3]^+ \xrightarrow{-CH_3} [CH_3\text{–}Se]^+ \xrightarrow{-CH_3} [Se]^+ \quad (6)$$
m/z 110 m/z 95 m/z 80

$$[CH_3\text{–}Se\text{–}Se\text{–}CH_3]^+ \xrightarrow{-CH_3} [CH_3\text{–}Se\text{–}Se]^+ \xrightarrow{-CH_3} [Se\text{–}Se]^+ \quad (7a)$$
m/z 190 m/z 175 m/z 160

$$[CH_3\text{–}Se\text{–}Se\text{–}CH_3]^+ \xrightarrow{-HSe} [CH_3\text{–}Se\text{–}CH_2]^+ \xrightarrow{-CH_4} [Se\text{–}CH]^+ \xrightarrow{-CH} [Se] \quad (7b)$$
m/z 190 m/z 109 m/z 93 m/z 80

$$[CH_3\text{–}Se\text{–}Se\text{–}CH_3]^+ \xrightarrow{-CH_3\text{–}Se} [CH_3\text{–}Se]^+ \xrightarrow{-CH_3} [Se]^+ \quad (7c)$$
m/z 190 m/z 95 m/z 80

different groups attached to the selenium atom (reaction 7b), which results in fragmentation at m/z 109 from loss of HSe followed by elimination of CH_4 group at m/z 93. The alternative pattern is the cleavage of the Se–Se bond resulting in fission of the molecule into two halves giving rise to fragment at m/z 95 (reaction 7c).

The clear interpretation from the spectra is the evidence of reactions 7b and 7c proved by the abundance of the prominent peak at m/z 93 from the addition of fragmentation CH–Se at m/z 93 (reaction 7b), of ^{80}Se isotope and the fragmentation of CH_3–Se at m/z 93 (reaction 7c), of isotope ^{78}Se.

4. Conclusions

The proposed procedure for high-temperature derivatization of low levels of selenium with 3-bromo-5-trifluoromethyl-1,2-diaminobenzene has been shown to be simple, rapid, sensitive and precise. The method has obvious advantages over other substituted diaminobenzene ligands, which involves the comparison of the sensitivity, retention time and clean chromatograms.

The method, which has been applied to assess the released organoselenium compounds from sediments should be applicable to the environmental, biological and geological samples.

5. Acknowledgements

The authors wish to acknowledge the award of the Secretariat of Energy (Libya) scholarship to one of them (A.E.) during the tenure of which this research work was carried out and to Dr. A. El-Hassnawi for all his help. They also to express their gratitude to Dr. S.J. O'Doherty for his help with the GC–MS analysis.

6. References

[1] P.J. Craig, in J. Craig (Editor), *Organometallic Compounds in the Environment*, Longman, Harlow, 1986, pp. 1–64.
[2] C.G. Wilber, *Clin. Toxicol.*, 17 (1990) 171.
[3] S.J. Deverel and S.P. Millard, *Distribution and Mobility of Selenium and Other Trace Elements in Shallow Ground Water of the Western San Joaquin Valley, California; Open File Report 86-538*, US Geological Survey, Sacramento, CA, 1986.
[4] S. Nakashima and K. Tôei, *Talanta*, 15 (1968) 1475.
[5] Y. Shimoishi, *J. Chromatogr.*, 136 (1977) 85.
[6] Y. Shimoishi and K. Tôei, *Talanta*, 17 (1970) 165.
[7] T. Stijve and E. Cardinal, *J. Chromatogr.*, 109 (1975) 239.
[8] C.F. Poole, N.J. Evans and D.G. Wibberley, *J. Chromatogr.*, 136 (1977) 73.
[9] S. Dilli and I. Sutikno, *J. Chromatogr.*, 298 (1984) 21.
[10] A.F. Al-Attar and G. Nickless, *J. Chromatogr.*, 440 (1988) 333.
[11] K. Johansson and A. Olin, *J. Chromatogr.*, 598 (1992) 105.
[12] P. Barth, V. Krivan and R. Hausbeck, *Anal. Chim. Acta*, 263 (1992) 111.
[13] Q. Zhang, H.G. Li and Z.Z. Qiao, *Lihua Jianyan, Huaxue Fence*, 28 (1992) 274.
[14] J.A. Blotcky, P.J. Claassen and P.E. Rack, *J. Radioanal. Nucl. Chem.*, 161 (1992) 11.
[15] P. Hitchen, R. Hutton and C. Tye, *J. Autom. Chem.*, 14 (1992) 17.
[16] J.T. Hang, X.Z. Zhang, S.S. Dong and Y. Zhu, *Talanta*, 39 (1992) 1277.

[17] J. Larsson and H. Pardue, *Anal. Chim. Acta*, 224 (1989) 289.
[18] P.S. Brimmer, W.R. Fawcett and A.K. Kulhavy, *Anal. Chem.*, 59 (1987) 1470.
[19] U. Karlson and W.T. Frankenberger, *Soil Sci.*, 149 (1990) 56.
[20] L. Campanella, T. Ferri and R. Morabito, *Analusis*, 17 (1989) 507.
[21] W.R. Wolf, D.E. LaCroix and J. Kochansky, *J. Micronutrient Analysis*, 4 (1988) 145.
[22] H.W. Allaway and E.E. Cary, *Anal. Chem.*, 36 (1964) 1359.
[23] C. Liteanu and I. Rica, *Statistical Theory and Methodology of the Trace Analysis*, Halsted Press/Wiley, Chichester. 1980, pp. 96–97.
[24] L.B. Agenas, in W.H.H. Günther and D.L. Klayman (Editors), *Selenium Compounds, Their Chemistry and Biology*, Wiley, New York, 1973, Ch. XV G, pp. 963–983.

ELSEVIER

Journal of Chromatography A, 664 (1994) 89–98

JOURNAL OF CHROMATOGRAPHY A

Analysis of polymerase chain reaction product by capillary electrophoresis and its application to the detection of single base substitution in genes

Hidetoshi Arakawa, Kunio Uetanaka, Masako Maeda, Akio Tsuji*

School of Pharmaceutical Sciences, Showa University, Hatanodai, Shinagawa, Tokyo 142, Japan

(First received August 6th, 1993; revised manuscript received October 25th, 1993)

Abstract

Capillary gel electrophoresis (CGE) was studied for the direct analysis of polymerase chain reaction (PCR) amplified samples. A low cross-linked polyacrylamide gel (3%T, 0.5%C) was used for CGE with treated and untreated silica capillaries. CGE showed high reproducibility and resolution in the separation of DNA fragments (*ca.* 100–1000 base pairs) produced by PCR. The CGE system was applied to the detection of an amplification refractory mutation system (ARMS) and PCR–restriction fragment length polymorphism (PCR–RFLP), which are detection methods of single base substitution in genes using PCR. With the CGE system, full automation of PCR product detection is feasible.

1. Introduction

DNA analysis is an analytical technique with great potential for the diagnosis of genetic and infectious diseases. The polymerase chain reaction (PCR) has been used to increase enzymatically the specific segment of a target gene, which produces 10^5 more target sequences [1]. Detection of the PCR product is generally accomplished by ethidium staining or hybridization with a radiolabelled DNA probe after separation by slab gel electrophoresis. The development of an automated PCR procedure that involves a detection system is desirable, but no detection system has yet proved suitable for automated PCR because of the problems of rapidity, quantification, reproducibility and the repeated use of slab gel separation. Analysis of double-stranded DNA fragments by capillary electrophoresis (CE) has used low- and zero-cross-linked polyacrylamide [2,3], agarose [4] and cellulose derivatives [5–8] as buffer additives for molecular sieving. CE with hydroxypropylmethylcellulose as the methylcellulose derivative has great potential, because CE conditioning can be performed by changing the sieving buffer. However, the PCR product must be submitted to ultrafiltration to remove PCR byproducts (dNTP, primers and enzyme) before analysis by CE, because PCR components co-migrate with the PCR product of interest in CE. On the other hand, capillary gel electrophoresis (CGE) with low- and zero-cross-linked polyacrylamide, which has a theoretical plate number as high as that of CE with a cellulose derivative, can be used for

* Corresponding author.

0021-9673/94/$07.00
SSDI 0021-9673(93)E1265-2

analysis of the PCR product directly without an ultrafiltration step.

We have studied the direct analysis of PCR products by CGE. A low-cross-linked polyacrylamide gel (3% T, 0.5% C)[a], which was developed by Heiger *et al.* [2], was used as a CGE system with treated and untreated silica capillaries. This system permitted standard DNA fragments [72–1315 base pairs (bp) of ΦX174 RF DNA–*HaeIII* digest], which correspond to specific segments amplified by conventional PCR, to be separated within 30 min. In this work, CGE was applied to the detection of an amplification refractory mutation system (ARMS) and PCR–restriction fragment length polymorphism (PCR–RFLP), which are detection methods of single base substitution in genes by PCR. The results show that analysis of PCR products by CGE is rapid, reproducible and quantitative and has promise for development into an automated PCR system capable of diagnosing genetic and infectious diseases.

2. Experimental

2.1. Apparatus

A Model 270A capillary electrophoresis system (ABI, Foster City, CA, USA) was used. The separations were monitored on-column at 254 nm. A P/ACE 2000 system with a laser-induced fluorescence (LIF) detector (Beckman, Fullerton, CA, USA) was used. Excitation was at 488 nm and a 530-nm band-pass filter was used for emission.

2.2. Materials

ΦX174 DNA–*HaeIII* digest (DNA MW Marker 4) was obtained from Nippon Gene (Osaka, Japan). γ-Methacryloxypropyltrimethoxysilane was purchased from Sigma (St. Louis, MO, USA) and acrylamide, Bis, N,N,N′,N′-tetramethylethylenediamine (TEMED) and ammonium peroxodisulphate (APS) from Wako (Osaka, Japan). Silica capillary tubing [50 cm (effective length 30 cm) × 100 μm I.D. × 375 μm O.D.) was obtained from GL Sciences (Tokyo, Japan). A Gene Amp PCR reagent kit with Amplitaq DNA polymerase was supplied by Perkin-Elmer (Norwalk, CT, USA). Primers A (PKU1), B (PKU2), PKU15w and PKU16m for phenylalanine hydroxylase gene and dried blood spot of phenylketonuria with $Arg^{413} \rightarrow Pro^{413}$ mutation site of exon 12 were generously donated by Professor K. Narisawa (Tohoku University, Medical School, Miyagi, Japan), Primer 1, primer 2 and dive E gene were generously donated by Professor R. Ohki (Kyourin University, Tokyo, Japan). *HaeIII* was purchased from Toyobo (Osaka, Japan). Thiazole orange was generously donated by Dr. T. Satow (Beckman Instruments, Tokyo, Japan). Other chemicals were of analytical-reagent grade.

2.3. CGE

Fused-silica capillary tubing [50 cm (effective length 30 cm) × 100 μm I.D.] was used for CGE. Acrylamide polymerization was accomplished in the capillary according to the methods of Paulus and Ohms [9] and Baba *et al.* [10]. The polymer was covalently attached to the walls of the fused-silica capillary by a bifunctional reagent, as follows. The capillary was rinsed with distilled water for 5 min, then a mixture of methanol and γ-methacryloxypropyltrimethoxysillane (50:50, v/v) was injected into the capillary and left there for 3 h. A 5-ml volume of a solution consisting of acrylamide and Bis dissolved in 100 m*M* Tris–250 m*M* borate buffer (pH 7.8) was carefully degassed by vacuum and introduced in the capillary after adding 2 μl of TEMED solution and 50 μl of 10% (w/v) APS. The polymerizing solution was quickly introduced into the treated capillary by a vacuum injection system equipped with an ABI Model 270A CE system for 10 min and left for at least 2 h. In a CGE experiment, the electrode of the injection side was attached to the negative side of a power supply. Sample injections were performed electrophoretically for typically 2 s at 5 kV. Electrophoresis was per-

[a] C = g N,N′-methylenebisacrylamide (Bis)/%T; T = (g acrylamide + g Bis)/100 ml solution).

formed with 100 m*M* Tris–borate buffer (pH 8.3) at 10 kV and 30°C. The DNA fragments were detected at 260 nm.

2.4. PCR

Amplification of λ phage DNA as a control was performed according to the procedure of the Gen Amp PCR kit (Perkin-Elmer, Norwalk, CT, USA).

2.5. ARMS for PKU

This process was carried out according to the method of Narisawa and co-workers [11,12]. DNA was extracted from dried blood specimens on Guthrie cards that are generally used for neonatal screening. Three discs (3 mm diameter) containing about 10.8 μl of blood were punched from a specimen with a steel punch and placed in a 1.5-ml polypropylene tube. The discs were methanol-fixed with 30 μl of methanol for 5 min at room temperature, dried under vacuum and incubated in 90 μl of a solution containing 50 m*M* KCl, 10 m*M* Tris–HCl (pH 8.3), 1.5 m*M* $MgCl_2$, 0.001% gelatin and 50 μg/ml proteinase K at 55°C for 1 h. The mixture was then heated at 99°C for 10 min and centrifuged at 15 000 *g* for 10 min. A 10-μl volume of the supernatant (extracted DNA) was subjected to PCR with primers A and B [13] to amplify 245 bp DNA fragments containing $Arg^{413} \rightarrow Pro^{413}$ at the mutation site of exon 12 in a hepatic phenylalanine hydroxylase (PAH) gene. The PCR reaction mixture consisted of 50 m*M* KCl, 10 m*M* Tris–HCl (pH 8.3), 1.5 m*M* $MgCl_2$, 0.001% gelatin, 200 μ*M* dNTPs (dATP, dCTP, dTTP and dGTP), 1 μ*M* each of the amplification primers, 10% dimethyl sulphoxide, 10 μl of extracted DNA and 1.5 units of Taq DNA polymerase in a total volume of 30 μl. Nucleotide sequences of the amplification primers were primer A and primer B. Primer A is complementary to the antisense DNA strand of intron 11, 58–77 nucleotides upstream from exon 12. Primer B is complementary to the sense DNA strand of intron 12, 33–52 nucleotides downstream of exon 12. A DNA thermal cycler (ATTO; Zymoreactor, Tokyo, Japan) was used to carry out 30 cycles of PCR according to the following programme: 1 min denaturation at 94°C, 1 min annealing at 56°C and 1 min extension at 74°C. This first amplified products were diluted 1:100 with water and amplified again with the primer-specific mutation site. A second PCR was separately amplified using primer A and PKU15w primer and primer A and PKU16m primer. This second PCR condition was the same as for the first PCR except for 20 cycles. The PCR product obtained was analysed by CGE with UV detection.

In the measurement of the PCR product with a high-sensitivity LIF detector, the first PCR is omitted. A 10-μl volume of the extracted DNA (supernatant) was subjected to PCRs of ARMS with primer A and PKU15w primer and primer A and PKU16m primer. The PCR condition was similar to that described above. The product obtained was analysed by CGE with LIF detection and the intercalating dye. Electrophoresis was performed with 100 m*M* Tris–borate buffer (pH 8.3) containing 0.1 μg/ml thiazole orange, 2 m*M* EDTA and CGE with 3% T, 0.5% C [capillary 37 cm (30 cm to detector) × 100 μm I.D.] at 10 kV and 30°C.

2.6. PCR–RFLP

This experiment was carried out with dive E 42 gene. DNAs, which were extracted from *E. coli* containing dive E gene, were generously donated by Professor R. Ohki. The PCR was performed according to the method and Ohki and co-workers [14,15]. Wild and mutant DNA of dive E were subjected to PCR with primer 1 and Primer 2. Primer 1 is complementary to the antisense DNA strand of dive E 42 gene (19–48 nucleotides). Primer 2 is complementary to the sense DNA strand (448–477 nucleotides). The PCR reaction mixture consisted of 50 m*M* KCl, 10 m*M* Tris–HCl (pH 8.3), 1.5 m*M* $MgCl_2$, 0.001% gelatin, 200 μ*M* dNTPs, 1 μ*M* each of amplification primers 1 and 2, 5 ng of extracted DNA and 1.5 units of Taq DNA polymerase in a total volume of 50 μl. PCR was carried out for 30 cycles according to the following programme:

1 min at 94°C, 2 min at 50°C and 5 min at 72°C. Two PCR products, which were generated from wild and mutant genes, were separately digested with *HaeIII*. A 21-μl volume of PCR product was incubated in 26.7 μl of solution containing 10 m*M* Tris–HCl (pH 7.5), 7 m*M* $MgCl_2$, 60 m*M* NaCl, 7 m*M* 2-mercaptoethanol, 0.1 mg/ml BSA and 52 U *HaeIII* for 3 h at 37°C. After incubation, 2.9 μl of 200 m*M* EDTA solution were added to inactivate the *HaeIII* enzyme. A sample was then analysed by CGE with UV detection.

3. Results and discussion

DNA restriction fragments and PCR product can be separated by CE in the presence of methylcellulose derivatives as buffer additives. Schwartz and co-workers [6,7] applied CE with a sieving buffer containing hydroxypropylmethylcellulose (HPMC) and ethidium bromide for the detection of a PCR-amplified restriction fragment length polymorphism of ERBB2 oncogene and PCR products of the human immunodeficiency virus 1. The PCR products were separated by this CE system in less than 30 min, and the capillary tube could be re-used by changing the sieving buffer. However, the PCR product could not be directly analysed with this CE system, because the PCR reaction mixture components (primer, dNTP) co-migrated with the PCR product of interest. Therefore, the system required an ultrafiltration step with the Centricon system before CE analysis. Although this method is very useful, the purification step makes the routine assay tedious. Therefore, we now describe the use of CGE for direct analysis of PCR products and its application to the detection of an ARMS and PCR–RFLP, which are detection methods of single base substitution in genes using PCR.

3.1. Migration and separation by CGE

It is well known that the resolving power of CGE is very high. The separation of ds DNA by CGE has been reported by Heiger *et al.* [2]. A gel-filled capillary was prepared as follows: first the inner surface of the capillary (50 cm × 100 μm I.D.) was treated with methacryloxypropyltrimethoxysilane as described by Paulus and Ohms [9], then a polyacrylamide gel-filled column was prepared by the method of Baba *et al.* [10] with minor modifications.

The effect of gel concentration (3%–9% T at 0 and 0.5% C) on the separation of the ds DNA fragment (ΦX174 RF DNA–*HaeIII* digest) was studied. Conditions of 3% T, 0.5% C and 8% T, 0% C polyacrylamide provide good resolution of ds DNA restriction fragments. Typical electropherograms obtained by ΦX174 RF DNA–*HincII* digest on 8% T, 0% C polyacrylamide and ΦX174 RF DNA–*HaeIII* digest on 3% T, 0.5% C are shown in Figs. 1 and 2, respectively. As can be seen, the separation of the ds DNA fragment obtained at 8% T, 0% C polyacrylamide gel, which showed the separation of fragments differing by 5–10 bp in length, was better than that at 3% T, 0.5% C. However, the analysis time (migration time) was long (about 40 min) and the mean precision of the migration time of each fragment on the separation of ΦX174 RF DNA–*HaeIII* digest on 8% T, 0% C (data not shown) was 3.42%, within-run ($n = 8$). These results were inferior to those with 3% T, 0.5% C described below. The condition of 3% T, 0.5% C polyacrylamide for the separation of ds DNA was used in the following experiment. The efficiency of this CGE (3% T, 0.5% C) was evaluated by the separation of ΦX174 RF DNA–*HaeIII* digest. The results showed large theoretical plate numbers of $2.5 \cdot 10^6$ for the 118 bp and $1 \cdot 10^6$ for the 310 bp. The precision of the migration time obtained by this CGE for ds DNA fragments ranging from 72 to 1353 bp was examined. The within-run ($n = 10$), day-to-day ($n = 8$) and gel-to-gel ($n = 12$) results are given in Table 1. The mean relative standard deviations obtained within-run, day-to-day and gel-to-gel were 0.47, 2.77 and 0.83%, respectively.

The detection limit of PCR-amplified λ phage obtained with this CGE method was 1 pg of a sample of PCR. This value was the same as that obtained for ethidium bromide-stained slab gel (data not shown). The life of this capillary gel

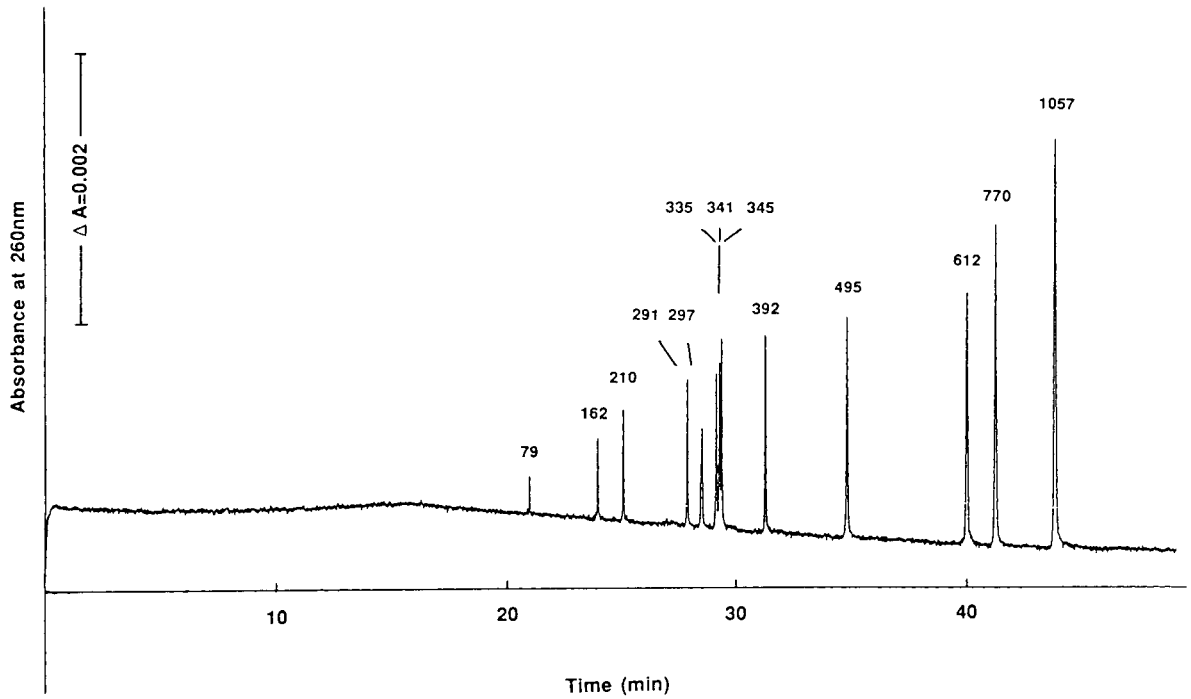

Fig. 1. Separation of *HincII* digest of ΦX174 RF DNA on a 8% T, 0% C polyacrylamide capillary.

was about 80 separations. In contrast, the life of a capillary gel without methacryloxypropyltrimethylsillane pretreatment is about 20 separations under the same conditions. Hence the use of a pretreated capillary gel appears to be a good method for the determination of PCR product.

3.2. Application of CGE analysis to the detection of single base substitutions in genes

Two methods using PCR have been developed to detect single base substitution in a gene. The ARMS is one method for the determination of point mutation in a gene [16]. This method depends on whether the PCR product is observed in slab gel electrophoresis after PCR with a primer-specific mutation site. The basis of this system is that oligonucleotides with a mismatched 3′-residue do not function. Narisawa and Matsubara have developed ARMS for the phenylketonuria mutation (PKU) ($Arg^{111} \rightarrow Ter$, Sp4, $Tyr^{204} \rightarrow Cys^{204}$, $Arg^{243} \rightarrow Gln^{243}$, $Arg^{413} \rightarrow Pro^{413}$, $Arg^{261} \rightarrow Gln^{261}$). We tried to apply CGE analysis to the detection of this ARMS technique for PKU. As a model, the PCR product obtained by ARMS of $Arg^{413}(CGC) \rightarrow Pro^{413}(CCC)$ of exon 12 in the hepatic PAH gene was detected by CGE (3% T, 0.5% C). DNA was extracted from dried blood specimens on Guthrie cards according to the method of Matsubara *et al.* [11]. The method is described in detail under Experimental and a scheme for ARMS is shown in Fig. 3.

Extracted DNA was first subjected to PCR to amplify the 245 bp fragment in exon 12. This region contains the mutation site $Arg^{413} \rightarrow Pro^{413}$. The 245 bp fragment was amplified by 30 cycles of PCR, and part of the amplified products were then further subjected to a second PCR according to the method of Matsubara *et al.* [11]. The second PCR was carried out separately using primer A and PKU15w primer, and primer A and PKU16m primer. PKU15w primer corresponds to the normal sequence at Arg^{413}(CGC) and PKU16m primer corresponds to the point mutation se-

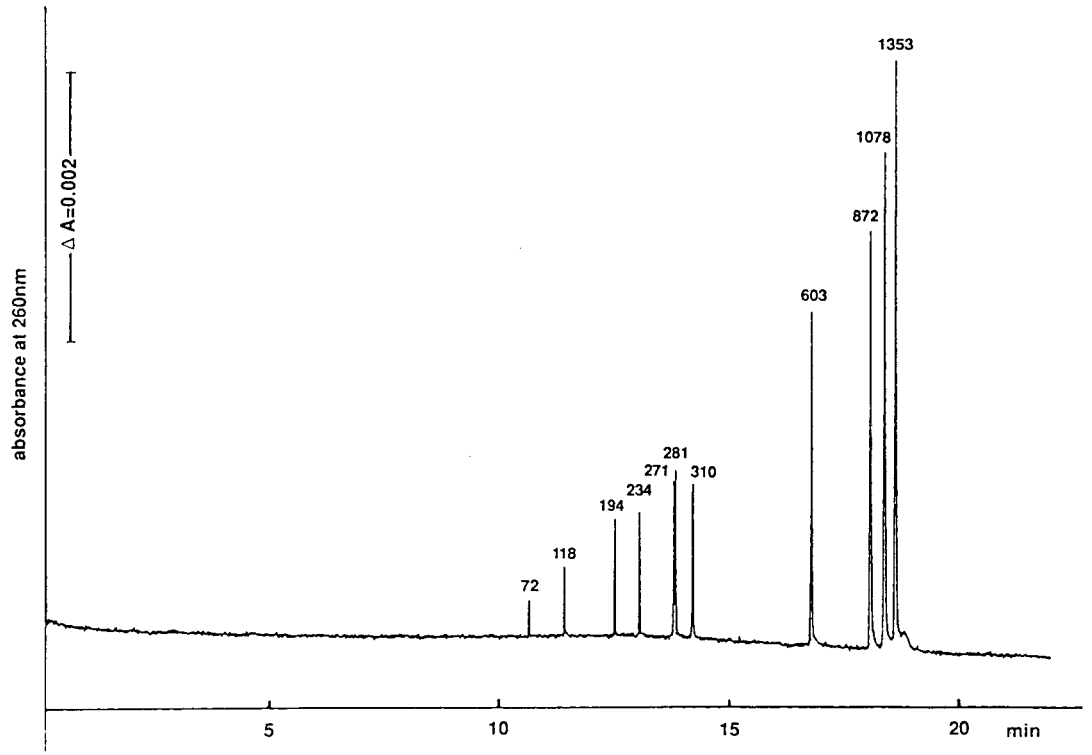

Fig. 2. Separation of *HaeIII* digest of ΦX174 RF DNA on a 3% T, 0.5% C polyacrylamide capillary.

quence at Pro^{413}(CCC). In a normal subject, the product (138 bp) was derived only from primer A and PKU15w, and no product was generated when the PKU16m primer was applied to normal DNA. On a patient's sample containing a point mutation at Pro^{413}, no product was generated by

Table 1
Precision of migration times for various DNA fragments on the separation of ΦX174 DNA–*HaeIII* digest

Base pairs	Within-assay (n = 10)		Day-to-day (n = 8)		Gel-to-gel (n = 12)	
	Mean (min)	R.S.D. (%)	Mean (min)	R.S.D. (%)	Mean (min)	R.S.D. (%)
72	10.53	0.46	10.99	2.49	10.97	0.74
118	11.29	0.47	11.78	2.50	11.75	0.70
194	12.38	0.46	12.90	2.61	12.88	0.73
234	12.92	0.45	13.46	2.66	13.43	0.70
271	13.67	0.44	14.23	2.71	14.19	0.74
281	13.71	0.44	14.28	2.72	14.24	0.77
310	14.08	0.44	14.66	2.75	14.62	0.76
603	16.61	0.47	17.30	2.93	17.24	0.92
872	17.85	0.48	18.61	3.02	18.54	1.03
1078	18.13	0.53	18.92	3.03	18.86	1.01
1353	18.37	0.52	19.17	3.02	19.11	0.99

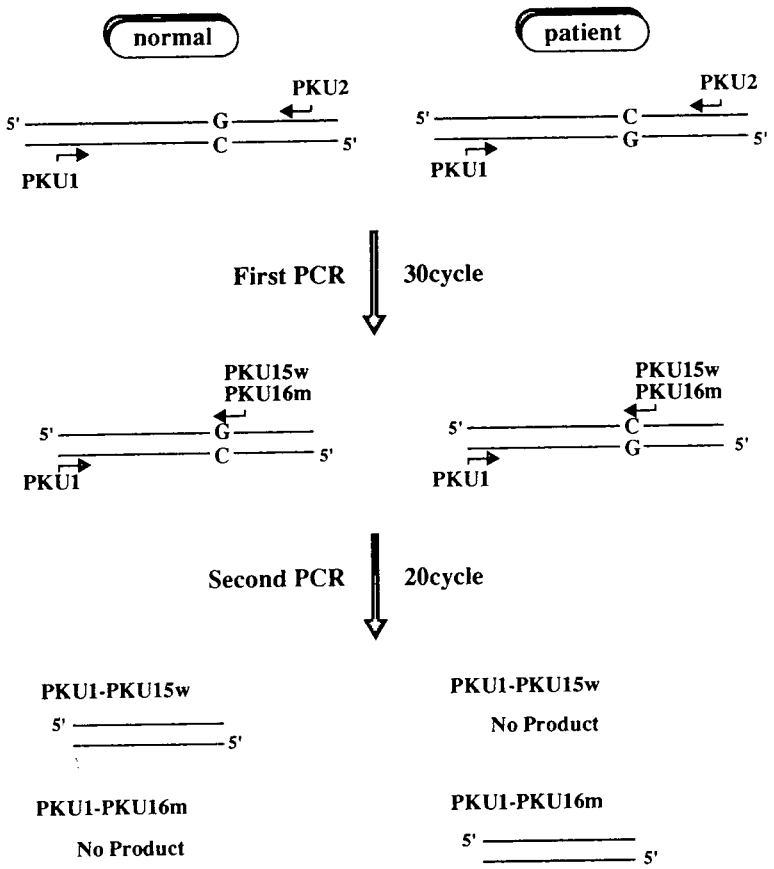

Fig. 3. Scheme of the method of ARMS.

primer A and PKU15w primer. However, product was observed when PKU15w primer was replaced with PKU16m primer. The PCR products thus obtained were analysed by CGE.

As shown in Fig. 4, the PCR product migrated to about 12.30 min. Comparison of these results should indicate whether or not the DNA sample has a point mutation at exon 12. In this work, the detection limit of DNA by CGE with UV detection was not adequate to detect a specific gene from a small amount of human DNA, even after 30 cycles of PCR. Therefore, the two PCR systems described above were required (the first PCR produced a 245-bp fragment which contained a mutation site, and this first PCR product was then used as a template for the second PCR). This system requires long reaction time, which might result in contamination of the DNA. This problem can be resolved by using the high-sensitivity CGE with LIF. Schwartz and Ulfelder [17] recently developed a highly sensitive method of separating PCR fragments by CE which used hydroxypropylmethylcellulose as sieving buffer with LIF. This method using thiazole orange as an intercalating dye is *ca.* 400 times as sensitive as UV detection. In this work, PCR products obtained directly from ARMS without the first PCR were analysed by CGE (3% T, 0.5% C) with LIF and the dye. The results are shown in Fig. 5. This CGE system with LIF and thiazole orange as an intercalating dye had higher sensitivity (λ phage 100 fg, PCR 25 cycles) and higher resolution (baseline resolution at 271 and 281 bp) than the CGE system

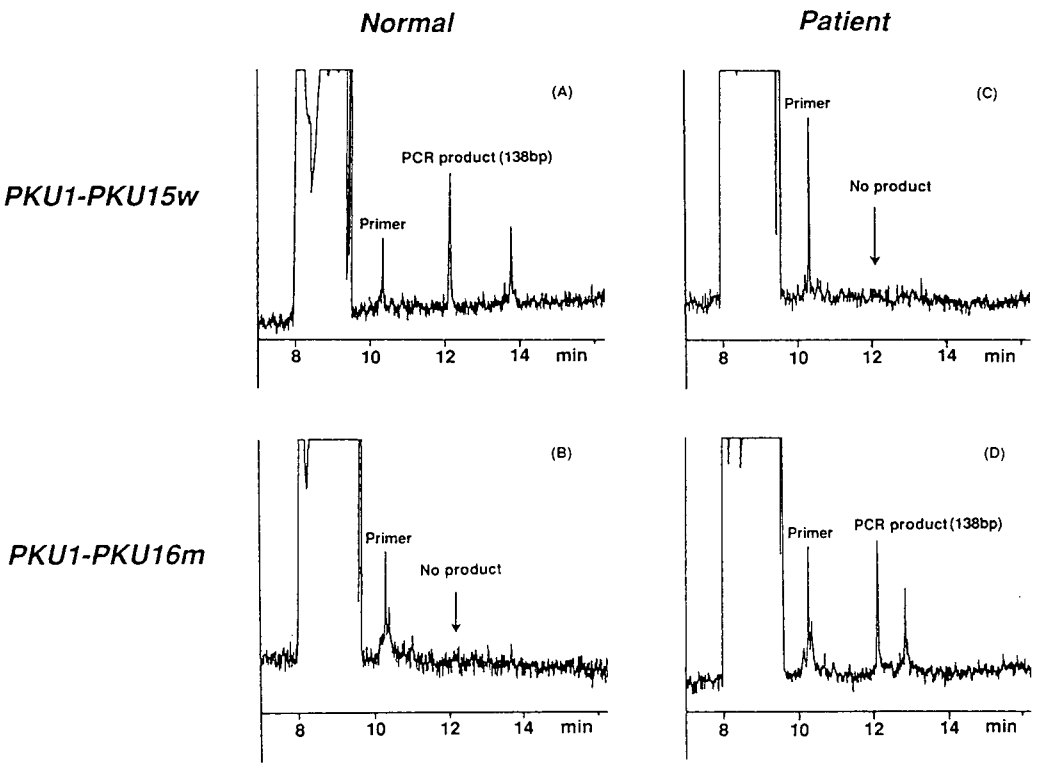

Fig. 4. Electropherograms of the products obtained by ARMS. (A) and (B) are the results for a normal subject with primer set primer A–PKU15w and primer A–PKU16m, respectively; (C) and (D) are the results for a PKU patient with primer set primer A–PKU15w and primer A–PKU16m, respectively.

with UV detection. The results will be described in detail elsewhere. This method has high potential for PCR product obtained from a human genome.

Another method to determine a single base mutation in a gene is PCR–RFLP using the restriction enzyme. PCR–RFLP has been used to diagnose many diseases. In this work, we tried to apply CE analysis to the detection of PCR–RFLP. The model used was the dive E 42 gene carrying wild- and mutant-type DNA. The mutant type of this DNA contains G→A point mutation at the 141 site. Wild and mutant DNA were subjected to PCR to amplify the 359 bp fragment in the dive E 42 gene. This region contains the mutation site of $G^{141} \rightarrow A^{141}$. Two PCR products generated from the wild and mutant gene are the ^{140}GGCC and ^{140}GACC sites in the 359 bp fragment. The restriction enzyme, *HaeIII*, cuts the GGCC site in the PCR product generated from a wild gene, whereas the PCR product of a mutant is not cut by this enzyme. Hence this *HaeIII* recognition site is lost in mutated DNA. The PCR reaction was carried out according to the method of Ohki and co-workers [14,15] described under Experimental. The amplification product was directly digested by the restriction enzyme, *HaeIII*, for 3 h at 37°C, and the sample was subsequently analysed by CGE in 3% T, 0.5% C. As predicted from the dive E sequence, *HaeIII* restriction enzyme cut the GGCC site in the PCR product of wild genes and produced two peaks (122 bp) at 11.35 min and (237 bp) at 12.98 min. In

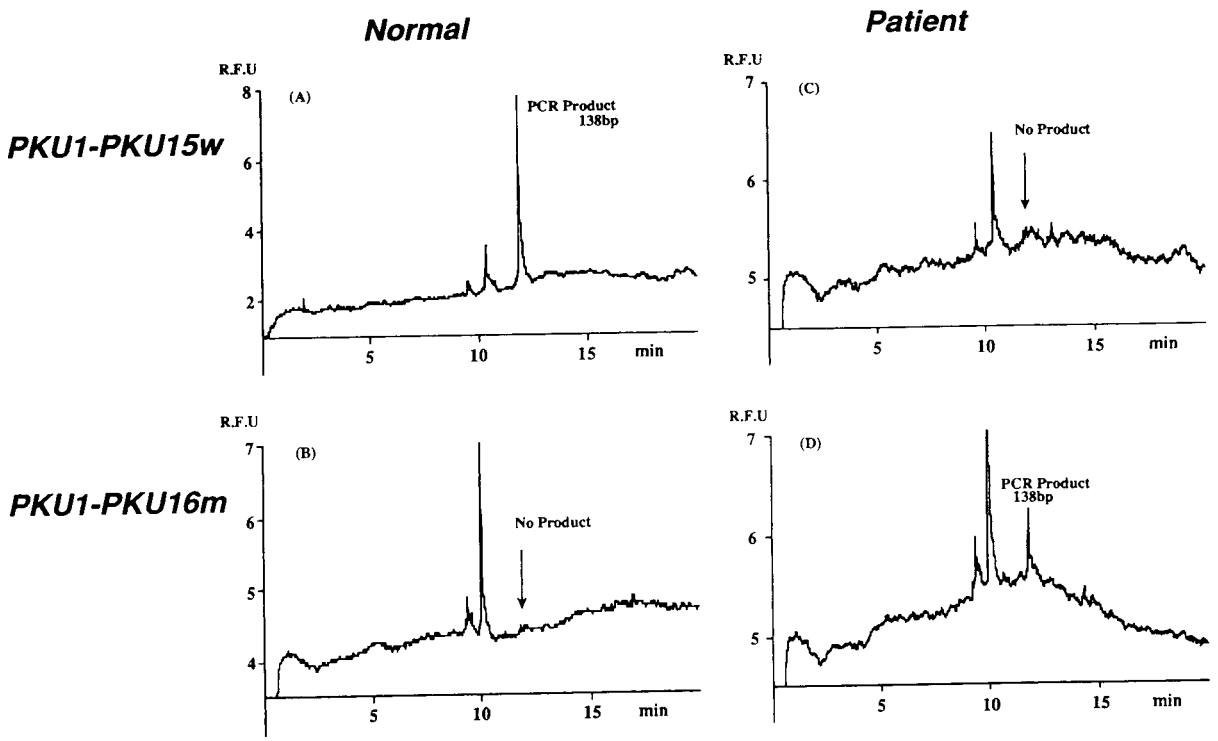

Fig. 5. CGE with LIF detection of *HaeIII* digest of ΦX174 DNA and the products obtained by ARMS. (A) and (B) are the results for a normal subject with primer set primer A–PKU15w and primer A–PKU16m, respectively; (C) and (D) are the results for a PKU patient with primer set primer A–PKU15w and primer A–PKU16m, respectively.

contrast, the PCR product of a mutant gene, digested by *HaeIII*, showed only one peak (359 bp) at 14.54 min. The results are shown in Fig. 6.

The results described above show that CE analysis of PCR–RFLP is a useful method to determine the point mutation in a gene.

4. Conclusions

We developed a method for the analysis of the PCR product by CGE. The separation of the DNA fragment obtained by CGE showed a high theoretical plate number, short analysis time and high precision. This method provides an efficacious means for the determination of PCR product. CGE was applied to the determination of single base mutation of a gene amplified by PCR. It was found that CGE is a useful technique for detection by the ARMS and PCR–RFLP. With this method, the PCR procedure for the diagnosis of genetic and infectious disease could be automated in the near future.

5. Acknowledgements

We thank Professor K. Narisawa and Associate Professor K. Matsubara, Medical School, Tohoku University, for kindly providing us with primers of ARMS and dried blood samples. We also thank Professor R. Ohki, School of Health Sciences, Kyorin University, for kindly providing us with primers of dive E and dive E gene, and Dr. T. Satow of Beckmann Instruments for kindly providing us with thiazole orange.

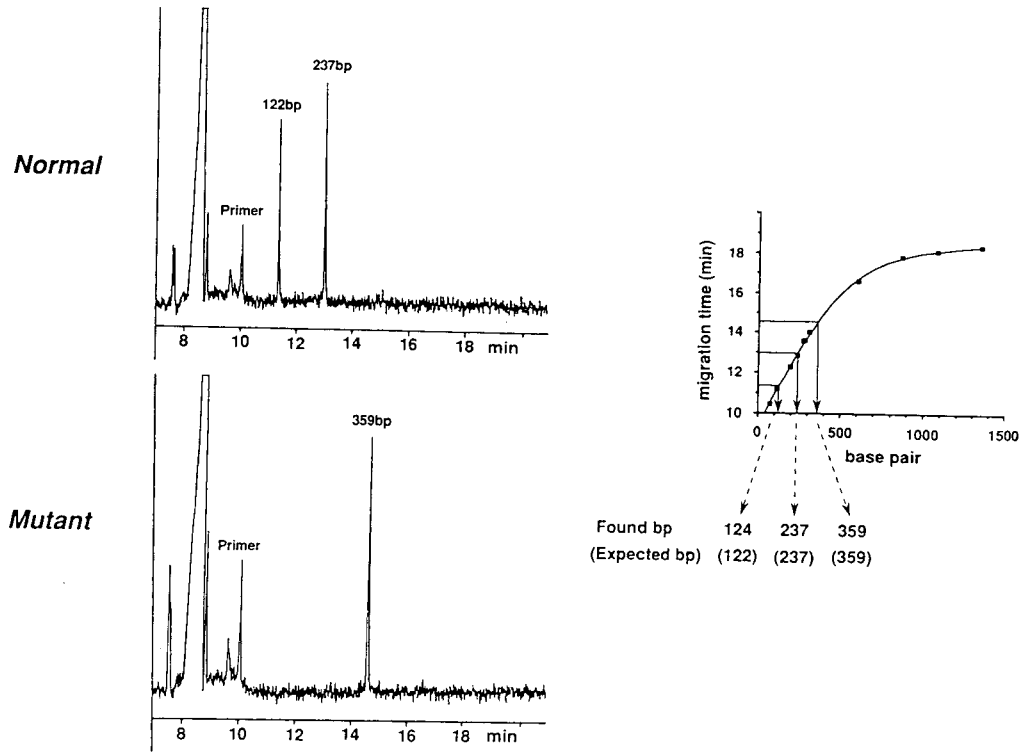

Fig. 6. Electropherograms of an *HaeIII* restriction digest of PCR products obtained from wild and mutant dive E gene.

6. References

[1] R.K. Saiki, S. Scharf, F. Faloona, K.B. Mullis, G.T. Horn, H.A. Erlich and N. Arnheim, *Science*, 230 (1985) 1350.

[2] D.N. Heiger, A. Cohen and B.L. Karger, *J. Chromatogr.*, 516 (1990) 33.

[3] A. Guttman and N. Cooke, *Anal. Chem.*, 63 (1991) 2038.

[4] P. Bocek and A. Chrambach, *Electrophoresis*, 12 (1991) 1059.

[5] M. Zhu, D.L. Hansen, S. Burd and F. Gannon, *J. Chromatogr.*, 480 (1989) 311.

[6] H.E. Schwartz, K.J. Ulfelder, F.J. Sunzeri, M.P. Bush and R.G. Brownlee, *J. Chromatogr.*, 559 (1991) 267.

[7] K.J. Ulfelder, H.E. Schwartz, J.M. Hall and F.J. Sunzeri, *Anal. Biochem.*, 200 (1992) 260.

[8] M.H. Kleemiss, M. Gilges and G. Schomburg, *Electrophoresis*, 14 (1993) 509.

[9] A. Paulus and J.I. Ohms, *J. Chromatogr.*, 507 (1990) 113.

[10] Y. Baba, T. Matsuura, K. Wakamoto and M. Tsuhako, *Chem. Lett.*, (1991) 371.

[11] Y. Matsubara, K. Narisawa, K. Tada, H. Ikeda, Y. Yegi, D.M. Danks, A. Green and R.B. McCabe, *Lancet*, 371 (1991) 552.

[12] K. Narisawa and Y. Matsubara, in preparation.

[13] A.G. Dilella, W.M. Hung and S.L.C. Woo, *Lancet*, ii (1988) 497.

[14] F. Tamura, S. Nishimura and M. Ohki, *EMBO J.*, 3 (1984) 1103.

[15] S. Kawamata and R. Ohki, *Kyorin Igaku Kaishi*, 24 (1993) 111.

[16] C.R. Newton, A. Graham, L.E. Heptinstall, S.J. Powell, C. Summers, N. Kalsheker, J.C. Smith and A.F. Markham, *Nucleic Acids Res.*, 17 (1989) 2503.

[17] H.E. Schwartz and K.J. Ulfelder, *Anal. Chem.*, 64 (1992) 1738.

ELSEVIER

Journal of Chromatography A, 664 (1994) 99–103

JOURNAL OF CHROMATOGRAPHY A

Short Communication

Molecular mass of proteins and their partitioning in aqueous two-phase systems

Peter A. Andreasen

Department of Molecular Biology, University of Aarhus, 130 C.F. Møller's Allé, 8000 Aarhus C, Denmark

(First received July 20th, 1993; revised manuscript received December 28th, 1993)

Abstract

Twenty proteins with molecular masses between 10^4 and 10^6 were partitioned in aqueous dextran–poly(ethylene glycol) two-phase systems with either 0.1 *M* KCl or 0.1 *M* KCl plus 3 *M* NaCl. The partition coefficient of all proteins were higher in the system with 0.1 *M* KCl plus 3 *M* NaCl than in the system with 0.1 *M* KCl alone. The ratios between the partition coefficients in the two systems were strongly correlated with the molecular masses of the proteins. This fact may be used for analytical as well as preparative purposes.

1. Introduction

When aqueous solutions of two polymers are mixed, two immiscible phases are formed. Cells, cell organelles, proteins and nucleic acids can be introduced into such systems without being damaged, and will assume a characteristic distribution between the two phases and/or their interface, depending on the properties of the phase system and of the partitioned substance. Aqueous two-phase partitioning can be used for a variety of analytical and preparative purposes in biochemistry, cell biology and biotechnology (for reviews, see refs. 1–4).

In aqueous dextran–poly(ethylene glycol) two-phase systems, proteins partition between the two phases. Their partition coefficients depend on net charge, surface hydrophobicity and specific interactions with the polymers ("affinity partitioning"). The influences of these parameters on protein partitioning have been studied in great detail (for reviews, see refs. 5 and 6). The influence of the molecular mass of proteins has been less well characterized. It has been a general finding that a protein tends to partition more one-sided, the larger its molecular mass. However, there are many exceptions to the rule, and no obvious correlation between molecular mass and partition coefficient has been established so far [5–8].

In the present communication, I describe a strong correlation between protein molecular mass and the ratio between the partition coefficient in phase systems with different salt concentrations.

2. Materials and methods

2.1. Materials

The following proteins were purchased from the indicated sources: alcohol dehydrogenase from baker's yeast (Sigma A 7011), rabbit muscle aldolase (Sigma A 7145), equine apoferritin (Sigma A 3641), bovine α-chymotrypsin (Sigma

0021-9673/94/$07.00
SSDI 0021-9673(94)00007-V

C 7762), bovine catalase (Sigma C 3155), chicken conalbumin (Sigma C 0755), equine cytochrome *c* (Sigma C 7752), equine ferritin (Sigma F 4503), porcine heart fumarase (Sigma F 1757), rabbit muscle glyceraldehyde-3-phosphate dehydrogenase (Sigma G 2267), bovine haemoglobin (Sigma H 2500), bovine β-lactoglobulin (Sigma L 0130), whale myoglobin (Sigma M 0380), chicken ovalbumin (Sigma A 2512), porcine pepsin (Boehringer-Mannheim), bovine ribonuclease A (Sigma R 4875), bovine serum albumin (Boehringer-Mannheim), bovine thyroglobulin (Sigma T 1001), bovine trypsin (Sigma T 8003), bovine pancreas trypsin inhibitor (Sigma A 1153) and soybean trypsin inhibitor (Boehringer-Mannheim). Dextran T500 (lot No. FA 13748) was from Pharmacia. Poly(ethylene glycol) 6000 was from Merck. All other chemicals were of analytical grade.

Before use, the proteins were dialysed extensively against a suitable buffer.

2.2. Two-phase systems and partitioning

Proteins were partitioned in 1 ml dextran T500–poly(ethylene glycol) 6000 two-phase systems, containing 6.25% (w/v) of each of the polymers, 6 m*M* Tris, 2 m*M* K_2HPO_4, pH 8.1, 10% (v/v) glycerol and salts as indicated below. Each phase system contained 1–5 mg protein. Partitioning was performed at 0–4°C. Each phase system was vortex mixed for 15 s, and centrifuged for 1 min at 10 000 *g* in order to accelerate separation of the bulk phases. The partition coefficients were calculated as the ratios between the absorbances at 280 nm of diluted aliquots of the top and the bottom phases. Each partition coefficient given below is the geometric mean of at least four determinations.

Phase diagrams were constructed by the cloud point method [9]. The concentrations of KCl plus NaCl in the phases were determined by measuring the conductivity of diluted aliquots of the phases and comparison to a standard curve.

The molecular masses, isoelectric points and the numbers of subunits of the proteins were those given in biochemistry textbooks or in refs. 10–13.

3. Results

A number of proteins were partitioned in aqueous dextran–poly(ethylene glycol) two-phase systems with 0.1 *M* KCl; with 0.1 *M* KCl plus 0.9 *M* NaCl; with 0.1 *M* KCl plus 3 *M* NaCl; and with 0.22 *M* KCl plus 0.26 *M* Li_2SO_4. Fig. 1 shows double-logarithmic plots of the partition coefficients *versus* the molecular masses. In the case of oligomeric proteins, the molecular masses of the oligomers were used. It is seen that the proteins tended to partition more one-sided, the larger their molecular mass, but the data points are quite scattered, particularly in the molecular mass range 10^4–10^5. For all tested

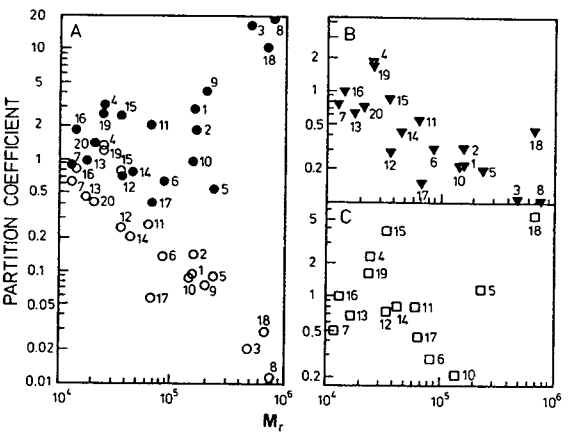

Fig. 1. Partition coefficients of proteins in phase systems with (A) 0.1 *M* KCl (○) and 0.1 *M* KCl + 3 *M* NaCl (●); (B) 0.1 *M* KCl plus 0.9 *M* NaCl (▼); (C) 0.22 *M* KCl plus 0.26 *M* Li_2SO_4 (□). The partition coefficients are plotted double-logarithmically *versus* their molecular masses. The partitioned proteins were: 1 = alcohol dehydrogenase (tetramer, M_r 150 000); 2 = aldolase (tetramer, M_r 156 000); 3 = apoferritin (24-mer, M_r 460 000–490 000); 4 = α-chymotrypsin (M_r 24 300); 5 = catalase (tetramer, M_r 230 000); 6 = conalbumin (M_r 84 000); 7 = cytochrome *c* (M_r 12 400); 8 = ferritin (24-mer, M_r 700 000–800 000); 9 = fumarase (tetramer, M_r 194 000); 10 = glyceraldehyde-3-phosphate dehydrogenase (tetramer, M_r 142 800); 11 = haemoglobin (tetramer, M_r 62 000); 12 = β-lactoglobulin (dimer, M_r 35 000); 13 = myoglobin (M_r 17 000); 14 = ovalbumin (M_r 43 000); 15 = pepsin (M_r 34 700); 16 = ribonuclease A (M_r 13 700); 17 = serum albumin (M_r 66 300); 18 = thyroglobulin (dimer, M_r 669 000); 19 = trypsin (M_r 24 000); 20 = soybean trypsin inhibitor (M_r 20 100). Partitioning of a few of the proteins was not performed in the systems with 0.1 *M* KCl plus 0.9 *M* NaCl and with 0.22 *M* KCl plus 0.26 *M* Li_2SO_4.

proteins, the partition coefficient in systems with KCl plus NaCl increased with the total salt concentration. The direction of the changes of the partition coefficients when going from systems with 0.1 *M* KCl plus 0.9 *M* NaCl to systems with 0.22 *M* KCl plus 0.26 *M* Li_2SO_4 (which have identical ionic strengths) is that expected from a protein net charge-dependent influence of the identity of the salts [5,14], considering the p*I* values and the pH of the phase systems (an increase for negatively charged proteins, a decrease for positively charged proteins).

Fig. 2 shows a double-logarithmic plot of the *ratio* between the partition coefficients in the phase systems with 0.1 *M* KCl plus 3 *M* NaCl and 0.1 *M* KCl *versus* the molecular masses. It is seen that there was a strong correlation between

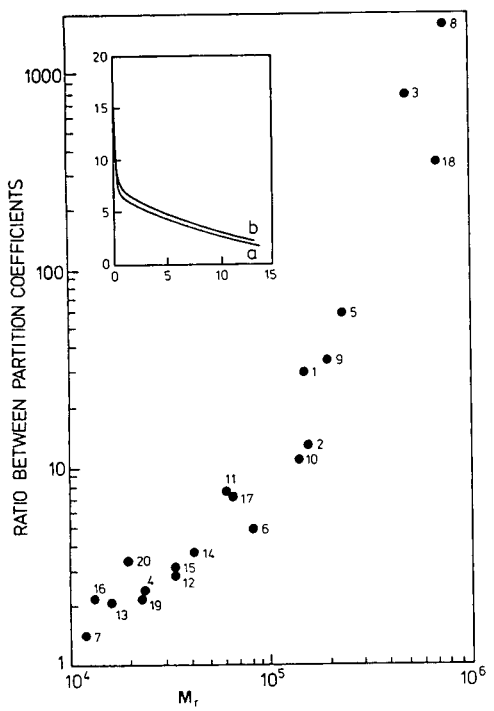

Fig. 2. Ratio between the partition coefficients of proteins in phase systems with 0.1 *M* KCl plus 3 *M* NaCl and 0.1 *M* KCl, plotted double-logarithmically *versus* their molecular masses. Numbering of partitioned proteins as in Fig. 1. The inset shows phase diagrams for systems with 0.1 *M* KCl (a) and 0.1 *M* KCl plus 3 *M* NaCl (b). The dextran T500 percentage is given on the abcissa, and the poly(ethylene glycol) 6000 percentage on the ordinate.

this ratio and the molecular mass. The ratio increased from 1–2 for proteins with molecular mass $1 \cdot 10^4$–$2 \cdot 10^4$ to more than 1000 for the largest proteins tested, having molecular masses of $7 \cdot 10^5$–$8 \cdot 10^5$. There was a nearly linear relationship between the ratio and the molecular mass in the range 10^4–10^5, although the correlation was not linear over the entire molecular mass range. The linear correlation coefficient in that range was 0.886, considerably better than those found for the direct plots of the partition coefficients *versus* molecular masses (−0.735 and −0.365 for 0.1 *M* KCl and 0.1 *M* KCl plus 3 *M* NaCl, respectively). The ratio did not decrease below 1 for substances with molecular masses smaller than 10^4. For instance, the ratio was 1.15 for bovine pancreas trypsin inhibitor (M_r 6500) and 1.19 for the steroid triamcinolone acetonide (M_r 434). A similar correlation existed for the ratios between the partition coefficients in systems with 0.1 *M* KCl plus 1 *M* NaCl and with 0.1 *M* KCl (data not shown).

With 0.1 *M* KCl, the volume of the top phase constituted 64% of the total volume; with 0.1 *M* KCl plus 3 *M* NaCl, it constituted 44% of the total volume. The phase diagrams were different for systems with 0.1 *M* KCl and for systems with 0.1 *M* KCl plus 3 *M* NaCl. With a given polymer composition, the high salt concentration moves the system closer to critical point (Fig. 2). The partition coefficient of KCl plus NaCl was not measurably different from 1 in any of the phase systems.

4. Discussion

Formally, the partition coefficients of proteins in aqueous two-phase systems may be split into several terms [1,2]:

$$\ln K = \ln K_{el} + \ln K_{hphob} + \ln K_{hphil} + \ldots$$

where K_{el}, K_{hphob}, K_{hphil} etc. represent the contribution to the partition coefficient from electrostatic, hydrophobic, hydrophilic etc. interactions between the protein and the phases. The strategy that has been employed for characteriza-

tion of a protein by aqueous two-phase partitioning consists in changing the composition of the phase system in a way believed to alter only one type of interaction between the protein and the phases. To the extent that each type of interaction can be varied independently of the others, the properties of the protein can be assessed from the variations of its partition coefficient in response to the changes in the composition of the phase system. This principle has for instance been employed for assessing (1) protein surface hydrophobicity, by measuring the change of partition coefficient of the protein in response to substitution of poly(ethylene glycol) with poly(ethylene glycol) esterified with fatty acids; (2) protein net charge, by measuring the change of partition coefficient of the protein in response to changes of the identity of the salts in the system (for instance, substituting NaCl with Li_2SO_4), which influences the interfacial potential [5]. Thus, it is the *ratio* between the partition coefficients at different partitioning conditions that is useful.

In the present investigation, the *ratio* between the partition coefficients of proteins at two different salt concentrations (0.1 *M* KCl plus 3 *M* NaCl and 0.1 *M* KCl) was shown to be correlated with their molecular masses. In contrast, there was no correlation between the absolute values of the partition coefficients and the molecular masses. The contribution from protein net charge was expected to be the same in systems with 0.1 *M* KCl plus 3 *M* NaCl and with 0.1 *M* KCl, and this was verified by finding that the partition coefficients of serum albumin and ovalbumin varied identically with pH in the two systems (data not shown). Thus, the contribution to the partition coefficient from protein net charge was removed by taking the ratio between the partition coefficients. But there was a lack of correlation of the molecular masses and the absolute values of the partition coefficients in systems with KCl plus Li_2SO_4 as well as in systems with only KCl and NaCl; partitioning in the former is almost insensitive to protein net charge [14]. It should also be noted that a lack of correlation between the molecular masses and the partition coefficients at the isoelectric points were previously reported for a group of haemo- and non-haemoproteins [8]. Therefore, the lack of correlation between the molecular masses and the absolute values of the partition coefficients is not only due to the contribution from protein net charge, and charge-*in*dependent contributions to the partition coefficient, except that from protein size, are also removed by taking the ratio between the partition coefficients at the two salt concentrations.

An increase of protein partition coefficients with increasing NaCl concentrations was first reported by Albertsson [1]. However, the physico-chemical basis of this salt effect is not understood. Generally, the effect of salts on the interactions between the polymer components is expected to have a pronounced effect on the composition of the phases, which may in turn influence protein partition coefficients; in addition, the presence of salts can influence the protein partitioning by modifying the intermolecular forces between the protein and the polymer coils [6]. In agreement with previous findings [1], the increase of the total salt concentration from 0.1 to 3.1 *M* was found here to change the composition of the phases. A number of models (based on the so-called osmotic virial-expansion approaches and lattice model approaches) have been developed recently to predict protein partitioning by physico-chemical calculations. These models do predict that changes of phase composition will influence protein partition coefficients in a way increasing with protein size, but they do not predict an elimination of other contributions (like interactions between polymer and protein) to the partition coefficient by taking the ratio between the partition coefficient at different phase compositions [4,6,15–17]. The most promising approach in the present context seems to be the scaling-thermodynamic formulation of Abbott *et al.* [18–21]. This theory emphasizes physical exclusion between polymer and protein as well as weak attractive forces between polymer and protein. Considering phases of individually dispersed polymers (as opposed to entangled polymer network), this theory was able to account qualitatively for the correlation between protein size

and the *ratio* between the partition coefficients in systems with poly(ethylene glycol)s of different molecular masses [22,23], in the absence of changes in the polymer concentrations of the phases. Although the effect of using poly(ethylene glycol)s of different molecular masses was considerably smaller than the salt effect described here, it seems possible that the scaling-thermodynamic theory may be developed to account for the present observation.

The finding reported here may be quite useful for an estimation of molecular masses of proteins. It can be employed to proteins in crude mixtures, provided that an assay for the protein is available. Aqueous two-phase partitionings are performed under non-denaturing conditions, so the method can also be employed to oligomeric proteins, provided that the oligomeric structure does not change with the salt concentration. The method is extremely rapid, since the partitioning can be performed in a few minutes. Sequential partitionings at different salt concentrations may be useful for preparative fractionations of proteins on the basis of molecular mass.

5. References

[1] P.-Å. Albertsson, *Partition of Cell Particles and Macromolecules*, Almquist & Wiksell, Stockholm, 2nd ed., 1971.
[2] P.-Å. Albertsson, *J. Chromatogr.*, 159 (1978) 111–122.
[3] H. Walter and G. Johansson, *Anal. Biochem.*, 155 (1986) 215–242.
[4] H. Walter, G. Johansson and D.E. Brooks, *Anal. Biochem.*, 197 (1991) 1–18.
[5] G. Johansson, in H. Walter, D.E. Brooks and D. Fisher (Editors), *Partitioning in Aqueous Two-Phase Systems —Theory, Methods, Uses, and Applications to Biotechnology*, Academic Press, Orlando, FL, 1985, pp. 161–226.
[6] N.L. Abbott, D. Blankschtein and T.A. Hatton, *Bioseparation*, 1 (1990) 191–225.
[7] P.-Å. Albertsson, *Nature*, 182 (1958) 709–711.
[8] S. Sasakawa and H. Walter, *Biochemistry*, 11 (1972) 2760–2765.
[9] S. Bamberger, D.E. Brooks, K.A. Sharp, J.M. van Alstine and T.J. Webber, in H. Walter, D.E. Brooks and D. Fisher (Editors), *Partitioning in Aqueous Two-Phase Systems —Theory, Methods, Uses, and Applications to Biotechnology*, Academic Press, Orlando, FL, 1985, pp. 85–130.
[10] P. Andrews, *Biochem. J.*, 96 (1965) 596–606.
[11] A.Bezkorovainy, D. Grohlich and C.M. Gerbeck, *Biochem. J.*, 110 (1968) 765–770.
[12] P. Lambin, *Anal. Biochem.*, 85 (1978) 114–125.
[13] D. Malamud and J.W. Drysdale, *Anal. Biochem.*, 86 (1978) 620–647.
[14] P.Å. Andreasen, *Mol. Cell. Endocrinol.*, 28 (1982) 563–586.
[15] J.N. Baskir, T.A. Hatton and U.W. Suter, *Macromolecules*, 20 (1987) 1300–1311.
[16] J.N. Baskir, T.A. Hatton and U.W. Suter, *J. Phys. Chem.*, 93 (1989) 2111–2122.
[17] D. Forciniti, C.K. Hall and M.R. Kula, *Biotechnol. Bioeng.*, 38 (1991) 986–994.
[18] N.L. Abbott, D. Blankschtein and T.A. Hatton, *Macromolecules*, 24 (1991) 4334–4348.
[19] N.L. Abbott, D. Blankschtein and T.A. Hatton, *Macromolecules*, 25 (1992) 3917–3931.
[20] N.L. Abbott, D. Blankschtein and T.A. Hatton, *Macromolecules*, 25 (1992) 3932–3941.
[21] N.L. Abbott, D. Blankschtein and T.A. Hatton, *Macromolecules*, 25 (1992) 5192–5200.
[22] P.-Å. Albertsson, A. Cajarville, D.E. Brooks and F. Tjerneld, *Biochim. Biophys. Acta*, 926 (1987) 87–93.
[23] H. Hustedt, K.H. Kroner, W. Stach and M.R. Kula, *Biotechnol. Bioeng.*, 20 (1978) 1989–1996.

ELSEVIER

Journal of Chromatography A, 664 (1994) 104–110

JOURNAL OF CHROMATOGRAPHY A

Short Communication

Direct high-performance liquid chromatographic separation of the racemates and diastereomers of nadolol

Masanori Hoshino*, Eiji Matsui, Koichi Yajima, Akira Okahira

Central Research Laboratories, Zeria Pharmaceutical Co., Ltd., 2512-1, Oshikiri, Konan-machi, Osato-gun, Saitama 360-01, Japan

(First received August 10th, 1993; revised manuscript received December 14th, 1993)

Abstract

The direct separation of the two racemates and four diastereomers of nadolol by high-performance liquid chromatography (HPLC) is described. The racemates were well separated on non-chiral ODS columns using mixtures of phosphate buffer and methanol. The diastereomers could be separated on commercial chiral columns, using organic and aqueous mobile phases. The analytical HPLC method using an organic mobile phase was applied to semi-preparative HPLC for diastereomers.

1. Introduction

Nadolol is an important β-adrenoceptor antagonist widely used in the treatment of cardiovascular disorders and essential hypertension. Although nadolol contains three asymmetric carbons, two hydroxy groups of the tetrahydronaphthalene ring form a *cis* configuration. Therefore, it has two racemates and four diastereomers. Commercial nadolol is a mixture of approximately equal proportions of the two racemates, namely + −/− + (*RS*/*SR*) and + +/− − (*RR*/*SS*) referred to as racemates A and B, respectively [1].

Matsutera *et al.* [2] and Lacroix *et al.* [3] have reported the high-performance liquid chromatographic (HPLC) separation of the two racemates of nadolol. Schill *et al.* [4] reported that each racemate of nadolol was resolved into its diastereomers by HPLC on an α_1-acid glycoprotein (α_1-AGP) column, but they did not report the separation of all four stereoisomers in a single run. Lee *et al.* [5] studied the direct separation of the four diastereomers of nadolol using various HPLC column packings, but the separation was successful only on an α_1-AGP column. Dyas *et al.* [6] separated the four diastereomers on a Pirkle-type chiral stationary phase after derivatization with 1-naphthyl isocyanate and assigned each peak to configurations.

This paper describes HPLC methods for the direct separation of the two racemates and four diastereomers of nadolol. The method for separating the diastereomers was used also for

* Corresponding author.

0021-9673/94/$07.00
SSDI 0021-9673(93)E0043-T

semi-preparative HPLC to isolate the four diastereomers.

2. Experimental

2.1. Reagents and chemicals

Nadolol (**1**) (Fig. 1) was purchased from Sigma (St. Louis, MO, USA). Methanol, *n*-hexane and 2-propanol were obtained from Wako (Osaka, Japan). Other chemicals were of analytical reagent grade.

2.2. Preparation of racemates

Compound **1** was dissolved in acetonitrile with slight warming. The two racemates were isolated by fractional crystallization from the solution. Two courses of fractional crystallization yielded white crystalline powders. Their melting points were 140.6 and 152.8°C, in close agreement with the melting points of racemates A and B prepared by Matsutera *et al.* [2]. The IR spectra of the two racemates (KBr disc) were examined with a Model IR-700 IR spectrometer (JASCO, Tokyo, Japan), and characteristic absorption bands were observed at 1260 cm^{-1} in racemate A and at 1240 and 3580 cm^{-1} in racemate B, consistent with the literature [1].

2.3. Preparation of diastereomers

A 1-g amount of **1** was dissolved in 20 ml of ethanol, 250 μl of the solution was injected into the preparative HPLC system and fractions of various diastereomers were repeatedly collected. The fractions were pooled and white powders were obtained by evaporating the solvent at ambient temperature under reduced pressure.

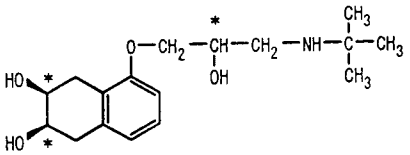

Fig. 1. Structure of nadolol. The asterisks denote the location of the chiral centres.

2.4. Apparatus and HPLC conditions

Analytical HPLC methods

The chromatograph was an LC100 system (Yokogawa, Tokyo, Japan) consisting of a pump (LC100P), an autosampler (LC100A), a column oven (LC100T) and a UV detector (LC100U). The racemates were separated on a Cosmosil $5C_{18}$ column (250 mm × 4.6 mm I.D., particle size 5 μm) (Nacalai Tesque, Kyoto, Japan) and an end-capped YMC-Pack ODS-AM-303 column (250 mm × 4.6 mm I.D., particle size 5 μm) (YMC, Kyoto, Japan). The diastereomers were resolved on an Ultron ES-OVM column (150 mm × 4.6 mm I.D., particle size 5 μm) (Shinwa, Kyoto, Japan), in which the glycoprotein ovomucoid was bound to aminopropylsilica gel, and a Chiralpak AD column (250 mm × 4.6 mm I.D., particle size 10 μm) (Daicel, Tokyo, Japan), in which a 3,5-dimethylphenylcarbamate derivative of amylose was bound to silica gel. The flow-rate was set at 0.5 or 1.0 ml/min and the detection wavelength at 220 or 230 nm. The column temperatures was maintained at 40°C for the analysis of the racemates and at 30 or 35°C for the analysis of the diastereomers. The mobile phases are specified in the figures and tables.

Preparative HPLC method

An HPLC system consisting of a Model LC-5A pump, FCV-100B fraction collector, SPD-2A UV detector, CR-3A Cromatopac recorder (Shimadzu, Kyoto, Japan) and Model AS-8010 autosampler (Tosoh, Tokyo, Japan) was used for preparative HPLC. A semi-preparative Chiralpak AD column (250 mm × 20 mm I.D., particle size 10 μm) (Daicel) was used. The flow-rate was 4 ml/min, the detection wavelength 230 nm and the column temperature 35°C. The mobile phase was *n*-hexane–2-propanol (80:20, v/v) containing 0.1% of diethylamine.

2.5. HPLC purities of the racemates

A 5-μl volume of a 1 mg/ml methanol solution of racemate A or B was injected into a Cosmosil $5C_{18}$ column mounted on the above HPLC

system, and the HPLC purity of each racemate was calculated from the peak areas other than those of the solvent peaks. The HPLC purities of racemates A and B were 98.1% and 90.1%, respectively. Under these conditions, the detection limits of racemates A and B were 0.05 and 0.07 μg, respectively ($S/N = 3$).

2.6. Contents of optical isomers of the isolated diastereomers

A 10-μl volume of a 2 mg/ml methanol solution of each diastereomer was injected into a Chiralpak AD column mounted on the above HPLC system and the contents of the optical isomers of each diastereomer were calculated from the peak areas other than those of the solvent peaks. Under these conditions, the detection limit of each diastereomer was 0.01, 0.014, 0.16, and 0.2 μg in the order of elution ($S/N = 3$).

2.7. Specific rotation

The specific rotation of a 5 mg/ml methanol solution of each stereoisomer was measured with a Model DIP-370 polarimeter (JASCO) using a quartz cell with a 100-mm layer length.

3. Results and discussion

3.1. Direct separation of the racemates

Tables 1 and 2 show the effect of the phosphate buffer concentration and the methanol contents in the mobile phase. The capacity factors (k') of racemates A and B decreased as the concentration of the phosphate buffer increased, but no marked changes were observed in the resolution (R_s) values. The methanol concentration in the mobile phase markedly affected the k' values. Therefore, 200 mM phosphate buffer (pH 7.5)–methanol (75:25, v/v) was used as the mobile phase in consideration of the analysis time and the R_s value. Racemate A was eluted more quickly than racemate B (Fig. 2A).

Table 1
Effect of buffer concentration on capacity factor (k') and resolution (R_s)

Buffer concentration (mM)	k'		R_s
	Racemate A	Racemate B	
10	10.01	10.92	0.70
50	6.48	7.05	0.76
100	5.53	6.01	0.76
200	4.28	4.64	0.79
300	3.75	4.05	0.80

Column, Cosmosil 5C_{18} (250 mm × 4.6 mm I.D.); mobile phase, methanol–phosphate buffer (pH 7.5) (3:7); flow-rate, 0.5 ml/min; column temperature, 40°C.

Similarly, the separation of the racemates was evaluated using the end-capped column. Complete separation was observed with a mobile phase of 50 mM phosphate buffer (pH 7.2)–methanol (70:30, v/v), and the elution time was markedly shorter compared with that without end-capping (Fig. 2B). This marked difference in the elution time is considered to be due to a decrease in the hydrogen bonding of residual silanol by end-capping and a resultant decrease in retention.

3.2. Direct separation of the diastereomers

The separation of the four diastereomers was studied with the Chiralpak AD column using

Table 2
Effect of mobile phase solvent ratio when using methanol as organic modifier on capacity factor (k') and resolution (R_s)

Methanol–buffer (v/v)	k'		R_s
	Racemate A	Racemate B	
20:80	10.00	11.33	2.21
25:75	5.63	6.36	1.63
30:70	2.89	3.25	1.48
35:65	1.99	2.23	1.39

Column, Cosmosil 5C_{18} (250 mm × 4.6 mm I.D.); mobile phase, methanol–200 mM phosphate buffer (pH 7.5); flow-rate, 0.5 ml/min; column temperature, 40°C.

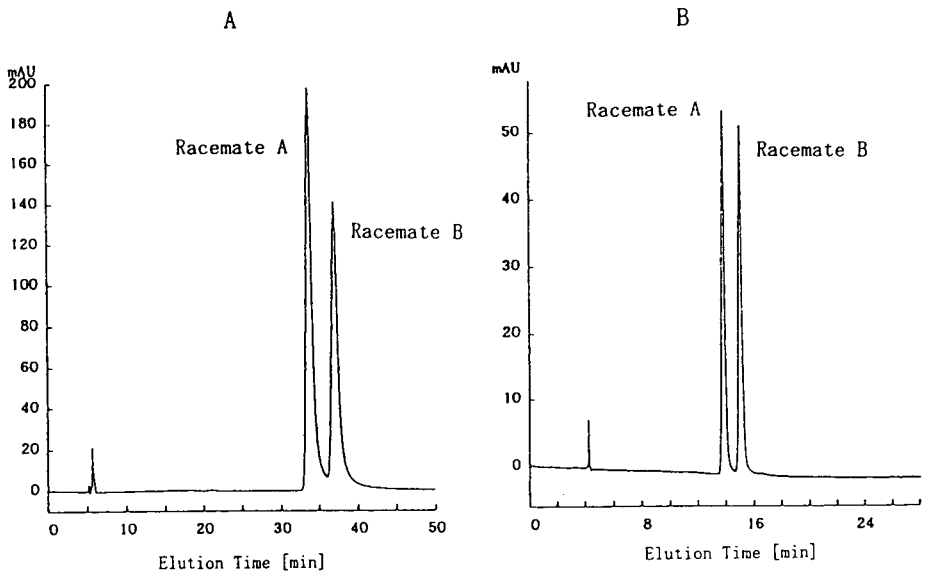

Fig. 2. Chromatograms of nadolol racemates A and B. (A) Column, Cosmosil $5C_{18}$ (250 mm × 4.6 mm I.D.); mobile phase, 200 m*M* phosphate buffer (pH 7.5)–methanol (75:25); flow-rate, 0.5 ml/min; column temperature, 40°C; volume injected, 5 μl (containing of 5 μg of nadolol). (B) Column, YMC-Pack ODS-AM-303 (250 mm × 4.6 mm I.D.); mobile phase, 50 m*M* phosphate buffer (pH 7.2)–methanol (70:30); flow-rate, 1.0 ml/min; column temperature, 40°C; volume injected, 5 μl (containing of 5 μg of nadolol).

n-hexane–2-propanol as the mobile phase and the Ultron ES-OVM column using an aqueous mobile phase of buffer solution–methanol. These mobile phases were recommended by the manufacturers of the columns to avoid their deterioration.

When the ratio of *n*-hexane and 2-propanol was changed from 60:40 (v/v) to 90:10 (v/v) with the addition of 0.1% diethylamine to improve the shape and the resolution of the peaks, the k' and R_s values improved as the proportion of *n*-hexane increased, but no changes were observed in the stereoselectivity (α). Even with the mobile phase that provided the best separation, the separation between the peak eluted first and that eluted second was insufficient, but other peaks were separated with $R_s > 2.0$ (Fig. 3A).

The elution behaviour with the Ultron ES-OVM column is reported to change with the pH of the mobile phase and the kinds and contents of organic modifiers [7,8]. From the results of a preliminary study, the composition of the mobile phase was determined as 20 m*M* phosphate buffer–methanol, and the effects of changes in the composition ratio and the pH of the phosphate buffer were evaluated.

When the pH of the phosphate buffer was below the isoelectric point of ovomucoid (p$I \approx$ 4), ovomucoid was positively charged and the analyte was scarcely retained because of the electrostatic repulsion between the stationary phase and the analyte. However, when the pH was above the isoelectric point, the k' values increased sharply. These findings were in agreement with the results of Fujima *et al.* [8] that ovomucoid becomes negatively charged and the k' value increases because of both electrostatic and hydrophobic interactions. The R_s and α values also increased with increase in pH (Table 3).

Concerning the effect of the content of methanol as an organic modifier, the k' value increased markedly and the α value increased gradually as the methanol content decreased (Table 4). This probably reflects changes in the ability to discriminate asymmetry with changes in the

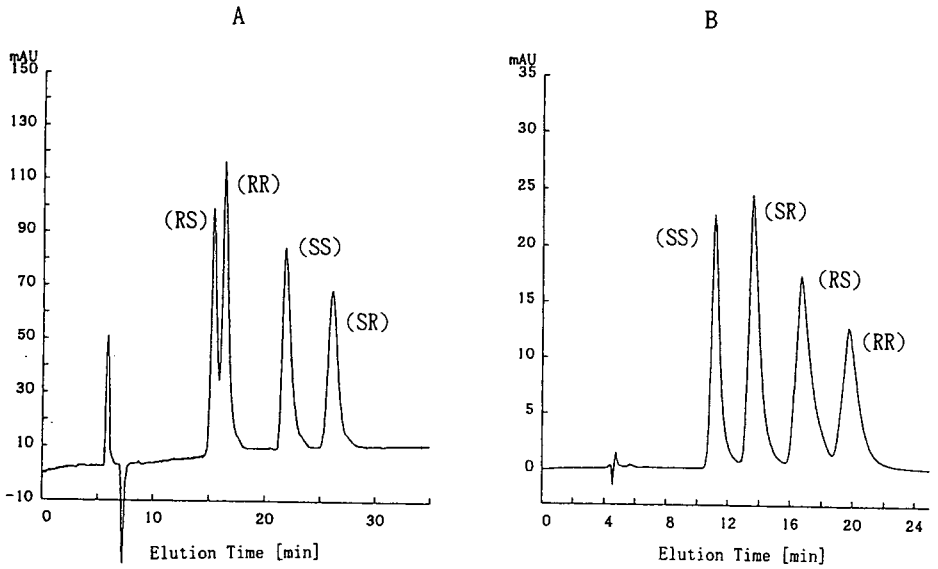

Fig. 3. Chromatogram of nadolol diastereomers. (A) Column, Chiralpak AD (250 mm × 4.6 mm I.D.); mobile phase, *n*-hexane–2-propanol (80:20) containing 0.1% of diethylamine; flow-rate, 0.5 ml/min; column temperature, 35°C; volume injected, 10 μl (containing of 10 μg of nadolol). (B) Column, Ultron ES-OVM (150 mm × 4.6 mm I.D.); mobile phase, 20 m*M* phosphate buffer (pH 6.0)–methanol (90:10); flow-rate, 0.5 ml/min; column temperature, 30°C; volume injected, 10 μl (containing of 10 μg of nadolol).

strength of the hydrophobic interaction and conformation of ovomucoid [8]. Fig. 2B shows a typical chromatogram. The peaks are mostly baseline resolved with R_s values of 1.9 or above.

3.3. Application to semi-preparative HPLC

Analytical HPLC for stereoisomers was applied to semi-preparative HPLC, and the four

Table 3
Effect of buffer pH on capacity factor (k'), resolution (R_s) and stereoselectivity (α)

pH	k'				R_s [b]			α [b]		
	Peak 1[a]	Peak 2[a]	Peak 3[a]	Peak 4[a]	Peaks 1–2	Peaks 2–3	Peaks 3–4	Peaks 1–2	Peaks 2–3	Peaks 3–4
3.0	0.00	0.00	0.00	0.00	–	–	–	1.00	1.00	1.00
3.5	0.00	0.08	0.08	0.08	0.83	–	–	1.00	1.00	1.00
4.0	0.24	0.55	0.64	0.79	2.52	0.52	0.66	2.35	1.16	1.21
4.7	0.34	0.70	0.81	0.98	2.89	0.63	0.76	2.06	1.15	1.20
5.5	0.94	1.78	2.19	2.90	3.15	1.06	1.34	1.90	1.23	1.32
6.0	3.17	5.77	7.35	9.77	4.50	1.85	2.66	1.81	1.27	1.32

Column, Ultron ES-OVM (150 mm × 4.6 mm I.D.); mobile phase, 20 m*M* phosphate buffer–methanol (97:3); flow-rate, 0.5 ml/min; column temperature, 30°C.

[a] Elution order on Ultron ES-OVM column.

[b] R_s and α values between each peak when the first-eluted peak = 1.

Table 4
Effect of mobile phase solvent ratio on capacity factor (k'), resolution (R_s) and stereoselectivity (α)

Composition[a] (v/v)	k'				R_s[c]			α[c]		
	Peak 1[b]	Peak 2[b]	Peak 3[b]	Peak 4[b]	Peaks 1–2	Peaks 2–3	Peaks 3–4	Peaks 1–2	Peaks 2–3	Peaks 3–4
80:20	1.04	1.16	1.40	1.60	0.64	1.12	0.93	1.11	1.20	1.14
85:15	1.16	1.43	1.83	2.21	1.40	1.84	1.49	1.23	1.28	1.20
87:13	1.27	1.66	2.18	2.68	1.83	2.03	1.66	1.30	1.31	1.23
90:10	1.55	2.19	2.93	3.75	2.38	2.00	1.93	1.40	1.33	1.27
95: 5	2.42	4.14	5.48	7.15	3.90	2.05	2.03	1.70	1.32	1.30
97: 3	3.17	5.77	7.35	9.77	4.50	1.85	2.66	1.81	1.27	1.32

Column, Ultron ES-OVM (150 mm × 4.6 mm I.D.); mobile phase, 20 m*M* phosphate buffer (pH 6.0)–methanol; flow-rate, 0.5 ml/min; column temperature, 30°C.
[a] Composition of 20 m*M* phosphate buffer (pH 6.0)–methanol.
[b] Elution order on Ultron ES-OVM column.
[c] R_s and α values between each peak when the first-eluted peak = 1.

nadolol diastereomers were isolated. The semi-preparative Chiralpak AD column was used, because the use of an organic solvent system as the mobile phase facilitates the treatments of collected fractions, the injection volume is greater and the peak shapes are not altered. The composition of the mobile phase was the same as in the analytical method. Table 5 shows the contents and specific rotations of each of the resolved diastereomers.

3.4. *Assignment of separated peaks*

The configurations of the four diastereomers separated by analytical HPLC were elucidated from racemates A and B and the resolved diastereomers. Racemates A and B were analyzed using each analytical column used for the analysis of diastereomers, and + − (*RS*) or − + (*SR*) and + + (*RR*) or − − (*SS*) was established from the retention time and the specific rotatior of each diastereomer of racemates A and B Further, to confirm these assignments, racemates A and B and the resolved diastereomers were analyzed by the method of Dyas *et al.* [6] using the same column. As a result, we determined the order of elution to be (*RS*), (*RR*), (*SS*) and (*SR*) from the Chiralpak AD column and (*SS*), (*SR*), (*RS*) and (*RR*) from the Ultron ES-OVM column.

Table 5
Stereoisomer contents and optical rotations of the isolated diastereomers from nadolol

Peak No.[a]	Content (%)[b]				$[\alpha]_D^{20}$ (°)[c]	Racemate
	Peak 1	Peak 2	Peak 3	Peak 4		
1	100.0	N.D.[d]	N.D.	N.D.	+9.2	A
2	2.40	97.59	N.D.	N.D.	+20.5	B
3	0.05	0.07	98.15	1.72	−22.8	B
4	N.D.	0.19	0.75	99.05	−14.1	A

[a] Elution order on Chiralpak AD column.
[b] Area percentage of peaks on Chiralpak AD column.
[c] See Section 2.7.
[d] N.D. = not detected.

In conclusion, we established methods for the direct HPLC separation of the two racemates and four diastereomers of nadolol. In the separation of the racemates, the hydrogen bonding of residual silanols in the packing was considered to affect the retention time. The diastereomers could be separated by organic and aqueous mobile phases, and the organic mobile phase could also be applied to semi-preparative HPLC.

4. References

[1] L. Slusarek and K. Florey, in K. Florey (Editor), *Analytical Profiles of Drug Substances*, Vol. 9, Academic Press, New York, 1980, p. 455.

[2] E. Matsutera, Y. Nobuhara and Y. Nakanishi, *J. Chromatogr.*, 216 (1981) 374.

[3] P.M. Lacroix, N.M. Curran and E.G. Lovering, *J. Pharm. Biomed. Anal.*, 10 (1992) 917.

[4] G. Schill, I.W. Wainer and S. Barkan, *J. Liq. Chromatogr.*, 9 (1986) 641.

[5] C.R. Lee, J.P. Porziemsky, M.C. Aubert and A.M. Krstulovic, *J. Chromatogr.*, 539 (1991) 55.

[6] A.M. Dyas, M.L. Robinson and A.F. Fell, *J. Chromatogr.*, 586 (1991) 351.

[7] J. Haginaka, C. Seyama, H. Yasuda and K. Takahashi, *J. Chromatogr.*, 598 (1992) 351.

[8] H. Fujima, H. Kitagawa, H. Kitamura and H. Wada, *Chromatography (Kuromatogurafi)*, 13 (1992) 385.

ELSEVIER

Journal of Chromatography A, 664 (1994) 111–116

JOURNAL OF CHROMATOGRAPHY A

Short Communication

High-performance liquid chromatographic characterization of monofluorophosphate, difluorophosphate and hexafluorophosphate

Norimasa Yoza*[,a], Sachiko Nakashima[a], Nobuyuki Ueda[a], Tohru Miyajima[a], Terumasa Nakamura[b], Pierre Vast[c]

[a]*Department of Chemistry, Faculty of Science, Kyushu University, Fukuoka 812, Japan*

[b]*School of Nursing and Medical Technology, University of Occupational and Environmental Health, Yahatanishi-ku, Kitakyushu 807, Japan*

[c]*Laboratory of Applied Chemistry, University of Science and Technology of Lille, 59655 Villeneuve d' Ascq Cedex, France*

(First received September 20th, 1993; revised manuscript received November 18th, 1993)

Abstract

The retention behaviour of fluorophosphates on an anion-exchange column was characterized and compared with that of phosphates. Postcolumn blue coloration of phosphorus with a molybdenum reagent allowed the sensitive detection of both fluorophosphates and phosphates. ^{31}P NMR measurements were also employed to provide complementary data for the identification of phosphorus compounds. The retention times of orthophosphate and its fluorine derivatives increased with increasing number of P–F bonds: $PO_4^{3-} < PO_3F^{2-} < PO_2F_2^- < PF_6^-$. Good separation among orthophosphate, monofluorophosphate and difluorophosphate was achieved, but hexafluorophosphate was adsorbed too strongly to be eluted. It is suggested that fluorine derivatives of diphosphate (pyrophosphate), $P_2O_6F^{3-}$ and $P_2O_5F_2^{2-}$, might be present as minor impurities in monofluorophosphate chemicals. A misleading suggestion as to the assignment of unknown peaks in a preliminary report was corrected. Retention times with elution using 0.18 *M* KCl of the authentic phosphates and fluorophosphates and the speculated diphosphate derivatives increased in the order $PO_4^{3-} < PO_3F^{2-} < P_2O_7^{4-} < P_2O_6F^{3-} < P_3O_{10}^{5-} < PO_2F_2^- < P_2O_5F_2^{2-} < P_3O_9^{3-} < PF_6^-$.

1. Introduction

Of the three fluorine derivatives of orthophosphate (P_1) [1] shown in Table 1, monofluorophosphate (MFP) has been widely used as a caries-preventive additive in dentifrices [2] and examined as a drug for the treatment of osteoporosis [3]. In connection with these important applications in biological systems, much attention has been focused on the bioavailability or enzyme-catalysed reaction of MFP. By employing high-performance liquid chromatography (HPLC), flow-injection analysis (FIA) and ^{31}P NMR spectrometry, we have demonstrated that alkaline phosphatase (EC 3.1.3.1) catalyses the hydrolysis of MFP with extremely high activity. The P–F bond cleavage to produce P_1 and fluoride ion at pH 7.2 is accelerated by a factor of as high as 10^{10} [4–6]. Such enzyme-catalysed reactions of inorganic phosphorus compounds,

* Corresponding author.

0021-9673/94/$07.00
SSDI 0021-9673(93)E0045-V

Table 1
Abbreviations for phosphorus compounds discussed in this paper

Abbreviation	Structural formula
P_1	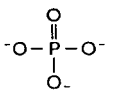
MFP	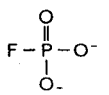
DFP	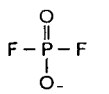
HFP	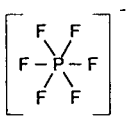
P_2	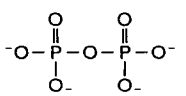
MFP_2	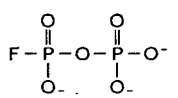
DFP_2	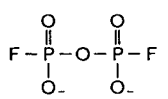

including the hydrolysis of diphosphate (pyrophosphate, P_2) by inorganic pyrophosphatase (EC 3.6.1.1) [7,8], have also been investigated to elucidate the role of inorganic phosphorus compounds in metabolic processes of organisms [9], prebiotic processes of evolution [10] and eutrophication processes of environmental water [11]. The results with MFP and P_2 stimulated our interest and studies were extended to the enzymatic degradation of other fluorophosphates [12] such as difluorophosphate (DFP), hexafluorophosphate (HFP) and derivatives of P_2 [13–15], monofluorodiphosphate (MFP_2) and difluorodiphosphate (DFP_2).

Advanced analytical techniques are needed in performing kinetic experiments on enzymatic reactions described above. This work was undertaken to establish an HPLC method for the determination of MFP, DFP and HFP. The successful separation of P_1, MFP and DFP and the extraordinarily strong adsorption of HFP on the column are described. ^{31}P NMR spectrometry was successfully employed as a complementary technique to HPLC for identifying phosphorus compounds for which authentic references were unavailable. The combined application of both HPLC and NMR methods to the fine characterization of several impurities in MFP chemicals is also described.

2. Experimental

Two samples of monofluorophosphate (Na_2PO_3F) from different sources were used: MFP-I was obtained from Aldrich (Milwaukee, WI, USA) and MFP-II was a gift from an industrial company. Sodium hexafluorophosphate ($NaPF_6$) was also available from Aldrich. Potassium difluorophosphate (KPO_2F_2) was prepared according to the literature [12].

The HPLC system consisted of a TSKgel SAX anion-exchange column (25 cm × 4 mm I.D.) and a postcolumn reaction detector as reported previously [4,5,7], except that a conventional spectrophotometric LC detector (Shimadzu SPD-6AV) was used instead of a photodiode-array detector. The conversion of phosphorus compounds into orthophosphate and the subsequent chromogenic reaction to form the so-called heteropoly blue was simultaneously achieved in a high-temperature reactor (140–150°C) using an acidic molybdenum(V)–molybdenum(VI) reagent. Retention times of anionic phosphorus compounds were effectively controlled by varying the potassium chloride concentrations of the eluents at a constant EDTA(4Na) concentration of 0.1% with a pH of *ca.* 10–10.5.

^{31}P NMR spectra were recorded at 25°C by using 10-mm tubes on a JEOL-GX-400 spectrometer operating at 162 MHz. Chemical shifts (δ values in ppm) are presented with respect to an external reference of 85% phosphoric acid, with positive values being downfield of the reference.

3. Results and discussion

The main objective of this work was to investigate the chromatographic retention behaviour of three fluorophosphates, MFP, DFP and HFP, on an anion-exchange separation column. Four phosphates, P_1, P_2, P_3 (triphosphate, $P_3O_{10}^{5-}$) and cP_3 (cyclotriphosphate, $P_3O_9^{3-}$), were used as reference samples. The reference samples are available commercially or can be prepared in the laboratory as sodium salts of high purity (>99%). HPLC data for these reference samples on the same anion-exchange separation column as used in this work have been reported previously [4,5,7]. A postcolumn chromogenic reaction system for phosphates and MFP using a molybdenum(V)–molybdenum(VI) reagent has been confirmed to be sensitive enough to permit the spectrophotometric detection of as low as $2 \cdot 10^{-7}$ *M* phosphorus(V) [4,7].

The successful separation of MFP from P_1, P_2 and P_3 has been reported in previous papers [4,5,7], but no chromatographic data were available for DFP and HFP. It was pointed out that MFP chemicals contain 6–13% of phosphorus as impurities. In addition to the peaks of P_1, P_2, and P_3 an unknown peak was observed between those of P_2 and P_3. We suggested that DFP, the closest homologue of MFP, might be one of the probable species assignable to this unknown peak. At that time DFP and HFP were not available as references. Further examination with additional use of authentic samples of DFP, HFP and cP_3 was attempted in this work. As will be mentioned later, neither DFP nor HFP was ascribable to the unknown peak.

3.1. ^{31}P NMR characteristics of fluorophosphate samples

As reliable standard methods for the purification and analysis of fluorophosphates have not been established, it seems difficult to obtain alkaline fluorophosphates of guaranteed high purity. Most MFP, DFP and HFP from commercial and industrial sources might contain considerable amounts of impurities that must often be analysed by users. Three fluorophosphates to be used for subsequent HPLC experiments were preliminarily analysed by ^{31}P NMR spectrometry to evaluate the approximate purity of each matrix compound and to identify the impurities. As shown in Figs. 1–3, MFP, DFP and HFP showed spectra with a doublet, triplet and septet, respectively, with $N + 1$ lines where N is the number of P–F bonds. The chemical shift (δ) and coupling constant ($^1J_{PF}$) of MFP were greatly affected by pH variations at pH <5, but remained unchanged in the pH range 6–11;

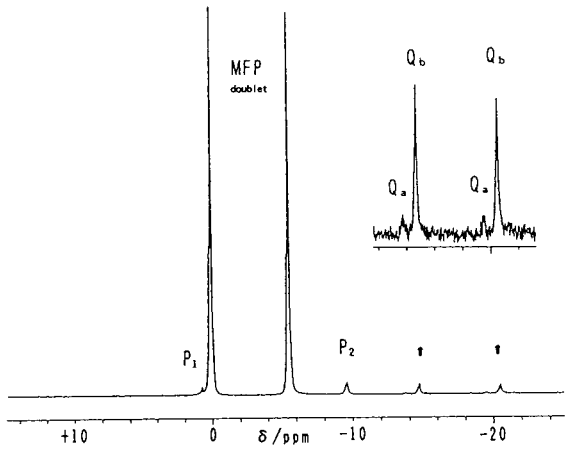

Fig. 1. ^{31}P NMR spectrum of monofluorophosphate. Sample, 0.1 *M* MFP-II (pH 4). P_1, P_2, Q_a and Q_b are impurities. Q_a and Q_b are discussed in Fig. 4. Small signals of P_3 may be included in the signal of P_2 and the upper field signal of Q_b.

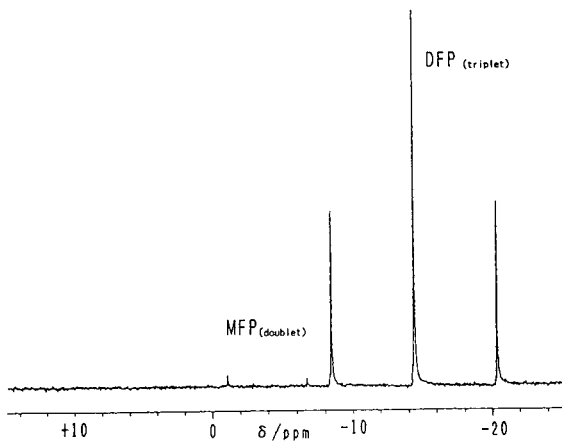

Fig. 2. ^{31}P NMR spectrum of difluorophosphate. Sample, 0.01 *M* DFP (pH 3.5). MFP is an impurity.

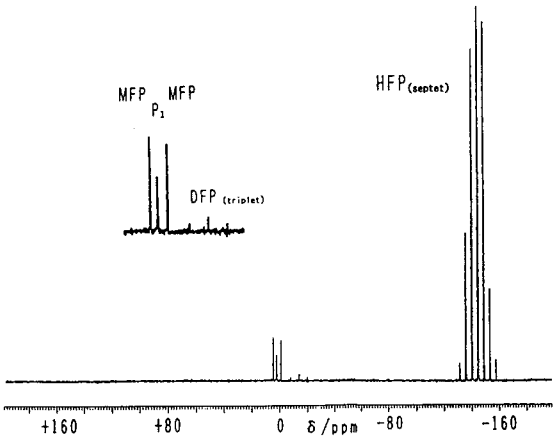

Fig. 3. ^{31}P NMR spectrum of hexafluorophosphate. Sample, 0.1 *M* HFP (pH 6.7). P_1, MFP and DFP are impurities.

$\delta = +1.3 \pm 0.2$ ppm and $^1J_{PF} = 869 \pm 2$ Hz [6]. On the other hand, the NMR parameters of DFP ($\delta = -14.2 \pm 0.1$ ppm, $^1J_{PF} = 962 \pm 1$ Hz) and HFP ($\delta = -144 \pm 1$ ppm, $^1J_{PF} = 712 \pm 1$ Hz) were independent of pH over the wide pH range of 3–10. Identification of most of the impurity signals was achieved as indicated in Figs. 1–3 by reference to published NMR data [1,6]. Detailed discussion as to the identification of Q_a and Q_b will be made late by cross-reference to both NMR and HPLC data.

3.2. HPLC profiles of reference samples

All chromatographic runs in this work were made by isocratic modes. Fig. 4 (top) shows an HPLC profile for a mixed solution of authentic samples, P_1, P_2, P_3 and MFP. The four components were well resolved with retention times (t_R) within 30 min. A cyclic reference sample, cP_3, appeared at 288 min far behind the linear phosphates. The HPLC profile will be referenced hereafter in assigning unknown peaks.

It was preliminarily confirmed by FIA [5,16] that DFP and HFP, in addition to MFP [4], were quantitatively detectable by the same post-column chromogenic reaction system as used for the above phosphates. HPLC of a freshly prepared aqueous solution of DFP gave a major

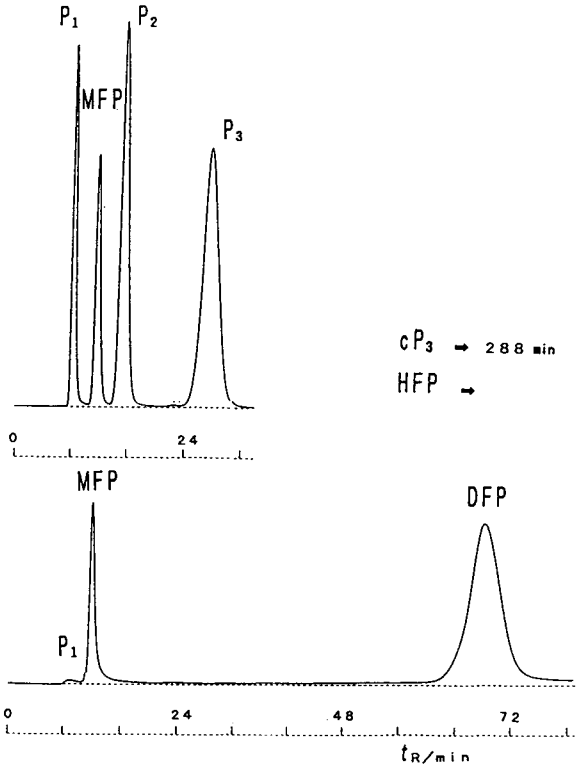

Fig. 4. HPLC profiles of an authentic mixture of monofluorophosphate, orthophosphate, diphosphate and triphosphate (top) and of difluorophosphate and its hydrolytic products (bottom). Eluent, 0.18 *M* KCl + 0.1% Na_4EDTA; sample, top, an equimolar mixture (0.1 m*M* each) of MFP, P_1, P_2, and P_3, and bottom, 0.22 m*M* DFP and its hydrolysate, MFP; detection, 690 nm, 0.16 AUFS (top) and 0.08 AUFS (bottom). cP_3 appeared at 288 min (not shown), but HFP was not eluted within 400 min.

peak of DFP at 68 min between the peaks of P_3 and cP_3. A small peak of MFP was also observed, indicating 98% purity of the DFP, as expected from the NMR data in Fig. 2. In order to elucidate the retention behaviour of DFP relative to that of MFP, the DFP sample solution including MFP, a hydrolysate produced during prolonged storage of DFP solution, was eluted. As shown in Fig. 4 (bottom) both peaks of MFP and DFP were well defined and separated. The retention behaviour of HFP was examined in a separate experiment. No positive appearance of

an HFP peak was observed within 400 min. The HFP might be strongly adsorbed on the column.

In order to shorten the retention times of DFP and HFP for practical purposes of routine analysis, the eluent concentration was increased from 0.18 *M* KCl to 0.35 and 0.40 *M* KCl. In both instances MFP, P_1, P_2 and P_3 were recorded as an unresolved muti-component peak at 8.0 min. DFP (40 min) appeared before cP_3 (45 min) with 0.35 *M* KCl, but the retention order was reversed with 0.40 *M* KCl; DFP (36 min) appeared after cP_3 (28 min). The effect of the eluent concentration on the retention time of DFP was smaller than that of cP_3 owing to the difference in the anionic charges of DFP and cP_3, −1 and −3, respectively [17]. Surprisingly, no peak of HFP was observed within 100 min, where most linear and cyclic oligophosphates were eluted [17,18]. Further attempts were made with stronger 1.0 *M* KCl but again without any positive appearance of HFP within 100 min.

3.3. Identification of impurities in MFP

Two MFP samples from different sources were eluted with the same eluent concentration as that in Fig. 4. As shown in the main profile (Fig. 5), MFP-II indicated five impurities; P_1, P_2 and P_3 were identified by reference to the standard profile (Fig. 4), but Q_a and Q_b are speculative. MFP-I (inset) contained a small amount of Q_a, but Q_b was not detected. In a previous paper [4] we carried out a similar experiment on MFP and observed unknown peaks of Q_a and Q_b. At that time DFP and HFP were not available as reference samples. It was speculated that Q_a and Q_b might be assignable to DFP and cP_3, respectively. The present re-examination with the additional use of DFP, HFP and cP_3, however, provided clear evidence that neither DFP, HFP nor cP_3 could be assigned to Q_a and Q_b (Fig. 5). A similar conclusion was also drawn from additional experiments with 0.35 *M* KCl eluent; Q_b

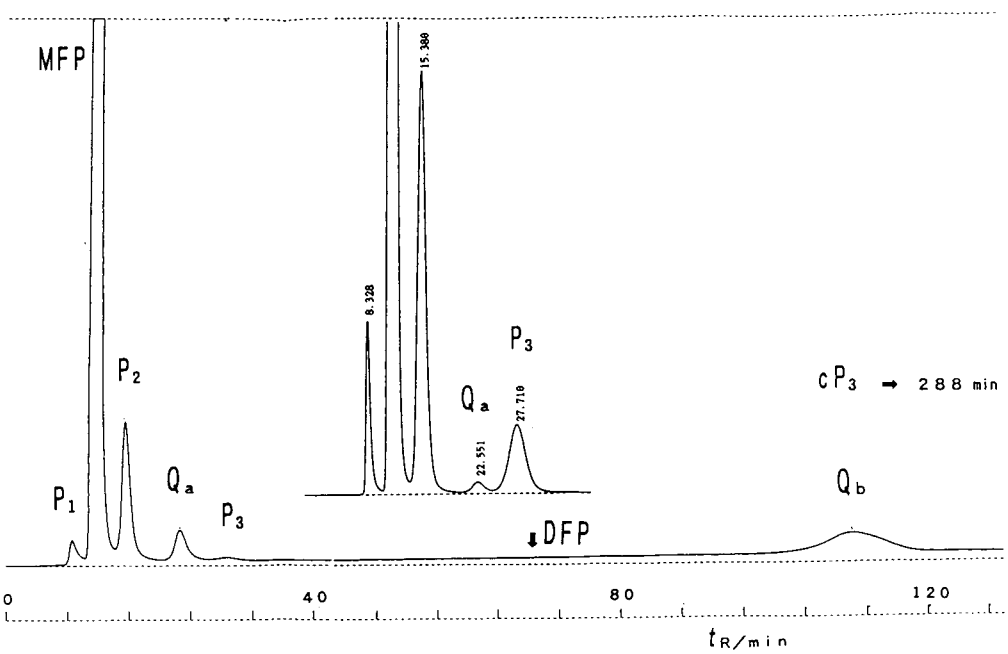

Fig. 5. HPLC profiles of two disodium monofluorophosphate samples from different sources and identification of impurities. Sample, 1 m*M* MFP-II and (inset) 1 m*M* MFP-I. Other conditions as in Fig. 4, except recording at 0.08 AUFS. Retention times of DFP and cP_3 from Fig. 4 are also indicated for comparison.

appeared at 36 min, *i.e.*, different from the retention times of cP_3 and DFP, with the order, $Q_b < cP_3 < DFP$.

4. Conclusions

None of the reference samples examined in this work is a candidate for Q_a and Q_b, and we must again speculate that some phosphorus compounds produced Q_a and Q_b. Fluorine derivatives of diphosphate (MFP_2 for Q_a and DFP_2 for Q_b) are considered to be the most probable candidates. Some reasons for suggesting such species are that (a) the relative amounts of Q_a and Q_b in the HPLC profile (Fig. 5) are in approximate agreement with those of the NMR signals of Q_a and Q_b in Fig. 1, (b) the anionic charges of Q_a and Q_b calculated from the effect of eluent concentration on retention time [17,18] were −3 and −2, respectively, and (c) a "doublet" peak of Q_b with $\delta = -17.7$ ppm and $J = 938$ Hz is similar to the doublet peak with $\delta = -17.8$ ppm and $^1J_{PF} = 943$ Hz of DFP_2 in the literature [14]. No information on the formation or NMR spectrum of MFP_2 is available, but the similarity between the large coupling constants of the Q_a "doublet" and Q_b "doublet" suggests that Q_a is assignable to MFP_2, although the small splitting of each signal of Q_a and Q_b has not been clarified.

The retention times in 0.18 *M* KCl (Fig. 4) of the seven authentic phosphates and fluorophosphates and the speculated derivatives of diphosphate decrease in the order $P_1 < MFP < P_2 < MFP_2 < P_3 < DFP < DFP_2 < cP_3 < HFP$. From the viewpoint of practical application it is worth noting that (1) the retention times of orthophosphate analogues increased with increasing number of P–F bonds, $P_1 < MFP < DFP < HFP$, and a good separation among P_1, MFP and DFP was achieved, whereas HFP was adsorbed too strongly to be eluted. Finally, we hope that MFP_2 and DFP_2 will become available as reference samples so that re-examination will become feasible to confirm the assignments of Q_a and Q_b speculated in this work.

5. References

[1] J.R. Van Wazer, *Phosphorus and Its Compounds*, Interscience, New York, 1958, Ch. 13.
[2] E.I.F. Pearce, *Caries Res.*, 17, Suppl. 1 (1983) 21.
[3] F. Liote, C. Bardin, A. Liou, A. Brouard, J.L. Terrien and D. Kuntz, *Calcif. Tissue Int.*, 50 (1992) 209.
[4] N. Yoza, S. Nakashima, T. Nakazato, N. Ueda, H. Kodama and A. Tateda, *Anal. Chem.*, 64 (1992) 1499.
[5] N. Yoza, S. Nakashima, I. Akazaki, N. Ueda, T. Nakazato, N. Tokushige and T. Yokota, *Mem. Fac. Sci. Kyushu Univ., Ser. C*, 18 (1992) 203.
[6] N. Yoza, N. Ueda and S. Nakashima, *Fresenius' J. Anal. Chem.*, in press.
[7] N. Yoza, I. Akazaki, T. Nakazato, N. Ueda, H. Kodama and A. Tateda, *Anal. Biochem.*, 199 (1991) 279.
[8] N. Yoza, H. Hirano, Y. Baba and S. Ohashi, *J. Chromatogr.*, 325 (1985) 385.
[9] H. Hirano, Y. Baba, N. Yoza and S. Ohashi, *Chem. Lett.*, (1986) 633.
[10] N. Yoza, N. Ueda, N. Tokushige, T. Miyajima, Y. Baba, M. Tsuhako and A. Tateda, *Inorg. Chim. Acta*, 202 (1992) 237.
[11] N. Yoza, S. Sagara, H. Morioka, T. Handa, H. Hirano, Y. Baba and S. Ohashi, *J. Flow Inject. Anal.*, 3 (1986) 37.
[12] P. Vast, G. Palavit and A. Semmoud, *Phosphorus Res. Bull.*, 1 (1991) 439.
[13] A. Addou, P. Vast and P. Legrand, *Bull. Soc. Chim. Fr.*, (1984) 55.
[14] H. Falius, *Angew. Chem., Int. Ed. Engl.*, 7 (1968) 622.
[15] U. Schulke and R. Kayser, *Z. Anorg. Allg. Chem.*, 600 (1991) 221.
[16] T. Nakazato and N. Yoza, *J. Chromatogr.*, 641 (1993) 221.
[17] Y. Baba, N. Yoza and S. Ohashi, *J. Chromatogr.*, 348 (1985) 27.
[18] G. Kura, E. Kitamura and Y. Baba, *J. Chromatogr.*, 628 (1993) 241.

ELSEVIER

Journal of Chromatography A, 664 (1994) 117–122

JOURNAL OF CHROMATOGRAPHY A

Short Communication

Effect of functional groups on the retention behaviour of anions in ion chromatography using a coated silica column

Yoshimasa Michigami*, Kanae Fujii, Kazumasa Ueda

Department of Chemistry and Chemical Engineering, Faculty of Technology, Kanazawa University, 2-40 Kodatsuno, Kanazawa 920, Japan

(First received October 19th, 1993; revised manuscript received December 28th, 1993)

Abstract

The effect of functional groups on the retention behaviour of some anions was investigated in ion chromatography using ODS columns coated with several quaternary ammonium or phosphonium salts that have various free alkyl groups on the nitrogen and phosphorus atoms. The retention behaviour of strongly retained monovalent anions, such as nitrate and bromide, was greatly affected by the alkyl groups. However, those of divalent and weakly retained monovalent anions were little affected. The retention of anions on the quaternary phosphorus atom were stronger than those on the quaternary nitrogen atom.

1. Introduction

Ion chromatography has become a popular technique for the determination of anions, which is usually difficult by classical techniques [1]. It has been reported based on chemical ion-exchange selectivities that variation of the resin matrix should have a large effect on the relative selectivities of different ions [2]. Some studies on the retention behaviour of ions on the functional groups of ion-exchange resins by ion chromatography have been reported [1–5]. In some studies [3,4] functional groups reacted with styrene–divinylbenzene copolymer (XAD-1) and quaternary ammonium salts were used, and in others [2,5] XAD-1 columns coated with quaternary ammonium salts were used. The effects of alkyl functional groups on the quaternary nitrogen atom was investigated by the use of chemically bonded trialkylammonium resins or other quaternary ammonium resins [1,3,4]. The retention of polarizable anions (NO_3^-, I^-, etc.) was stronger than that of the other anions and increased with increasing R groups on the nitrogen atom. This was explained by the phenomenon of "water structure induced by ion pairing" [1,3].

Column coating techniques for anion chromatography have been reported [2,6–9]. The advantage of such techniques is the easy preparation of columns with various ion-exchange groups and capacities.

In this work, the effect of free alkyl groups on the quaternary nitrogen atom on the retention behaviour (or relative selectivities) of anions was studied by ion chromatography using ODS col-

* Corresponding author.

0021-9673/94/$07.00
SSDI 0021-9673(94)00009-X

Table 1
Chromatographic conditions

Separation column	Octadecylsilica (ODS) columns dynamically coated with various quaternary ammonium or phosphonium salts
Column temperature	35°C
Sample loop	100 μl
Detection wavelength	210 nm
Flow-rate	1.0 ml min^{-1}
Eluent	1.0 mmol l^{-1} citrate (pH 6.5)

umns coated with several quaternary ammonium or phosphonium salts and with a citrate eluent. The local electrical densities (or bacisities) on the quaternary nitrogen and phosphorus atoms in the ion-exchange process are briefly discussed.

2. Experimental

The ion chromatographic equipment consisted of a pump (CCPD; Tosoh, Tokyo, Japan), a variable-wavelength ultraviolet detector (UV-8011 or UV-8000; Tosoh), an injector (Rheodyne, Cotati, CA, USA), a column oven (CO-8000; Tosoh) and a pen recorder (YEW type 3066; Yokogawa, Tokyo, Japan). The operating conditions are given in Table 1.

All chemicals were of analytical-reagent grade, and deionized, distilled water, further filtered through a 0.45-μm membrane filter, was used.

The eluent was 1 mmol l^{-1} citrate, adjusted to pH 6.5 with dilute sodium hydroxide solution. The eluent was degassed ultransonically before use.

The quaternary ammonium and phosphonium salts used and their abbreviations are given in Table 2. CTBuABr was synthesized according to the following procedure, which was a modification of the procedure used by Ohki *et al.* [10]. Cetyl bromide (5 mmol), tri-*n*-butylamine (5 mmol) and methanol (5 ml) were placed in a glass tube, which was sealed under vacuum after several freeze–pump–thaw cycles. The sealed tube was heated for 8 h at 100°C and shaken intermittently. The synthesized CTBuABr was passed through a glass column packed with silica gel (Wakogel C-100; Wako, Osaka, Japan), after dissolution in 30% methanol solution. The column was washed with about 50 ml of 70% methanol and CTBuABr was obtained by evaporating the elute and washings. Other synthetic cetyltrialkylammonium salts and cetyltriphenylphosphonium salts were prepared from the corresponding cetyl halides and tri-

Table 2
Quaternary ammonium and phosphonium salts

Abbreviation	Compound	Source
CTMABr	Cetyltrimethylammonium bromide	Commercially available
CTEABr	Cetyltriethylammonium bromide	Synthesized
CTPrABr	Cetyltripropylammonium bromide	Synthesized
CTBuABr	Cetyltributylammonium bromide	Synthesized
CPyCl	Cetylpyridinium chloride	Commercially available
CDMEABr	Cetyldimethylethylammonium bromide	Commercially available
CDMBuABr	Cetyldimethylbutylammonium bromide	Synthesized
CDMBnACl	Cetyldimethylbenzylammonium chloride	Synthesized
CTBuPBr	Cetyltributylphosphonium bromide	Commercially available
CTPhPI	Cetyltriphenylphosphonium iodide	Synthesized

alkylamines or triphenylphosphine in a procedure similar to the synthesis of CTBuABr except for the heating temperature; CTEABr 90°C, CTPrABr 100°C and CTPhPI 130°C. All of the compounds were similarly purified with silica gel. CDMBuABr and CDMBnACl were synthesized from cetyldimethylamine and *n*-butyl bromide and benzyl chloride, respectively, and similarly purified with silica gel.

Dynamically coated columns were prepared from columns (50 × 4.6 mm I.D.) packed with ODS resin (Capcell Pak C_{18}, AG-120, 5 μm particle size; Shiseido, Tokyo, Japan), which has no silanol groups. No retention of anions was observed on this ODS resin. The coating procedure was similar to that used by DuVal and Fritz [2] and Mullins [9]. The column was coated with about 70 ml of 0.01 mol l^{-1} quaternary ammonium or phosphonium salt in about 10% methanol solution at a flow-rate of 0.5 ml min^{-1}. The end of the coating procedure was confirmed by absorbance monitoring during elution. They were then conditioned with the eluent before testing. The column capacities were calculated from the measurement of the eluate absorbance during the eluent conditioning.

3. Results and discussion

The effect of trialkyl (R) groups in cetyltrialkylammonium groups ($C_{16}R_3N^+$) on the capacity factors of some anions was examined. The results obtained are given in Table 3 and the chromatograms of some anions of CTMABr- and CTBuABr-coated columns are shown in Figs. 1 and 2, respectively. The effect of the column capacity on the retention of anions could be ignored, as almost identical column capacities were obtained, as shown in Table 3. The retention of polarizable (or strongly retained) monovalent anions, such as nitrate, nitrite and bromide, increased with the larger R groups, whereas this tendency was only slight for weakly retained monovalent anions, such as chloride, fluoride, phosphate and hydrogencarbonate. Benzoate, iodide and thiocyanate as monovalent anions were very strongly retained on the coated columns and their retention behaviour could not be observed. However, the retention of divalent anions, such as oxalate, sulphate and thiosulphate, decreased with the larger R groups. A change in the elution order was also observed on these coated columns; the larger R groups reversed the elution order of nitrate and thiosulphate and of nitrite and sulphate. This retention behaviour of monovalent and divalent anions was similar to that reported by Barron and Fritz [3,4]. They explained the effect by stronger ion pairing, resulting from disruption of the water structure by the anions and by tightening of the water structure surrounding the ion pair by the larger R groups for poorly hydrated anions, such as bromide, iodide and nitrate. On the other hand, the retention of nicotinate as a monovalent anion also decreased. This may be due to the size exclusion effect for bulky nicotinate anion.

The local electrical densities (or basicities) on the nitrogen atom were decreased with the larger R groups, because the local electron supply to the nitrogen atom from the surrounding R groups was decreased with the larger R groups. Hence the retentions of polarizable anions were increased. However, those of divalent anions were decreased, because two sites of nitrogen atoms may be necessary for their retention in the ion-exchange process and the steric hindrance may be increased.

For the cetylpyridinium group with no free alkyl groups on the quaternary nitrogen atom, the retentions of anions were slightly weaker than those for CTMABr which had the smallest R groups, as shown in Table 3. This may be due to higher local electrical density on the nitrogen atom in the pyridinium ring.

However, the retentions of polarizable and weakly retained monovalent anions decreased with the larger monosubstituted R groups and those of divalent anions decreased slightly or were almost constant for cetyldimethylalkylammonium groups ($C_{16}Me_2RN^+$), as shown in Table 3. The results for monovalent anions from dimethylalkylammonium groups showed the opposite tendency to those from trialkylammonium groups. However, the results for divalent anions

Table 3
Capacity factors for anions on columns coated with quaternary ammonium or phosphonium groups

Anion	Capacity factor (k')									
	CTMABr (0.15)[a]	CTEABr (0.14)	CTPrABr (0.14)	CTBuABr (0.17)	CPyCl (0.16)	CTBuPBr (0.11)	CTPhPI (–)	CDMEABr (0.17)	CDMBuABr (0.15)	CDMBnACl (0.18)
Benzoate	>60	>60	>60	>60	>60	>60	>60	>60	>60	>60
Bromide	11.3	11.7	13.0	13.3	8.3	24.0	28.0	7.4	7.1	16.8
Chloride	2.4	2.3	2.3	2.3	2.3	3.8	2.7	1.9	1.8	3.4
Fluoride	0.7	0.7	0.7	0.7	0.7	0.7	0.8	0.7	0.7	0.8
Hydrogen carbonate	0.7	0.7	0.7	0.7	0.7	0.7	0.8	0.7	0.7	0.8
Iodide	>60	>60	>60	>60	>60	>60	>60	>60	>60	>60
Nicotinate	13.1	–	–	4.7	11.7	5.9	–	11.1	4.6	7.0
Nitrate	19.5	21.7	31.3	41.3	12.0	55.0	65.7	13.7	12.1	25.7
Nitrite	6.0	6.7	6.7	8.0	4.0	10.0	8.5	4.2	3.7	6.6
Oxalate	7.8	–	–	3.9	7.0	6.3	10.7	–	7.6	7.9
Phosphate	1.3	1.3	1.3	0.7	1.0	1.1	0.8	–	0.9	0.8
Sulphate	6.3	4.3	3.3	3.0	5.3	4.0	2.3	5.1	4.6	6.6
Thiosulphate	25.7	19.7	13.3	13.3	19.3	30.0	16.6	–	20.7	55
Thiocyanate	>60	>60	>60	>60	>60	>60	>60	>60	>60	>60

Chromatographic conditions as in Table 1.
[a] Values in parentheses are ion-exchange capacities of the coated columns in mequiv. per column.

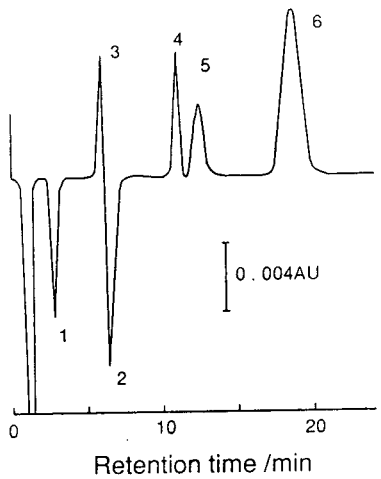

Fig. 1. Separation of anions on CTMABr-coated column. Peaks: 1 = chloride (10 μg ml^{-1}); 2 = sulphate (40 μg ml^{-1}); 3 = nitrate (1 μg ml^{-1}); 4 = bromide (6 μg ml^{-1}); 5 = nicotinate (60 μg ml^{-1}); 6 = nitrate (4 μg ml^{-1}). Conditions as in Table 1. Peaks as in Fig. 1.

from both groups showed similar a tendency and no change in the elution order of anions was observed. The effect of alkyl groups on the local electron supply to the nitrogen atom for dimethylalkylammonium groups is much smaller than that for trialkyl groups, and the effect of the hydrophobic mono-R groups for the retention of anions increased with the larger R groups. This was also indicated by a stronger retention of anions on the CDMBnACl-coated column, as shown in Table 3.

Quaternary phosphonium groups ($CTBuP^+$ and $CTPhP^+$) instead of quaternary ammonium groups were also examined. The retention of most anions, especially polarizable anions, increased on the CTBuPBr-coated column compared with the CTBuABr-coated column, in spite of low ion-exchange capacity on the former column, as shown in Table 3 and Figs. 1 and 3. This may be explained by the difference in electronegativities between nitrogen and phosphorus atoms.

The anions may be retained on the resins in ion chromatography by complex interactions, such as ion-exchange processes, hydrophobic interactions and the ion-pairing effect. In this paper, the retention of anions has been discussed from the point of view of the local electrical densities (or bacisities) on the quaternary nitrogen atom in the ion-exchange process. The retention behaviour of polarizable (strongly retained) monovalent anions, such as nitrate and bromide, was greatly influenced by the free alkyl groups on the quaternary nitrogen atom, but that of divalent and weakly retained monovalent anions varied little. Hence the selection of functional groups also contributes to the improvement of the resolution of anions (especially monovalent and divalent anions) in ion chromatography.

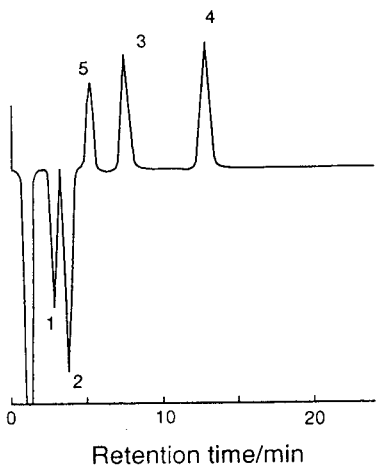

Fig. 2. Separation of anions on a CTBuABr-coated column. Conditions as in Table 1. Peaks as in Fig. 1.

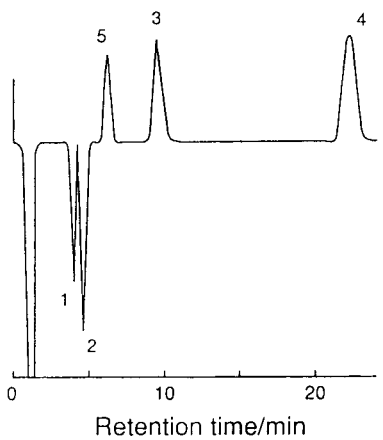

Fig. 3. Separation of anions on a CTBuPBr-coated column. Conditions as in Table 1. Peaks as in Fig. 1.

4. References

[1] D.T. Gjerde and J.S. Fritz, *Ion Chromatography*, Hüthig, Heidelberg, 2nd ed., 1987, pp. 166 and 174.
[2] D.L. DuVal and J.S. Fritz, *J. Chromatogr.*, 295 (1984) 89.
[3] R.E. Barron and J.S. Fritz, *J. Chromatogr.*, 284 (1984) 13.
[4] R.E. Barron and J.S. Fritz, *J. Chromatogr.*, 316 (1984) 201.
[5] A.S. AL-Omair and S.T. Lyle, *Talanta*, 34 (1987) 361.
[6] R.M. Cassidy and S. Elchuk, *Anal. Chem.*, 54 (1982) 1558.
[7] K. Ito, Y. Ariyoshi, F. Tamabuki and H. Sunahara, *Anal. Chem.*, 63 (1991) 273.
[8] R.M. Cassidy and S. Elchuk, *J. Chromatogr., Sci.*, 21 (1983) 454.
[9] F.G.P. Mullins, *Analyst*, 112 (1987) 665.
[10] A. Ohki, K. Dohtsu and M. Takagi, *Benseki Kagaku*, 33 (1984) E187.

ELSEVIER

Journal of Chromatography A, 664 (1994) 123–128

JOURNAL OF CHROMATOGRAPHY A

Short Communication

Influence of eluent anions in boronate affinity chromatography

Pamela R. Westmark, Linbee S. Valencia, Bradley D. Smith*

Department of Chemistry and Biochemistry, University of Notre Dame, Notre Dame, IN 46556, USA

(First received October 20th, 1993; revised manuscript received January 10th, 1994)

Abstract

The influence of various anions on the retention of nucleosides and nucleotides to a boronate affinity chromatography column was examined. At pH 7.0, F^- ions were found to produce the strongest affinity and the best separation of nucleosides from their 2′-deoxy analogues. ^{11}B NMR studies indicated this was due in part to the propensity of F^- to form tetrahedral fluoroboronate complexes. Using an eluent of 50 m*M* 4-(2-hydroxyethyl)-1-piperazineethanesulfonic acid and 500 m*M* KF at pH 7.0, the nucleotides nicotinamide–adenine dinucleotide and flavin–adenine dinucleotide were found to be strongly retained on a boronate column. These nucleotide-saturated columns were examined for their ability to retain the nucleotide-binding enzymes, glucose-6-phosphate dehydrogenase, lactate dehydrogenase and galactose oxidase. No retention of the enzymes was observed.

Introduction

Immobilized boronic acids are used as affinity adsorption ligands for the separation of a wide range of biological molecules, especially compounds containing vicinal diols such as saccharide derivatives [1–4]. The most important factors known to effect retention on a boronate column are: (i) the diol configuration, (ii) other substituents within the diol compound, (iii) the acidity of the immobilized boronic acid, (iv) the pH of the eluent and (v) the ionic strength and valency of the cations in the eluent. Commercially available boronate affinity columns utilize immobilized derivatives of 3-aminophenylboronic acid which has a pK_a value of 8.75 [1]. Consequently, standard binding conditions usually require an eluent of pH 8.0–9.0 and high ionic strength. Since many biological samples are unstable under these conditions, there is a need to develop boronate chromatography systems that can bind effectively at neutral pH. One approach has been to develop matrices containing more acidic boronic acid derivatives and recent attempts have made significant progress [1,2,5]. However, none of these new ligands are readily available and their preparations are difficult for the non-specialist.

The major equilibrium responsible for the diol-selective binding in boronate chromatography is thought to be formation of the anionic tetrahedral boronate complex, **1**, X = OH, as shown in Fig. 1. Two mechanisms have been postulated for boronate–diol complex formation; (i) condensation of the diol with the anionic boronate, **2**, X = OH, as depicted in pathway A in Fig. 1 [6,7] and (ii) direct complexation of the diol with the neutral trigonal boronic acid as

* Corresponding author.

0021-9673/94/$07.00
SSDI 0021-9673(94)00030-D

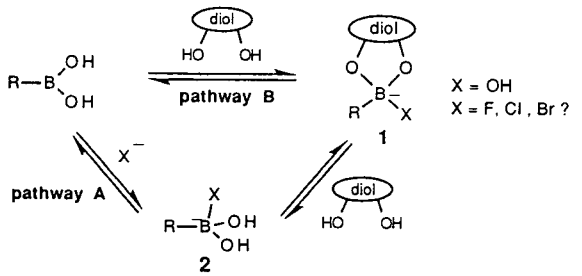

Fig. 1. Reversible complexation of a diol and a boronic acid mediated by an anion X^-.

shown in pathway B [1,8]. Recently, we reported indirect evidence for the formation of the fluoroboronate structure, **1**, X = F, which we believe is formed via the fluoroboronate, **2**, X = F [9]. Accordingly, we were interested if the effects of this complexation would have any significance in boronate chromatography. In this report, we correlate observed nucleoside and nucleotide retention volumes on a commercially available boronate affinity column with the nature of the eluent anions. In agreement with our initial premise, we find that at pH 7.0, F^- ions enhance nucleoside binding more effectively than any other anion examined. This finding has potential practical value as a simple method of increasing diol-specific binding while maintaining near physiological conditions, as well as providing insight into the mechanism of boronate–diol complexation.

2. Experimental

2.1. Materials

AffinityPak polyacrylamide–boronate columns (1 ml, catalogue No. 20368) were purchased from Pierce. The enzymes and reagents were obtained from Sigma and Aldrich, and used without further purification. ^{11}B NMR spectra were acquired on a GE NT-300 spectrometer, and UV spectra were collected using a Perkin-Elmer Lambda 2 instrument.

2.2. Nucleoside and nucleotides binding

Nucleoside and nucleotides (100 μg) were loaded onto a 1-ml boronate column that was presaturated with the appropriate eluent [10]. Fractions (0.5 ml) were collected and monitored for absorption at 260 nm except for reduced nicotinamide–adenine dinucleotide phosphate (NADPH) (338 nm) and nicotinamide–adenine dinucleotide (NAD^+) (259 nm). The columns were re-used after they were washed with water, two column volumes of 1 *M* guanidine (enzyme denaturant), and two column volumes of 0.02% sodium azide (a preservative for column storage).

2.3. Enzyme binding

A 1-ml boronate column was presaturated with a solution of nucleotide cofactor in the appropriate buffer. An aliquot of pure enzyme (100 μl) was then loaded and eluted. The eluent was collected in 0.5-ml fractions, and the protein concentration and enzymatic activity determined by Bradford's reagent and enzymatic assay. Glucose-6-phosphate dehydrogenase [11] and lactate dehydrogenase [12] were monitored for their abilities to convert nicotinamide–adenine dinucleotide phosphate (NADP) to NADPH, the formation of which can be monitored by the change in absorbance at 340 nm. The activity of galactose oxidase was determined via the standard coupled assay with *o*-tolidine and peroxidase to produce a chromophore at 420 nm [11].

3. Results and discussion

A technique which preceded boronate chromatography, combined borate sugar complexation with ion exchange to separate mixtures of sugars, and phosphorylated sugars [13]. During this work the effects of ionic strength were noted; however, since retention was a function of multiple equilibria, a detailed interpretation could not be made. In boronate chromatography, where retention is a function of a single binding equilibrium, the effects of eluent cations

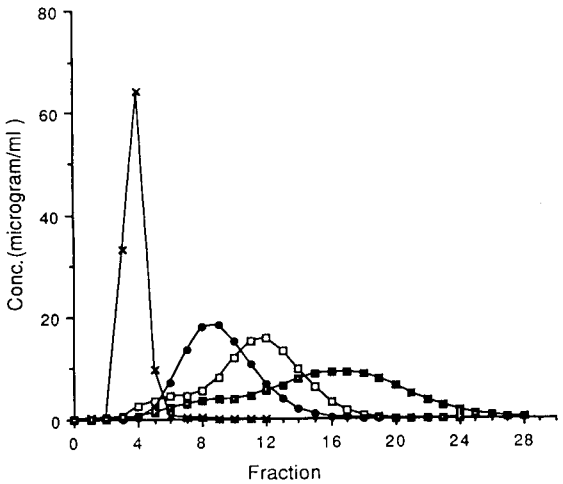

Fig. 2. Chromatographic profile of adenosine on a 1-ml polyacrylamide–boronate column. The column was pre-equilibrated and then eluted with 50 m*M* HEPES, pH 7.0 containing 500 m*M* of (■) KF, (□) KCl, (●) KBr, × no salt. Fractions of 0.5 ml were collected and monitored for absorbance at 260 nm.

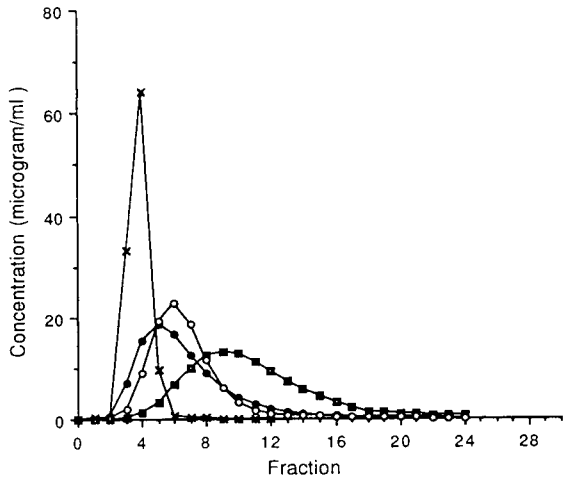

Fig. 3. Chromatographic profile of adenosine on a 1-ml polyacrylamide–boronate column. The column was pre-equilibrated and then eluted with 50 m*M* HEPES, pH 7.0 containing 500 m*M* of tetamethylammonium (■) fluoride, (○) chloride, (●) bromide, × no salt. Fractions of 0.5 ml were collected and monitored for absorbance at 260 nm.

on retention volumes have been summarized, but to our knowledge there has been no systematic study of eluent anions [2,3]. Fig. 2 shows the effect of different potassium halide salts on the retention of adenosine on a commercially available, polyacrylamide-based, low-pressure boronate column at pH 7.0. One of the reasons we chose this column support is that polyacrylamide matrices are known to slowly degenerate under alkaline conditions, so the need to work under mild conditions is emphasized [2]. In the event, the observed order of binding effectiveness was KF > KCl > KBr. We also examined other potassium salts such as phosphate, 4-(2-hydroxyethyl)-1-piperazineethanesulfonic acid (HEPES) and nitrate; none were as effective as KF. To minimize the electrostatic contributions of the cation, the elution experiments were repeated with the eluent containing added tetramethylammonium halide salts. Again the retention volumes increased in the order $F^- > Cl^- > Br^-$ (Fig. 3). These results strongly suggest the anions are providing a stabilizing influence on boronate–diol complexation and that the stabilization increases with the charge to surface ratio of the anion.

Fig. 4 shows the separation of a mixture of adenosine and 2′-deoxyadenosine using an eluent of 50 m*M* HEPES buffer at pH 7.0 and (i) no added salt, (ii) added 500 m*M* KCl or (iii) added 500 m*M* KF. Only in the presence of added salt could a successful separation be achieved at pH 7.0 and the best resolution was obtained with added KF. Similar experiments were run with other nucleoside–deoxynucleoside mixtures (uridine, cytidine and inosine) and in each case KF provided the best separation.

Fig. 5 compares the ability of added KF and KCl to retain the nucleotide coenzyme NAD^+ on a boronate column at pH 7.0. In the presence of 500 m*M* KF the NAD^+ was strongly retained on the column and only when the eluent was changed to a "no salt" buffer system did the NAD^+ emerge. With the same amount of added KCl the binding capacity was clearly lower, as about half of the NAD^+ had leaked from the column by the time the "no salt" buffer was added. Under identical conditions, the cofactor

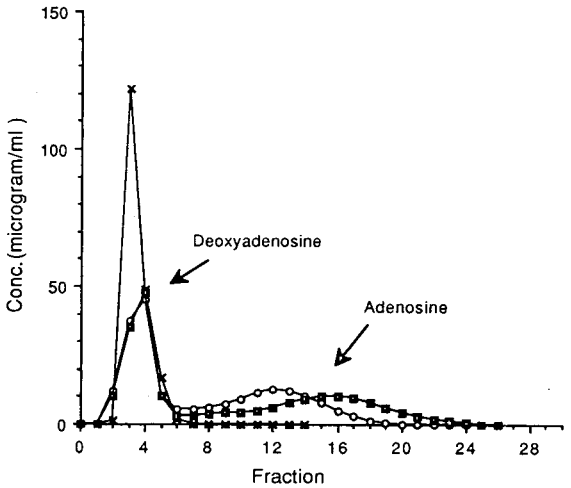

Fig. 4. Separation of adenosine from 2′-deoxyadenosine on a 1-ml immobilized polyacrylamide–boronate column. The column was pre-equilibrated and then eluted with 0.05 *M* HEPES, pH 7.0 containing 500 m*M* of (□) KF, (○) KCl, × no salt. Fractions of 0.5 ml were collected and monitored for absorbance at 260 nm.

flavin–adenine dinucleotide (FAD) displayed very similar binding characteristics, whereas other nucleotide derivatives such as ATP, UMP and NADPH did not bind to the column and were collected in the void volume. The higher affinities of NAD^+ and FAD relative to the other nucleotides have been noted and discussed by previous workers [3,10].

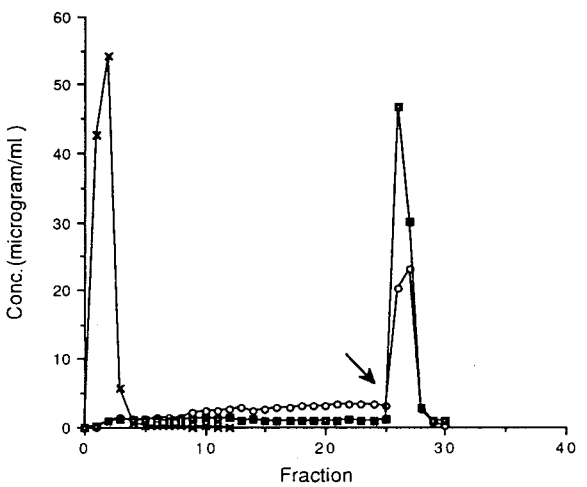

Fig. 5. Chromatographic profile of NAD^+ on a 1-ml polyacrylamide–boronate column. The column was pre-equilibrated and then eluted with 50 m*M* HEPES, pH 7.0 containing 500 m*M* of (□) KF, (○) KCl, × no salt. The arrow indicates a change of eluent to 50 m*M* HEPES, pH 7.0 with no added salt. Fractions of 0.5 ml were collected and monitored for absorbance at 260 nm.

It is known from the literature that retention on a boronate column increases with ionic strength. This phenomenon has been attributed to the electrostatic effects of the eluent cations stabilizing the anionic boronate complexes, divalent cations being the most effective [3]. Our observation that retention is quite sensitive to the nature of the eluent anions is difficult to rationalize using this electrostatic argument. Anions would be expected to destabilize the anionic boronate complexes and reduce retention, with the "harder" anions (anions with a higher charge to surface ratio) having the strongest effect. This is the opposite to that observed (for the halides the order was $F^- > Cl^- > Br^-$) and consequently an alternative explanation is needed. One possible mechanism for complex stabilization by an anion, X, involves the tetrahedral boronate, **2**, and pathway A in Fig. 1. In an attempt to confirm this mechanism, we examined the ability of various anions to form structures analogous to **2** using ^{11}B NMR. It is well known that the ^{11}B chemical shift of a tetrahedral boronate is approximately 20 ppm upfield from a trigonal boronic acid signal [1,14]. The rate of exchange between trigonal and non-chelated tetrahedral boron species is fast on the NMR time scale such that a single resonance is observed whose chemical shift is a measure of the fraction of tetrahedral boron species present. Table 1 shows the results of adding various salts to a solution of phenylboronic acid, buffered at pH 7.0. Only in the case of added KF was there a measurable upfield shift in the ^{11}B signal, indicative of the presence of tetrahedral phenylfluoroboronate anions. From these NMR studies we conclude that F^- is the only anion other than OH^- that can measurably complex with trigonal boronic acid derivatives in aqueous solution and form tetrahedral boronates. Thus, only in the case of X = F is there NMR evidence that the increased retention may be due to the participation of pathway A in Fig. 1.

Table 1
^{11}B NMR chemical shifts for phenylboronic acid as a function of added salt

Added salt (500 m*M*)[a]	^{11}B chemical shift[b] (ppm)
KF	23.9
KCl	28.5
KBr	28.6
Potassium phosphate	28.0
No added salt	28.9
KOH, pH 12	8.0

[a] Salt added to a solution of phenylboronic acid in 50 m*M* HEPES, pH 7.0.
[b] Referenced to external borontrifluoride etherate at $\delta = 0.0$ ppm.

Since diol retention at pH 7.0 is increased by the presence of divalent cations and F^- anions, the logical additive to maximize diol-specific retention at pH 7.0 would be salts such as MgF_2 and CaF_2. Unfortunately, the low solubility of these salts limits their practical utility. As a useful substitute we found that a freshly prepared eluent containing 25 m*M* $MgCl_2$ and 25 m*M* KF provided a maximal adenosine retention volume at pH 7.0 (data not shown).

A potentially attractive application of boronate chromatography is the technique of "exchangeable-ligand chromatography" or "piggyback chromatography" where the boronate column is presaturated with a diol-containing ligand such as a nucleotide cofactor, and the enzyme-binding affinity of the ligand is used to selectively retain enzymes [10,15]. The technique has been reported only a few times with boronate columns, and mixed results have been obtained. A successful example is the purification of UDP–glucose pyrophosphorylase from slime mold using a UTP-saturated boronate matrix [15]. We briefly examined the ability of boronate columns presaturated with NAD^+ (pH 7.0, 50 m*M* HEPES and 500 m*M* KF) to retain the enzymes, glucose-6-phosphate dehydrogenase and lactate dehydrogenase [10]. In addition, boronate–FAD columns were examined under similar conditions for their ability to retain galactose oxidase. In each case, no significant retention of the enzyme was observed. The lack of enzyme binding may be due to a number of reasons. Two possibilities are; (i) the dinucleotide diols that are needed for binding to the column are also required for binding to the enzymes, if this is the case then the generality of the method is severely limited [16]; (ii) the enzyme active site may be too deep for the boronate-bound dinucleotides to form stabilizing interactions, the use of longer spacers connecting the boronate ligands to the column support should, in principle, alleviate this problem [2,17].

In conclusion, we have provided evidence that eluent anions increase diol retention on a boronate affinity column by stabilizing boronate–diol complexation. Although we cannot unambiguously assign the stabilization to the mechanism of pathway A in Fig. 1, we believe pathway A is a reasonable explanation. In any case, it is clear the identity and concentration of the eluent anions are parameters that should be considered when optimizing separations by this chromatographic method.

4. Acknowledgements

This study was funded in part by the US National Science Foundation. L.S.V. was a Howard Hughes Undergraduate Research Fellow.

5. References

[1] R.P. Singhal, B. Ramamurthy, N. Govidraj and Y. Sarwar, *J. Chromatogr.*, 543 (1991) 17.
[2] R.P. Singhal and S.S.M. DeSilva, *Adv. Chromatogr.*, 31 (1992) Ch. 5, pp. 293–336.
[3] A. Bergold and W.H. Scouten, in W.H. Scouten (Editor), *Solid Phase Biochemistry, Analytical and Synthetic Aspects*, Wiley, New York, 1983, Ch. 4.
[4] J.H. Hageman and G.D. Kuehn, in A. Kenney and S. Fowell (Editors), *Methods in Molecular Biology*, Marcel Dekker, New York, 1992, Vol. 11, p. 45–71.
[5] S. Soundararajan, M. Badawi, C.M. Kohlrust and J.H. Hageman, *Anal. Biochem.*, 178 (1989) 125.
[6] R. Pizer and C. Tihal, *Inorg. Chem.*, 31 (1992) 3243–3247.
[7] J.P. Lorand and J.O. Edwards, *J. Org. Chem.*, 24 (1956) 769.

[8] S.A. Barker, A.K. Chopra, B W. Hatt and P.J. Somers, *Carbohydr. Res.*, 26 (1973) 33.
[9] M.F. Paugam and B.D. Smith, *Tetrahedron Lett.*, 34 (1993) 3723.
[10] V. Bouriotis, I.J. Galpin and P.D.G. Dean, *J. Chromatogr.*, 210 (1981) 267.
[11] C.C. Worthington (Editor), *Worthington Enzyme Manual*, Worthington Biochemical Corporation, Freehold, 1988.
[12] H.U. Bergmeyer, in H.U. Bergmeyer (Editor), *Methods in Enzymatic Analysis*, Vol. 2, Verlag Chemie, Weinheim, 3rd ed., 1983, pp. 163–167.
[13] A.A. Benson, *Methods Enzymol.*, 3 (1957) 110–129; and references cited therein.
[14] G.R. Kidd, in P. Lazlo (Editor), *NMR of Newly Accessible Nuclei*, Vol. 2, Academic Press, New York, 1983, pp. 49–77.
[15] R.R. Maestas, J.R. Prieto, G.D. Kuehn and J.H. Hageman, *J. Chromatogr.*, 189 (1980) 225.
[16] C. Branden and J. Tooze, *Introduction to Protein Structure*, Garland, New York, 1991, Ch. 10.
[17] G. Wulff, W. Dederichs, R. Grotstollen and C. Jupe, in T.C.J. Gribnau, J. Visser and R.J.F. Nivard (Editors), *Affinity Chromatography and Related Techniques*, Elsevier, Amsterdam, 1982, p. 207.

ELSEVIER

Journal of Chromatography A, 664 (1994) 129–134

JOURNAL OF CHROMATOGRAPHY A

Short Communication

Separation of metallothionein isoforms by micellar electrokinetic capillary chromatography

John H. Beattie*,[a], Mark P. Richards[b]

[a]*Division of Biochemical Sciences, Rowett Research Institute, Greenburn Road, Bucksburn, Aberdeen AB2 9SB, UK*
[b]*US Department of Agriculture, Agricultural Research Service, Non-ruminant Animal Nutrition Laboratory, Beltsville, MD 20705, USA*

(First received June 1st, 1993; revised manuscript received December 28th, 1993)

Abstract

Current techniques for the separation and quantification of metallothionein isoforms have limited value for routine analysis. Isoforms having a similar charge have been separated successfully using reversed-phase HPLC but this technique suffers from a slow sample turnover time. The use of the surfactant sodium dodecyl sulphate for the separation of metallothionein isoforms by micellar electrokinetic capillary chromatography (MECC) is described. The charge-different isoforms MT-1 and MT-2 from rats, rabbits and sheep were separated within 9–12 min. In addition, a varying degree of heterogeneity was observed in purified samples of human MT-1, rat MT-2, rabbit MT-1, rabbit MT-2 and sheep MT-1. The behaviour of chicken MT was different from that of any other species. The separation of sheep liver extracts indicated the potential of MECC as the basis for a quantitative assay for both charge-different and charge-similar metallothionein isoforms.

1. Introduction

Multiple genes for the metal-binding protein metallothionein (MT) have been detected in several mammals [1]. These genes have been cloned, sequenced and a considerable amount is now known about their promoter sites and the regulation of transcription [2–4]. There is, however, virtually no information concerning their translation and the synthesis of the corresponding protein isoforms because of limitations in the methodology for their quantification. Questions concerning the function of individual isoforms cannot therefore be easily addressed.

MT is often measured by isoform insensitive methods such as the Ag [5] or Cd [6] saturation assays although immunological assays specific to the major charge-separable isoforms, MT-1 and MT-2 have been reported [7,8]. The method of choice to study the multiple isoforms of MT-1 and MT-2 is reversed-phase HPLC (RP-HPLC), since the isoforms which do not differ greatly in charge show differences in hydrophobicity [9]. There are however significant disadvantages of RP-HPLC for routine analysis which include the lengthy separation time and the requirement for relatively large sample volumes. A rapid method for the separation and quantification of the major MT isoforms using capillary zone electrophoresis (CZE) has recently been developed

* Corresponding author.

0021-9673/94/$07.00
SSDI 0021-9673(94)00034-7

[10,11]. Further recent developments indicate that by changing the pH of the electrolyte, it is possible to separate several components from purified MT samples using CZE [12].

Micellar electrokinetic capillary chromatography (MECC) was developed by Terabe and co-workers [13,14] and is a technique using capillary electrophoresis instrumentation with the addition of a micelle-forming ionic surfactant to the electrolyte [15]. The technique has been successfully used to separate proteins [16] so we therefore decided to investigate the separation of MT isoforms and to investigate the potential of MECC for the study of these proteins in tissue extracts.

2. Experimental

2.1. Purified MT samples

Purified metallothionein samples were obtained from several different sources. Rabbit MT (MT-1 and MT-2) and horse MT samples were purchased from Sigma (St. Louis, MO, USA) and rat CdMT-2 and human MT-1 were gifts from Dr. Chiharu Tohyama (National Institute of Environmental Studies, Tsukuba, Japan). Sheep and rat ZnMT isoforms were separated and purified from the livers of animals injected with Zn, using gel filtration and ion-exchange chromatography [17]. Chicken MT was prepared in the same way from birds injected with Cd but was then re-purified by RP-HPLC [18].

2.2. Preparation of liver samples

Chicken livers were obtained from birds which had been injected with Cd. Sheep liver was obtained from a Zn-injected grey-faced ewe [10] and all liver samples were frozen until required. Unless otherwise stated, 100-mg samples of liver were weighed into eppendorf tubes followed by the addition of 200 μl of deionised water. After disruption of the tissue by sonication, 200 μl of acetonitrile were added slowly, while vortexing, to a 200-μl aliquot of the homogenate. The samples were immediately centrifuged at 13 000 rpm (10 000 *g*) for 5 min and 200 μl of the supernatant were dried using a centrifugal vacuum evaporation system (Speedvac, Savant, NY, USA). The residue was re-dissolved in 20–50 μl of electrolyte buffer prior to analysis.

2.3. Electrophoresis conditions

Samples were analysed using Beckman P/ACE 2100 or 2050 capillary electrophoresis systems fitted with cartridges containing a polyimide-coated fused-silica capillary (Beckman, Fullerton, CA, USA: 50 cm × 75 μm, untreated). Unless otherwise stated, the electrolyte used was 100 m*M* borate buffer pH 8.4, made by adjusting the pH of a 25 m*M* solution of sodium tetraborate with 100 m*M* boric acid, and containing 75 m*M* sodium dodecyl sulphate (SDS). Samples (0.5–1.0 mg MT isoform ml^{-1} water) were loaded by pressure injection for 1 s and separations were performed at 10 kV and 25°C. Separated components were routinely detected at 200 nm but also at 214, 254 and/or 280 nm using a UV monitor.

In order to evaluate the most suitable concentration of SDS for the electrophoresis of MT samples and liver extracts, separations were performed at a range of different surfactant concentrations and were monitored as described above.

3. Results

3.1. Purified MT samples

Electropherograms for some purified MT samples are shown in Figs. 1–3. Rat MT-2 (Fig. 1), horse MT and rabbit MT-1 (Fig. 2) were both found to contain two components which were well resolved. The purified MT-1 components from sheep and human (Fig. 2) showed evidence of more than two isoforms whereas only one was found in electropherograms of rat MT-1 (Fig. 1), rabbit MT-2 and sheep MT-2 (Fig. 2). The results for chicken MT (Fig. 3) were unlike those obtained with MT samples from other species in

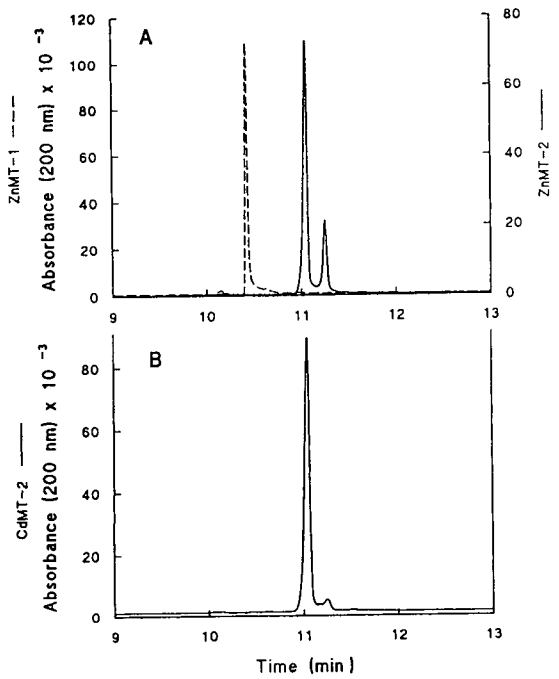

Fig. 1. Separation of purified rat liver ZnMT-1, ZnMT-2 (A) and CdMT-2 (B) (all 1 s injection, 1 mg ml^{-1}) at 10 kV and 25°C using a 57 cm × 75 μm I.D. untreated capillary and a 100 m*M* borate buffer pH 8.4 containing 75 m*M* SDS.

that the resolution of the protein peak was very poor. Variations in migration times of MT-1 and MT-2 between the profiles of purified proteins in Figs. 1–3 may in part be related to species differences in protein structure.

3.2. Liver samples

Preliminary studies to investigate the influence of electrolyte SDS concentration on the separation and resolution of low-M_r components in liver extracts demonstrated that the optimum concentration was between 50 and 75 m*M* SDS (Fig. 4). Migration times increased at higher SDS concentrations which were thought to encourage micelle partitioning and enhance the association of SDS with larger molecules. No improvement in separation or resolution was found by increasing the SDS concentration to 100 m*M* (results not shown) although migration times were further increased. Thus a concentration of 75 m*M* SDS was used routinely in electrolyte buffers.

Standard addition studies with sheep liver extract using purified sheep MT (not shown) had the effect of increasing the absorbance peaks corresponding to components in the purified MT alone. By monitoring at different wavelengths, it was possible to obtain some spectral information concerning all separated components in the native sheep extract (Fig. 5). These profiles demonstrated that the components labelled a, b and c in Fig. 5 showed little absorbance at 280 nm, indicating a low aromatic amino acid content which is characteristic of MT.

4. Discussion

The critical micelle concentration for SDS is reported to be 8.2 m*M* [19] although a much higher concentration is often used for the optimal separation of compounds by MECC [15]. We found that a concentration of 75 m*M* gave the optimum separation for chicken liver extract (Fig. 4) and that these conditions were also suitable for sheep liver extract (Fig. 5). As the SDS concentration was increased from 25 to 75 m*M*, the migration time also increased (Fig. 4) indicating a greater partitioning of the extract components into the micelles.

The electroosmotic front (EOFront) marks the position of zero net charge, which in the present work was observed at 8.5–9.0 min. MT-1 proteins were found to migrate at 1.1–1.2 × the EOFront with MT-2 proteins following at 1.2–1.3 × the EOFront. In comparison to RP-HPLC, the migration times and sample turnover times for MT isoforms were very favourable. The charge-separable isoforms referred to as MT-1 and MT-2 due to their sequential separation on conventional ion-exchange chromatography, often showed evidence of heterogeneity which could indicate the presence of additional isoforms. However, there are a number of other possible explanations including sample contamination, degradation/aggregation or the formation of different metalloforms. Analysis of the purified proteins by laser desorption ionisation

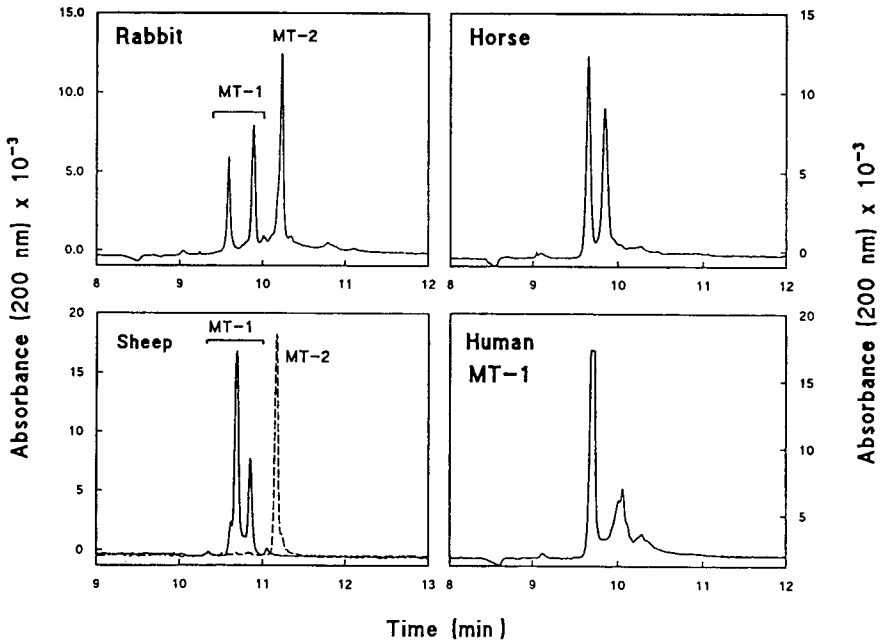

Fig. 2. Separation of rabbit and sheep liver MT, human liver MT-1 and horse kidney MT (all 1 s injection, 1 mg ml^{-1}) using the conditions described in Fig. 1.

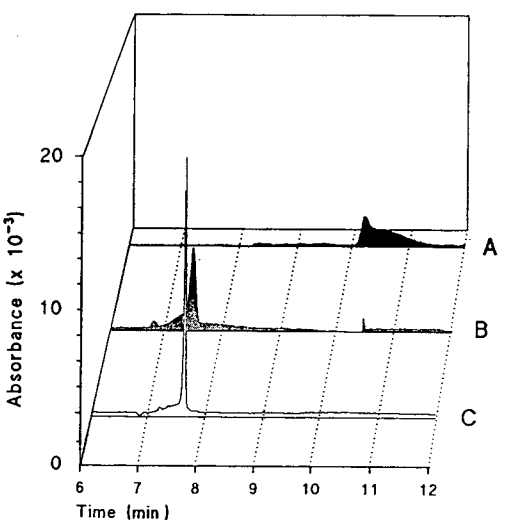

Fig. 3. Separation of purified chicken liver CdMT (A) at 10 kV and 25°C. SDS was ommitted from the electrolyte but not the sample buffer (B) and from both the electrolyte and the sample buffer (C). All samples contained 0.5 mg MT ml^{-1} (1 s injection).

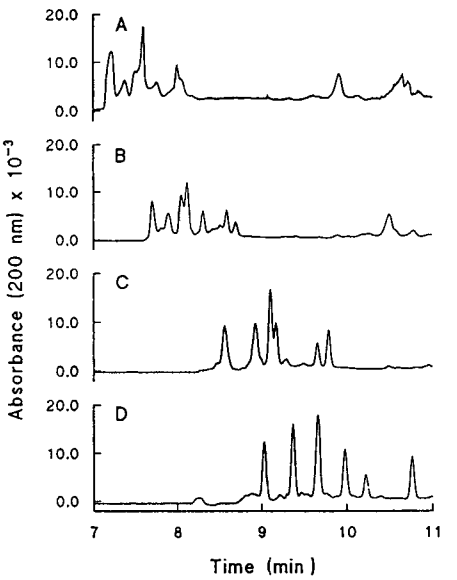

Fig. 4. Effect of increasing the electrolyte SDS concentration on the separation of low-M_r components in a chicken liver extract. The electrolytes contained 100 m*M* sodium borate pH 8.4 and (A) 0, (B) 25, (C) 50 and (D) 75 m*M* SDS.

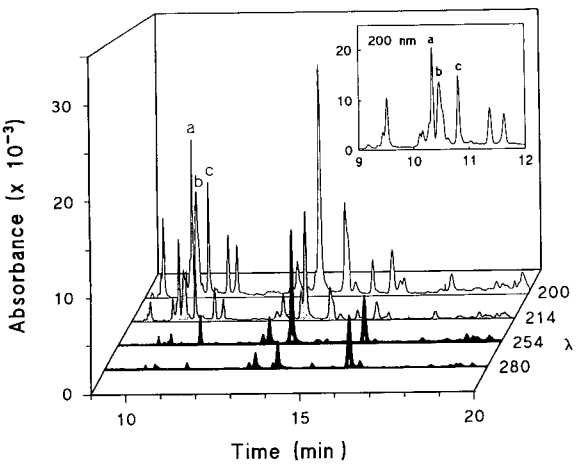

Fig. 5. Separation of sheep liver extract at four different wavelengths using the conditions described in Fig. 1 and detail of the MT peaks at 200 nm are shown inset. Peaks a and b contain MT-1 species whereas peak c is MT-2.

mass spectrometry did not indicate contamination or degradation/aggregation with the possible exception of horse MT. Sheep have at least three functioning MT-1 genes [20] and amino acid analyses of the hepatic protein gave a composition characteristic of MT. This supports UV spectral data showing low absorbance at 280 nm and indicating the absence of aromatic amino acids in all the MECC separated components. Separation of sheep MT-1 by CZE at pH 2.5, 7.0 and 11.0 in each case gave a single, well resolved absorbance peak [12] and this indicates homology of acidic and basic amino acid residues between the two main components separated by MECC. SDS is reported to encourage the formation of inter- and/or intramolecular linkages of MT through cysteine groups, resulting in broad obscure bands with SDS–polyacrylamide gel electrophoresis [21]. However, in all but one MT sample, the components separated using SDS-MECC were of high resolution and were highly reproducible both as regards component migration time and peak area. The single exception was chicken MT which appeared to be adversely affected by the SDS in the sample buffer and/or in the electrolyte. Chicken MT is unusual in that it contains two additional amino acids and the terminal carboxyl residue is a histidine [22]. Thus its uncharacteristic behaviour with MECC conditions may be related to these modifications.

Finally, we investigated the possibility that the various components observed when separating purified MT isoforms could be metalloforms of the same protein but found, at least as regards rat (Fig. 1) or rabbit (not shown) ZnMT-2 and CdMT-2, that there was no difference in migration time relating to the species of metal bound.

The separation of purified rat ZnMT-2 showed two components, one major and one relatively minor which concurs with the previous evidence for two Zn-containing components in rat MT-2 samples separated by ion-exchange HPLC [23]. Two components have also been isolated from mouse liver MT-2 [24], although there is as yet no evidence for three functioning MT genes in these rodents. The occurrence of 2 or more isoforms of MT-2 would be unusual since most of the heterogeneity in many species occurs in the MT-1 form. CdMT-2 was prepared from Sprague–Dawley rats in a Japanese laboratory, separated using the same conditions as for the rat ZnMT-2 (Hooded Lister rats) and the electropherogram also showed evidence of a component with a similar migration time (Fig. 1B), albeit at lower concentration. The appearance of a similar component in MT-2 specifically from Zn-treated mice has been noted previously [23].

The results of rabbit MT separations show two major MT-1 components and one prominent MT-2 protein. These results are in agreement with CZE electropherograms of rabbit MT-1 and MT-2 proteins at low pH which show a total of three prominent components [12]. There is evidence for the existence of six MT isoforms in rabbit tissues, some of which are minor as regards their cellular concentration but which nevertheless show relatively high levels of induction by metals [25]. The separation of horse MT was unusual since the difference in migration time between the two partially separated components was uncharacteristic of that normally found for MT-1 and MT-2. The CZE separation of horse MT at pH 11 showed three distinct components indicating the presence of one or more proteins with a charge uncharacteristic for MT at this pH [12]. The heterogeneity of human

MT-1 is well known [26] and we have partially resolved three of the proteins so far identified.

Using the MECC conditions described here, we have separated smaller related peptides such as oxidised and reduced glutathione, which migrate at approximately 1.5 and 1.6 × the EO-Front, respectively (data not shown). Although we have not yet identified many of the components separated by MECC of liver extracts, there is clearly great potential for the simultaneous quantification of low-M_r cell components including metallothionein and glutathione. The acetonitrile extraction procedure which removes most proteins and complex carbohydrates is simple, rapid and compatible for direct analysis by MECC. Investigations are continuing on improvements to the preparation procedure and assay conditions which will permit the complete separation of MT isoforms from contaminating components in tissues from a wide variety of different animal species. We conclude that MECC is a useful method for the separation of MT isoforms and that this technique shows considerable potential for their rapid quantification.

5. Acknowledgements

The authors wish to thank Dr. Ian Bremner for his critical review of the manuscript. This work was funded by the Scottish Office Agriculture and Fisheries Department, UK and the US Department of Agriculture.

6. References

[1] P.E. Hunziker and J.H.R. Kägi, *Curr. Topics Nutr. Dis.*, 18 (1988) 349.
[2] D.H. Hamer, *Ann. Rev. Biochem.*, 55 (1986) 913.
[3] R.D. Palmiter, in J.H.R. Kägi and Y. Kojima (Editors), *Metallothionein II*, Birkhäuser, Basle, 1987, p. 63.
[4] G.K. Andrews, *Prog. Food Nutr. Sci.*, 14 (1990) 193.
[5] A.M. Scheuhammer and M.G. Cherian, *Methods Enzymol.*, 205 (1991) 78.
[6] D.L. Eaton and M.G. Cherian, *Methods Enzymol.*, 205 (1991) 83.
[7] R.K. Mehra and I. Bremner, *Biochem. J.*, 213 (1983) 459.
[8] H.M. Chan, M.G. Cherian and I. Bremner, *Toxic. Appl. Pharmacol.*, 116 (1992) 267.
[9] M.P. Richards, *Methods Enzymol.* 205 (1991) 217.
[10] J.H. Beattie, M.P. Richards and R. Self, *J. Chromatogr.*, 632 (1993) 127.
[11] M.P. Richards, J.H. Beattie and R. Self, *J. Liq. Chromatogr.*, 16 (1993) 2113.
[12] M.P. Richards and J.H. Beattie, *J. Chromatogr.*, 648 (1993) 459.
[13] S. Terabe, K. Otsuka, K. Ichikawa, A. Tsuchiya and T. Ando, *Anal. Chem.*, 56 (1984) 111.
[14] S. Terabe, K. Otsuka and T. Ando, *Anal. Chem.*, 57 (1985) 834.
[15] G.M. Janini and H.J. Issaq, *J. Liq. Chromatogr.*, 15 (1992) 927.
[16] M.A. Strege and A.L. Lagu, *Anal. Biochem.*, 210 (1993) 402.
[17] R.K. Mehra and I. Bremner, *Biochem. J.*, 227 (1985) 903.
[18] M.P. Richards and N.C. Steele, *J. Chromatogr.*, 402 (1987) 243.
[19] K. Klepárník and P. Bocek, *J. Chromatogr.*, 569 (1991) 3.
[20] M.G. Peterson and J.F.B. Mercer, *Eur. J. Biochem.*, 174 (1988) 417.
[21] M. Kimura, S. Koizumi and F. Otsuka, *Methods Enzymol.*, 205 (1991) 114.
[22] G.K. Andrews and L.P. Fernando, in C.D. Klaasen and K.T. Suzuki (Editors), *Metallothionein in Biology and Medicine*, CRC Press, Boca Raton, FL, 1991, p. 103.
[23] K.T. Suzuki, H. Uehara, H. Sunaga and N. Shimojo, *Toxicol. Lett.*, 24 (1985) 15.
[24] S. Kobayashi and J. Sayato-Suzuki, *Biochem. J.*, 251 (1988) 649.
[25] M. Wan, P.E. Hunziker and J.H.R. Kägi, *Biochem. J.*, 292 (1993) 609.
[26] A.K. West, R. Stallings, C.E. Hildebrand, R. Chiu, M. Karin and R.I. Richards, *Genomics*, 8 (1990) 513.

ELSEVIER

Journal of Chromatography A, 664 (1994) 135–137

JOURNAL OF CHROMATOGRAPHY A

Book Review

Chromatography today, by C.F. Poole and S.K. Poole, Elsevier, Amsterdam, 1991, XI + 1026 pp., price US$ 147.50, Dfl. 295.00, ISBN 0-444-88492-0.

Chromatography today is a worthy successor to its forerunner, *Contemporary practice of chromatography*, a textbook which is regarded by both novice and veteran chromatographers as one of the most comprehensive works published on separation science in the last decade. Like its predecessor, *Chromatography today* is not for the casual chromatographer. The minute detail in which the theoretical, practical and instrumental aspects of chromatographic techniques are discussed may deter the occasional user but certainly makes essential reading for those routinely involved in separation technologies.

The book is written in a modular fashion so that particular sections may be selected for individual course components or study interests. An extensive bibliography is provided at the end of each chapter —in fact so large are the number of references that a separate index listing reference authors in alphabetical order may be considered for future editions. This is a reasonably theoretical book which provides an enormous depth of information on the fundamental aspects of chromatography. Little or no emphasis is placed on describing various applications though the work is so extensively referenced that the reader is easily guided to both general and specific applications. The text is also highly accessible, since it is written in a clear, flowing and very readable style.

Although much of the material (particularly the tables and figures) will be familiar to existing readers of *Contemporary practice of chromatography*, it is evident by the number of references which post date the previous text that the content has considerably updated. The book is composed of a manageable nine chapters, one devoted to basic chromatographic principles, two each to gas and liquid chromatography, and one each to supercritical fluid chromatography (SFC), thin-layer chromatography (TLC), sample preparation and hyphenated methods such as GC–MS and LC–MS. Chapter 1 covers fundamental relationships in chromatography and deals in reasonable mathematical detail with aspects such as the factors contributing to band broadening, leading ultimately to a derivation of the Van Deemter equation. A new addition in this chapter is a section on peak shape models which are used to estimate how far peaks deviate from the Gaussian ideal. In the two subsequent chapters on GC, certain procedures —such as film formation on glass surfaces, reactions to deactivate silanol groups on glass surfaces and methods for coating open tubular columns— are described in detail. Though of undoubted academic interest, it is questionable how useful such sections would be to most practising chromatographers. Efficiency and quality tests are discussed in detail as are retention phenomena in gas–liquid chromatography; retention index schemes are also provided. Instrumental aspects of GC are covered in Chapter 3 and much space is devoted to various injection techniques, some-

SSDI 0021-9673(93)E0086-A

thing which will prove beneficial to those involved in the practical application of gas chromatography.

Chapter 4 (The column in liquid chromatography) contains a useful table covering the physical and chemical properties of some commercially available silicas. Surface modification of silicas with organosilane and other reagents is extensively discussed and the factors influencing the degree of coverage attainable are clearly outlined. Such descriptions should give the student a better appreciation of the complexities of reversed-phase separations where retention mechanisms are strongly influenced by secondary interactions. These widely observed phenomena of secondary interactions in reversed-phase chromatography are treated from a theoretical standpoint supported by a number of mathematical equations. A more specific description of the interaction between cations and residual silanol groups on reversed-phase chromatography phases may have been useful, since this is the most dominant of the secondary equilibria and is the least understood by less experienced chromatographers. A helpful section on column test methods and evaluation protocols provides guidance in the evaluation of both commercially packed columns and columns packed in the laboratory.

Chiral separations in both GC and LC are, for some reason, located in Chapter 8 (Sample preparation). Considering the explosive growth in (particularly LC) chiral chromatography in the last decade, the separation of enantiomers is, in my view, at least as deserving of a full chapter as SFC, which constitutes the sole topic of Chapter 6. In addition, since many enantiomeric separations are nowadays carried out on speciality chiral sorbents, it is not clear why chiral separations should necessarily come under the aegis of "Sample preparation" in the first place. Notwithstanding its location, however, this subject is covered in a most comprehensive fashion and will provide most readers with a thorough appreciation of this complex chromatographic mode.

The eluotropic series of solvents for different normal phase sorbents is given on p. 383, though other tables, complementary to this one, and providing useful reference information in the selection of mobile phases, are scattered throughout the chapter (buffer salts, p. 433; physical properties of solvents, p. 459; solvent strengths and selectivity parameters, p. 462). The text contains a vast number of very useful tables and figures such as these, but since they may be difficult to locate solely for reference purposes, some kind of separate listing for these may be considered in the future also.

Another burgeoning technique, capillary electrophoresis, has been inserted at the end of the chapter on column in liquid chromatography. Perhaps because the title of the book contains the word "chromatography" the authors felt that detailed treatment of electrophoretic techniques would not have been part of the remit of this text, but a chapter, or at least a major section, devoted to this important and growing separation mode would have been appropriate and may be included in future editions.

Chapter 5 (Instrumental requirements for high-pressure liquid chromatography) incorporates relatively recent instrumental developments such as photodiode array detection. There is also some discussion on the instrumental modifications required to carry out small-bore chromatography, an approach which appears to be gaining popularity more rapidly than capillary liquid chromatography for which the instrumental requirements are more stringent.

A chapter on TLC is a welcome addition since there have been a number of developments in this field over the past five years. Most notable are high efficiency plates and Empore TLC sheets for quantitative analysis, automated multiple development (permitting spot concentration) in addition to improved techniques for sample application.

The penultimate chapter, on sample preparation, deals with all aspects of the subject ranging from chiral separations to analyte isolation by distillation. This chapter includes interesting and informative schemes for the solvent extraction of acids, bases and neutral compounds from a variety of aqueous and non-aqueous matrices. Solid-phase extraction is discussed in some depth

and greater emphasis is given to the isolation of trace organics from water than to other applications such as the extraction of drugs from biological fluids. It is also noteworthy that restricted access phases are mentioned here in relation to their use as solid-phase extraction sorbents, but I could find no reference to them with respect to the purpose for which they were originally designed —speciality analytical columns permitting the direct injection of biological samples without prior extraction. Multimodal and multidimensional techniques are also included in this chapter. Although these are important topics which merit inclusion in a book such as this, in a significant number of instances, multidimensional techniques are used not for sample preparation but simply to enhance the resolving power of the chromatograph. For this reason, this component may have been better placed in a different section or in a separate chapter.

The final chapter is devoted to hyphenated techniques such as GC–MS, LC–MS and SFC–MS. This chapter also discusses the development of Fourier transform IR as a detection scheme in both HPLC and GC. At least one gas chromatograph combining both MS and Fourier transform IR detection may be obtained commercially, so it is useful that some theoretical discussion on the principles and potential uses for such instruments is available.

In view of the fact that many modern laboratories are highly automated, some reference to the instrumentation for automated sample handling, laboratory management and data manipulation could have been included, as could some reference to some of the capabilities of the currently available software packages for data reduction and manipulation. Furthermore a modern textbook on chromatography would benefit from some attention to basic statistical concepts such as linear regression, standard deviation, relative standard deviation, standard of error etc. —essential elements in many of the routine tests used for the evaluation of chromatographic assays.

It is important to stress again that this not a book of chromatographic applications —it is a text which is most useful to teachers of chromatography and to undergraduate students at a reasonably advanced level specialising in separation technology.

This is the type of book which would be an important, if not vital, addition to any institution where chromatography is taught or is used and I have no doubt that like *Contemporary practice of chromatography*, this book will, for many students and teachers alike, become the definitive general textbook in this vast subject area for many years to come.

Dublin (Ireland) Mary Kelly

PUBLICATION SCHEDULE FOR THE 1994 SUBSCRIPTION

Journal of Chromatography A and *Journal of Chromatography B: Biomedical Applications*

MONTH	O 1993	N 1993	D 1993	J	F	M	A	
Journal of Chromatography A	652/1 652/2 653/1	653/2 654/1 654/2 655/1	655/2 656/1 + 2 657/1 657/2	658/1 658/2 659/1 659/2	660/1 + 2 661/1 + 2 662/1 662/2	663/1 663/2 664/1	664/2 665/1 665/2 666/1 + 2 667/1	The publication schedule for further issues will be published later.
Bibliography Section						681/1		
Journal of Chromatography B: Biomedical Applications				652/1	652/2 653/1	653/2 654/1	654/2 655/1	

INFORMATION FOR AUTHORS

(Detailed *Instructions to Authors* were published in *J. Chromatogr. A*, Vol. 657, pp. 463–469. A free reprint can be obtained by application to the publisher, Elsevier Science B.V., P.O. Box 330, 1000 AH Amsterdam, Netherlands.)

Types of Contributions. The following types of papers are published: Regular research papers (full-length papers), Review articles, Short Communications and Discussions. Short Communications are usually descriptions of short investigations, or they can report minor technical improvements of previously published procedures; they reflect the same quality of research as full-length papers, but should preferably not exceed five printed pages. Discussions (one or two pages) should explain, amplify, correct or otherwise comment substantively upon an article recently published in the journal. For Review articles, see inside front cover under Submission of Papers.

Submission. Every paper must be accompanied by a letter from the senior author, stating that he/she is submitting the paper for publication in the *Journal of Chromatography A* or *B*.

Manuscripts. Manuscripts should be typed in **double spacing** on consecutively numbered pages of uniform size. The manuscript should be preceded by a sheet of manuscript paper carrying the title of the paper and the name and full postal address of the person to whom the proofs are to be sent. As a rule, papers should be divided into sections, headed by a caption (*e.g.*, Abstract, Introduction, Experimental, Results, Discussion, etc.). All illustrations, photographs, tables, etc., should be on separate sheets.

Abstract. All articles should have an abstract of 50–100 words which clearly and briefly indicates what is new, different and significant. No references should be given.

Introduction. Every paper must have a concise introduction mentioning what has been done before on the topic described, and stating clearly what is new in the paper now submitted.

Experimental conditions should preferably be given on a *separate* sheet, headed "Conditions". These conditions will, if appropriate, be printed in a block, directly following the heading "Experimental".

Illustrations. The figures should be submitted in a form suitable for reproduction, drawn in Indian ink on drawing or tracing paper. Each illustration should have a caption, all the *captions* being typed (with double spacing) together on a *separate sheet*. If structures are given in the text, the original drawings should be provided. Coloured illustrations are reproduced at the author's expense, the cost being determined by the number of pages and by the number of colours needed. The written permission of the author and publisher must be obtained for the use of any figure already published. Its source must be indicated in the legend.

References. References should be numbered in the order in which they are cited in the text, and listed in numerical sequence on a separate sheet at the end of the article. Please check a recent issue for the layout of the reference list. Abbreviations for the titles of journals should follow the system used by *Chemical Abstracts*. Articles not yet published should be given as "in press" (journal should be specified), "submitted for publication" (journal should be specified), "in preparation" or "personal communication".

Vols. 1–651 of the *Journal of Chromatography*; *Journal of Chromatography, Biomedical Applications* and *Journal of Chromatography, Symposium Volumes* should be cited as *J. Chromatogr.* From Vol. 652 on, *Journal of Chromatography A* (incl. Symposium Volumes) should be cited as *J. Chromatogr. A* and *Journal of Chromatography B: Biomedical Applications* as *J. Chromatogr. B.*

Dispatch. Before sending the manuscript to the Editor please check that the envelope contains four copies of the paper complete with references, captions and figures. One of the sets of figures must be the originals suitable for direct reproduction. Please also ensure that permission to publish has been obtained from your institute.

Proofs. One set of proofs will be sent to the author to be carefully checked for printer's errors. Corrections must be restricted to instances in which the proof is at variance with the manuscript.

Reprints. Fifty reprints will be supplied free of charge. Additional reprints can be ordered by the authors. An order form containing price quotations will be sent to the authors together with the proofs of their article.

Environmental Analysis

Techniques, Applications and Quality Assurance

Edited by **D. Barceló**

Techniques and Instrumentation in Analytical Chemistry Volume 13

Three aspects of environmental analysis are treated in this book:

- the use of various analytical techniques
- their applications to trace analysis of pollutants, mainly organic compounds
- quality assurance aspects, including the use of certified reference materials for quality control of the entire analytical process.

The book will serve as a general reference for post-graduate students as well as a practical reference for environmental chemists who need to use the analytical techniques for environmental studies. Analytical chemists needing information on the complexity of environmental sample matrices and interferences will also find this an invaluable reference.

Contents: Part 1. Field Sampling Techniques and Sample Preparation. 1. Sampling techniques for air pollutants (R. Niessner). 2. Sample handling strategies for the analysis of organic contaminants from environmental samples (M.-C. Hennion, P. Scribe). 3. Extraction, clean-up and recoveries of persistent trace organic contaminants from sediment and biota samples (D.E. Wells).
Part 2. Application Areas. 4. Current developments in the analysis of polychlorinated biphenyls (PCBs) including planar and other toxic metabolites in environmental matrices (D.E. Wells). 5. Official methods of analysis of priority pesticides in water using gas chromatographic techniques (D. Barceló). 6. Coupled-column reversed phase liquid chromatography as a versatile technique for the determination of polar pesticides (E.A. Hogendoorn, P. van Zoonen). 7. Liquid chromatographic determination of phenols and substituted derivatives in water samples (G. Marko-Varga). 8. HPLC methods for the determination of mycotoxins and phycotoxins (J.F. Lawrence, P.M. Scott). 9. Determination of radionuclides in environmental samples (V. Valkovic).
Part 3. Quality Assurance and Reference Materials. 10. Quality assurance in environmental analysis (W.P. Cofino). 11. Certified reference materials for the quality control of measurements in environmental monitoring (E.A. Maier). 12. Standard reference materials for the determination of trace organic constituents in environmental samples (S.A. Wise).
Part 4. Emerging Techniques. 13. Application of fluorescence spectroscopic techniques in the determination of PAHs and PAH metabolites (F. Ariese, C. Gooijer, N.H. Velthorst). 14. Characterization of surfactants in water by desorption ionization methods (F. Ventura). 15. Utilization of various LC-MS interfacing systems in environmental analysis; application to polar pesticides (M.H. Lamoree, R.T. Ghijsen, U.A.Th. Brinkman). 16. Hyphenated techniques applied to the speciation of organometallic compounds in the environment (O.F.X. Donard, R. Ritsema). 17. The potential of capillary electrophoresis in environmental analysis (M.W.F. Nielen).
Subject index.

© 1993 660 pages Hardbound
Price: Dfl. 465.00 (US $ 265.75)
ISBN 0-444-89648-1

ELSEVIER SCIENCE B.V.

ORDER INFORMATION

For USA and Canada
ELSEVIER SCIENCE INC.
P.O. Box 945
Madison Square Station
New York, NY 10160-0757
Fax: (212) 633 3880

In all other countries
ELSEVIER SCIENCE B.V.
P.O. Box 330
1000 AH Amsterdam
The Netherlands
Fax: (+31-20) 5862 845

US$ prices are valid only for the USA & Canada and are subject to exchange rate fluctuations; in all other countries the Dutch guilder price (Dfl.) is definitive. Customers in the European Community should add the appropriate VAT rate applicable in their country to the price(s). Books are sent postfree if prepaid.